FACULTY OF
BIOSCIENCE ENGINEERING

Human exposure and potential health effects of marine compounds in sea spray aerosols

ir. Emmanuel Van Acker

Thesis submitted to fulfill the requirements for the degree of
Doctor (PhD) of Bioscience Engineering

Academic year: 2020 – 2021

GHENT
UNIVERSITY

“Celui qui a respiré une fois aux bords de la mer, oublie difficilement le sentiment de bien-être qu’il y a éprouvé”

Dr. Louis Verhaege, 1843

Promoters

Prof. dr. Colin Janssen

Prof. dr. ir. Karel De Schamphelaere

Ghent University, Faculty of Bioscience Engineering

Department of Animal Sciences and Aquatic Ecology

Dean

Prof. dr. ir. Marc Van Meirvenne

Rector

Prof. dr. ir. Rik Van de Walle

FACULTY OF
BIOSCIENCE ENGINEERING

Human exposure and potential health effects of marine compounds in sea spray aerosols

ir. Emmanuel Van Acker

Thesis submitted to fulfill the requirements for the degree of
Doctor (PhD) of Bioscience Engineering

Academic year: 2020 – 2021

GHENT
UNIVERSITY

Promotors: **Prof. dr. Colin R. Janssen**

Ghent University, Faculty of Bioscience Engineering

Department of Animal Sciences and Aquatic Ecology

Prof. dr. ir. Karel A. C. De Schamphelaere

Ghent University, Faculty of Bioscience Engineering

Department of Animal Sciences and Aquatic Ecology

Members of the examination committee:

Prof. dr. ir. Nico Boon (Chairman)

Ghent University, Faculty of Bioscience Engineering

Department of Biotechnology

Prof. dr. ir. Jana Asselman (Secretary)

Ghent University, Faculty of Bioscience Engineering

Department of Animal Sciences and Aquatic Ecology

Prof. dr. ir. Christophe Walgraeve

Ghent University, Faculty of Bioscience Engineering

Department of Green Chemistry and Technology

dr. ir. Charlotte Grootaert

Ghent University, Faculty of Bioscience Engineering

Department of Food Technology, Safety and Health

Prof. dr. ir. Lynn Vanhaecke

Ghent University, Faculty of Veterinary Medicine

Department of Veterinary Public Health and Food

Prof. dr. Jan Mees

Flanders Marine Institute (VLIZ)

Ghent University, Faculty of Sciences

Department of Biology

Prof. dr. Erik Smolders

KU Leuven, Faculty of Bioscience Engineering

Department of Soil and Water Management

Dean: **Prof. dr. ir. Marc Van Meirvenne**

Ghent University, Faculty of Bioscience Engineering

Rector: **Prof. dr. ir. Rik Van de Walle**

Ghent University

Dutch translation of the title:

Humane blootstelling en potentiële gezondheidseffecten van mariene componenten in zeespray aerosolen

Refer to this work as:

Van Acker, E. 2021. Human exposure and potential health effects of marine compounds in sea spray aerosols. PhD Thesis, Ghent University, Ghent, Belgium.

ISBN-number: *will be added when available*

DANKWOORD

Amai, we zijn zover. Het moment waar iedere PhD student naar uitkijkt: het laatste stukje tekst van zijn boekje neerschrijven. De pagina's die tevens het meest gelezen worden. Op zo'n moment denk je dan hoe dit alles is begonnen.

We schrijven vrijdag 17 november 2014 omstreeks 14:00:

> *Ik ben in de Gentse Stropstraat mijn valies aan het pakken voor het aankomende leidersweekend van mijn teerbeminde scoutsgroep. Plots krijg ik telefoon van een onbekend nummer. De essentie van het daaropvolgend gesprek is iets als volgt:*
>
> > *Hallo met Emmanuel Van Acker.*
> >
> > > *Dag Emmanuel, met Prof. Colin Janssen hier. (…) Zou je geïnteresseerd zijn om te appliqueren op de vacature van academisch assistent aan ons labo. Zo'n positie komt niet vaak vrij en ik denk dat dit wel iets voor jou is.*
> >
> > *Ja, dat lijkt me een interessante job. (…) Ik zal er zeker over nadenken.*
> >
> > > *Nu zit er wel een addertje onder het gras. De vacature sluit vanavond om 23:59. Mocht je interesse hebben zal je lang mogen twijfelen. Alle info over vacature vind je op de site van de universiteit.*
> >
> > *Eu, ok, ik zal dan snel beslissen. Bedankt professor voor je telefoontje. (…)*
>
> *Na even kort denken, boks ik snel een CV in elkaar en begin ik aan een motivatiebrief. Deze laatste vervolledig ik in het dorpje waar we dat weekend verblijven. Michiel L. leest hem nog eens na en vervolgens ga ik met Theo B. op zoek naar een internet hotspot in de buurt. Na even wandelen, staan we op een donkere oprit van een huis en verstuur ik mijn documenten ruim op tijd … omstreeks 23:35.*

Na één sollicitatiegesprek met prof. Janssen en prof. De Schamphelaere werd ik aangenomen. Ik bleef wel met één vraag zitten: was die last-minute sollicitatie een voorbode van wat zou volgen? Nee hoor, er waren de afgelopen 6 jaar zeker ook momenten dat we ruim op tijd klaar waren en niet tegen de deadline aan werkten.

Gedurende 6 jaar als assistent werken in een labo als het onze levert heel wat onvergetelijke momenten op: Kerstfeestjes, sportdagen, Gentse feesten, end-of-the-month-drinks, congressen en PhD verdedigingen, die al dan niet werden afgesloten in

de binnenstad. Als één van de laatste der Plateau'iaan PhD studenten heb ik een hele reeks gezichten zien passeren, maar vooral veel vriendschappen opgebouwd. Een ferme dank je wel is meer dan terecht voor de mensen die deze 6 jaar hebben ingekleurd met hun hulp, steun en ambiance. Laten we beginnen met de meest beruchte persoonlijkheid van ons labo, jawel den ouwen (zoals hij zichzelf graag noemt), mijn hoofdpromotor Prof. Janssen.

Assistent zijn van Colin brengt zoals gezegd een beetje deadline-werk met zich mee, maar ook zoveel meer! De meester (of beter) professor tacticus leert je niet per se alles over statistiek maar wel hoe je je onderzoek best in de picture zet, hoe je studenten kan begeesteren, hoe je op de interfase van disciplines vaak ontdekkingen doet, en hoe samenwerkingen en connecties je snel vooruit kunnen helpen. Dank je Colin voor je (mariene) leerschool, je vele revisies van mijn geschreven werk, je vertrouwen in het pad dat ik langzaam maar zeker bewandelde, en de vele constructieve wetenschappelijke en persoonlijke babbels. De voornaamste locaties van deze babbels zullen me dan ook blijblijven: je chique ovalen desk, de plateau-koer tussen je sigarenrook, je nette coupure-bureau aan de andere kant van de kastenrij (is-hij-er-kijk-sprongetjes werden er een vaste gewoonte), een lunch restaurantje en tenslotte je old-school krab/kreeft achtergrond bij een corona-safe Teams call.

Het moet wel gezegd, mijn doctoraatonderwerp was en is (na microplastics) één van Colin zijn kindjes. Falen was dus geen optie. Om een snelle start van mijn onderzoek te verzekeren plaatste hij twee thesisstudenten onder mijn hoede. Gezien ik zelf nog maar half wist wat mijn onderzoek inhield, was dit geen makkelijke opdracht. Met wat steun en advies van mijn oude thesisbegeleider (en vriend) Maarten De Rijcke kwam dit toch tot een goed einde. Vele thesisstudenten volgden en bleken zeker tijdens de eerste jaren cruciaal om naast de vele taken als assistent aan onderzoek toe te komen. De zeven master studenten (Myrthe, Tine, Sam, Emily, Waut, Elisabeth, en Jasmijn) die onder mijn vleugels hard werkten en goede tot uitstekende thesissen schreven wil ik dus ook erg bedanken.

Ik ook vaak rekenen op de steun van mijn co-promotor Karel De Schamphelaere. Naast zijn grondige en kritische reviews van mijn manuscripten, kwam zijn nuttig advies steeds van pas als ik een ander perspectief kon gebruiken. In de tweede helft

van mijn termijn kon ik ook bij Jana Asselman terecht voor raad en daad. Ik wens jullie beide te bedanken voor de fijne en goede samenwerking! Maarten zijn advies verminderde daarentegen in de tijd, maar bleef wel een constante. Zeker omdat hij in zijn nieuwe job bij het VLIZ onderzoek bleef voeren op hetzelfde thema. De verderzetting van onze samenwerking bleef dus verzekerd en dit bleek een succesvol recept. Dikke merci voor alles copain!

Nog zo een persoon waar ik ongedwongen advies aan kon vragen was Nancy De Saeyer: de stille rots in de branding van ons labo. Je bereidwilligheid om iedereen zo goed mogelijk te helpen en de vele taken dat je opknapt om het labo te doen draaien zijn onmisbaar! Ik wil je daarnaast ook bedanken om je analytische ervaring met me te delen en voor je interesse in mijn werk. Emmy, Jolien en Gisèle, de lieve laboranten van ons labo, wil ik heel erg bedanken voor hun hulp bij de voorbereiding van practica, het uitvoeren van in vitro experimenten en extracties, het bestellen van materiaal, en de om-ter-beste sfeer tussen daphnia's en algen. Ook een dikke merci aan Marc, voor het bouwen van mijn eigen zeespray toestel. Als assistent kom je naast het labo ook vaak op het secretariaat. Naast de snoepjes vond ik daar bij Marianne (en Sigrid) een aangename babbel en veel hulp bij administratie voor mezelf, de cursussen, projecten en de (agenda's van) proffen. Ongelofelijk bedankt dames!

Gezien mijn doctoraat nogal interdisciplinair was, heb ik heb vele uren in andere labo's (en aan zee) doorgebracht. Zonder de hulp van de professionals in deze labo's was mijn onderzoek niet mogelijk. Dank je wel, Prof. Lynn Vanhaecke en je ganse team (Steve, Gabriel, Lieven, Beata, Dirk, …) voor de analyses die ik in Merelbeke met jullie deskundige hulp kon uitvoeren. Dank je wel, Dr. Ilse Beck, Karlien Van Wesenmael en Dr. Charlotte Grootaert voor de initiatie tot het kweken van cellijnen en allerlei assays. Dank je wel Maarten De Rijcke, Mattias Bossaer, Jan Vermaut, Michiel Suerinck en de andere VLIZ medewerkers voor de samenwerking en hulp bij allerhande staalnames.

Na Olivier's vertrek (in 2016), stond ik er een lastige semester alleen voor als assistent. Tot mijn grootte blijdschap deed Ilias daarna zijn intrede en nam hij in een record tempo veel verantwoordelijkheid op. Ondanks dat onze stijlen initieel wel eens durfden te botsten, slaagden we er in een complementair team te vormen dat elkaars sterktes wist te vinden. Oprechte dank Ilias voor op je te kunnen bouwen en je enorme inzet!

Als jonge PhD student arriveerde ik op de Plateau in een levendig labo met veel *bons vivants* die al graag eens op zwier gingen. Merci voor de vele toffe avonden (tot in de late uurtjes als stickers) Karel Vi., Maarten, Charlotte, Tina, Jenni, Cecilia, David, Jan, Lisbeth, Gert en Jonathan. Na de verhuis naar de Coupure veranderden er enkele gewoontes. Vaak liep ik (of Sacha) op vrijdag het landschapsbureau af op zoek naar kandidaten om de Koepuur (of de Walrus) onveilig te gaan maken. Thanks Samuel, Joao, Wout, Niels, Daniel, Arne, Josef, Sacha, Karel Vl., Simon, Kristi, Nathalia, Long, Tiptiwa, Sharon, Maaike, Stijn, Abegail, Quying, Miao en Zixia. Het was zalig vertoeven in jullie gezelschap. Vanzelfsprekend ook een dikke merci aan mijn sport en rode duivel maatje Samuel, zonder wie mijn tijd aan het labo en de lunchpauzes niet hetzelfde zouden geweest zijn!

Verder wil ik heel specifiek mijn ouders, broer en zus te bedanken voor de steun en liefde die ze me de laatste 30 jaar hebben geboden. Zonder hen was er nooit sprake geweest van de dr. en ir. die nu voor mijn naam mogen staan. Ook mijn schoonouders/gebuurs mag ik niet vergeten te bedanken, gezien ik te pas en te onpas bij hen binnenval voor wat hulp. Tot slot rest mij enkel nog de belangrijkste persoon te bedanken: mijn ongelofelijk topvrouwtje en beste vriend Laura. Van meet af aan leefde je mee met de ups en downs van dit avontuur. In beide gevallen was je er en hielp je me het belang ervan te relativeren, iets wat soms al eens nodig is wanneer ik teveel in mij werk verzonken was. We zullen ons toekomstig kleintje binnenkort wel duidelijk moeten maken dat hij bij jou moet zijn wanneer hij een dokter (i.p.v. doctor) nodig heeft voor een pijntje. Hoe dan ook staat er een mooie toekomst voor onze deur, laten we snel opendoen…

Emmanuel Van Acker

Avelgem, 26 August 2021

CONTENTS

ABBREVIATIONS

1-9	4E-BP1	Eukaryotic translation initiation factor 4E-binding protein 1
A	AIC	Akaike information criterion
	Akt	Protein kinase B
	AZA	Azaspiracid
B	BGC	Biosynthetic gene cluster
C	CYP1B1	Cytochrome P450 family 1 subfamily B member 1
	C18	Octadecyl
D	DA	Domoic acid
	DE	Differentially expressed
	DMPC	Dimyristoylglycerophosphocholine
	DMEM	Dulbecco's Modified Eagle Medium
	DPPC	Dipalmitoylphosphatidylcholine
	DRC	Dose response curve
	DSP	Diarrhetic shellfish poisoning
	DTX	Dinophysistoxin
E	ECx	Effect concentrations for x% of the cells
	EF_{LSA}	Enrichment factor in lake spray aerosols
	EF_{SSA}	Enrichment factor in sea spray aerosols
	EF_{SSML}	Enrichment factor in the sea surface microlayer
	ERSEM	European Regional Seas Ecosystem Model
F	FDR	False discovery rates
	FWHM	Full width at half maximum
G	GSEA	Gene set enrichment analysis
	GLM	Generalized linear model
H	HAB	Harmful algal bloom
	HCD	High energy collision dissociation
	HESI	Heated electrospray ionization
	HRMS	High-resolution mass spectrometry
	hYTX	Homoyessotoxin
I	ICP-OES	Inductively coupled plasma-optical emission spectroscopy
	IS	Internal standard
J-K	/	
L	LOD	Limit of detection
	LOQ	Limit of quantification
M	MART	Marine aerosol reference tank
	mTOR	Mechanistic target of rapamycin
	MTT	3-(4,5-dimethylthiazol-2-yl)-2,5-diphenyltetrazolium bromide
N	NCE	Normalized collision energy
	NPZD	Nutrient-phytoplankton-zooplankton-detritus (model)
O	OA	Okadaic acid
	OHH	Ocean(s) and human health
	OVTX	Ovatoxin

P	PADI3	Peptidyl arginine deiminase 3
	PbTx	Brevetoxin
	PCSK9	Proprotein convertase subtilisin/kexin type 9
	PhyC	Phytoplankton biomass expressed as concentrations of carbon
	PI3K	Phosphatidylinositol-3 kinase
	PRM	Parallel reaction monitoring
	PTFE	Polytetrafluoroethylene
	PTX	Pectenotoxin
Q	Q1-8	Research question 1 to research question 8
R	R^2	Coefficient of determination
	RDS	Respiratory distress syndrome
	RH	Relative humidity
	Rs	Chromatographic resolution
	RSD	Relative standard deviation
	RSM	Response surface modelling
	RT	Retention time
S	S6RP	S6 ribosomal protein
	S_b	Between-group standard deviation
	SCD	Stearoyl-CoA desaturase
	SE	Standard error
	SI	Supportive information
	S_I	Intermediate precision or within-laboratory S_r
	SMIM 29	Small integral membrane protein 29
	SNRPE	Small nuclear ribonucleoprotein polypeptide E
	SPE	Solid phase extraction
	SPX	Spirolide
	S_r	Repeatability standard deviation
	SRT	Surfactant replacement therapies
	SREBF1	Sterol regulatory element binding transcription factor 1
	SSA	Sea spray aerosol
	SSML	Sea surface microlayer
	SSW	Subsurface water
	$S_{y/x}$	Error of estimate
T	TMM	Trimmed mean of M-values
	$Time_{seawind}$	The time the wind (direction) blew from across the sea
	TSP	Total suspended particles
U	UHPLC	Ultra-high-performance liquid chromatography
	UN	United Nations
V	VIF	Variance inflation factor
	VLIZ	Flanders Marine Institute
W	$WH_{seawind}$	One-week average wave height during periods with seawind
X	/	
Y	YTX	Yessotoxin
Z	/	

Chapter 1

General introduction and outline

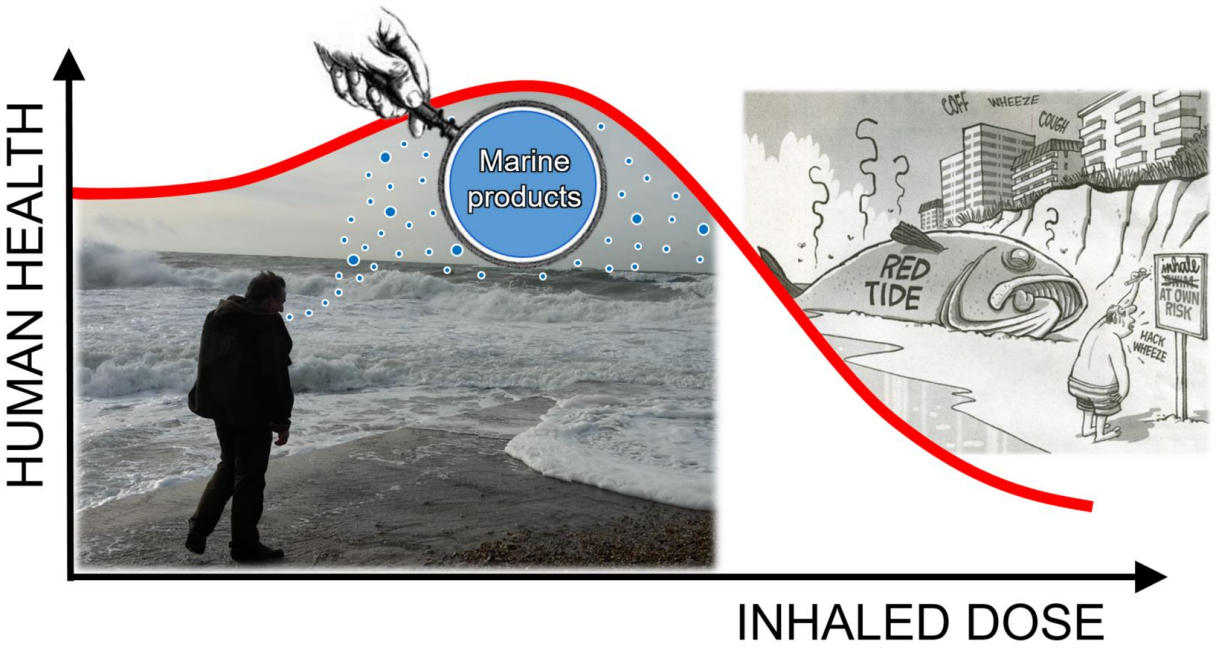

Chapter contents

Preface

It is generally believed that living and taking recreation near the sea is beneficial for human health. Especially the air we breathe in these marine environments has long been attributed health promoting properties. This is something my grandmother also told me when I was still a child. It is, however, not entirely clear where the idea of ‘healthy coastal air’ comes from. It seems that along with the development of human medicine and at a later stage with coastal tourism, it has evolved into a kind of "folk wisdom". Nonetheless, the ancient concept of thalassotherapy has regained scientific interest in recent years. Researchers are investigating the interconnections between the ocean and the health of human coastal populations. Still, to date, strong scientific evidence has remained absent to reveal whether and how coastal air could improve the health of coastal populations.

In this PhD thesis, I have investigated one of the major aspects that distinguishes coastal air from inland air: sea spray aerosols (SSA). Both the biogenic composition of SSAs and the potential effects on human health have been dealt with. Before going into detail on the performed research, you will find a holistic summary of the historical context and current knowledge on the various aspects of this research topic. In the last section of this introduction Chapter 1, the rationale, objectives and outline of this PhD thesis are explained.

1 Historical context

Marine environments have been important throughout the history of humankind. Both the image of a dangerous ocean that takes lives, as that of an ocean providing essential resources and opportunities have been common all over the world. In recent years, the ancient idea that coastal environments are health promoting has gained scientific interest. While the first written references of the curative uses of seawater and coastal air date back to the Ancient Greeks, there is evidence that ocean-therapy was used to treat health conditions in Ancient Egypt over 5000 years ago.[1,2] The Greek philosopher and medical theorist Alcmaeon of Croton (ca. 470 B.C.) is considered the first to formally link human health to water quality. In his treatise 'Airs, waters and places' (ca. 400 B.C) Hippocrates built on this idea and linked the location one lives with the prevalence of diseases. As such the distance to the sea and the climate were seen as important driving factors for human health.[3] Hippocrates also suggested the inhalation of steam from (boiling) salty water (i.e., seawater) as a curative method.[4] Back then, no one realized that the bursting bubbles of boiling water produce an aerosol. Even nowadays many people still confuse aerosolization (see section 3) with the volatilization or evaporation (i.e., gas phase) of chemical compounds.

In the 18th and 19th century the ancient ocean-therapy concept was revived by various physicians. First in England (e.g., Dr. R. Russel; Figure S1.1) and later also on the European mainland due to prominent doctors such as L. Bagot, J. La Bonnardière and A. Delcroix.[5–7] In Belgium the work of Dr. L Verhaeghe (1843) '*Les Bains de mer d'Ostende, leurs effects physiologiques et thérapeutiques*' was an important milestone.[8] Among others, he raised the new question: "what are the characteristics that make coastal air so beneficial" and stated that "this question was far from receiving its last answer". Verhaeghe was right, up to the present day a fair number of researchers have examined the characteristics of coastal air in an attempt to address this question. A few years before, Roubardi (1833) suggested that the composition of coastal air changes when the sea is rough, due to the entrainment of water in a form of fog.[9] We currently know this better as a sea spray aerosols (SSAs), i.e., a suspension of seawater drops small enough to reside for some time in the atmosphere. In 1865, Dr. J. La Bonnardière introduced the term 'thalassotherapy'.[7] Derived from the Greek words *thalassa* (i.e., sea) and *therapeia* (i.e., treatment), it refers to the

therapeutic use of seawater, marine products and the seashore climate (e.g., coastal air).[10] In the late 19th and early 20th century the reinvented thalassotherapy led to the establishment of health facilities and sanatoria along the European shores of the Atlantic Ocean (Figures 1.1A, S1.2, S1.3) and North Sea (Figure 1.1B). These sanatoria often had large terraces or balconies which allowed patients, who often suffered from tuberculosis or rheumatism,[6] to be exposed to the sun and coastal air.

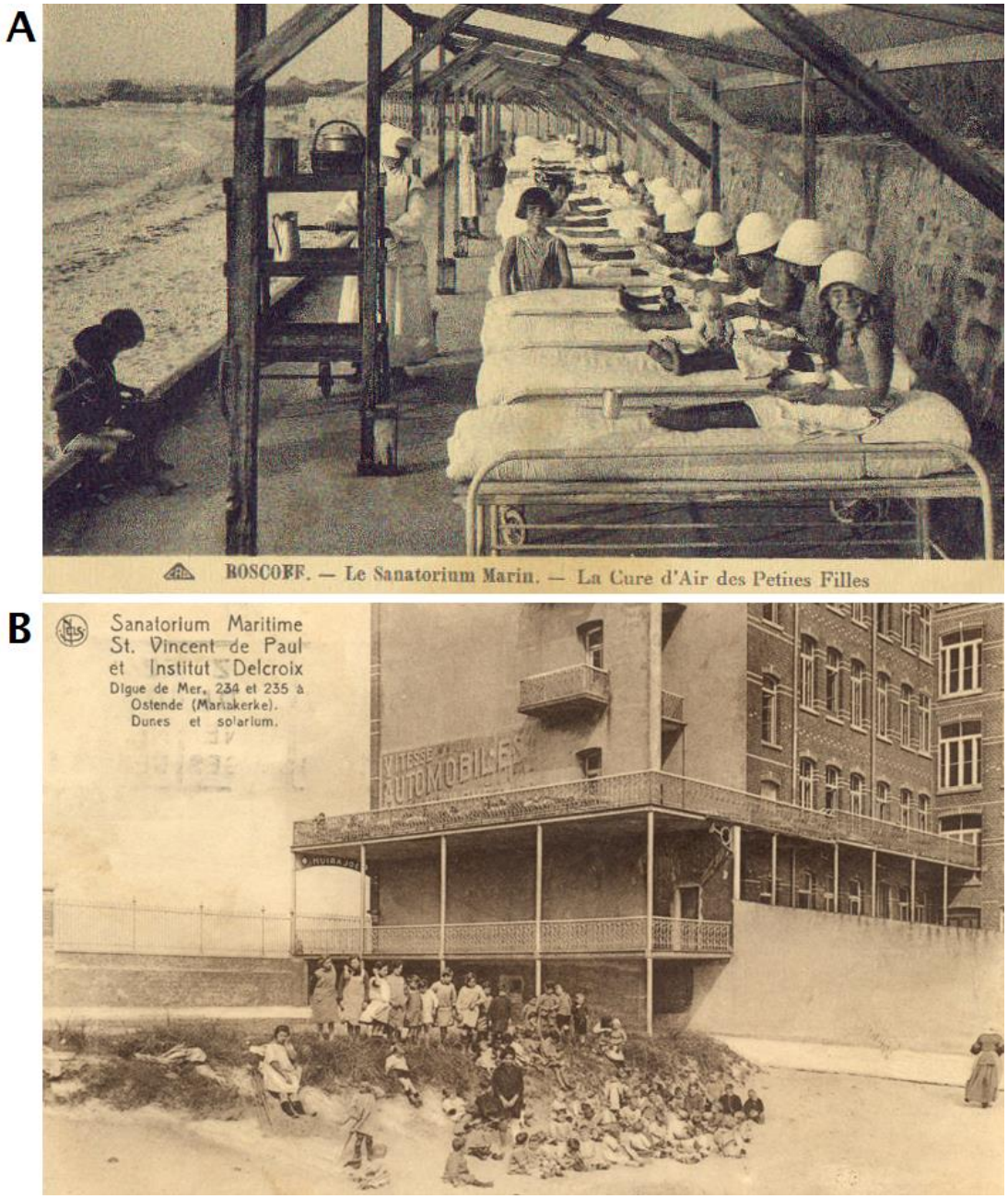

Figure 1.1: (A) Outdoor facilities of the marine sanatorium in Roscoff, France, founded by Dr. Louis Bagot (1899).[5] Picture geneanet.org. (B) Building and outdoor balcony of the institute Sint Vincentius à Paulo in Ostend, Belgium. It was founded by Dr. Armand Delcroix (1897) and served as a marine sanatorium.[6] After world war II, the hospital (and sanatorium) was rebuild through the efforts of Dr. Edouard Delcroix. © beeldbankkusterfgoed.be.

At that time, scientists and doctors mainly focused on the inorganic content (e.g., salts) of coastal air. Consequently, one of the common (urban) legends was that the apparent coastal health promoting effect originated from a high airborne iodine exposure. It is true that coastal air has higher Iodine concentrations (±5-30 ng m^{-3}).[11] The ocean is after all the main source[12] for both gaseous (67-80%) and particulate (20-33%) forms of iodine in the atmosphere.[11] Iodine is an essential element for human physiology and has a prominent function in the hormone production of the thyroid gland.[13] Iodine-deficiency disorders, leading to mental impairment and adverse growth and development, result from an insufficient intake (<150 µg day^{-1} for adults).[13] Based on the above and the findings of Smyth et al.,[14] the inhalation of coastal air (i.e., maximum 10-25 m^3 day^{-1}) can only account up to 0.5-1% of the recommended daily iodine intake. Smyth et al.[14] did show that this airborne iodine exposure can increase up to about 10% of the recommended daily intake when (continuously) inhaling the air above seaweed beds, which is rich in gaseous I_2. The latter is, however, an unrealistic scenario. It can thus be concluded that the airborne iodine supplement in coastal regions cannot explain the suggested health effects.

It was only from 1948 onwards, when Woodcock[15] started his research on the human respiratory irritation during Florida red tides (Figure 1.2A), that research on organic (biogenic) compounds in sea spray aerosols (SSAs) was initiated. Red tides are the old and popular terminology for harmful algal blooms (HABs) that discolor seawater due to the high cell density of (red) pigmented dinoflagellates or diatoms.[16] The frequent reoccurring HABs in Florida and the Gulf of Mexico are caused by *Karenia brevis* (Figure 1.2B), which produces brevetoxins (PbTxs).[17] Similar to the above discussed method of Hippocrates, Woodcock boiled seawater containing toxic algae and exposed his face to the “vapors”. He discovered that he only experienced respiratory irritation if air bubbles were formed in the boiling water. As such he discovered that not the steam but the produced aerosol caused the irritation. Before Woodcock[15] and Taylor[18], who first pointed to *K. brevis* HABs as the main culprit in 1917, the respiratory irritations were already associated with massive fish-mortality events (i.e., co-occurring harmful effects of these HABs).[19] To date, about a dozen studies have investigated the aerosolization of algal toxins or so called phycotoxins.[20–25] Contrary to most phycotoxins, an increasing number of marine compounds are being identified as having a positive pharmacological activity[26,27] (see section 4). Airborne

exposure to SSAs, which has mainly been investigated for their harmful effects, may therefore also induce beneficial effects. This hypothesis, which is further discussed in section 2, could explain the results of recent epidemiological studies that indicate a coastal proximity health effect (see section 2) and support (if proven to be correct) the ancient thalassotherapy concept.

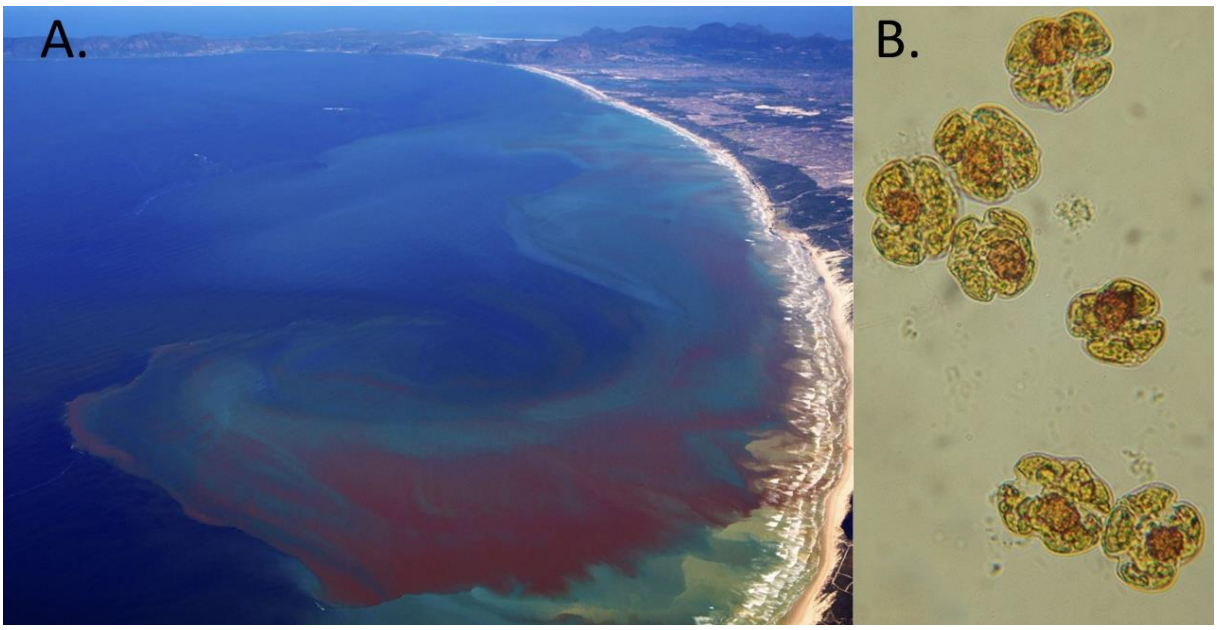

Figure 1.2: (A) Red tide event caused by a HAB of (B) Karenia brevis which have red pigments and can produce brevetoxins (PbTxs). © Awesomeocean.com © Mote Marine Laboratory.

2 Ocean and human health epidemiology and hypotheses

World-wide, coastal regions are by far the most densely populated areas.[28] In many cases, however, we are not aware of or do not understand how we impact marine environments and vice versa.[29] Indeed, changes in marine ecosystems can have (as discussed below) direct and indirect impacts on human health. These anthropogenic activities and impacts include eutrophication, overfishing, mariculture, introduction of invasive species, chemical contamination (e.g., industrial chemicals, wide dispersive use chemicals and radioisotope discharges), coastal zone destruction (e.g., shipping, dredging, land reclamation), sewage discharge (e.g., spread of infectious diseases), as well as indirect consequences of atmospheric pollution (e.g., global warming and ocean acidification). The increasing awareness of this high interconnectivity, as displayed in Figure 1.3, resulted in a new inter-disciplinary research field that links the 'ocean and human health' (OHH).[30] A key aspect that is addressed in this field is the vulnerability of marine ecosystems and the related negative consequences for

humankind. Research towards (threatened) marine ecosystem services that have positive effects on human health is also included. In fact, it is believed that (commercial) opportunities and benefits of a healthy ocean are a stronger convincing argument to protect marine systems than the risks related to an unhealthy ocean.[31]

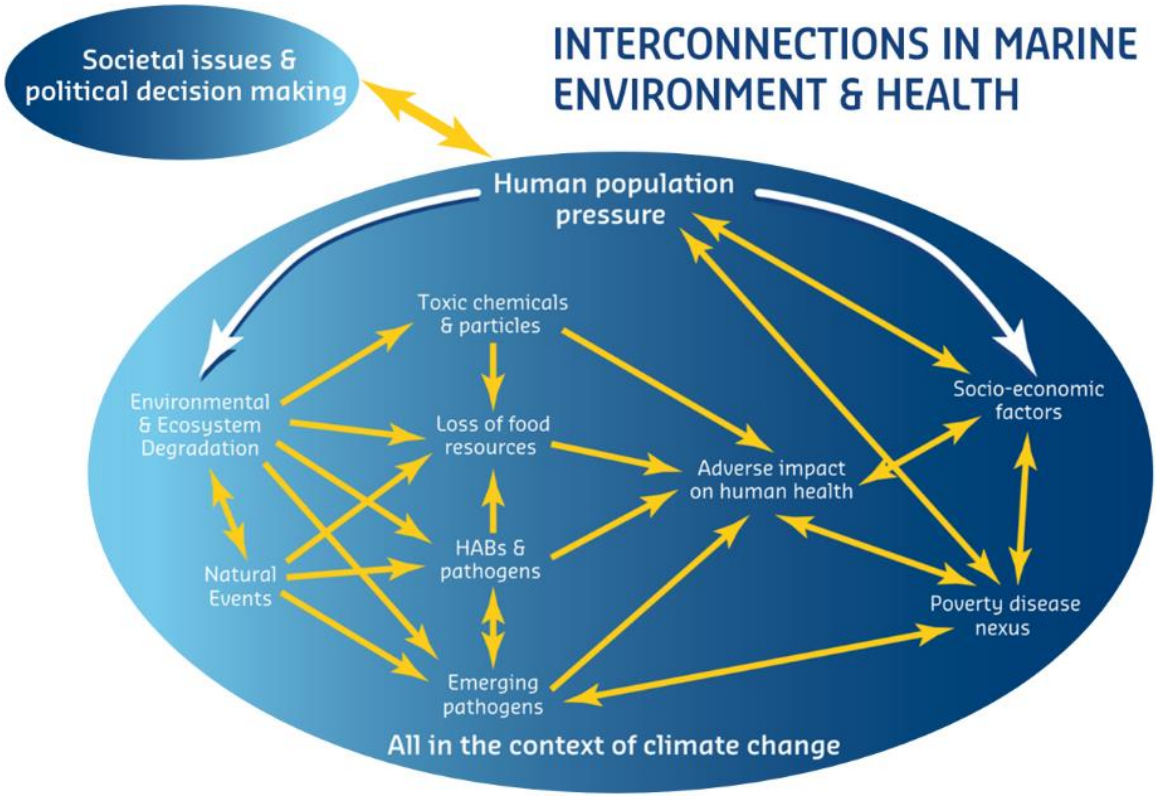

Figure 1.3: Summary of key processes in the marine environment with a negative public health relevance. Many of these processes are disturbed or influenced by anthropogenic activities. Natural processes with a positive health relevance are not incorporated. (from Moore et al.).[30]

Despite the fact that the idea of a health promoting coastal environment has always been around, there is little scientific evidence regarding specific effects or mechanisms to support this claim/believe. In the last decade epidemiological studies[32–36] have started to reveal a coastal proximity health effect. They showed that good health and happiness are more prevalent the closer one lives to the sea. An additional finding was that positive effects were greater amongst more economically deprived communities.[33] Several hypotheses have been proposed to explain the coastal proximity health effect. To date beneficial effects have been mainly attributed to psychological mechanisms, based on the premise that humans recognize harmful environments that induce stress.[37] Natural environments (i.e., blue and green spaces) would therefore promote wellbeing as they conjure positive feelings, thus reducing stress-related inflammation.[38] Depledge and Bird[39] combined this psychological theory with

mechanisms that are linked to the coastal environments, such as increased relaxation, restoration, exposure to sunlight, social contact and physical exercise. Their so-called 'Blue Gym' hypothesis would explain the improved health and wellbeing of coastal populations. The recent epidemiological study by Hooyberg et al.[35] considered the proposed mechanisms of the Blue gym theory (i.e., mental health, physical activity levels, and social contact). Although they did found a significant improved health effect in Belgian coastal populations, none of the investigated mechanisms, including a lower air pollution (i.e., PM10 concentrations at 0-5 km from the shoreline), could provide an explanation.[35] A number of studies, however, did demonstrate a significant increase of mental health[34,40] and physical exercise for different coastal populations.[41–44]

Yet, all of these mechanisms are unlikely to explain long-term physiological benefits according to Rook[45] and Moore[46]. These authors both proposed a new and interesting hypothesis to explain the coastal proximity health effect. Both their theories are not contradictory but rather complementary to previously proposed hypotheses which focused on physiological mechanisms (see Figure S1.4).[39,47,48] Rook[47] attributed the beneficial effects of marine environments to an improved immunoregulation, which is also referred to as the "old friends" theory. It states that a reduced exposure to microorganisms leads to poorer response to inflammations and may even lead to psychiatric disorders.[47] The airborne exposure to diverse microbiota via SSAs[48] would therefore stimulate the immune system and human health in general. Moore[46], on the other hand, suggested through his 'biogenics hypothesis' that the regular airborne exposure to natural compounds and (fragments of) microbiota in natural aerosols (e.g., SSAs) is health promoting. Moore postulated that this is caused through the downregulation of the phosphatidylinositol-3 kinase/protein kinase B/mechanistic target of rapamycin (PI3K/Akt/mTOR) cell signaling pathway (hereafter referred to as the mTOR pathway), as many natural products (e.g., from bacteria, algae, and fungi) have been shown to inhibit the activities of these protein kinases.[46]. The proposed theory (see Figure 1.4) is based on the fact that the mTOR pathway controls many aspects of cellular physiology such as protein synthesis, cell growth, autophagy, apoptosis, innate immunity, neurodegeneration, longevity, cortisol concentration and iodine uptake,[46] while enhanced activity of the pathway is related to multiple pathological conditions (e.g., cancers, type 2 diabetes, neurodegenerative diseases).[49] The mTOR pathway activity is regulated by the integration of various signals including

growth factors, insulin, nutrients, exercise, energy availability, vitamin D and cellular stressors such as hypoxia, osmotic stress, reactive oxygen species (ROS) and viral infection.[46,49,50] Other mTOR-related interconnected pathways such as NF-κB (nuclear factor kappa-light-chain-enhancer of activated B cells) and PTEN (phosphatase and tensin homologue) are also included in the biogenics hypothesis.[46] NF-κB induces among others the expression of various pro-inflammatory genes and will upon deregulation contribute to various inflammatory diseases,[51] while PTEN is a tumour suppressor protein.[46,52]

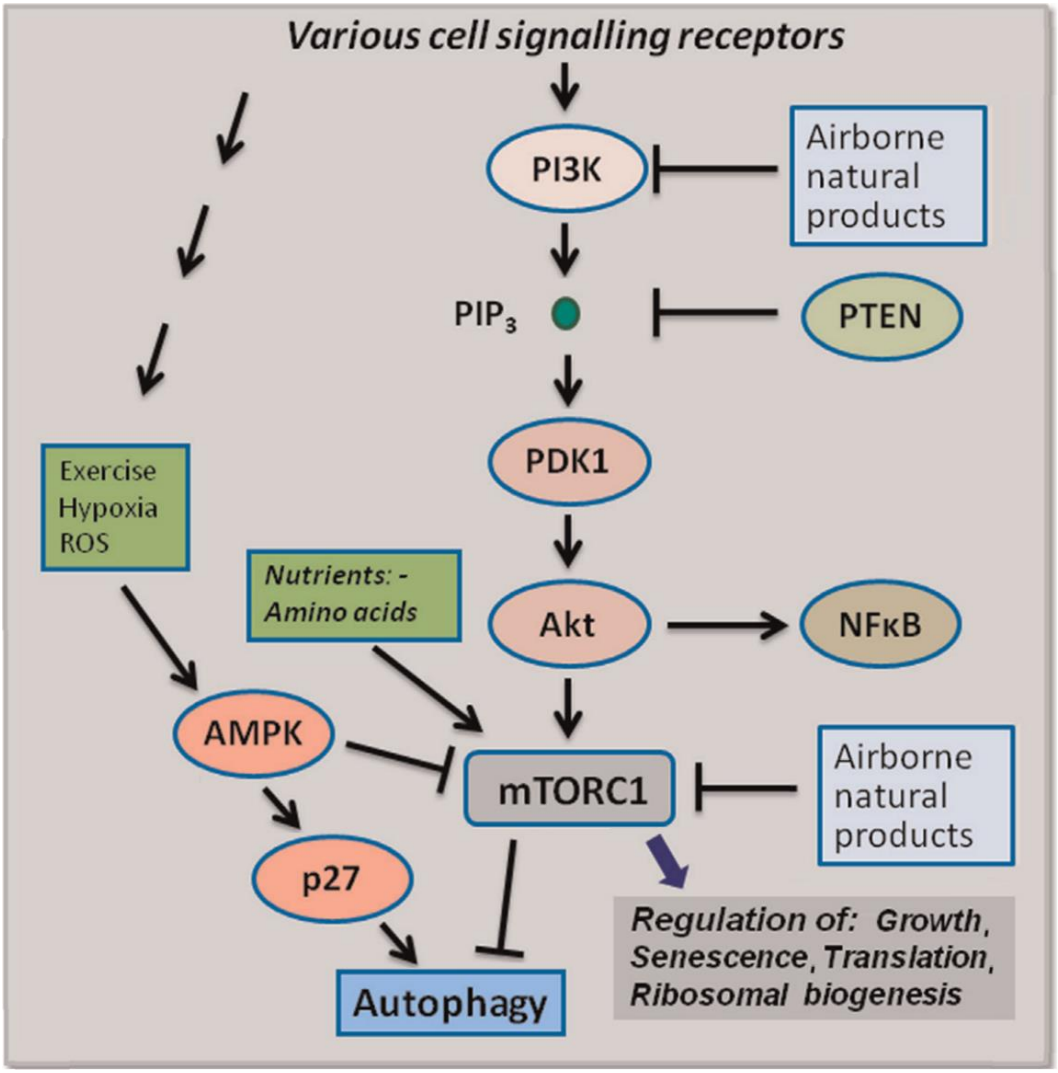

Figure 1.4: Diagram of the cell signaling systems involved in the biogenics hypothesis.[46] *Particularly the phosphatidylinositol-3 kinase/protein kinase B/mechanistic target of rapamycin complex 1 (PI3K/Akt/mTORC1) cell signaling pathway, hereafter referred to as the mTOR pathway, is suggested to be a crucial target. This intracellular signaling pathway is strongly linked to the regulation of cell growth, autophagy, apoptosis and longevity.*[49] *PIP3 – phosphatidylinositol 3,4,5 trisphosphate; NF-κB – nuclear factor kappa-light-chain-enhancer of activated B cells; PTEN – phosphatase and tensin homologue; AMPK – 5' adenosine monophosphate-activated protein kinase; p27 – cyclin-dependent kinase inhibitor; ROS – reactive oxygen species. Activation ↑; inhibition ⊤. Figure from Moore.*[46]

3 Sea spray aerosols (SSAs)

An aerosol is defined as a suspension of non-gaseous (i.e., liquid or solid) particles in an atmosphere. They can originate from both anthropogenic and/or natural emissions. Just like smoke, dust or pollen, a sea spray aerosol (SSA) is a primary aerosol, as it is directly emitted in the air from its (liquid or solid) source medium (i.e., seawater). Secondary aerosols, on the contrary, are formed by gaseous molecules which nucleate and aggregate to particles within the atmosphere.[53] Many aerosols, however, have a hybrid character. An example of such a hybrid aerosol are (natural) pollen that adsorb exhaust particles and (soluble) gaseous pollutants (e.g., SO_2, NO_2, NO_3 and NH_3) on their (wet) surface.[54,55] It was hypothesized that such polluted pollen have synergistic effects regarding respiratory allergies[54] and explain the augmented hay fever in urban areas.[56–58] SSAs also contain a certain fraction of secondary origin, such as iodine (see section 1) originating from gaseous molecules (e.g., HOI, IO, I_2, CH_3I).[11,12] SSAs disperse globally and constitute circa 90% of the marine aerosols, almost 50% of the total natural aerosol flux, and over 33% of the global aerosol flux (i.e., including anthropogenic productions).[59] They act as cloud nucleation sites,[60] influence atmospheric chemical reactions, and scatter and absorb short-wave and long-wave radiation, respectively.[59] Research on the production and behaviour of SSAs, has mainly been conducted in a meteorological, climatological or biogeochemical context. Potential human health effects of airborne SSA exposure remain almost unexplored.

3.1 Effective SSA production

SSAs are primarily produced by bubble bursting processes occurring after the breaking of waves. This occurs continuously in the shallower depths of the surf zone (i.e., near shore), and in open seas when the wind reaches speeds above 3 to 5 m s^{-1}.[53,61] The wind speed and the fetch (i.e., the distance over which the wind blows over the sea) are two environmental variables that are positively related to wave height, and thus to wave breaking and the production of SSAs.[62] Breaking waves entrap air and create underwater bubbles that range from less than 100 µm to about 10 mm in size.[63] When the air bubbles reach the surface they create foam or so-called whitecap. The fractional whitecap coverage of seas is often used as a proxy for SSA production.[53,64] Air bubbles that burst at the seawater surface eject aerosol drops into the atmosphere by means of two consecutive mechanisms.[65,66] Fine film drops, of 0.01 to >10 µm, are first

created out of the bursting bubble film. The largest (bursting) bubbles can produce up to several hundreds of film drops. The seawater that subsequently fills the bubble cavity may overshoot and detach from the water surface. As such, a few somewhat larger jet drops of 1 to >100 µm can thus be ejected in the atmosphere.[61] Above a wind speed threshold of 7 to 11 m s^{-1} an additional SSA production mechanism starts to take place.[53] Large spume drops of 20 to 1000 µm[67] are then directly torn from the crests of breaking waves.[68] Spume drops are, however, often too large to have a relevant atmospheric residence time.[59] The different SSA production mechanisms are illustrated in Figure 1.5.

It should be noted that there are a few other (minor) processes that also lead to underwater air bubbles and thus produce SSAs. Vents and seeps release gases (e.g., H_2S, CH_4, H_2) and thus create bubbles that rise from the sea floor. Next, there are also some anthropogenic disturbances that create underwater bubbles such as shipping traffic and dredging. The most important additional process forming underwater bubbles is the impact of rain on the sea surface.[68,69] The impact of rain and breaking waves can, apart from forming air bubbles, also bounce back and form a sort of splash-up.[70] The majority of these so-called splash drops are, just like spume drops, often too large to have a significant atmospheric residence time.[59]

Immediately after their production, SSAs shrink through evaporation until they reach a vapor pressure that is in equilibrium with the partial pressure of water vapour in the surrounding air. The latter is alternatively expressed as the relative humidity (RH). SSAs therefore shrink or grow (continuously), when the RH decreases or increases. The size (distribution) of SSAs is commonly assessed at a RH of 80%. As demonstrated in Figure 1.6, at this RH the radius of (liquid) SSA drops (r) is just about twice as large as that of dry (solid) SSA particles (r_0). The RH in the marine boundary layer (i.e., atmosphere that is directly influenced by the ocean) generally ranges between 70 and 90%,[61] and SSAs stay in an aqueous state. When the RH, however, decreases below ±45% the dissolved salts (in the SSAs) form crystals and the remaining water is lost via evaporation. The subsequent dry aerosols have a solid state and are therefore often referred to as sea salt aerosols. In Figure 1.6, a summarizing representation of these dehydration (i.e., shrinking) and hydration (i.e., growing) processes is given. It is clear that these processes have important implications on the size and thus the atmospheric residence time of SSAs (as discussed below).

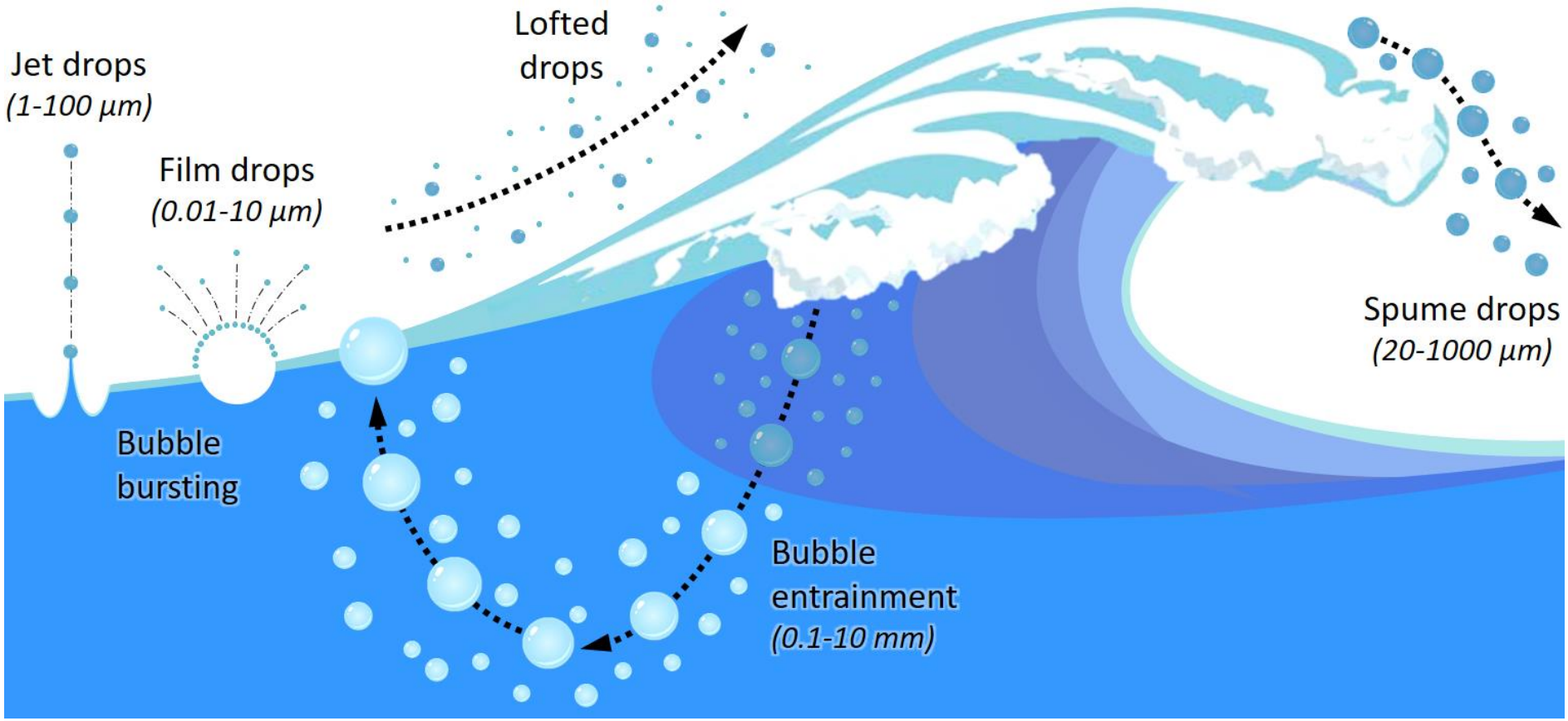

Figure 1.5: Conceptual illustration of the SSA production processes of film, jet and spume drops. Modified from Richter and Veron.[67]

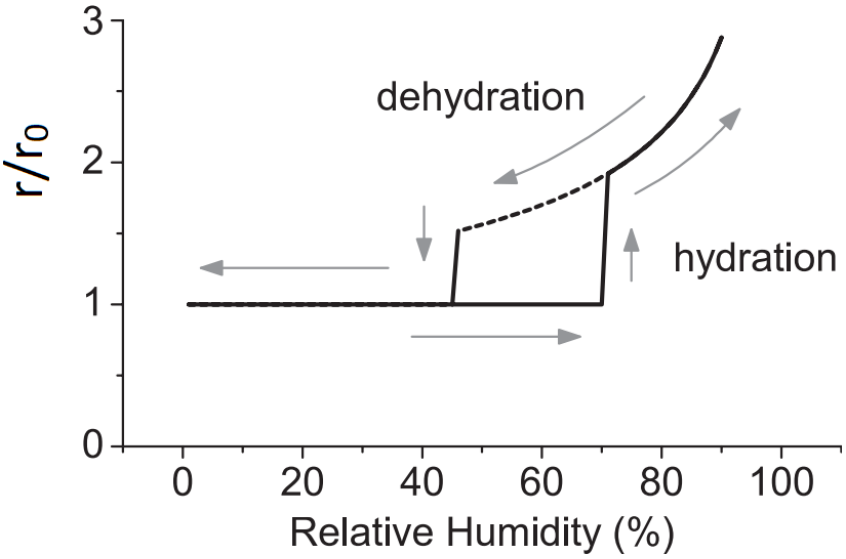

Figure 1.6: SSA particle radius (r) over the dry (solid) particle radius (r_0) as a function of the relative humidity (RH). Note that the dehydration of (liquid) drops follow a different path as compared to the hydration of dry (solid) particles. Modified from Saltzman.[61]

Film drops are by far the most abundantly produced SSA type. Due to their small size, however, they have a volume production flux which is a couple orders of magnitude lower than that of jet drops.[67] At high wind speeds, spume drops can exceed the volume production flux of the other SSA types.[67] Due to their limited production and short atmospheric retention time, spume drops have a small contribution and are often ignored.[61] The fraction of the SSA production that has a sufficient retention time and contributes appreciably to marine aerosols is denoted as the effective SSA production flux.[62] Processes keeping SSAs suspended in the air must compete against gravitational settling. Retention times are thus mainly dependent on the SSA size and the (upward) motions in the atmosphere (e.g., turbulent eddies, advection due to convection). The smallest SSAs (<0.1 µm) are mainly lost due to coagulation (see Figure 1.7). Via a strong diffusion by Brownian motion they collide with other SSAs and grow.[61] The middle sized SSAs (0.1-1 µm) have the longest atmospheric retention time and are referred to as 'accumulation mode aerosols'. They have a slower diffusion and coagulation, and are still small enough to largely overcome gravitational settling. For this size range, hygroscopic growth in clouds and subsequent rainout are the principal removal process.[61] The largest SSAs (>1 µm) are mainly lost via dry deposition by gravitational settling or inertial impaction (see Figure 1.7). Wet deposition, however, also occurs for coarse/large SSAs through impaction by rain drops or other types of precipitation.[61,71,72] Due to the variable atmospheric retention time from seconds to weeks, SSA transport ranges from very local to global distances.[61,62]

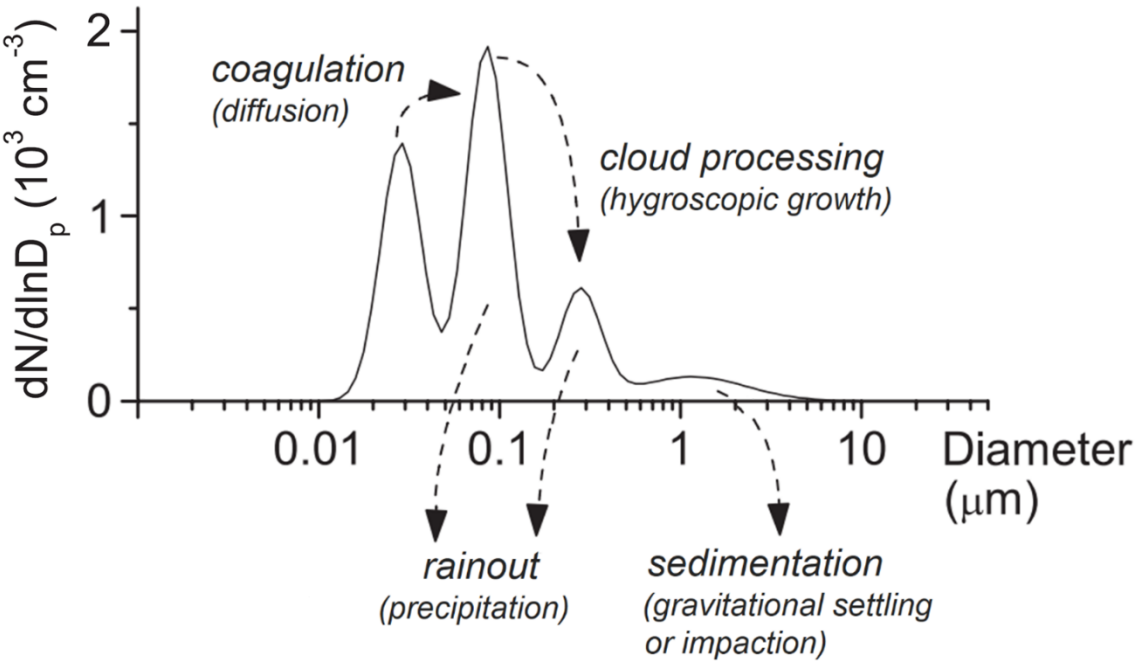

Figure 1.7: Marine aerosol number as a function of the particle size. The dominant removal processes are added per size range. Modified from Saltzman.[61]

3.2 SSA composition and enrichment processes

Although sea spray aerosols (SSAs) are, after evaporation, sometimes referred to as sea salt aerosols, they are far more complex than merely aerosolized water with a high salinity. The major dissolved components of seawater (i.e., Cl^-, Na^+, SO_4^{2-}, Mg^{2+}) were always assumed to be found at (approximately) the same concentrations in freshly emitted SSAs.[62,73] In recent years, however, studies showed that this is not always the case.[73–75] In Chapter 5 of this thesis, we discuss this matter in further detail and provide additional (environmental) evidence from our own research. Environmental sampling[76–82] and experiments with SSA generators[73,83–85] have also shown that SSAs introduce particulate matter, bacteria, viruses, algae, fatty acids, carbohydrates, sterols and proteins into the atmosphere. These aerosolized microorganisms[86] and organic compounds[73,83,87] are often found at (much) higher concentrations than in the originating subsurface water (SSW). Such so-called enrichment processes (relative to the SSW) can also occur in the sea surface microlayer (SSML).[73,86,87] The SSML is a thin film (20-400 μm) found at the air-water interface of the ocean surface which is chemically distinct from the SSW.[88,89] Magnitudes of enrichment are usually expressed as an enrichment factor (EF). Such EF_i can be quantified for both phases of i (SSML and SSA), relative to the SSW, and generally use Na^+ as an normalization factor (see eq. 1.1). Na^+ is a widely used proxy to quantify SSA densities and is considered to

have a negligible enrichment.[62] As discussed below, surprisingly little is known about the enriched aerosolization of (bioactive) organic compounds and their consequent human health effects upon inhalation.[61]

$$\mathrm{EF_i} = \frac{[\mathrm{TOX}]_\mathrm{i} \,/\, [\mathrm{Na^+}]_\mathrm{i}}{[\mathrm{TOX}]_\mathrm{SSW} \,/\, [\mathrm{Na^+}]_\mathrm{SSW}} \qquad \text{(eq. 1.1)}$$

3.3 Artificial SSA production

To examine SSA production and transfer processes for diverse compounds, and to test and optimize sampling procedures, repeatable and controllable SSA generators are required. Several systems are used as such, ranging from pressurised atomizers (Figure 1.8A), (underwater) aeration systems using sintered filters or materials (Figure 1.8B), and wave flumes or plunging water jet systems (Figure 1.8C).[90]

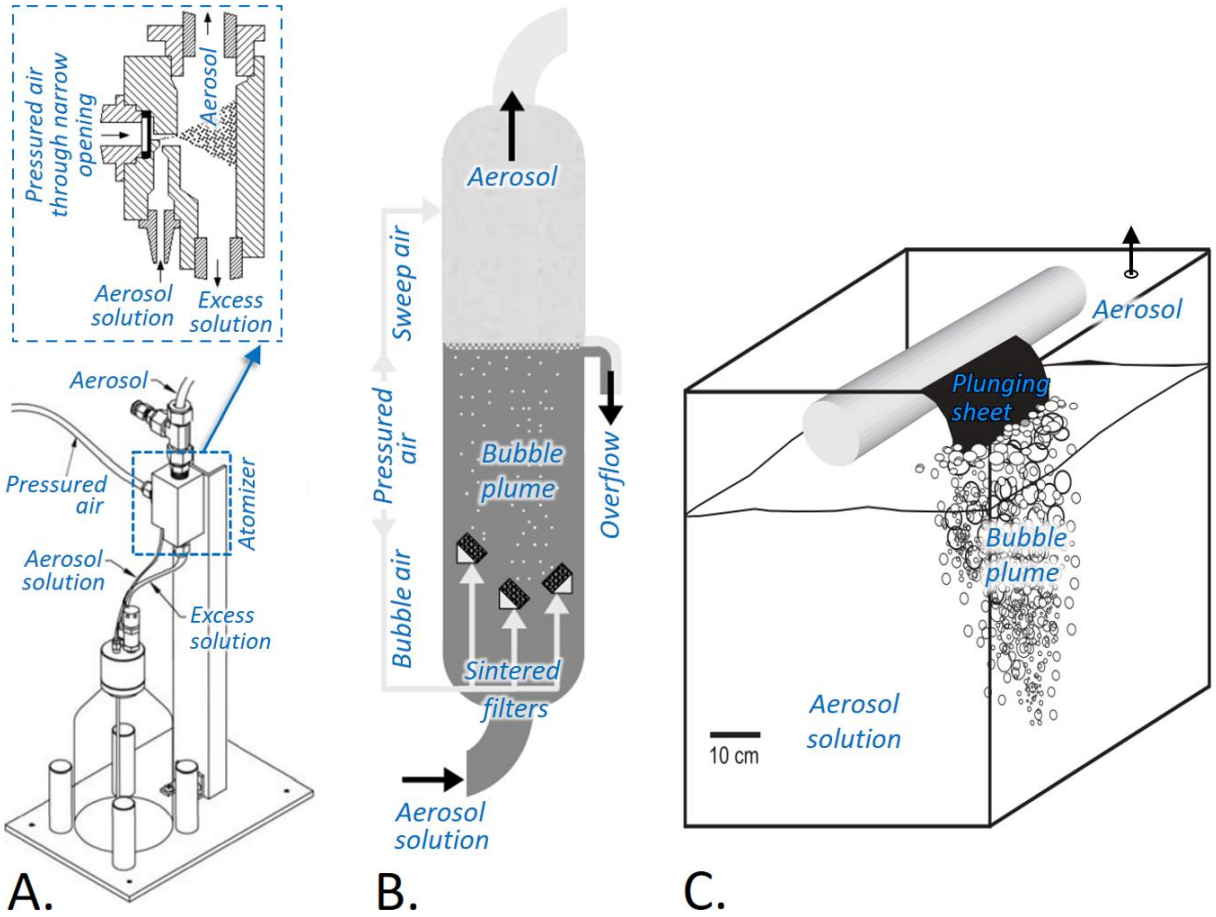

Figure 1.8: Different types of aerosol generators based on (A) pressurised atomizers,[91] (B) aeration systems using sintered materials,[92] and (C) plunging water jet systems such as the marine aerosol reference tank (MART).[90,93] The figures are adapted from TSI®,[94] Keene et al.,[92] and Callaghan et al.[93], respectively.

The latter breaking wave simulation systems (Figure 1.8C) have shown to produce the most diverse (i.e., bubbles ranging from 0.1 to 10 mm) and representative air bubble plume. [95,96] As such these breaking wave simulation systems are best suited to mimic SSA production and water-air transport processes for dissolved chemicals and particulate fractions. A relatively small plunging water jet system was introduced by Stokes et al.[90] They designed the so-called marine aerosol reference tank (MART), which in essence is a 210 L (air-closed) aquarium equipped with a system that produces an intermittent plunging water sheet (Figure 1.8C).

4 Marine bioactive compounds

A bioactive compound is a substance that has a positive or negative effect on a living organism, tissue or cell.[97] One could ask why the marine environment is so rich in bioactive compounds? Marine organisms often live in complex and hostile habitats under extreme conditions. The biosynthesis of unique secondary metabolites with a specific bioactivity therefore helps them to function and survive.[27,98] These bioactive compounds have direct positive effects (e.g., antitumor, antiproliferative, photoprotective, antioxidant, anticoagulant, anti-inflammatory) on the organism itself or negative effects (e.g., antibiotic, antiviral, antifungal, antifouling, cytotoxic, neurotoxic) on parasites, competitors or predators which threaten them.[27,99,100] The unique character and reason why many of these marine compounds cannot be found in terrestrial organisms, can be attributed to the fact that the marine environment hosts a much higher biodiversity (based on phylogeny). About half of the 36 described animal phyla for example can only be found in the marine environment, while only one phylum (i.e., *Onychophora*) is unique to the terrestrial environment.[26,101] One of the important messages of this section is: by protecting marine ecosystems, we preserve the source of undiscovered natural compounds, all of which may have a pharmacological, nutritional, agricultural and/or industrial use.

4.1 Marine pharmacology

It is obvious that we first focused on terrestrial environments to find natural compounds with a pharmacological potential. Indeed, the early cases of bioactive compounds isolated from organisms are morphine from *Papaver somniferum* (1803)[102] and the first antibiotic from *Penicillium chrysogenum (1929)*.[103] Natural drug discovery in marine

environments only slowly accelerated from the 1970's.[104] From the few ten thousand marine compounds that are currently described,[26] 21 compounds (or derivatives) have already made it to marketed drugs (Table S1.1) and at least 23 are currently being tested in clinical trials (i.e., latest development stage).[105,106] Besides having a pharmacological potential, new marine compounds also revolutionize our understanding on the biochemistry of some diseases. A large portion of the current marine drugs are used for cancer treatments (Figure 1.9 and Table S1.1). This can be attributed to the relative larger funding sources for cancer research as compared to other less occurring pathologies.[107]

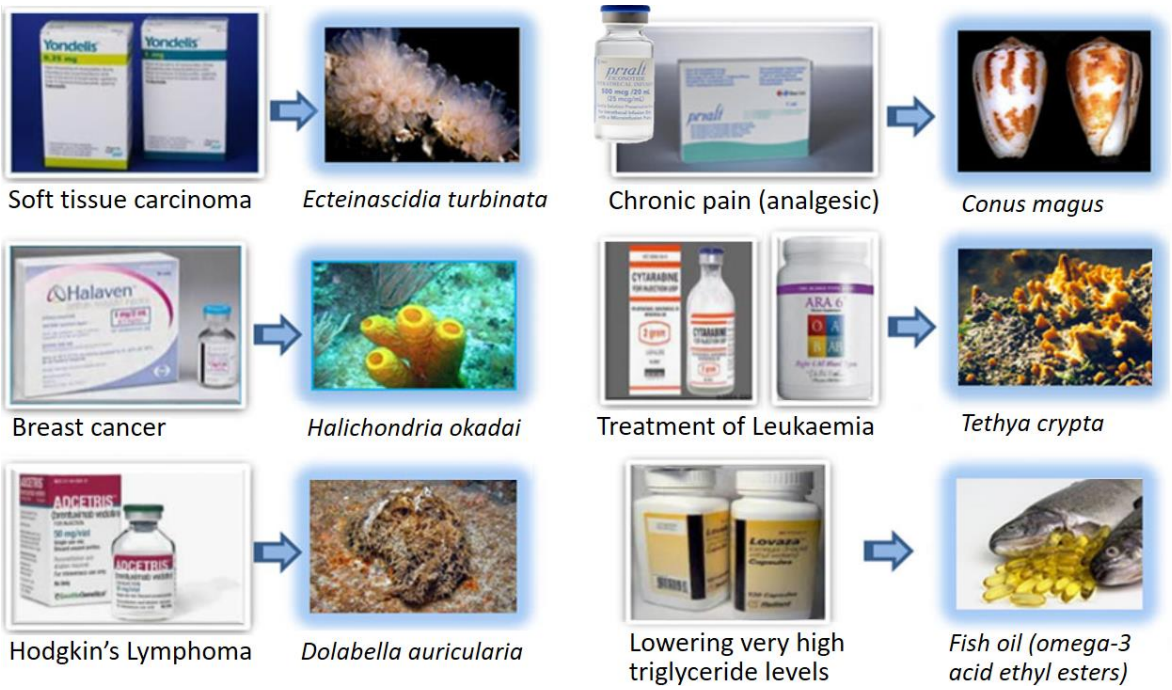

Figure 1.9: Marketed pharmaceuticals that originate from marine life. From Jaspars et al.[108]

During the past two decades, genome sequencing technologies have developed very rapidly and have revolutionized the strategies to discover natural bioactive compounds.[26,109] The classic top-down approach uses bioassays to screen for the activity of a specific biomass (extract), after which the pure bioactive compound is enriched and tracked by means of several rounds of fractionation and purification.[109] While this activity-guided approach (Figure 1.10A) simultaneously reveals the bioactivity of the new discovered compound, it misses out compounds which (1) are not targeted in these bioassays, (2) are transcriptionally silent or (3) remain undetectable (i.e., low concentrations).[109] The newer bottom-up genome mining approach (Figure 1.10B) is based on experimental evidence that the (microbial) genes encoding for the biosynthesis of a natural compound are typically clustered in a

genome as a biosynthetic gene cluster (BGC).[110] After BGC identification, using powerful bioinformatics tools, the clusters are activated using various synthetic biology tools to produce the natural compound. Although many new natural compounds have been discovered using genome mining approaches, the identification of the molecular targets and biological functions of these compounds is most challenging.[109]

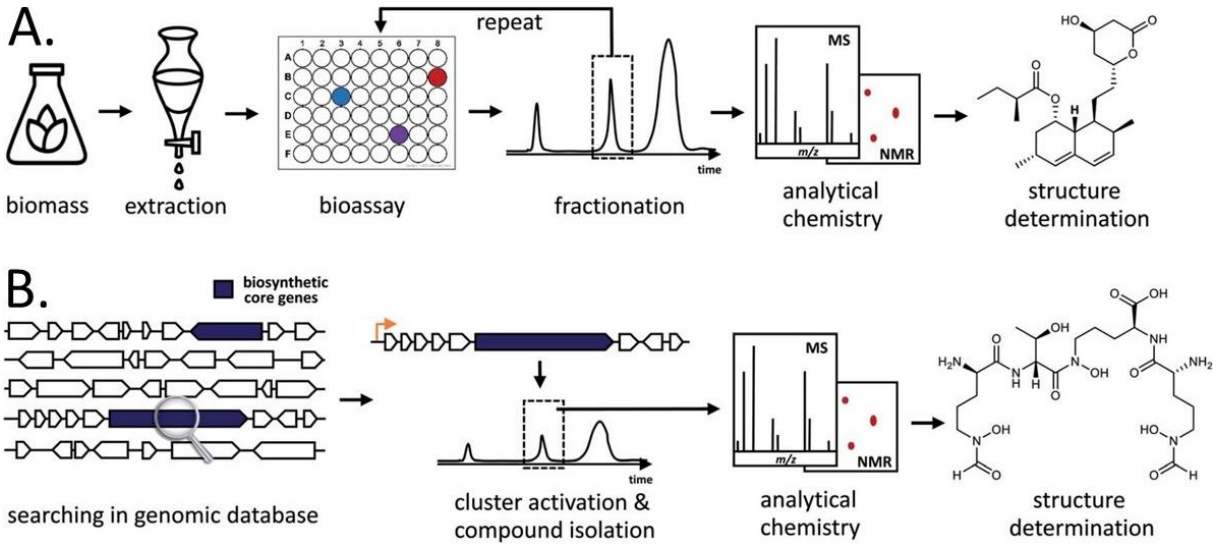

Figure 1.10: Strategies to discover natural compounds: (A) classic top-down activity-guided approach and (B) newer bottom-up genome mining approach. From Yan et al.[109]

The marine biotechnology sector is rapidly expanding as the projected value (>$6.4 billion by 2025)[105] of products and processes derived from marine compounds or marine genetic resources is enormous. Since the 'Nagoya protocol on access to genetic resources and the fair and equitable sharing of benefits arising from their utilization' (2014) exclusive private access to marine genetic resources in territorial waters is forbidden.[111] Nonetheless, by 2018 over 13,000 genetic sequences extracted from 862 marine species had been patented by companies and institutes to ensure exclusive access to potential economic opportunities.[105,112] As many unique marine species live in areas beyond national jurisdiction, the exploitation of their genetic resources are not protected. Especially species associated with deep-sea hydrothermal vents, which have unique adaptations to survive, are of particular interest.[112] Since its General Assembly resolution 72/249 of December 2017, however, the United Nations (UN) have been working on an international legally binding instrument under the UN Convention on the Law of the Sea.[113] This new treaty on the conservation and sustainable use of marine biodiversity in areas beyond national jurisdiction has a particular focus on the utilization of marine genetic resources.[105,114]

4.2 Human's natural exposure

It is clear that throughout history humans (living in coastal areas) have been exposed - via natural routes - to a large number of marine bioactive compounds. The most straightforward active exposure route is of course via the consumption of seafood. Indeed, seafood contains - among others - essential amino acids, photosynthetic pigments, vitamins, and minerals.[27] One of the most popular examples of health promoting marine compounds are n-3 fatty acids in fish. Although many health benefits of n-3 fatty acids have been reported in literature (e.g., cognitive development, mental illnesses),[115] there are also some controversies about their efficacy and benefits for certain pathologies (e.g., cardiovascular diseases, diabetes).[115–117]

Seafood can on the contrary also be contaminated with harmful chemicals (e.g., Hg, dioxins and polychlorinated biphenyls).[118] Contamination with natural compounds is predominantly caused by phycotoxins. About 100 HAB-species are classified as toxin producing algae.[119] These phycotoxins have very diverse structures and bio-activities, and can be extremely potent.[120] In 2000, Van Dolah[121] reported an global incidence of >60,000 intoxications year^{-1} and an average mortality of 1.5% over all phycotoxin seafood poisoning syndromes (see Table 1.1). The reported global occurrence of (toxic) HABs has also increased in the last decades.[122,123] The increase of HABs are most often linked to several anthropogenic activities such as fisheries, aquaculture, shipping and eutrophication. Indeed, fisheries have depleted the fish stocks of many carnivorous fish[124] resulting in increasing populations of small planktivorous fish and thus a decrease in the phytoplankton grazing pressure (by zooplankton).[125] Second, some HAB species have been dispersed over the world as alien species through shellfish seeding operations and the ballast water of ships.[122,123,126] A third important factor linked to an increased frequency of HABs is coastal eutrophication.[123,127,128] The increased concentrations of the two most limiting nutrients, i.e., nitrogen and phosphorus, by the use of fertilizers does not only enhance the general primary productivity, it can also shifts nutrient ratios relative to silicon. Non-siliceous phytoplankton species can therefore be favored in such conditions and induce (harmful) blooms.[123] Until this year's paper of Hallegraef et al.,[129] climate change was also assumed to enhance many factors (e.g., seawater temperatures, surface stratification, dissolved CO_2 and pH) which could favor the productivity of certain algal (harmful) species and increase HABs worldwide.[125,130] Hallegraef et al.,[129] however,

concluded that there is no global trend in the occurrence of HABs that can be discerned from that of the increased observational efforts. In addition, methodologies to detect HABs and their phycotoxins in different marine matrices (e.g., seawater,[131] algae,[132] seafood[131,133,134]) have improved substantially over the last decades. There are not only much more reference materials available for phycotoxins, the tremendous improvements in analytical techniques like liquid chromatography-mass spectrometry (LC-MS) induce among others a faster analysis with lower operating costs and a higher sensitivity, specificity, accuracy, and precision.[135]

As discussed above, human exposure to marine compounds can also occur via the inhalation of SSAs, i.e., a more continuous and passive exposure route for coastal populations. Research on the aerosolization of marine bioactive compounds is limited and has mainly been focused on the phycotoxins that induce respiratory syndromes, i.e., brevetoxins (PbTxs)[20,21] and ovatoxins (OVTXs).[22] These respiratory syndromes include among others coughing, wheezing, irritation, airflow reduction and chest tightness.[136–138] The latter algal toxin or phycotoxin is produced by the micro-algal species *Ostreopsis ovata* and has been suspected to be the causal agent for a respiratory syndrome during HABs in the Mediterranean Sea.[139] Airborne exposure to these two aerosolized phycotoxins induce respiratory distress (i.e., nose/throat irritation, coughing, wheezing, chest tightness, shortness of breath), especially in vulnerable groups (i.e., people with underlying respiratory conditions).[21] Many other toxin-producing algae are, however, non-severe blooming species,[140] and the phycotoxin content (i.e., proxy for production) in HAB-species is certainly not lower for PbTxs (14-30 pg $cell^{-1}$)[137] as compared to other major phycotoxins like okadaic acid (OA; 6.7-15.8 pg $cell^{-1}$),[141] dinophysistoxin-1 (DTX-1; 0.12-0.39 pg $cell^{-1}$),[141] or yessotoxin (YTX; 2.9-33.6 pg $cell^{-1}$).[142,143] The air concentrations of these aerosolized phycotoxins (and other marine chemicals) are therefore expected to (much) lower than the PbTx (1.3-180 ng m^{-3})[23,24,144] and OVTX (2.4 ng m^{-3})[22] concentrations measured during HABs. Many marine compounds - including some phycotoxins[145] - are also linked to positive therapeutic effects. Moore's biogenics hypothesis described above is therefore not that strange.

Table 1.1: Overview of the different phycotoxin seafood poisoning syndromes, together with their main causal toxins, producers and clinical manifestations. Based on Botana,[146] De Rijcke,[147] Minns[148] with additional information.[145,149,150] More physico-chemical information on the individual phycotoxins can be found in found in Table 1.2.

Phycotoxin seafood syndrome	Main toxin(s)	Main producer(s)	Clinical manifestations
Diarrhetic shellfish poisoning (DSP)	Okadaic acid (OA), Pectenotoxin (PTX), Dinophysistoxin (DTX)	*Dinophysis spp., Prorocentrum spp.*	Acute gastroenteritis
Amnesic shellfish poisoning (ASP)	Domoic acid (DA)	*Pseudo-nitzschia spp., Nitzschia spp.*	Gastroenteritis, neurological damage, anterograde memory disorder, death
Neurotoxic shellfish poisoning (NSP)	Brevetoxin (PbTx)	*Karenia spp.*	Circumoral paresthesias, ataxia, gastroenteritis, death
Paralytic shellfish poisoning (PSP)	Saxitoxin (STX), Gonyautoxin (GTX)	*Alexandrium spp., Pyrodinium spp., Gymnodinium spp.,*	Paresthesias of face and extremities, paralysis, respiratory failure, death
Hepatotoxic shellfish poisoning (HSP)	Microcystin (MC), Nodularin (NOD), Cylindrospermopsin (CYN)	*Microcystis spp., Anabaena spp., Cylindrospermopsis spp.*	Kidney/liver damage, ear/eye irritation, gastroenteritis, flu-like symptoms, death
Ciguatera fish poisoning (CFP)	Ciguatoxin (CTX), Maitotoxin (MTX)	*Gambierdiscus spp.*	Gastroenteritis followed by neurologic symptoms
Spiroimine shellfish poisoning (SSP)	Spirolide (SPX), Gymnodimine (GYM), Pinnatoxin (PnTX)	*Alexandrium spp., Karenia spp., Vulcanodinium spp.*	Fast neurological symptoms, respiratory failure, death
Azaspiracid poisoning	Azaspiracid (AZA)	*Azadinium spp., Protoperidinium spp.*	Gastroenteritis
Palytoxin poisoning	Palytoxin (PLTX), Ovatoxin (OVTX)	*Ostreopsis spp.*	Gastroenteritis, spasms, cardiac alterations, respiratory failure, death
Yessotoxin poisoning	Yessotoxin (YTX), Homoyessotoxin (hYTX)	*Protoceratium spp., Lingulodinium spp., Gonyaulax spp.*	Unclear

Table 1.2: Overview of the main North Sea phycotoxins that were used and/or investigated in this PhD research.

Phycotoxin	Reported status in the North Sea	Mw (Da)	log Kow	Chemical structure
Okadaic acid (OA)	DSP toxins (i.e., OA and DTXs) are the dominant phycotoxins in the North Sea.[151–153] Their concentrations in phytoplankton samples reach up to 0.8 µg kg^{-1} and in shellfish up to 60 µg kg^{-1} (wet weight) [151]	805.0	3.4	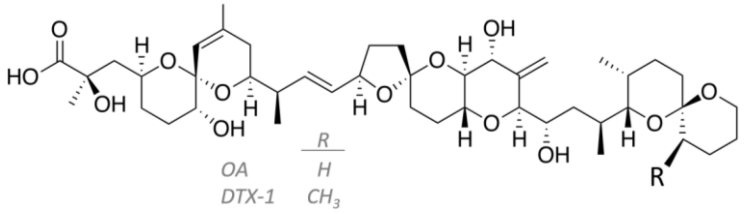
Dinophysistoxin-1 (DTX-1)		819.0	3.8	
Yessotoxin (YTX)	YTXs concentrations in phytoplankton samples reach up to 0.3 µg kg^{-1} and in shellfish up to 170 µg kg^{-1} (wet weight). [151]	1143.4	3.4	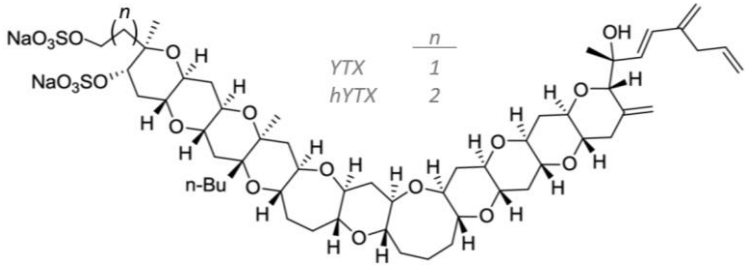
Homoyessotoxin (hYTX)		1157.4	3.7	
Azaspiracid-1 (AZA-1)	Particulate concentrations range from a few pg to 1.4 ng AZA per L of seawater in the northern areas of the North Sea.[154]	842.1	3.7	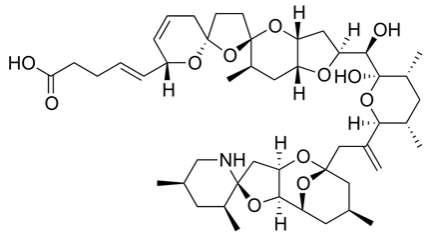
Brevetoxin-2 (PbTx-2)	The occurrence of PbTxs or their producer (*Karenia brevis*) have never been reported in the North Sea.	895.1	3.7	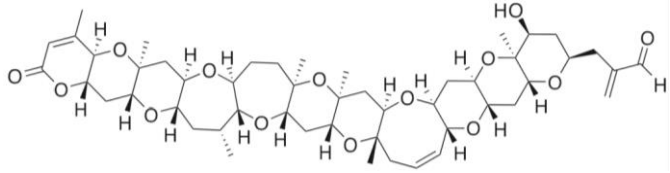
Domoic acid (DA)	DA is strongly excreted in the water (± 80%) by *Pseudo-nitzschia sp*. Concentrations peak in Spring (≤263 pg mL^{-1}) and are lower but still high (>100 pg mL^{-1}) in Autumn.[155]	311.3	-1.3	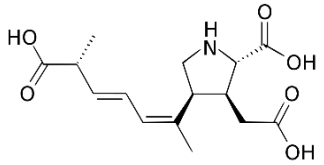

5 Thesis rationale, objectives and outline

Despite the common believe that coastal air induces beneficial health effects, the composition of SSAs has mainly been investigated from a meteorological or biogeo-chemical perspective and not in a health context. Research on the aerosolization and airborne-mediated effects of marine bioactive compounds has been scarce and mainly focused on the two known harmful cases of phycotoxins inducing respiratory syndromes (i.e., brevetoxins (PbTxs) and ovatoxins (OVTXs)). The need to investigate such harmful effects seems to have suppressed the interest to examine potential beneficial effects of coastal environments, which apparently are taken for granted.

The **main objective of this PhD thesis** was to perform an exploratory assessment of the airborne exposure to and potential health effects of marine compounds in SSAs. As illustrated above in the conceptual dose response curve, of this chapter's abstract art, we intended to include both the harmful and beneficial sides of airborne exposure to SSAs. Human health effects can be induced via numerous modes of action. Here we started to investigate potential **beneficial effects** of SSAs in the light of the above mentioned **biogenics hypothesis** (see section 2 and Figure 1.4). Conversely, to investigate **harmful effects** we performed research on the only group of marine compounds known to induce respiratory syndromes: **phycotoxins**. There are only two phycotoxins (PbTxs, OVTXs) that have been detected and quantified in SSAs. Other globally occurring phycotoxins, which are also frequently found in the North Sea, have never been examined on their aerosolization capacity or their potential airborne health effects. This is a crucial knowledge gap in the context of the OHH research field, certainly because some phycotoxins have also been linked to beneficial health effects.

It is clear that this exploratory PhD research could only be performed using an **interdisciplinary approach**. Setting up collaborations with other laboratories and institutes, to perform state-of-the-art chemical analysis, coastal sampling campaigns, and in vitro studies, was thus one of the crucial first steps. Indeed, we opted to assess potential health effects using **in vitro studies** with lung cells as a model for the human respiratory system. To investigate aerosolization processes and exposure scenarios, on the other hand, we constructed a **SSA generator**. Using both these effect and exposure model systems, in combination with some existing and newly developed methodologies, we addressed the following first set of **research questions:**

- Q1: *Can low doses of phycotoxins induce negative health effects via SSAs?* ***(Chapter 2)***
- Q2: *Can phycotoxins induce positive health effects via the mTOR pathway, as suggested by the biogenics hypothesis?* ***(Chapter 2)***
- Q3: *Are these phycotoxins easily aerosolized via sea spray and which factors affect these water-air transfer processes?* ***(Chapter 3)***
- Q4: *What are the phycotoxin air concentrations occurring at the Belgium coast, and do they pose a potential risk or benefit to human health?* ***(Chapter 3)***

The above questions can provide valuable answers demonstrating the basic principles of the biogenics hypothesis. It is important to underline that the performed research may provide supporting evidence, but will – at this stage – not prove/disprove this hypothesis. In the second stage of this PhD research we aimed to improve the environmental realism of this kind of OHH research. To this end, our first approach was to use natural SSA sample extracts in our in vitro effect studies. By measuring the differential gene expression in the exposed lung cells we analyzed an endpoint giving a general overview of the induced effects. Secondly, we analyzed a one-year series of natural SSA samples and targeted compounds with well-known effects on the respiratory system. As such, we aimed to answer this next set of **research questions:**

- Q5: *Which effects, after respiratory exposure, can marine compounds in SSAs have at the molecular level?* ***(Chapter 4)***
- Q6: *How do these effects of natural SSAs, at a molecular level, relate to the effects induced by specific phycotoxins?* ***(Chapter 4)***
- Q7: *Which marine bioactive compounds are present in SSAs at concentrations that can influence human health?* ***(Chapter 5)***
- Q8: *Are the coastal air concentrations of these compounds related to the ecological and/or meteorological state of the marine environment?* ***(Chapter 5)***

In the final part of this thesis **(Chapter 6)** the main findings and conclusions of this PhD research are reviewed and important knowledge gaps are identified. Next the current and future human health risks and benefits of SSA exposure are assessed. Finally, perspectives and recommendations for future research are formulated. These perspectives are not only important from a scientific point of view, they will also help to further unravel the (main) question of this research area: Do marine compounds in coastal air affect or improve human health via inhalation of SSAs?

Chapter 2

Potential health effects of phycotoxin exposure via sea spray aerosols

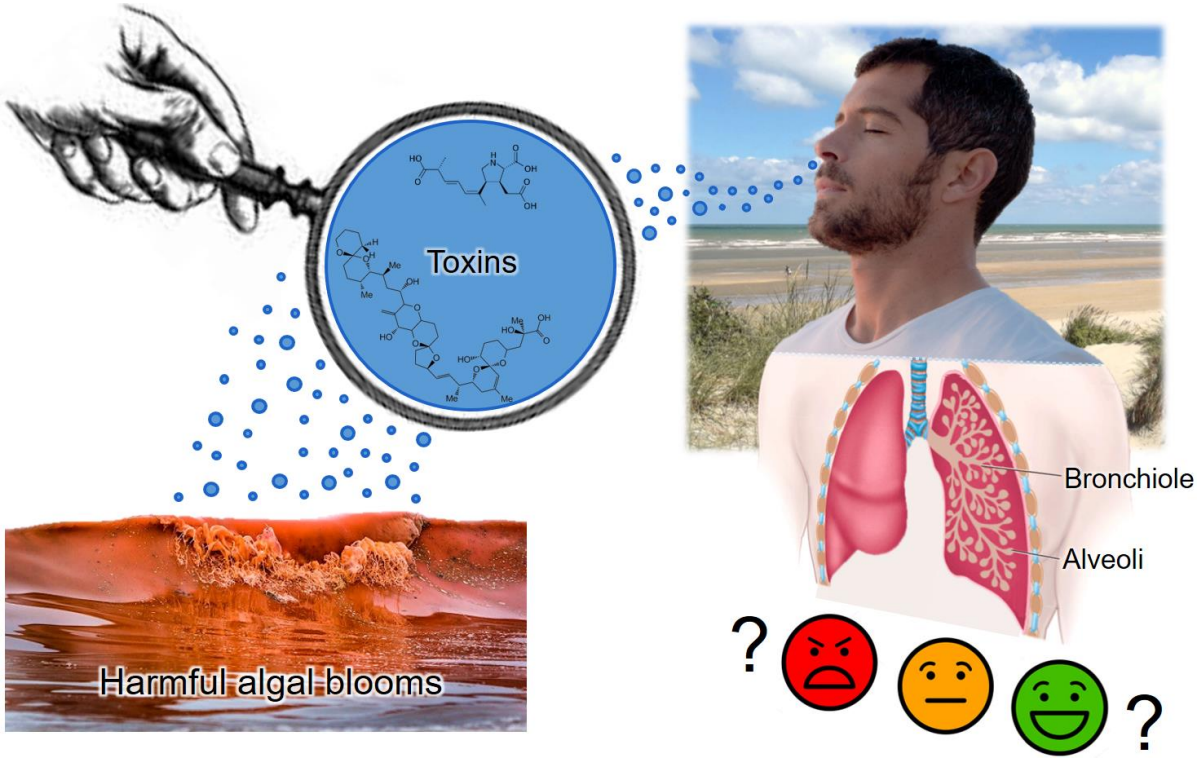

Redrafted from:

Van Acker, E.; De Rijcke, M.; Asselman, J.; Beck, I. M.; Huysman, S.; Vanhaecke, L.; De Schamphelaere, K.; Janssen, C. Aerosolizable Marine Phycotoxins and Human Health Effects: In Vitro Support for the Biogenics Hypothesis. Marine Drugs ***2020****, 18, 1–13.*

Chapter contents

Abstract

Airborne exposure to marine phycotoxins is of increasing concern. Inhalation of sea spray aerosols (SSAs) during harmful algal blooms (HABs) of *Karenia brevis* and *Ostreopsis ovata* blooms induces respiratory distress among others. The biogenics hypothesis, however, suggests that regular airborne exposure to natural products is health promoting via a downregulation of the mechanistic target of rapamycin (mTOR) pathway. Until now, little scientific evidence supported this hypothesis. The current explorative in vitro study investigated both health-affecting and potential health-promoting mechanisms of airborne phycotoxin exposure, by analyzing cell viability effects via cytotoxicity assays and effects on the mTOR pathway via western blotting. To that end, A549 and BEAS-2B lung cells were exposed to increasing concentrations (ng L^{-1} - mg L^{-1}) of (1) pure phycotoxins and (2) the extract of a laboratory-generated SSA containing homoyessotoxin (hYTX). Unlike the other phycotoxins, the examined yessotoxins (YTXs) initiated mechanisms which did not lead to direct cell mortality. The observed partial effects of YTXs on the cell viability can be attributed to the inhibition of cell growth and induction of apoptosis, both protective cell mechanisms that are linked to a downregulated activity of the mTOR pathway. Indeed, we showed that YTXs can downregulate the mTOR pathway and could therefore, in the light of the biogenics hypothesis, induce positive instead of negative health effects. Conversely, we found that okadaic acid (OA) and brevetoxin-2 (PbTx-2) initiated mechanisms leading to the direct mortality of the exposed lung cells. While PbTx-2 is known to induce a respiratory syndrome via SSAs, the producing algal species (*K. brevis)* is only dominant in the Gulf of Mexico. OA on the contrary is the primary marine phycotoxin in the North Sea and could potentially also induce negative effects upon airborne exposure to a sufficiently high dose. To perform a first risk or benefit assessment for OA and YTXs, reliable information on their potential airborne exposure is needed. When this study was performed, however, no information on the aerosolization or potential coastal air concentrations was available for these phycotoxins.

1 Introduction

Toxin-producing marine HAB species have received considerable attention since the 1970s. Algal toxins or phycotoxins, are best known for the seafood poisoning they may cause.[121] HAB events in the Gulf of Mexico and the Mediterranean Sea have, however, also caused respiratory distress and other human health conditions. In these cases, elevated concentrations of brevetoxins[156] and ovatoxins[22] were present in sea spray aerosols (SSAs). Such harmful exposures to aerosolized phycotoxins are rather rare events, requiring a combination of favorable weather conditions for SSA production and a severe toxin-producing HAB. Many toxin-producing algae, however, are non-severe blooming species[140] and most HABs are ephemeral phenomena. Air concentrations of aerosolized phycotoxins are therefore generally low. It has been suggested that these background concentrations could induce positive instead of negative human health effects.[46] Recent research interest into the positive bioactivity of some phycotoxins, like yessotoxin (YTX), also point to their potential therapeutic use.[145,157]

Throughout humankind's history, exposure to seawater and coastal air has been linked to positive health effects.[8,158] Fairly recently, epidemiological studies have started to reveal a coastal proximity health effect.[32–36] As discussed above in Chapter 1 section 2, several hypotheses have been raised to explain why coastal residents are – on average – healthier. Moore's biogenics hypothesis[46] is one of the central ideas which is investigated throughout this thesis. He suggested that the observed coastal health effects are caused by the regular exposure to natural compounds in SSAs, which downregulate the activity of the phosphatidylinositol-3 kinase/protein kinase B/mechanistic target of rapamycin (PI3K/Akt/mTOR) cell signaling pathway; hereafter referred to as the mTOR pathway. This is based on the fact that the augmented activity of this kinase pathway is related to multiple pathological conditions (e.g., cancers, type 2 diabetes, neurodegenerative diseases)[49] while inhibition or downregulation of this pathway has been associated with anti-cancer therapies and positive health effects.[49]

In this chapter, using explorative in vitro experiments, we aimed to investigate the potential health effects of airborne exposure to marine phycotoxins. Adverse effects were evaluated through the assessment of cell viability effects using cytotoxicity assays. The potential downregulation of the mTOR pathway was evaluated via western

blotting methods. Furthermore, given the importance of the mTOR pathway in both normal and cancer cells, we used both normal (BEAS-2B) and adenocarcinoma (A549) human lung cells in our study. We first studied the effects of pure phycotoxins, and subsequently the effects of homoyessotoxin (hYTX) in a more realistic SSA matrix.

2 Materials and methods

2.1 Chemicals and extracts

Yessotoxin (YTX) and homoyessotoxin (hYTX) were purchased as certified reference material (CRM) from the National Research Council Canada. All other toxins were analytical-grade products and dissolved, depending on their lipophilic properties, in 50 or 100% methanol or ethanol. Okadaic acid (OA) was purchased from LC Laboratories, domoic acid (DA) at Sigma-Aldrich (Saint Louis, MO, USA), brevetoxin-2 (PbTx-2) from MARBIONC, and Torkinib (PP242) – a known mTOR kinase inhibitor – from MedChem Express. The structural formulas of the phycotoxins are available in Table 1.2. These phycotoxins were selected based on: (1) potential presence in the North Sea (PbTx-2 was added as a well-studied reference compound), (2) tendency for aerosolization (less relevant for hydrophilic toxins such as DA), and (3) purchasability of chemical standards and algal strains producing the phycotoxins.

An laboratory-generated SSA extract, containing hYTX, was generated using a marine aerosol reference tank (MART). This MART was constructed as described by Stokes et al.[90] The MART tank was filled with artificial seawater (i.e., L1-medium; Annex III section 1) and inoculated with the dinoflagellate *Protoceratium reticulatum* (SCCAP K-1474) at a density of 10^6 cells L^{-1}. The used methods to culture these algae are described in detail in Annex III section 1. A prior chemical analysis, following the exact procedures described by Orellana et al.,[132] showed that this algal strain primarily produced hYTX. As hYTX is structurally similar to YTX, i.e., one functional group contains an additional methylene bridge (-CH2-) (see Table 1.2), its amphiphilic properties and tendency towards sea spay aerosolization are most likely similar. The SSAs generated in the MART were sampled in triplicate on Whatman® QM-A quartz microfiber filters (Ø 47 mm; see Chapter 3 section 2.3 for more details), enclosed in stainless steel in-line filter holders (Pall Corporation), over which an airflow of 9 ± 1 L min^{-1} was applied during 16 h using vacuum pumps (LABOPORT®). These

SSA filter samples were extracted and analyzed for their Na^+ and phycotoxin (i.e., hYTX) contents following the dedicated methods described in Chapter 3 (sections 2.3-2.5). The filter extracts were subsequently stored at -20°C until they were used as a treatment for our in vitro experiments. This laboratory-generated SSA treatment, which is further referred to as the lab SSA (extract), thus contained a known hYTX concentration and a mixture of other aerosolizable compounds (with unknown concentrations). Therefore it represents a more realistic exposure scenario as compared to dosing pure phycotoxins.

The Na^+ analysis in the lab SSA samples determined the SSA density (i.e., the collected SSA per volume of air), and provided information on the amount of collected SSA that was dosed to the lung cells. As such, the highest concentration treatment of the lab SSA (extract) contained 2.8 µg Na^+ $well^{-1}$. This information is also used below in Chapter 4, where this lab SSA extract was also used.

2.2 Lung cell culturing

To assess the potential effects of airborne exposure to marine phycotoxins, two epithelial lung cell lines were used in a series of in vitro experiments: The adenocarcinoma alveolar basal A549 cell line and the normal bronchial BEAS-2B cell line. As inhibition or downregulation of the mTOR pathway has been associated with anti-cancer therapies and positive health effects, we indeed opted to use both a normal (BEAS-2B) and adenocarcinoma (A549) human lung cell line in our study. As such, these cell lines served as models for (both normal and malignant) exposed lung tissues and, more generally, the lower respiratory tract. The choice to use cell lines originating from the lower respiratory tract is discussed in Annex II section 4. These historical cell lines were originally set up in collaboration with the laboratory of experimental cancer research at Ghent University. Culture methods and conditions were identical for both cell lines, and only differed in the splitting ratio (see below). The cells were grown in Dulbecco's modified eagle medium (DMEM), including phenol red, 10% heat-inactivated fetal bovine serum (FBS), 100 U mL^{-1} penicillin, and 100 µg mL^{-1} streptomycin, at 5% CO_2, 37 °C, and >95% relative humidity. Confluent cultures were sub-cultured, using 0.5% Trypsin–EDTA, and split twice a week in a ratio of 1:6 (BEAS-2B) or 1:8 (A549), or used in the experiments as explained below. Throughout our research, the passage number of the lung cell cultures never exceeded a value of 50.

2.3 MTT cell viability assays

To assess the effects of phycotoxins on the viability of cultured lung cells, MTT concentration–response assays were conducted. Upon trypsinization, cells were re-suspended in DMEM (i.e., medium) with the additives as described above, but without phenol red and only 5% of FBS. The cell suspension was diluted and seeded in 96-well plates at 3000 cells well^{-1} in 75 µL of medium. 10 h after incubation, adhered cells were exposed to phycotoxins (i.e., YTX, hYTX, OA, PbTx, DA), added as single substances in 25 µL of medium. Six replicates were used per concentration treatment. Negative, positive, and solvent control treatments were included in each experiment. For the negative control treatments, nothing was added to the 25 µL of medium, and for the positive control treatments, 3% SDS was added. The solvent control contained the same methanol or ethanol concentration as that used in the highest phycotoxin concentration treatments (maximum 2.9% ethanol). After a 43 h exposure period, the cell morphology and confluence were visually assessed and photographed using an inverted microscope (100× magnification). Then 40 µL Dulbecco's phosphate-buffered saline (D-PBS; see Annex II section 1) containing 5 mg mL^{-1} of 3-(4,5-dimethylthiazol-2-yl)-2,5-diphenyltetrazolium bromide (MTT) was added to each well. Next plates were wrapped in aluminum foil and incubated for another 2.5 h. Finally, 100 µL of 10% SDS/0.01 M HCl solution was added in each well and the plates were analyzed, after an overnight incubation at 20 °C, using a spectrophotometer (Multiskan Ascent, Thermo Labsystems) at 570 nm and a reference wavelength of 650 nm.

2.4 SDS-PAGE and western blotting

SDS-PAGE and western blotting were used to assess the mTOR pathway activity of exposed lung cells, allowing us to study the potential positive health effects of phycotoxins as suggested by the biogenics hypothesis. Since the phosphorylation of mTOR has been shown to be a less reliable marker,[52,159] we opted to evaluate two downstream phosphorylation targets of mTORC1 (i.e., S6RP, 4E-BP1) instead of the protein itself.[52,159] Next to the two downstream targets of mTORC1, an important upstream kinase in the mTOR pathway (i.e., Akt) was also analyzed via SDS-PAGE and western blotting. The cell exposure setup to analyze the mTOR pathway activity was largely comparable to that used for the MTT viability assays. Cells were seeded in 6-well plates, using 3 mL of DMEM (i.e., medium) with the additives as described

above, at a density of 320,000 and 425,000 cells well^{-1} for the A549 and BEAS-2B cell lines, respectively. 10 h after incubation, phycotoxins (i.e., OA, PbTx, YTX, hYTX, and hYTX in the lab SSA extract) were first diluted in methanol to 50× the desired concentration and consequently added in a volume of 60 µL well^{-1} (i.e., in 3 mL of medium). The test concentrations ranged from 10^{-6} µg L^{-1} up to (approximately) the EC_{10} values reported for the cell viability assays (see Table S2.1). Three replicates were used per phycotoxin treatment. Negative (i.e., 2% methanol) and positive (i.e., 0.3 µM Torkinib/PP242) control treatments were included in every experiment. The solvent control was identical to the negative control (i.e., one and the same treatment), as all treatments contained the same methanol concentration (i.e., 2%).

After a 43 h exposure period, protein cell extracts were prepared and analyzed with SDS-PAGE and western blotting procedures, as discussed in SI (Annex II section 1). SDS-PAGE was performed with 12% acrylamide precast gels (Bio-Rad, Hercules, CA, USA) and blotting with PVDF membranes (Bio-Rad, Hercules, CA, USA). Western blotting was first performed with phospho-specific antibodies directed against phospho-4E-BP1 (Ser65), phospho-S6RP (Ser240/244), and phospho-Akt (Ser473). After analysis with a Chemidoc Imaging CCD-camera (Bio-Rad), antibodies were stripped from the membranes and the procedure was repeated with non-phospho-specific antibodies directed against 4E-BP1, S6RP, and Akt. All primary antibodies were rabbit antibodies used at a 1/1000 dilution. The secondary antirabbit immunoglobuline G (IgG), HRP-linked antibody was used at a 1/3000 dilution. All antibodies were purchased from Cell Signaling Technologies.

2.5 Data processing, regression and statistics

The raw data of the MTT assays consisted of absorbance measurements. Using the RStudio software, cell viability dose response curve (DRC) models were fitted to these data. The exact procedure of how the raw absorbance data were transformed to cell viability values and how the final DRC models were made is explained in SI (Annex II section 2). Consequently, the effect concentrations for a 10% (EC_{10}) and 50% (EC_{50}) decrease in cell viability were derived from the DRC models.

The raw data of the western blot analyses were image-derived chemiluminescent response values. We were specifically interested in the down or upregulation in the phosphorylation of the three targeted proteins. To that end, the ratio of the phospho-

specific and non-phospho-specific signals was divided by the ratio of these measurements of the corresponding negative control (on the same blot) and subtracted with 1. In this way, for all treatments and examined proteins, a down (<0%) or upregulation (>0%) in phosphorylation, as compared to the negative control (=0%), was determined. Data within each treatment were checked for normality with a Shapiro–Wilk test ($p>0.05$). Subsequently, one-sample t-tests were performed to check for significant differences ($p<0.05$) with the negative control (=0%).

3 Results

3.1 Cell viability effects

Two different cell lines were used in this study: adenocarcinoma alveolar (i.e., A549) and normal bronchial (i.e., BEAS-2B) cells. The dose response curves (DRCs) for both cell lines and for the different phycotoxins are plotted in Figure S2.1 (supportive information). From these results, it is clear that the two cell lines are comparable in sensitivity towards these phycotoxins. Therefore, we focused on the results of the A549 cell line. All the data and results for the BEAS-2B cells are available in SI (Annex II).

Figure 2.1 gives a representative overview of the main cell viability results of the MTT assays performed with the A549 cell line and the five different phycotoxins. To illustrate the goodness of fit of the DRCs, the same graph containing all data points is available in SI (Figure S2.2). All toxins, except domoic acid (DA), exerted a negative effect on cell viability. The lowest cell viability effect concentrations were found for YTX and hYTX. Contradictory to the other examined toxins, these two YTXs only induced a partial cell viability decrease at the highest test concentrations. OA and PbTx-2 induced complete mortality, but their effects started at higher test concentrations as compared to the YTXs. A results summary of all MTT assays for both cell lines, containing the derived EC_{10} and EC_{50} values and DRC parameter estimates, is given in Table S2.1.

To test the effect of the use of different starting cell densities, part of the MTT assays testing YTX were performed at 8000 cells $well^{-1}$. This was performed using only the A549 cells, as from previous experimental results, we would not expect a different outcome for the BEAS-2B cells. A comparison between these two starting cell densities

(i.e., 3000 vs. 8000 cells well^{-1}) is made in Figure S2.3. Again, it is clear that the difference in effects due to a different starting density (3000 vs. 8000 cells well^{-1}) is smaller than the variability between successive experiments.

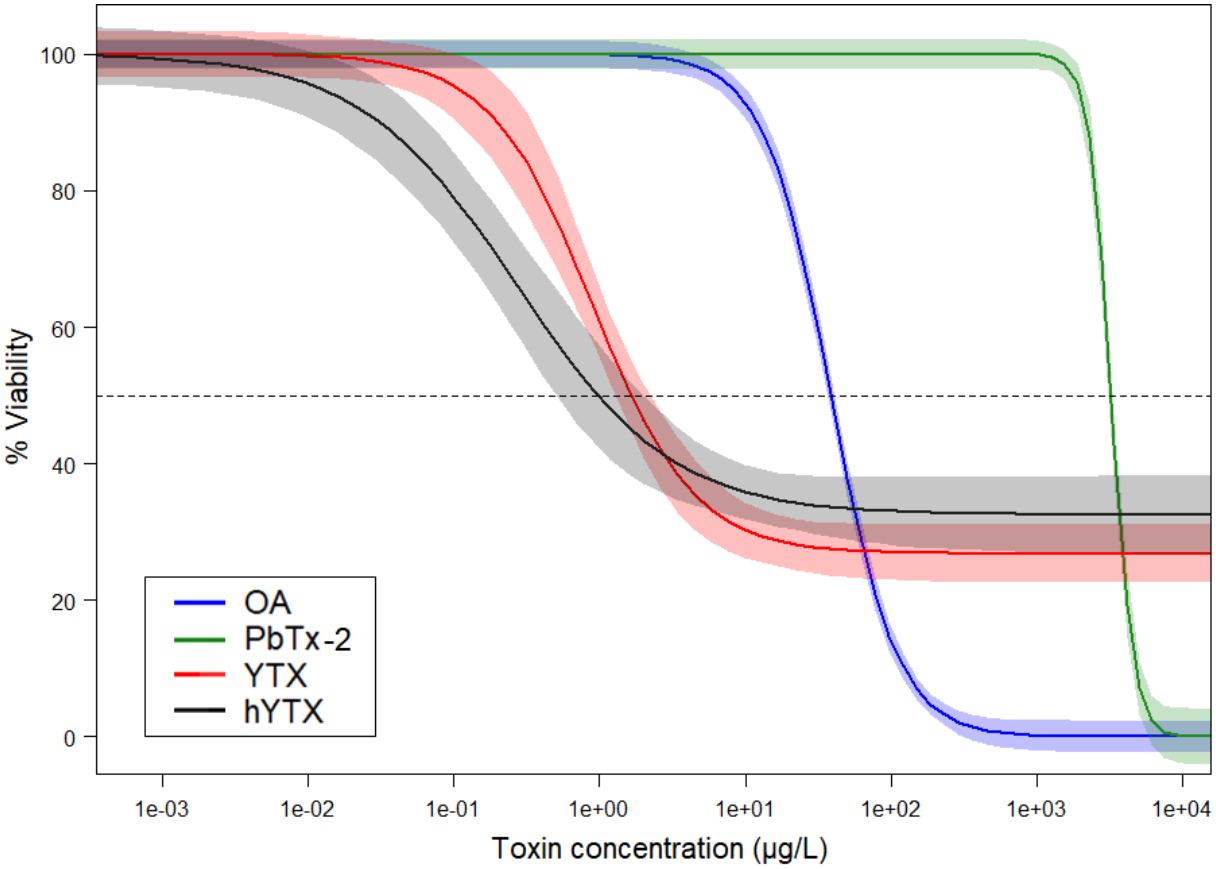

Figure 2.1: Log-logistic dose response models for four phycotoxins derived from the results of MTT cell viability assays performed on A549 cells over an exposure period of 43 h. The different phycotoxins are okadaic acid (OA), brevetoxin-2 (PbTx-2), yessotoxin (YTX), and homoyessotoxin (hYTX). The light-colored bands are 95% confidence bands. The start cell density was 3000 cells well^{-1} for all experiments. Parameter estimates (i.e., estimate ± SE) for all dose response models are available in Table S2.1 under experiment 3-A549 and 9-A549. Note that the DRC models were fitted using all test concentrations, including lower concentrations than the range shown here. To illustrate the goodness of fit of the DRCs, the same graph containing all raw data points is available in the supportive information (SI; Figure S2.2). The results for domoic acid (DA) are not shown on this graph as there were no effects observed at the highest possible test concentration.

Following every 43 h exposure period, the cell morphology and density were visually assessed and photographed at 100× magnification. In Figure 2.2, the effect of YTX on A549 cells is shown for different concentrations. In the negative control, a regular confluent cell culture is observed while in the high concentration treatment (i.e., 400 µg YTX L^{-1}), a much lower cell density and a high frequency of abnormal cell

morphology is visible. In the mid-concentration range (i.e., 0.5 µg L^{-1}), somewhat intermediate results are observed, with a slightly lower cell density and a relatively lower amount of normal-shaped cells. These results are complementary with the western blot results (see discussion).

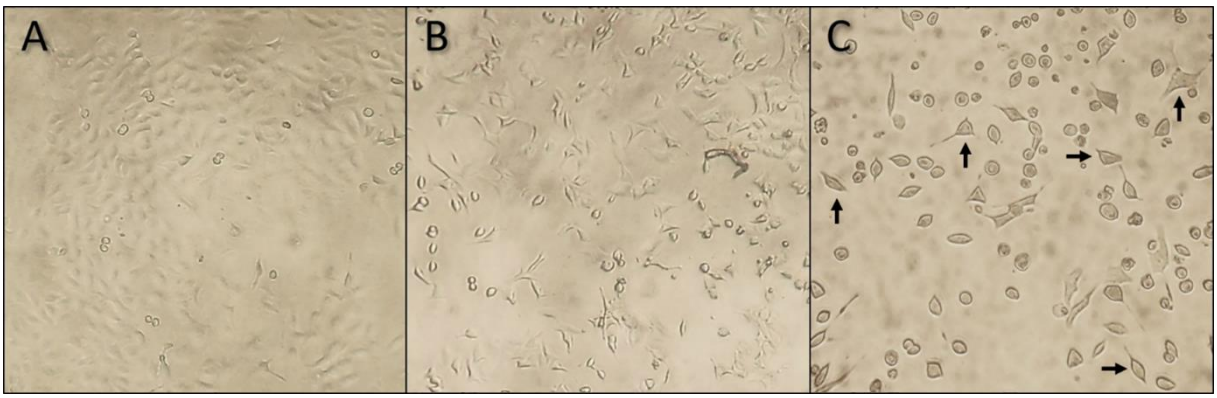

Figure 2.2: Microscopic images (100× magnification) of A549 cells after a 43 h treatment with pure YTX. The three different images represent three different concentration treatments: (A) negative control without YTX, (B) 0.5 µg YTX L^{-1}, and (C) 400 µg YTX L^{-1}. These visual observations are in line with the cell viability results. In the negative treatment (A), a nearly confluent cell culture can be seen. In the mid (B) and high (C) concentration treatments, cell cultures become less confluent and an increasing number of cells lose their normal cell morphology and deform into round cells. In the high concentration treatment (C), a few cells with a more or less normal cell morphology, as indicated with the arrows, are still present.

3.2 Effects on mTOR pathway activity

In exploratory western blotting experiments, only YTX exhibited an inhibitory effect on the phosphorylation of S6 ribosomal protein (S6RP), i.e., a downstream phosphorylation target of mTORC1. Therefore, all further experiments were conducted with YTX and analogues of YTX, like hYTX (see chemical structures in Table 1.2), using wide concentration ranges.

In the first main experiment, the effects of YTX on both the A549 and BEAS-2B cell lines were examined. The differential phosphorylation for the examined markers of the mTOR pathway (i.e., protein kinase B (Akt), S6RP, eukaryotic translation initiation factor 4E-binding protein 1 (4E-BP1)) is shown in Figure 2.3. For each of the two cell lines, a representative example of one of the blots is shown as a cropped non-edited version in Figure S2.4. In this experiment (Figure 2.3), significant effects were observed at the highest concentration (i.e., 1 µg L^{-1}) for all the examined markers. The downstream targets (i.e., S6RP, 4E-BP-1) showed a significant decrease in

phosphorylation for both cell lines (i.e., A549 and BEAS-2B) while the phosphorylation of Akt only showed a significant increase for the BEAS-2B cells. An explanation for these variable Akt results is given below. Overall, the results are largely comparable for both cell lines and show an inhibitory effect of YTX on the mTOR pathway. This effect (at 1 µg YTXL^{-1}) is even more expressed than the inhibitory effects of the positive control treatment, a known mTOR inhibitor (i.e., Torkinib/PP242 at 0.3 µM).

In a subsequent experiment, (pure) hYTX and hYTX in the lab SSA extract (produced as described above) were dosed to lung cells (Figure 2.4). Due to the limited size of the lab SSA extract, the maximum feasible concentration was limited to 0.5 µg hYTX L^{-1} and only A549 cells were incorporated in this experiment. A representative example of one of the blots is shown, as a cropped non-edited version, in Figure S2.5. The results demonstrate a significant decrease in phosphorylation for one of the target proteins (i.e., S6RP) for the highest concentration of hYTX. Due to the reduced hYTX concentration (i.e., 0.5 vs. 1 µg L^{-1}) and the complex mixture of the lab SSA treatment, the results of this experiments are less pronounced. They, however, still support the previous experiments (see discussion).

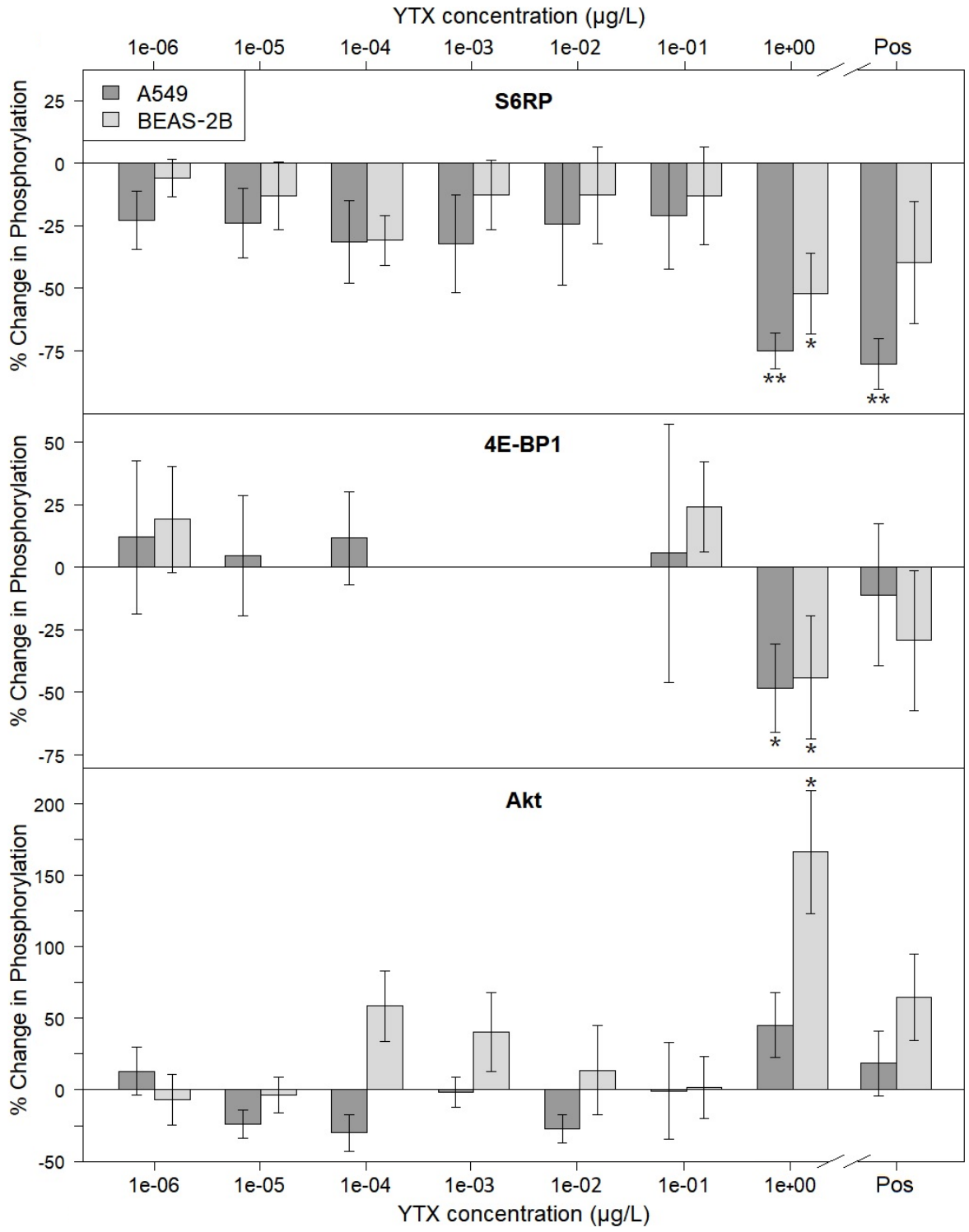

*Figure 2.3: Results of the western blotting experiment examining the effects of YTX on mTOR pathway activity, for both the A549 and BEAS-2B cell line. The change (%) in phosphorylation for the three examined proteins (i.e., S6RP, 4E-BP1, Akt) was obtained by normalizing the ratio of the phospho-specific and non-phospho-specific responses against the ratio of these measurements of the corresponding negative control treatment. Error bars present the standard error (n = 3). The positive control treatment, (i.e., 0.3 µM of Torkinib/PP242; a known mTOR inhibitor) is indicated as Pos on the x-axis. Significant changes in phosphorylation are indicated with asterisk symbols (*p<0.05, **p<0.01). The results for the 4E-BP1 marker are only shown for the lowest and highest concentration treatments. This is due to distortions on the lower part of the middle blotting lanes (i.e., mid-range concentrations; see Figure S2.4).*

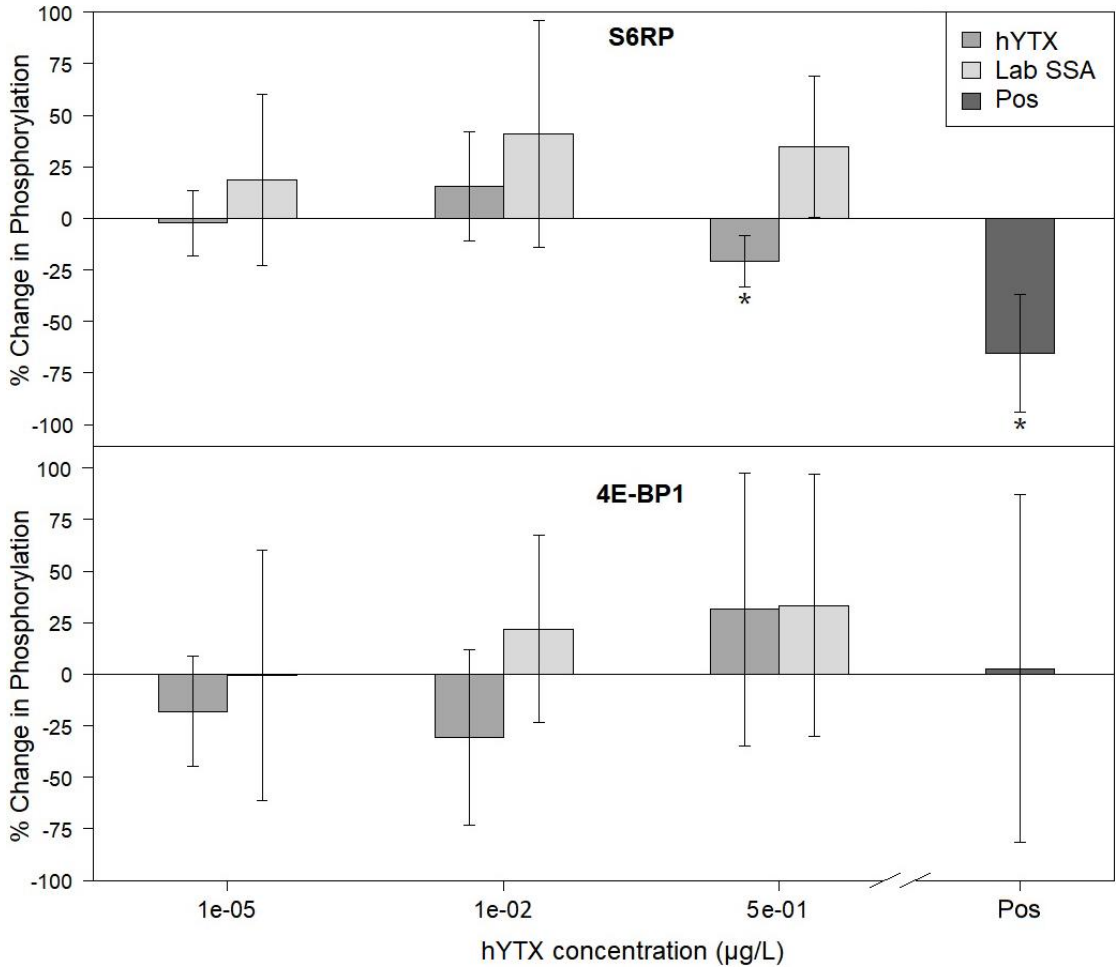

*Figure 2.4: Results of the western blotting experiment examining the effects of pure homoyessotoxin (hYTX) and the lab SSA extract (containing hYTX) on the mTOR pathway activity. Only the A549 cell line was used throughout this experiment. The % change in phosphorylation for the examined proteins (i.e., S6RP, 4E-BP1) was obtained by normalizing the ratio of the phospho-specific and non-phospho-specific responses against the ratio of these measurements of the corresponding negative control treatment. Error bars present the standard error (n = 3). The positive control treatment, containing 0.3 µM of the mTOR inhibitor Torkinib/PP242, is indicated as Pos on the x-axis. Significant changes in phosphorylation are indicated with asterisk symbols (*p<0.05).*

4 Discussion

4.1 Cell viability effects

Our results (Figure 2.1 and Table S2.1) indicate the importance of investigating the effects of marine phycotoxins besides the ones (e.g., brevetoxins, ovatoxins) that are currently known to cause adverse health effects in coastal environments.[21,22] PbTx-2 was the only phycotoxin examined in our study, for which elevated environmental air concentrations and respiratory distress have been reported during toxic HABs (and

SSA exposure).[21] Our cell viability experiments, however, show remarkably lower effect concentrations (i.e., higher toxicity or inhibitory potency) for OA and the two examined YTXs than for PbTx-2. This may indicate a higher pulmonary sensitivity towards these toxins.

Few comparable in vitro experiments have been performed so far. To the best of our knowledge, there were no PbTx(-2) effect data for lung cells available in the literature. One of the few records concerning the cell viability effects of PbTx-2 was found for a leukemic T cell line (Jurkat cells). Although Walsh et al.[160] did not report exact effect concentrations, their 48 h EC_{50} value was between 500 and 1000 µg L^{-1}. Wang et al.[161] exposed the A549 cell line (3000 cells $well^{-1}$) to OA and reported, using MTT cell viability assays, a 48 h EC_{50} value of 34 µg L^{-1}. Based on the cell morphology, they proposed apoptosis as the main cause for the negative cell viability effect. Botana et al.[162] performed sulforhodamine B cell cytotoxicity assays on A549 cells and reported 48 h EC_{50} values for YTX and hYTX of 3.2 and 0.62 µg L^{-1}, respectively. Depending on the exposure period they used in their experiments, the observed effects of YTXs were attributed to apoptosis or autophagy mechanisms.[162] In general, the scarce published data corroborate our experimental results.

YTXs are, in terms of exposure via ingestion (food), considered as the least potent group of phycotoxins. No human intoxications have been reported so far.[145] YTXs are, however, very toxic (LD_{50} of 100–500 µg kg^{-1}) in mice following intraperitoneal injection.[163] The exposure route for these toxins therefore seems of crucial importance in determining toxicity. In our study, YTXs demonstrated very low effect concentrations on lung cells in terms of cell viability. In addition, the shape of their DRCs (Figure 2.1) differed from the other examined phycotoxins since no complete mortality was obtained at the highest test concentrations. Instead, cell viability (on average) levelled off at around 30%. These findings were also visually confirmed using microscopy (Figure 2.2), as viable cells were still observed at 400 µg YTX L^{-1}. A decreasing viability trend could, however, still be observed in the high concentration range for YTX and hYTX (Figure S2.2). If more concentrated YTX standards were available and higher test concentrations were feasible, complete mortality would probably be observed in a higher concentration range. It is, however, clear from the shape of the DRCs that the effect of YTXs we currently encountered in the 0.05 to 100 µg L^{-1} concentration range

cannot be attributed to an adverse outcome pathway leading to direct cell mortality. It should be noted that for YTX and hYTX a small stimulation effect was sometimes visible at an even lower concentration of 0.01 µg L^{-1} (see Figure S2.2). This may indicate that the cell viability was not yet affected at this low concentration, but that the mitochondrial activity was stimulated due to a higher energy demand for homeostasis or detoxifying mechanisms. Although the mode of action of YTX is not completely understood, YTX has been shown to modify second messenger levels (cAMP), protein levels, and T-lymphocytes, and activate different types of induced cell death.[145] Based on in vitro studies with human lymphocytes, Botana et al.[162] suggested a different mode of action for YTX in tumor cells compared to that in normal cells and therefore highlights its potential as an anticancer drug. They point out that tumor cells undergo apoptosis, paraptosis, and autophagy-induced cell death while in normal cells, only cell proliferation is arrested. Based on this information, one could expect a different cell viability effect in carcinoma A549 cells and normal BEAS-2B cells. This is, however, not confirmed by our cell viability results, which showed little to no difference between the effect on the carcinoma A549 and normal BEAS-2B cell lines. The western blot experiments (discussed below), however, corroborate the findings of Botana et al.[162] as the inhibitory effects on the mTOR pathway were less pronounced for the normal BEAS-2B cells as compared to the carcinoma A549 cells.

4.2 Effect on mTOR pathway activity

The results from the western blot experiments, summarized in Figures 2.3 and 2.4, indicate that both examined YTXs indeed affect the mTOR pathway activity. The highest test concentration (i.e., 1 µg L^{-1}) of pure YTX induced a significant downregulation of the phosphorylation of both downstream targets of mTORC1 (i.e., S6RP and 4E-BP1) for both the normal BEAS-2B and carcinoma A549 lung cell lines. Such an inhibitory effect of YTX on mTOR pathway activity was until now only described for human glioma cells exposed to much higher concentrations of 34 and 286 µg L^{-1}.[164] Such a downregulated mTOR pathway leads to autophagy effects, inducing decreased cell proliferation and apoptosis.[49,165] The consequent (partial) decrease in cell viability was also observed in the same concentration range (Figure 2.1), and is therefore expected to be a consequence of this downregulation of the mTOR pathway.

In Figure 2.3, significantly increased phosphorylation of Akt for the BEAS-2B cells is shown. The feedback loops, activating Akt upon inhibition of mTORC1 phosphorylation, described by O'Reilly et al.[166] and Carracedo et al.[167] could explain these results. The rather smaller inhibitory effects for the downstream phosphorylation targets (i.e., S6RP and 4E-BP1) observed for the BEAS-2B cells, as compared to the A549 cells, may also be linked to these feedback mechanisms. Next, this could also explain the difference in the effect on carcinoma cells (e.g., A549) and normal cells (e.g., BEAS-2B), as suggested by Botana et al.[162] and discussed in section 4.1.

The highest test concentration (i.e., 0.5 µg L^{-1}) of pure hYTX induced significant downregulation of S6RP phosphorylation (Figure 2.4). Although still present, the effects are less strong as compared to the highest test concentration (i.e., 1 µg L^{-1}) of pure YTX in the previous experiment (Figure 2.3). This can be attributed to the two-fold lower highest test concentration. It is clear that the DRC slope (Figure 2.1) is sharp in this concentration range and that such a concentration difference may result in a smaller effect. For the lab SSA treatments, no significant effects were observed. Although these treatments had the same hYTX concentrations, they may contain (1) other organic compounds or small aerosolizable organic matter that bind or interact with hYTX or (2) other YTX analogues or metabolites with potentially weaker effects that compete with hYTX for molecular binding sites and uptake. Both suggestions imply a decreased bioavailability and lead to weaker effects. The results of Chapter 4 corroborate the current results on the weaker effects of this lab SSA extract and the significant influence of YTXs on the mTOR pathway.

4.3 General discussion

In this study, we aimed to investigate potential human health effects of airborne exposure to phycotoxins that can be present in SSAs. Until now, only a few PbTxs and OVTXs have been detected and quantified in environmental SSAs. Reported PbTx air concentrations during HAB events of *Karenia brevis* ranged from 3 to 180 ng m^{-3}.[156,168] Although it was not our direct research goal, the production and analysis of the laboratory-generated SSA proved that other phycotoxins can also aerosolize when present in seawater. Phycotoxin concentrations in SSAs will, among others, be dependent on the density of the toxin-producing algal species in seawater. As YTXs are produced by HAB species that do not bloom to very high densities, their

concentrations in the water and consequent SSA phase will never come close to those reported for PbTxs during strong HAB events. Especially as the maximum phycotoxin production per algal cell is nearly the same for YTXs and PbTxs (see Annex II section 4). The aerosolization and coastal air concentrations of other phycotoxins than PbTx were investigated within this PhD thesis and are discussed in detail in Chapter 3.

Throughout our in vitro experiments we consistently used an exposure period of 43 h. We opted for this (maximum) duration, as experiments could not be prolonged without splitting the cells. This was indeed an option but would have lowered the experiment's repeatability. A longer exposure period could emphasize cell viability effects and resemble a more (realistic) chronic exposure. Conversely, in vitro experiments analyzing the activity and thus phosphorylation of the mTOR pathway are often somewhat shorter in time (from 0.5 to 24 h).[159,169,170] The phycotoxins we spiked do have a high stability and reasonable solubility (see Kow), lung cells will thus rather be exposed to the phycotoxins over the whole experimental duration. The used 43 h exposure period is thus somewhat of a compromise to analyze both effects over the same period. Nonetheless, the cell viability effects of YTXs we observed may still be attributed to the downregulation of the mTOR pathway. Of course, this does not prove that YTXs (or any other marine chemicals) are the causal agent in SSAs improving the health of coastal populations. To that end, one needs to quantify and assess the ratio of exposure (i.e., air concentrations) and in vivo doses and effects of (sea spray) aerosolized chemicals. Our study rather provides proof of principle for the biogenics hypothesis, showing that aerosolizable marine compounds (e.g., YTXs) can downregulate the mTOR pathway and are potential therapeutic tools. Moreover, YTXs can be put forward as interesting target compounds to investigate the marine biogenics hypothesis. Finally, this study also stresses (1) the difference in the sensitivity of different exposure routes, as YTXs are considered to be the least potent phycotoxin group via ingestion exposure and (2) the complexity (e.g., bioavailability) of effects of bioactive substances in realistic environmental (mixture) matrices.

Chapter 3

Phycotoxin-enriched sea spray aerosols: methods, mechanisms, and human exposure

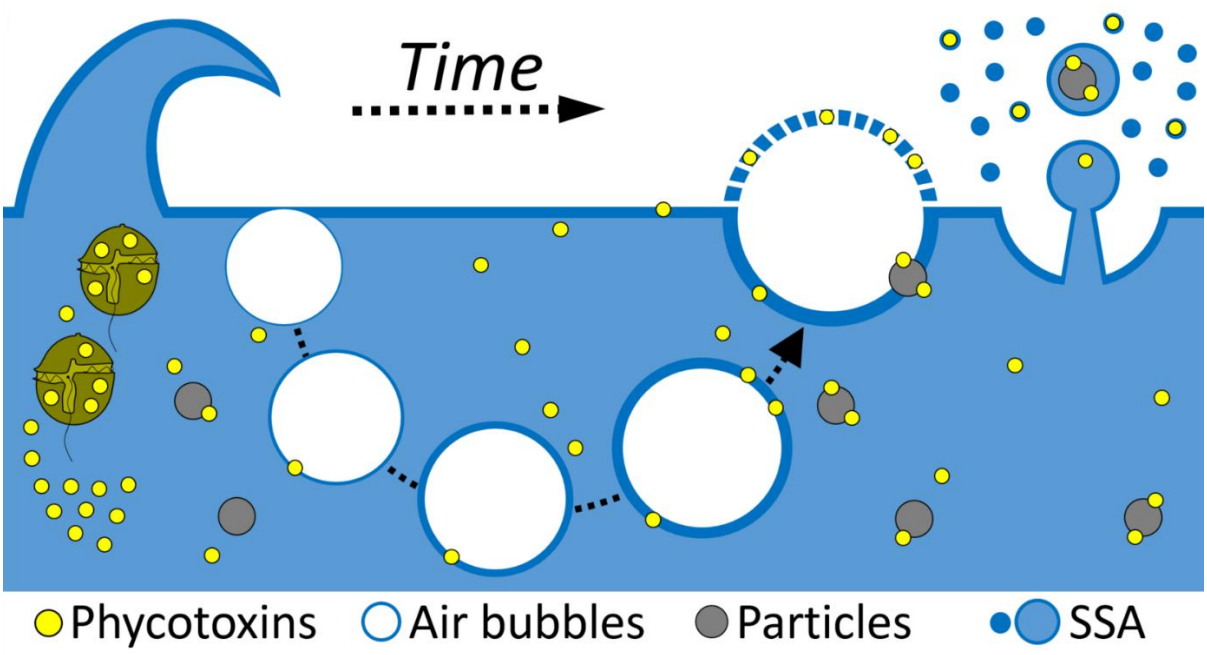

Redrafted from ([§] shared last):

Van Acker, E.; Huysman, S.; De Rijcke, M.; Asselman, J.; De Schamphelaere, K.; Vanhaecke, L.[§]; Janssen, C.[§] Phycotoxin-enriched sea spray aerosols: methods, mechanisms, and human exposure. Environmental Science & Technology ***2021****, 55, 6184-6196.*

Chapter contents

Abstract

To date, few studies have examined the role of sea spray aerosols (SSAs) in the human exposure to harmful and beneficial marine compounds. Two groups of phycotoxins (brevetoxins (PbTxs) and ovatoxins (OVTXs)) have been reported to induce respiratory syndromes during harmful algal blooms. The aerosolization and coastal air concentrations of other common marine phycotoxins have, however, never been examined. This study provided the first (experimental) evidence and characterization of the aerosolization of okadaic acid (OA), homoyessotoxin (hYTX) and dinophysistoxin-1 (DTX-1), by using artificial and natural seawater spiked with toxin-producing algae in a marine aerosol reference tank (MART). The high potential for aerosolization of these phycotoxins was demonstrated by their 78 to 1769-fold enrichment in SSAs relative to the subsurface water. To obtain and support these results, we first tested and validated our MART set-up, and optimized or developed new sampling, extraction and analytical methodologies. Our validated analytical method for the determination of phycotoxin concentrations in SSAs showed good linearity (R^2>0.99), recovery (85.3-101.8%), and precision (RSDs≤17.2%). We also investigated natural phycotoxin air concentrations by means of an environmental SSA sampling campaign which was combined with concurrently performed MART aerosolization experiments using (pure) natural seawater. This approach allowed us to indirectly quantify the (harmless) magnitude of OA concentrations (0.6-51 pg m^{-3}) in Belgium's coastal air. Overall, this study provided new insights into the enriched aerosolization of marine compounds and proposed a framework to assess their airborne exposure and potential effects on human health.

1 Introduction

As coastal regions are by far the most densely populated areas,[28] research that investigates possible relationships between the ocean and human health (OHH) has increased during the past few decades.[30] One of the emerging aspects in this research field is the airborne exposure to marine compounds via sea spray aerosols (SSAs). SSAs are far more than merely aerosolized seawater droplets.[171] Environmental sampling[76–79] and experiments with SSA generators[73,83–85] have shown that SSAs introduce particulate matter, microorganisms, fatty acids, carbohydrates, sterols and proteins into the atmosphere. Moreover, SSAs often contain (much) higher concentrations of microorganisms[86] and (hydrophobic or amphiphilic)[171,172] organic compounds[73,83,87] than the originating subsurface water (SSW). Such enrichment processes also occur in the sea surface microlayer (SSML).[73,86,87] The magnitude of enrichment is expressed as enrichment factors (EFs) and is usually determined relative to sodium (Na^+). Na^+ is a common proxy to quantify SSA densities and is considered to have no enrichment.[62]

During the past century, marine systems have experienced increasing pressure by global change and other stressors.[173,174] Many of these (e.g., eutrophication and invasive species) are linked to an increased (reported) occurrence of harmful algal blooms (HABs).[123,130,175] Human intoxications with algal toxins or so-called phycotoxins mainly occurs via seafood consumption.[176] The ingestion of shellfish contaminated with okadaic acid (OA) or dinophysistoxin (DTX), for example, causes gastrointestinal symptoms (e.g., vomiting and diarrhea) known as diarrhetic shellfish poisoning (DSP).[121] HAB events of *Karenia brevis* in the Gulf of Mexico[17] and *Ostreopsis ovata* in the Mediterranean Sea[138] are known to induce human respiratory syndromes (e.g., coughing, wheezing, irritation, airflow reduction and chest tightness)[136–138] caused by inhalation of aerosolized phycotoxins (i.e., brevetoxins (PbTxs) and ovatoxins (OVTXs), respectively). Vulnerable groups, such as asthma patients, have been reported to be more sensitive to aerosolized brevetoxins.[177]

Conversely, no human intoxication has ever been reported for yessotoxins (YTXs).[145] Recent research into the bioactivity of YTXs even points to their potential therapeutic use.[145,162,178] YTXs have been shown to downregulate the mammalian target of

rapamycin (mTOR) pathway.[145,179,180] The downregulation of this cell signaling pathway is crucial in Moore's biogenics hypothesis[46] as it has been associated with longevity, anti-cancer properties and other beneficial health effects.[49] Indeed, Moore[46] hypothesized that regular airborne exposure to aerosolized natural compounds causes health promoting effects via a downregulation of the mTOR pathway. Although there is currently too little evidence to prove or disprove this hypothesis, it highlights the relevance of the SSA exposure route for a whole spectrum of marine compounds with (potential) positive pharmacological effects.[26,27] SSA exposure is thought to contribute to the coastal proximity health effect, which is increasingly observed in epidemiological research.[32–36] Overall, the inhalation of aerosolized phycotoxins and other marine compounds is a poorly studied exposure pathway that could lead to negative but possibly also positive health effects. Appropriate (analytical) methodologies to quantify and assess this airborne exposure are, however, lacking.

To this end, the first goal of this study was to develop and validate new (analytical) methodologies to quantify phycotoxins in SSAs. Seven marine lipophilic phycotoxins were included in the method development and analysis: okadaic acid (OA), homoyessotoxin (hYTX), yessotoxin (YTX), dinophysistoxin-1 (DTX-1), azaspiracid-1 (AZA-1), pectenotoxin-2 (PTX-2) and 13-desmethyl spirolide C (SPX-1). These phycotoxins are important representatives of different groups of marine phycotoxins[181,182] that occur (almost) globally[121,182] and are routinely monitored in consumable shellfish products (i.e., their best known exposure route).[133,183] In our proposed method, SSA samples were concurrently analyzed for their Na^+ content, allowing a better characterization of any enrichment processes involved in the aerosolization of phycotoxins. Next, we performed diverse experiments with a marine aerosol reference tank (MART), wherein we investigated the phycotoxin transfer from micro-algae to the subsurface water (SSW), the sea surface microlayer (SSML), and ultimately the air/atmosphere via SSAs. Finally, the magnitude and risks of the phycotoxin air concentrations at the Belgium coast were assessed by combining environmental SSA sampling, experimental SSA production and toxicological data from literature.

2 Materials and methods

2.1 Toxins and algae

All seven phycotoxins included in this study (i.e., OA, hYTX, YTX, DTX-1, AZA-1, PTX-2 and SPX-1) were purchased as certified reference standard solutions (in methanol) from the National Research Council Canada. Two toxic micro-algae were used. The *Prorocentrum lima* strain (CCAP1136/9) was supplied by the Culture Collection of Algae and Protozoa and produced the two phycotoxins OA and DTX-1.[132] The *Protoceratium reticulatum* strain (SCCAP K- 1478) was supplied by the Scandinavian Culture Collection of Algae and Protozoa and produced the phycotoxin hYTX.[132] Algal culturing methods are described in detail in supportive information (SI; Annex III section 1). These phycotoxins were selected based on: (1) potential presence in the North Sea, (2) tendency for aerosolization, and (3) purchasability of chemical standards and algal strains producing the phycotoxins.

2.2 Experimental SSA production and sampling

To examine SSA production and transfer processes, and to optimize sampling procedures, a marine aerosol reference tank (MART) was constructed (Figure S3.1) as described by Stokes *et al*.[90] A MART is essentially an (air-closed) aquarium or tank equipped with a system that produces an intermittent plunging water sheet. It is designed to mimic the underwater air bubble plume, and thus SSA production, of breaking waves.[90,93] Further details of our self-constructed MART system can be found in SI (Annex III section 2).

Our MART set-up allowed SSA sampling in triplicate. This was performed using membrane filters (Ø 47 mm), enclosed in stainless steel in-line filter holders (Pall Corporation), over which an airflow of 9 ± 1 L min^{-1} was applied using vacuum pumps (LABOPORT®). Handling and field blanks were incorporated in all experiments and environmental sampling campaigns to confirm the absence of phycotoxin and Na^+ contamination and to account for the filter background of Na^+. Unless stated differently, MART experiments were performed in a thermostable room at 20 ± 1°C and allowed a minimum seawater (temperature) acclimation period of 8 h (prior to the start of the aerosolization experiments).

2.3 Preliminary testing and optimization

To determine which membrane filter was best suited to retain and analyze aerosolized phycotoxins and Na^+ (i.e., a proxy for the collected SSA quantity),[62] three filter types were tested: (1) a quartz microfiber filter (QM-A, Whatman®), (2) a glass microfiber filter (EPM2000, Whatman®), and (3) an octadecyl (C18) bonded silica solid phase extraction (SPE) disc (Empore™). Quartz and glass fiber filters have been used for SSA sampling by other studies.[22,24,184] These filters have respective pore sizes of 2.2 and 2 µm, and more importantly (according the product certificate) an air retention >99.95% for 0.3 µm particle. They thus collect total suspended particles (TSP). The C18 SPE disk was explored as a new alternative with a lipophilic binding affinity. Details of how these filters were tested are provided in SI (Annex III section 3). In short, filters were deployed in MART experiments using artificial seawater with and without toxin-producing algae. Phycotoxin extractions were performed using the (initial) procedure described below. Throughout this study, Na^+ extractions were performed by eluting filters three times with 5 mL of 0.14 M HNO_3. After filtration with a 0.45 µm filter (Acrodisc®), the Na^+ analysis was performed with inductively coupled plasma - optical emission spectroscopy (ICP-OES; Thermo Scientific iCAP 7000 series).

Following the selection of the quartz filter (as discussed below), our SSA sampling methods and MART set-up were further optimized as described in Annex III section 4. In short, we examined (among others) if the filter holder's frontal support screen should be removed to increase the filter collection efficiency, and if a filter pretreatment (i.e., rinsing steps with 0.14 M HNO_3 and H_2O) would improve the Na^+ analysis.

2.4 Extraction method optimization

At first, a preliminary procedure for phycotoxin extraction from SSA filter samples was designed. The different steps[132,156,185] and alkaline conditions[185] of the methanolic eluent[132,133,183,186–188] were based on published methods and preliminary experiments. A two-step statistical workflow was used to optimize this initial extraction methodology. The statistical software JMP 12.0 (SAS Institute Inc) was used to select, evaluate and model the appropriate experimental designs. First, a fractional factorial Plackett-Burman design[189] of 24 runs was used to screen the effect of 11 parameters or factors (see Table S3.1) on the extraction efficiency. The qualitative factors that significantly

(p<0.1, 90% confidence level) improved the extraction efficiency, were retained in the final procedure. As a second step, the significant quantitative factors were further optimized through response surface modelling (RSM) using a Box-Behnken design[190] of 15 runs (see Table S3.2). Prior to the extractions related to both experimental designs described above, filters were spiked with 1.25 ng of each phycotoxin. Organic solvents used for extraction purposes were of analytical grade.

Final extraction procedure

The deployed quartz filters were cut in two. One half was used for Na^+ analysis, and the other half was placed in a 15 mL polypropylene tube and used for phycotoxin analysis. Methanol (10 mL) containing 26 mM ammonium hydroxide (NH_4OH) was added as eluent, and samples were sonicated for 5 min. This elution was repeated using 3 mL of eluent. The primary and secondary extracts (10+3 mL) were combined and filtered using 0.2 µm polytetrafluoroethylene (PTFE) filters (Phenex™). Intermediate tubes, syringes, and PTFE filters were rinsed with 1 mL of (additional) eluent. Extracts were subsequently dried, under a gentle N_2 stream at 40°C, until a single drop was obtained and reconstituted in 50 µL of acetonitrile and 200 µL of H_2O both containing 6.7 mM NH_4OH. After a purification centrifugation step (5 min, 7200 g), the supernatant was transferred to a glass insert in a LC-MS vial prior to the analysis.

2.5 Phycotoxin analysis

Phycotoxin analysis was performed in a targeted manner (i.e., with certified reference standards) using ultra-high-performance liquid chromatography hyphenated to high-resolution Orbitrap mass spectrometry (UHPLC-HR-Orbitrap-MS) following the procedures reported by Orellana *et al*.[132] In brief, chromatographic separation was carried out by reversed phase chromatography using a C18 gravity column (1.8 µm, 50 × 2 mm, Macherey-Nagel). Detection was performed using an Exactive™ benchtop Orbitrap MS (Thermo Fisher Scientific), preceded by heated electrospray ionization (HESI-II) operating in positive and negative ionization modes. Mass resolution was set at 50,000 full width at half maximum (FWHM), and detection within a mass extraction window of 5 ppm was pursued. Instrument control and data processing were performed using Xcalibur 2.1 software (Thermo Fisher Scientific). $^{13}C/^{12}C$ isotopic ratios, determined at the highest peak intensities, were used as a second diagnostic criterion for compound identification.

2.6 Validation of the analytical method

Environmental SSA samples will, depending on the ambient conditions, contain a variable salt content. Prior to the validation, we successfully verified that these salts did not interfere with the phycotoxin analysis (Annex III section 5). The actual method validation followed the guidelines of Eurachem,[191] CD 2002/657/EC[192] and dedicated reviews.[193,194] The validation experiments were designed to evaluate linearity, limit of detection (LOD), limit of quantification (LOQ), selectivity, specificity, trueness, and precision. Linearity, LOD and LOQ were investigated by constructing a 10-point matrix-matched calibration curve (0, 0.5, 1.0, 1.5, 2.0, 2.5, 4.0, 6.0, 8.0, and 10 ng mL^{-1}) for all selected phycotoxins in each validation experiment. Furthermore, the selectivity, accuracy, and precision were evaluated at 1.5, 2, and 2.5 times the LOQ-level. This was performed in each validation experiment and in 6-fold per concentration level by extracting spiked quartz filter (halves). Three validation experiments were performed on three different days by the main operator and repeated a fourth time by a second operator. In addition, spiked and non-spiked SSA loaded filters (i.e., true blanks containing salts that were produced with the MART; see Annex III section 5) were used to evaluate the method's specificity.

2.7 Laboratory SSA experiments using spiked seawater

To characterize the SSA processes of phycotoxins, two near-identical MART experiments were performed wherein only the seawater differed. The first experiment was performed using filtered (0.2 µm) artificial seawater (i.e., L1-medium; Annex III section 1). The second used non-filtered natural seawater, collected in the surf zone near Ostend, Belgium (51°12′13.9″N, 2°50′55.5″E) on April 29, 2017, which represented a more realistic environment including natural dissolved compounds, particulate matter, and organisms.

Selected phycotoxins (i.e., OA, hYTX and DTX-1) were indirectly introduced in the MART by adding the micro-algae *P. lima* and *P. reticulatum*, both at a density of 500 cells mL^{-1}. This density is approximately 2 to 3 orders of magnitude higher than the environmental maximum for these algae.[195–198] In this context it should be considered that these proof-of-principle MART experiments helped us to study the fundamental aerosolization processes of the selected phycotoxins. Four hours later

the MART was activated and the produced SSA was sampled in triplicate for 12 h. Filters were subsequently cut in two and analyzed for their respective Na^+ and phycotoxin contents following the methods described above. As SSAs are partly retained by the filter holder's frontal half, these were collected by rinsing the holders four times with 5 mL of methanol. Half of the filter holder extract was dried, reconstituted in 10 mL of 0.14 M HNO_3 and analyzed for its Na^+ content. The other half was treated as a SSA filter extract and analyzed for phycotoxins.

To characterize the processes influencing the aerosolization and enrichment of phycotoxins, three distinct water layers were sampled in the MART. The (1 cm) bottom layer and the bulk subsurface water (SSW) were sampled using a glass pipet. The sea surface microlayer (SSML; i.e., 60-100 µm) was sampled using the glass plate method described by Harvey and Burzell.[199] In short, a clean glass plate (± 0.18 m^2) provided with a handle was immersed vertically in the water and carefully withdrawn at a rate of ±20 cm sec^{-1}. In this way a layer of approximately 60-100 µm thick was retained.[199] The surface film/water layer adhering to the plate was subsequently scraped off at both sides, with a precleaned metal blade, and collected in a 100 mL Erlenmeyer.

Three replicate (10 mL) samples of each water layer (i.e., bottom, SSW and SSML) were collected 1 h before and 1 h after the (12 h) active MART period. The samples were subsequently analyzed to determine the phycotoxin (and Na^+) concentration in the dissolved (<0.2 µm), small particulate (0.2-5 µm), and large particulate (>5 µm) size fractions. The extraction procedures for these different size fractions are described in Annex III section 6. The separation of these different size fractions for analysis was performed to provide important information on the potential SSA fate of phycotoxins. The size of a particulate, for example, likely determines the minimum size of the SSA droplet wherein it can be incorporated. The dissolved fraction can therefore be incorporated in all film droplets. Conversely, the large particulate fraction (i.e., mainly intracellular toxins) can only be aerosolized in larger sized jet droplets, which have a shorter atmospheric retention time[61] and are found to a lesser extent in environmental SSAs.[80,200]

Having analyzed the Na^+ and phycotoxin concentrations ([TOX]) in the SSAs, SSML, and SSW, we calculated the phycotoxin enrichment factor (EF_i) for both phases of i

(SSML and SSA). It should be noted that $[TOX]_{ssw}$ in the following equation only accounts for the dissolved and small particulate fractions (i.e., primary aerosolized fractions):

$$EF_i = \frac{[TOX]_i / [Na^+]_i}{[TOX]_{ssw} / [Na^+]_{ssw}} \quad \text{(eq. 3.1)}$$

Finally, to control the collection efficiency of our SSA sampling, we used an additional sampling technique during these two MART experiments. In short, the air passing through the quartz filters was drawn (in bubbles) through ultra-pure water following sampling as described by Tsunogai *et al*.[201] These samples were analyzed for phycotoxins and Na^+. More details of this additional SSA sampling method are provided in SI (Annex III section 7).

2.8 Estimated coastal air concentrations

A dual sampling campaign at the Belgian coast, with an (almost) daily interval, was performed in July 2017. Environmental SSAs were sampled from a beach, and more concentrated experimental SSA samples were concurrently produced from the same natural seawater using the MART in a (nearby) laboratory. Both the beach and MART SSA sampling were performed to (directly or indirectly) quantify phycotoxin coastal air concentrations ($[TOX]_{coastal\ air}$) and to assess the potential human airborne exposure.

The Twins beach club in between Ostend and Bredene (Belgium, 51°14′46.9″ N, 2°57′02.7″ E), situated ±50 m from the high-water mark, was the main environmental sampling station. Additional SSA samples were taken using a lifeguard chair (Figure S3.2). This mobile sampling station moved as tides changed and remained at 10 ± 5 m from the actual waterline. Environmental SSA sampling was performed with battery-powered Leland Legacy personal sampling pumps (SKC) at a constant air flow of 12 L min^{-1}. The duration of the SSA sampling at the Twins beach club was between 3 and 7 h and near the waterline (using the lifeguard chair) between 1 and 2.5 h.

The concurrent MART experiments were performed at an ambient temperature (19.7 ± 2.7°C) with 100% natural seawater (i.e., without deliberate introduction of toxin-producing algae). For every (near-daily) experiment, the MART was drained, cleaned

and refilled with seawater that was collected in the surf zone near Ostend (51°14′22.2″ N, 2°55′44.9″ E). The collected seawater had a temperature between 19.1 and 21.6°C and was directly used in the MART without an acclimation period. The experimental SSAs were sampled over 16-20 h periods. During weekends and holidays MART experiments were run for 40 or 70 h (i.e., 2 or 3 days).

After every environmental sampling or MART aerosolization experiment, deployed SSA filters were cut in two equal pieces. These filter halves were stored at 4°C in 5 mL of 0.14 M HNO_3, and at -20°C in 10 mL of methanol containing 26 mM NH_4OH (i.e., the initial eluents for the respective Na^+ and phycotoxin extractions). Further extraction and analysis were performed following the methods described above. The only difference was that in addition to Na^+, the Mg^{2+} content of these SSA samples was also measured using the ICP-OES analysis. This was performed to confirm, using Na^+/Mg^{2+} mass ratios,[202] that the Na^+ analyzed originated indeed from seawater and thus from the sampled SSAs.

In the case where the phycotoxin contents in the environmental (beach) SSA samples were undetectably low (<LOD), the concurrently performed MART experiments provided an additional strategy to (indirectly) quantify coastal air concentrations (i.e., $[TOX]_{coastal\ air}$). These experimental samples reached quantifiable phycotoxin concentrations (>LOQ) much more easily, as the SSAs collected in the relatively small headspace of the MART had a higher density (i.e., less diluted in air). Moreover, sampling times were extended over a longer period in the MART. The MART experiments were used to assess the phycotoxin composition of nascent SSAs, determined as the $[TOX]_{SSA}/[Na^+]_{SSA}$ ratio, on a near-daily-basis. This experimental ratio was then multiplied by the environmental SSA density (i.e., $[Na^+]_{coastal\ air}$) of the corresponding day to quantify $[TOX]_{coastal\ air}$ at our beach sampling sites (i.e., near the waterline and/or 50m inland):

$$[TOX]_{coastal\ air} = \frac{[TOX]_{SSA,\,MART}}{[Na^+]_{SSA,\,MART}} \times [Na^+]_{coastal\ air} \qquad \text{(eq. 3.2)}$$

Note that this indirect quantification strategy (eq. 3.2) assumes that the environmental samples consist of nascent SSAs and thus have the same $[TOX]_{SSA}/[Na^+]_{SSA}$ ratio as the MART samples.

3 Results

3.1 Preliminary testing and optimization

The comparison of the three different filter types showed that the highest phycotoxin yields were obtained with the quartz and glass fiber filters (Figure S3.3). The collected Na^+ as a function of the MART sampling time showed good linearity (R^2>0.90) for the quartz fiber filter (Figure S3.4), while this was not the case (R^2<0.05) for the glass fiber filter (Figure S3.5). We therefore concluded that the quartz filter was best suited to quantify aerosolized phycotoxins and Na^+.

Further optimization of our SSA sampling method resulted in the pretreatment of the quartz filter (i.e., rinsing steps with 0.14 M HNO_3 and H_2O; see Annex III section 4), the removal of the filter holder's frontal support screen, and extraction and analysis of the filter holder upon sampling. The latter was performed as about 50% of the collected Na^+ was retained by the filter holder's frontal half (Figures S3.6 and S3.7). The quartz filter pretreatment was introduced as it reduced the Na^+ background content of extracts with 69 ± 5% (n=2×6) and lowered the variability in the Na^+ content of replicate samples, expressed as the relative standard deviation (RSD), from 30 ± 9% (n=8×3) to 17 ± 6% (n=6×3). Throughout the study, after implementation of this filter pretreatment, the blank samples contained an average Na^+ background of 6.1 ± 1.4 µg (n=22). As shown in Figure S3.6, the frontal support screen retained 17 ± 5.3% of the total collected Na^+. Its removal increased the collection efficiency of the quartz filter in a similar way (18 ± 1.5%).

3.2 Extraction method optimization

The applied Plackett-Burman design evaluated the effect of 11 parameters or factors (Table S3.1) on the extraction efficiency of the selected phycotoxins. These results are summarized per phycotoxin in Figure 3.1 using the t-statistic or t-value, that is, the difference of the estimated (high level) parameter value from its hypothesized (no-effect) value represented in units of standard error. The sonication step during elution and the rinsing of the intermediate tube and PTFE filter significantly increased ($p<0.1$; 90% confidence level) the extraction efficiency for at least one phycotoxin. As such, these two steps were retained in the final procedure. The initial elution volume, NH_4OH

concentration in the eluent and centrifugation purification step had a significant effect ($p<0.1$; 90% confidence level) on the extraction efficiency in either a positive (i.e., higher) or negative (i.e., lower) manner. The optimum levels (i.e., giving maximum extraction efficiency) for these three quantitative factors were determined through response surface modelling (RSM), as graphically demonstrated in Figure S3.8. The RSM results and overall optimum levels are listed in Table S3.3. The six other factors had a negative ($p<0.1$) or non-significant effect ($p>0.1$) on the extraction efficiency and were not retained.

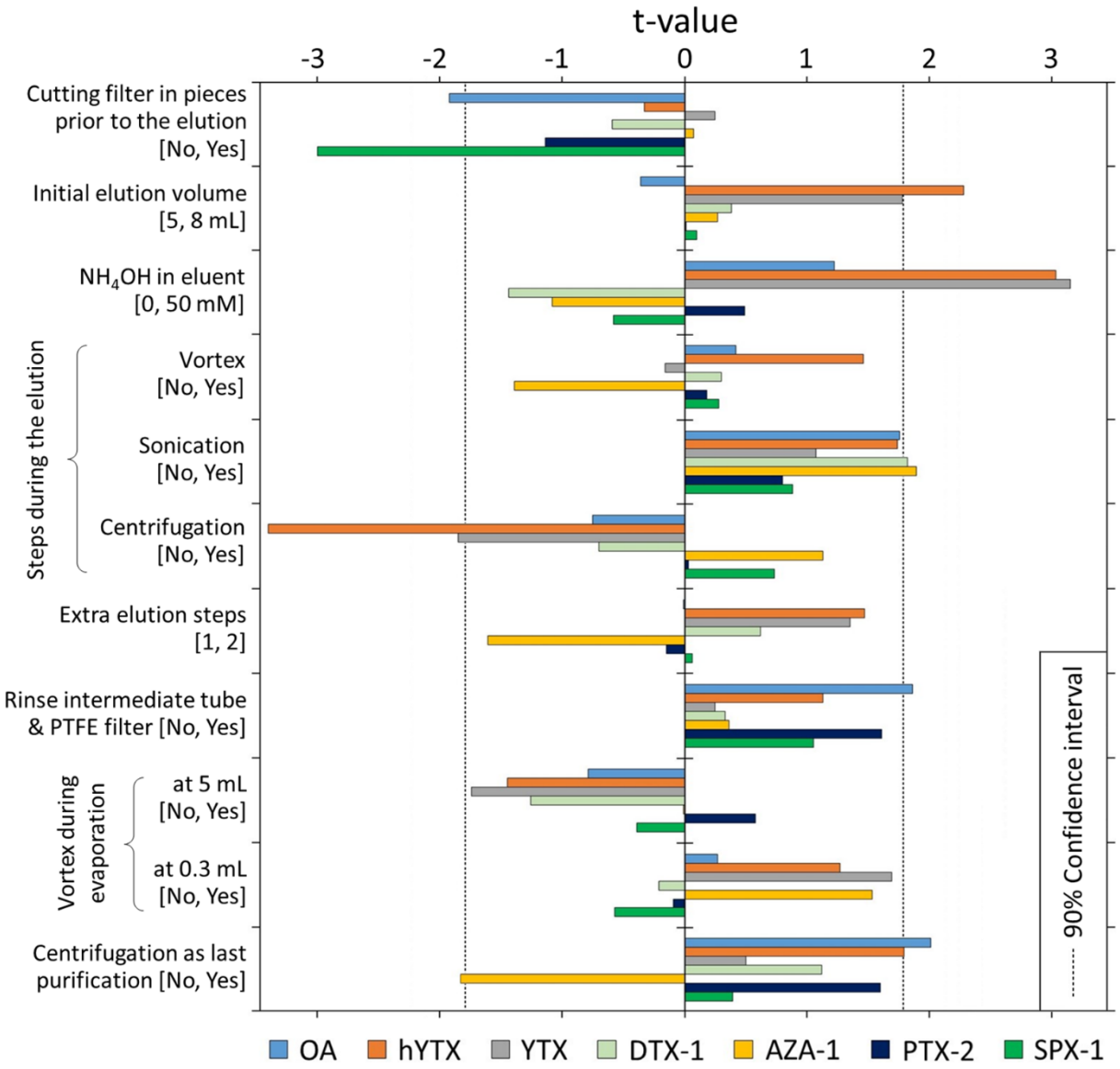

Figure 3.1: t-value diagram illustrating the effect and significance of the screened factors on the extraction efficiency. The two levels at which each factor was examined (see Table S3.1) are shown in brackets on the vertical axis. The bars that exceed the dashed lines indicate that the examined high level of the factor significantly decreases (negative t-value) or increases (positive t-value) the extraction efficiency with a confidence level of 90%.

3.3 Validation of analytical method

To ensure the method's fitness for purpose, that is, quantification of low phycotoxin concentrations in SSAs, the developed analytical methodology was evaluated with respect to its linearity, LOD, LOQ, selectivity, specificity, trueness, and precision. As SPX-1 had inadequate selectivity and specificity (as discussed below), its results are not presented for the other validation criteria.

Linearity

The linearity was evaluated using the matrix-matched calibration curves and the least squares method for linear regression.[194] These linear models showed good linearity (R^2>0.99), which was confirmed with a lack-of-fit analysis (F-test, p>0.05, 95% confidence level). Table 3.1 shows the average coefficients of determination (R^2) of all four calibration curves (one per validation experiment).

LOD and LOQ

The LODs and LOQs were determined using the standard deviation of the response, that is, the error of estimate ($S_{y/x}$), and the slope of the calibration curve.[193,203] These LODs and LOQs (in the final 250 µL extract) ranged from 0.17 to 0.40 ng mL^{-1} and 0.58 to 1.20 ng mL^{-1}, respectively (Table 3.1). In a 2 m^3 air sample, these LOQs correspond to air concentrations ranging from 145 to 400 pg m^{-3}. The ^{13}C-isotopes of the adduct ions were always detectable at the LODs and provided, as discussed below, two additional identification criteria. All targeted phycotoxins had LOQs near 1 ng mL^{-1}. The three concentration levels (i.e., 1.5, 2.0, and 2.5 × LOQ) used in the validation experiments to evaluate the selectivity, specificity, trueness and precision were therefore rounded to 1.5, 2, and 2.5 ng mL^{-1}.

Selectivity and specificity

To meet the CD 2002/657/EC[192] requirements (i.e., three identification points), compound identification was based on: (1) the accurate mass (*m/z*) of the adduct ion, (2) the accurate mass (*m/z*) of its ^{13}C-isotope ion, (3) the $^{13}C/^{12}C$ isotope ratio within the tolerance range of CD 2002/657/EC,[192] and (4) the specific retention time (RT). These four identification criteria were evaluated relative to the results of the certified reference standards of these seven phycotoxins (Table S3.4). As this method was

developed for low concentrations, we evaluated the selectivity at the lowest examined concentration level (i.e., 1.5 × LOQ). Over 3 days (n=24), RTs showed small deviations (Δ≤0.06 min) from the pure standards. Only AZA-1 showed somewhat larger RT deviations (Δ≤0.09 min). In addition, an adequate chromatographic resolution (R_S>2) was found for all phycotoxins except for SPX-1. Deviations from the accurate *m/z* never exceeded 1.5 ppm and were on average (per phycotoxin) below 0.75 ppm. ^{13}C-isotopes were always detectable at the same RT (Δ≤0.01 min) and also showed only small *m/z* deviations, with maximum and average deviations below 1.75 and 1 ppm, respectively. The $^{13}C/^{12}C$ isotope ratios differed, on average, less than 2% from the ratios of the pure reference standards (Table S3.4). All these results (Table S3.5) confirm the method's adequate selectivity for all phycotoxins except for SPX-1.

To evaluate the specificity, both spiked (n=9) and non-spiked SSA loaded filters (n=9) (i.e., true filter blanks containing salts; see Annex III section 5) were extracted and analyzed. Spiked samples (Figure S3.9A) showed a significant increase in the peak area intensity at their accurate *m/z* and specific RT (Table S3.4). No interfering matrix constituents, with a similar RT, were found in a mass extraction window of 5 ppm (Figure S3.9A/B) for six targeted phycotoxins. Indeed, throughout this study, we observed no background concentrations of these six phycotoxins in the blank samples (n=26). For SPX-1, however, two interfering matrix constituents were present (RTs of 3.24 and 3.46 min) which did not show a constant intensity over different samples (RSDs of 74 and 113%). The analysis therefore showed to be specific for all targeted phycotoxins except for SPX-1, for which this method proved to be inappropriate.

Trueness

In the absence of certified reference materials for SSA samples, the trueness was alternatively evaluated as the recovery of spiked samples.[192] Recoveries were determined on four occasions, for three concentration levels with six replicates, using the matrix-matched calibration curves. Average recoveries ranged between 85.3 and 101.8% (RSD<8.2%) and are summarized in Table 3.1.

Precision

The repeatability and the within-laboratory reproducibility were evaluated using the recovery data. The repeatability standard deviation (s_r) and the intermediate precision or the within-laboratory reproducibility standard deviation (s_I) were assessed following the guidelines of Eurachem.[191] The relative s_r (i.e., repeatability RSD) was determined from the results (n=18) of the main operator (i.e., three experiments under repeatable conditions over 3 days). The relative s_I (i.e., within-laboratory reproducibility RSD) included the additional results of the second operator (n=24) and combined the within- (s_r) and between- (s_b) group variance. The method showed an adequate precision, as both the repeatability and reproducibility RSDs were between 5.8 and 17.2% (Table 3.1).

Table 3.1: Multiple day validation results for the phycotoxin extraction and analysis from quartz filters. The three concentration levels spiked on these quartz filters represent 1.5, 2 and 2.5 times the (rounded) LOQ-levels (i.e., 1 ng mL^{-1}).

Compound	Level (ng mL^{-1})	Recovery (%) (average ± SD)	LOD (ng mL^{-1})	LOQ (ng mL^{-1})	Precision		Linearity (R^2)
					Repeatability RSD (%) (n=18)	Within-lab reproducibility RSD (%) (n=24)	
OA	1.50	85.7 ± 6.4	0.17	0.58	13.3	15.0	0.995
	2.00	91.0 ± 3.1			15.2	15.9	
	2.50	94.5 ± 3.6			14.9	15.8	
hYTX	1.50	85.3 ± 6.5	0.33	1.01	12.5	13.6	0.997
	2.00	92.1 ± 3.6			17.2	16.6	
	2.50	93.4 ± 4.9			15.5	15.2	
YTX	1.50	88.3 ± 7.1	0.32	0.96	12.8	15.3	0.996
	2.00	93.4 ± 7.5			16.4	16.8	
	2.50	96.1 ± 7.2			9.0	12.9	
DTX-1	1.50	94.0 ± 4.5	0.32	0.98	8.8	11.5	0.998
	2.00	98.2 ± 5.6			8.2	11.4	
	2.50	96.6 ± 5.4			13.4	13.7	
AZA-1	1.50	97.1 ± 2.8	0.25	0.75	7.2	9.8	0.999
	2.00	101.5 ± 0.8			6.0	6.9	
	2.50	101.8 ± 4.3			5.8	7.2	
PTX-2	1.50	92.3 ± 7.5	0.40	1.20	14.9	16.0	0.990
	2.00	100.1 ± 4.0			16.0	14.6	
	2.50	99.8 ± 6.4			10.4	12.9	

3.4 Laboratory SSA experiments using spiked seawater

The two MART experiments, using artificial and natural seawater (both) spiked with toxin-producing algae, were conducted to characterize the basic and (more) realistic SSA processes of selected phycotoxins (OA, hYTX and DTX-1). The phycotoxin enrichment in the produced SSAs and SSML was determined, in addition to the phycotoxin concentrations of different size fractions in the three analyzed water layers (Figure 3.2A/B). The determined EF_{SSA} values (eq. 3.1) for the artificial seawater experiment ranged from 488 to 1769. This strong SSA enrichment explain the high phycotoxin air concentrations (0.93-13.3 ng m^{-3}) that were measured. The EF_{SSA} values for the natural seawater experiment ranged from 78 to 520, and were significantly ($p<0.05$; 95% confidence level) lower for hYTX and DTX-1 as compared to the artificial seawater. These MART experiments showed that aerosolization and enrichment processes can be influenced by environmental factors (e.g., particulate organic matter concentration and foam stability due to natural surfactants). The EF_{SSML} values were relatively low and ranged from 2.9 to 5.7 and 1.3 to 6.4 for the artificial and natural seawater, respectively.

Note that the air concentrations and EF_{SSA} values were calculated using the combined results of the filter and filter holder extracts (i.e., total collected SSA). The Na^+ and phycotoxin distribution between the filter and its holder (Figure S3.10) was not different except for hYTX which had a significantly higher ($p<0.05$; 95% confidence level) $[TOX]_{SSA}/[Na^+]_{SSA}$ ratio (and thus EF_{SSA}) for the filter holder sample than for the filter sample. As discussed below, this differential distribution can be attributed to a higher particulate fraction of hYTX in the SSW and SSML. In addition, these experiments confirmed the good collection efficiency of our sampling method, as the extra control SSA sampling generally showed a low Na^+ and phycotoxin breakthrough (as further discussed in Annex III section 7).

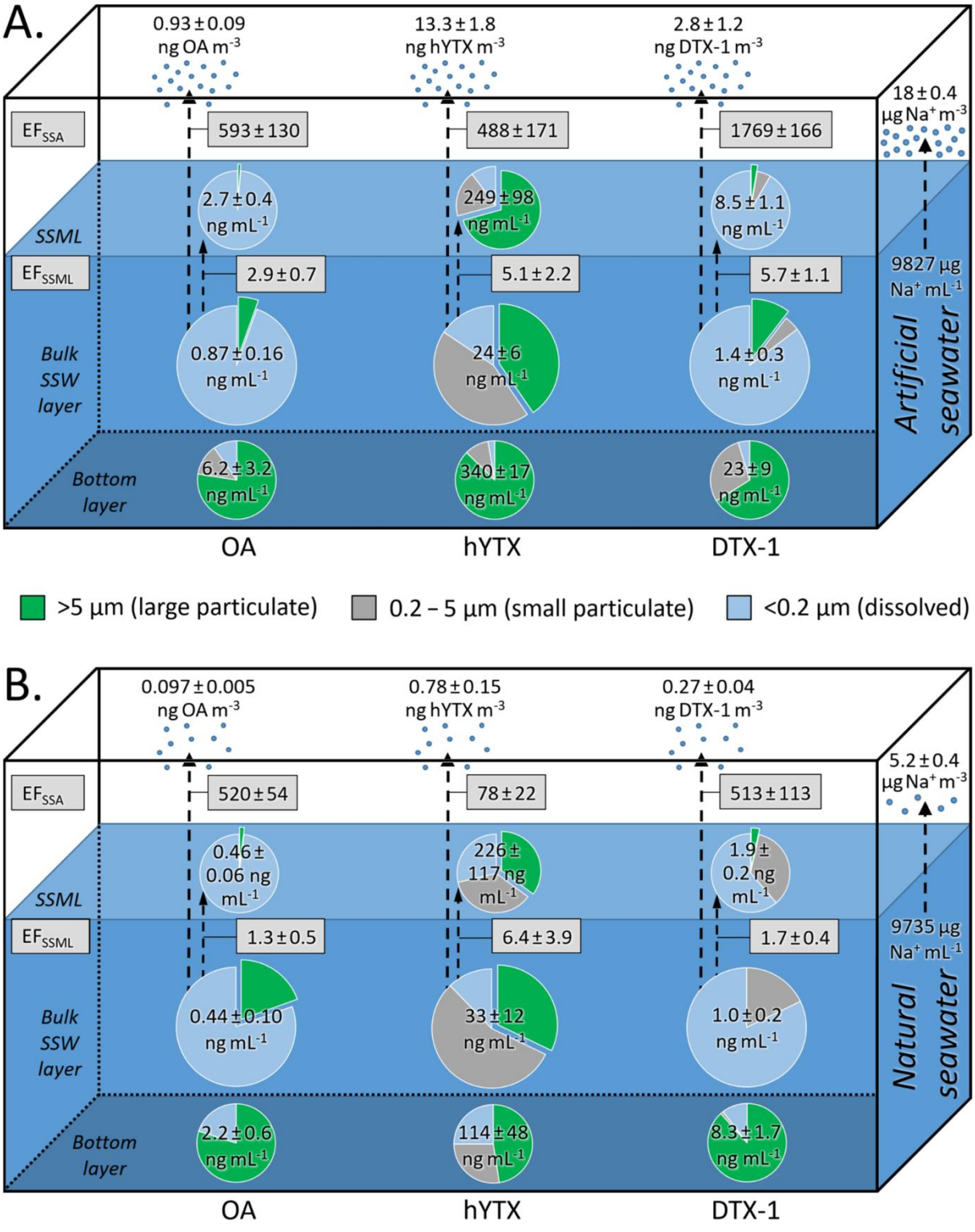

Figure 3.2: MART experiments using (A) artificial and (B) natural seawater, spiked with P. lima and P. reticulatum. The total OA, hYTX and DTX-1 concentrations in the (1cm) bottom layer, subsurface water (SSW) layer and sea surface microlayer (SSML) are shown with their respective distribution over the different size fractions. The Na^+ and phycotoxin air concentrations are displayed in the headspace. The mean phycotoxin enrichment factors (i.e., EF_{SSA} and EF_{SSML}) are presented in gray rectangles.

3.5 Estimated coastal air concentrations

The SSAs collected on the beach (seven beach club and three lifeguard chair samples) did not contain detectable phycotoxins, hence only environmental $[Na^+]_{coastal\ air}$ values are reported (Table 3.2A). In the eight concurrent MART experiments with pure natural seawater, however, OA was always detected. The concentrations in the SSA extracts ranged from 0.17 to 0.81 ng mL^{-1}, representing concentrations up to 34 pg m^{-3} in the MART's headspace. OA could be quantified in at least two of the three replicate SSA samples during each MART experiment. The measured Na^+ concentrations in the MART's headspace ranged from 6.5 to 16.3 µg m^{-3}. The magnitude of SSA production was thus between those measured in the previous MART experiments using artificial and natural seawater spiked with toxin-producing algae (Figure 3.2A/B). For every MART experiment a $[OA]_{SSA}/[Na^+]_{SSA}$ ratio (Table 3.2B) was determined. Using this empirical ratio, the measured $[Na^+]_{coastal\ air}$ and the strategy summarized in eq. 3.2, we indirectly quantified $[OA]_{coastal\ air}$ at every beach sampling site for each sampling day (Table 3.2C). On days when $[Na^+]_{coastal\ air}$ was measured but no MART experiments were performed, $[OA]_{coastal\ air}$ values were calculated using the average of the preceding and succeeding $[OA]_{SSA}/[Na^+]_{SSA}$ ratio.

Table 3.2: Results of (A) the SSA sampling events performed on a beach during July 2017 (i.e., $[Na^+]_{coastal\ air}$), (B) the simultaneously performed MART experiments using (pure) natural seawater (i.e., $[OA]_{SSA}/[Na^+]_{SSA}$ ratios), and (C) the subsequent (indirectly) quantified OA concentrations in the coastal air (i.e., $[OA]_{coastal\ air}$) using the strategy summarized in eq. 3.2. Cells denoted with (-), indicate that no samples were collected for that time point. Note that the OA content in the environmental samples was always below the LOD and are thus not given.

	A. Environmental $[Na^+]_{coastal\ air}$ (µg m^{-3}) *(sampled air volume)*		**B.** Experimental MART-based $[OA]_{SSA}/[Na^+]_{SSA}$ (pg μg^{-1})	**C.** Environmental indirectly quantified $[OA]_{coastal\ air}$ (pg m^{-3})	
	Beach club	*Lifeguard chair*		*50 m inland*	*Near waterline*
04-jul-2017	-	-	2.00 ± 0.32	-	-
06-jul-2017	2.1 (*4.9 m³*)	-	1.45 ± 0.18	3.0	-
07-jul-2017	1.2 (*4.5 m³*)	-	-	1.3	-
10-jul-2017	1.8 (*4.7 m³*)	-	0.73 ± 0.07	1.3	-
12-jul-2017	-	28.1 (*0.46 m³*)	-	-	49
13-jul-2017	0.23 (*4.0 m³*)	-	2.76 ± 0.96	0.62	-
18-jul-2017	12 (*3.9 m³*)	64.0 (*1.87 m³*)	0.80 ± 0.06	9.5	51
19-jul-2017	-	-	1.58 ± 0.31	-	-
20-jul-2017	4.9 (*4.5 m³*)	-	-	5.6	-
24-jul-2017	8.4 (*4.3 m³*)	-	0.71 ± 0.16	6.0	-
26-jul-2017	-	9.0 (*1.1 m³*)	-	-	7.3
28-jul-2017	-	-	0.91 ± 0.32	-	-

In addition, the average Mg^{2+}/Na^{+} mass ratios of the environmental SSA samples (11.7 ± 0.7%) and the MART SSA samples (12.1 ± 0.8%) were consistent with the ratio in seawater (11.9%).[204,205] These results thus confirm the SSA origin of the analyzed Na^{+}.

4 Discussion

Both in the context of the observed negative effects of red tide aerosols[17] and the beneficial biogenics hypothesis,[46] research on the aerosolization of marine phycotoxins is gaining interest. In this study, we investigated the aerosolization of marine phycotoxins that have not (yet) been associated with harmful effects on the human respiratory system.

4.1 Method development

As appropriate methodologies to quantify this airborne exposure were largely lacking, our first aim was to develop such dedicated tools. We optimized a sampling method for SSAs. Following optimization, the linearity of the collected Na^{+} as a function of the MART sampling time (R^2>0.90; Figure S3.4), and the low (filter) breakthrough of Na^{+} and phycotoxins (see Annex III section 7) demonstrated the good collection efficiency of our final SSA sampling method. Next, we optimized and successfully validated the UHPLC-HR-Orbitrap-MS method to analyze phycotoxins in SSA samples, according to dedicated guidelines.[191–194] This method was specific to six phycotoxins and showed a good linear response (R^2>0.99), low LOQ levels (0.58-1.20 ng mL^{-1}), high and stable recoveries (85.3-101.8%), and acceptable precision (RSDs between 5.8 and 17.2%). In comparison with analytical methods for the same phycotoxins in different matrices (e.g., bivalves,[131,133,134] algae,[132] and passive samplers[131]), our method showed similar or better results for the described validation criteria. The method's applicability was extensively demonstrated in the subsequently performed MART experiments. These aerosolization experiments produced the first quantitative detection for OA, hYTX and DTX-1 in an (experimental) SSA phase. The determined LOQ and indirectly quantified $[OA]_{coastal\ air}$ values (Table 3.2C) suggest that direct phycotoxin quantification in environmental SSAs is possible using the developed method. Such direct quantification, however, requires the sampling of larger air volumes (i.e., one order of magnitude higher).

4.2 Laboratory SSA experiments using spiked seawater

In the next stage of our study, the concurrent measurement of Na^+ and phycotoxins in both the SSW and SSA samples allowed us to characterize the enriched aerosolization of phycotoxins (Figure 3.2). A good quantitative understanding of these enrichment processes is of major importance as these may greatly increase the air concentrations ($[TOX]_{coastal\ air}$) that humans are exposed to. To our knowledge, Pierce *et al*.[206] are the only ones who have quantified SSA enrichment for harmful phycotoxins prior to our study (i.e., EF_{SSA} from 5 to 50 for PbTxs). They used the micro-algae *Karenia brevis* in combination with a SSA generator. Their EF_{SSA}-range is 1 to 2 orders of magnitude lower than that determined in this study for OA, hYTX and DTX-1. This difference cannot be attributed to hydrophobicity properties, as the principal PbTx(-2) analogue[206] had a log Kow value (i.e., 3.7) similar to OA, hYTX and DTX-1 (i.e., 3.4-3.8). Olson et al.[207] – who recently performed lake spray aerosol (LSA) experiments - found that aerosolization of diverse microcystins was dependent on their hydrophobicity. They[207] reported an EF_{LSA} value of 10 for the hydrophilic microcystin-RR (log Kow = -0.2), while the hydrophobic microcystin-LA (log Kow = 3.5) had an EF_{LSA} of 2000. The limited available literature on SSA enrichment processes (overview in Table S3.6), shows that EF_{SSA} values can vary greatly depending on the compound's chemical properties and that enrichment is inversely related to the SSA size. The latter observation can be attributed to the different SSA production mechanisms.[73,87]

Fine film drop SSAs are produced by the bursting bubble films[61,62] which are highly enriched with hydrophobic and surface-active materials.[59,208–210] Conversely, the coarser jet drop SSAs, produced by the overshooting water jet,[61,62] include a large fraction of non-enriched SSW.[88] The study by Keene et al.[92] mainly confirms this inverse relation between enrichment and SSA size, but reports a somewhat contradictory trend for the largest size fractions. They collected SSAs using an 8-stage impactor (i.e., 10 size fractions) and found a significantly higher organic carbon (OC) enrichment in the two largest fractions ($EF_{SSA} = \pm10^3$ and $\pm10^4$ for 10-18 µm and >18 µm, respectively) as compared to the third largest fraction ($EF_{SSA} = \pm10^2$ for 5.6-10 µm). These observations[92] can be explained by the short-lived jet drop[85] aerosolization of large particulate matter[76] or (fragments of) microorganisms (e.g., algae).[80–82] Aerosolized (toxin-producing) algae are basically dense accumulations of (non-excreted) phycotoxins[142] and other organic compounds. The consistently higher

deposition of hYTX on our filter holders as compared to Na^+, OA and DTX-1 (Figure S3.10), can be explained by the above-cited (literature) findings because (1) the largest SSAs have a relatively higher deposition on the filter holder than on the filter (due to gravitational settling)[211] and (2) the large particulate fraction in the SSW and SSML was much higher for hYTX than for OA and DTX-1 (Figure 3.2). The latter can be attributed to the fact that hYTX was produced by the pelagic *P. reticulatum,* which accumulated in the SSML. For the artificial seawater experiment for example, *P. reticulatum* cell counts were, on average, five times higher in the SSML as compared to the SSW, while *P. lima* concentrated in the bottom layer (see Figure S3.11).

Quinn *et al*.[85] performed aerosolization experiments using polystyrene beads that, like *P. reticulatum*, tend to float in the SSML. Higher concentrations of these polystyrene particles, however, did not result in higher aerosolization. It appears that jet drops have a limited capacity to aerosolize the particulate fractions in the SSML. Our finding that the hYTX EF_{SSA} was 6.2 times lower in the natural seawater experiment (Figure 3.2A/B) may be explained by the naturally occurring particles and microorganisms, in this (unfiltered) seawater, which competed for jet drop aerosolization. In addition, the lower large particulate fraction of hYTX in the SSML (Figure 3.2A/B) may increase this competition effect. For OA, which was nearly entirely dissolved in the SSW and SSML, the EF_{SSA} did not differ significantly ($p>0.05$; 95% confidence level) between the natural and artificial seawater experiments. This may suggest that the aerosolization of the dissolved fraction is much less susceptible to interference of other dissolved compounds in seawater.

SSA enrichment is usually attributed to the preceding enrichment in the SSML. Our results and the literature summarized in Table S3.6, clearly show that the EF_{SSML} values are often a few orders of magnitude lower than the corresponding EF_{SSA} values. Hoffman and Duce[208] also showed a positive relation between the distance traveled by rising air bubbles and the EF_{SSA}. In agreement with Quinn *et al*.'s work,[87] we conclude that the scavenging (enrichment) process of rising air bubbles determines the EF_{SSA} of (dissolved) compounds like phycotoxins to a far greater extent than SSML enrichment does. Another interesting observation made during the natural seawater experiment was the high foam stability (Figure S3.12). Medina-Pérez et al.[25] observed – using

Ostreopsis cf. *ovata* cultures in a SSA generator – a very large counter effect of foam stability on the aerosolization of amphiphilic, surface active ovatoxins (OVTXs). Foam stability is generally attributed to (marine) surfactants, which increase the bubble lifetime at the surface,[212,213] resulting in a more depleted/thinner bubble film and ultimately a lower SSA production.[85,213] This decreased production was also observed in our natural seawater experiment during which a 3.5 times lower $[Na^+]_{air}$ values was measured (Figure 3.2A/B). We therefore recommend using natural seawater in SSA experiments to examine the (realistic) aerosolization of particulate fractions, while artificial seawater can also be used for dissolved organic compounds.

4.3 Coastal air concentrations and human health

In the final stage of our study, we combined the results of the ambient SSA samples (beach) and experimental (MART) SSA samples (Table 3.2A/B) to indirectly quantify environmental air concentrations (i.e., $[OA]_{coastal\ air}$ = 0.62-51 pg m^{-3}; Table 3.2C). Note that, due to the assumption that beach samples mainly contain nascent SSAs and thus have the same $[TOX]_{SSA}/[Na^+]_{SSA}$ as in the MART experiments, this concentration range should be viewed as an order of magnitude rather than exact values. During the sampling period, no HAB events were observed. The quantified $[OA]_{coastal\ air}$ values are therefore much lower than those reported in the literature for sea spray aerosolized $[PbTx]_{coastal\ air}$ (1.3-180 ng m^{-3})[23,24,144] and $[OVTX]_{coastal\ air}$ (2.4 ng m^{-3}),[22] or freshwater microcystins (<2.89 ng m^{-3})[214] aerosolized via lake spray.[207,215] These reported high PbTx and OVTX exposure levels induced respiratory syndromes.[17,138] For the lake spray aerosolized microcystins there have been no reported cases inducing negative health effects. It has however been shown that mice are 10 times more sensitive to microcystins via inhalation than via ingestion.[216,217] As further discussed in Chapter 6 section 2-Q4, due to the absence of (in vivo) toxicological data for the respiratory exposure to OA, a robust risk assessment for the highest $[OA]_{coastal\ air}$ (i.e., 51 pg m^{-3}) determined here is currently not possible and too arbitrary to be trustworthy. To date, there have been no reported (medical) cases of respiratory syndromes upon airborne exposure to SSAs, during HABs of OA-producing algae. It therefore seems rather unlikely that the current $[OA]_{coastal\ air}$ induce negative health effects. We also do not expect health risks related to any other phycotoxin, because (1) DSP toxins (i.e., OA and DTXs) are the dominant phycotoxins in the North Sea[151–153] and (2) no other phycotoxins were detected in our MART experiments using pure natural seawater.

In previous studies, we[179,180] and others[145] have studied the potential positive health effects of airborne exposure to other phycotoxins (beside OA) using in vitro assays. These studies showed, among others, that YTXs can downregulate the mTOR pathway, that is, the crucial cellular pathway in Moore's biogenics hypothesis.[46] The current study demonstrates the potential for exposure to YTXs through SSAs and therefore supports, combined with the above-cited effect studies,[145,179,180] the principles of the biogenics hypothesis. This highlights that, in addition to adverse effects of phycotoxins, SSAs can provide an exposure route for a whole spectrum of marine compounds with positive pharmacological effects.[26,27]

Chapter 4

Sea spray aerosols interact with the mTOR pathway at a molecular level

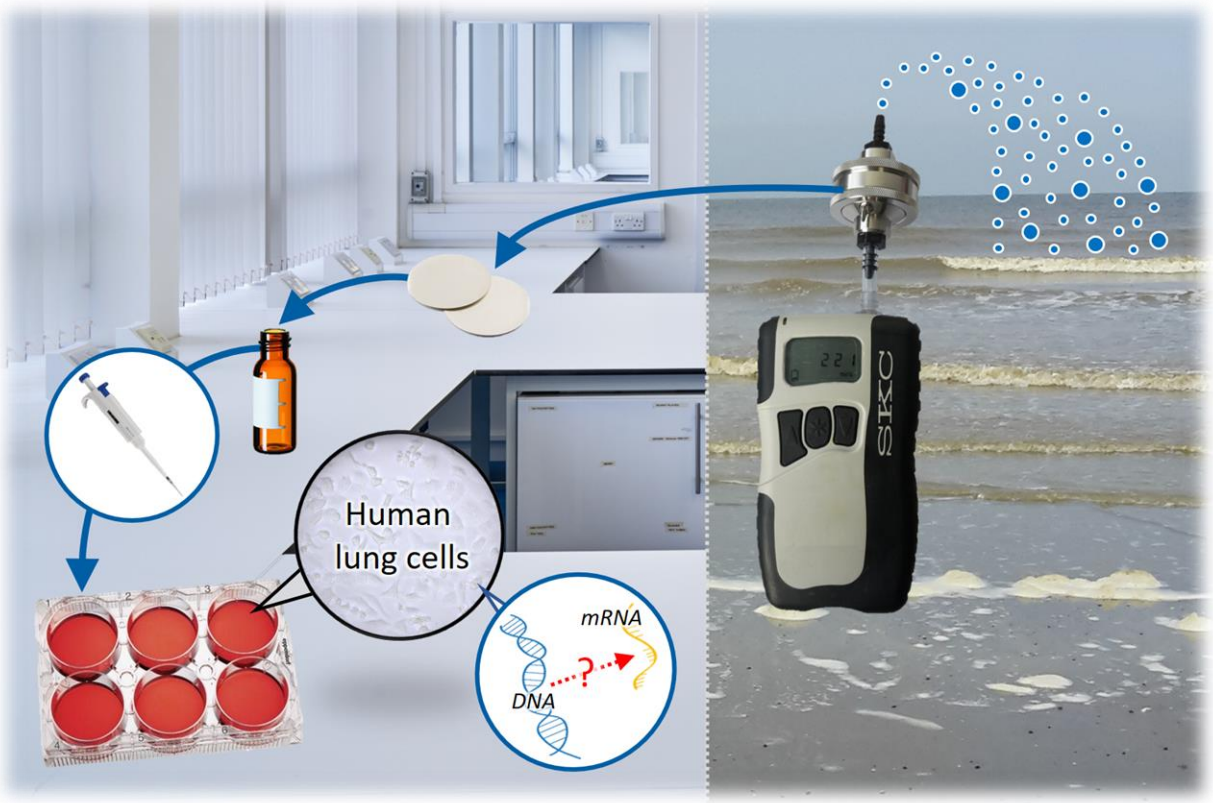

Redrafted from ([§] shared first):

Asselman, J.[§]; Van Acker, E.[§], De Rijcke, M.; Tilleman, L.; Van Nieuwerburg, F.; Mees, J.; De Schamphelaere, K..; Janssen, C. Marine biogenics in sea spray aerosols interact with the mTOR signaling pathway. Scientific Reports ***2019****, 9, 1–10*

Chapter contents

Abstract

SSAs contain microbiota and natural compounds which could affect human health. Yet the exposure and effects of SSAs on human health remain poorly studied. Here, we exposed human lung cancer cells during an exposure period of 43 h to (1) the extract of a natural SSA, (2) the marine phycotoxin hYTX, (3) the extract of a laboratory-generated SSA containing hYTX, and (4) a chemical inhibitor of the mTOR pathway. By using RNA sequencing, we characterized the molecular responses (i.e., differential gene expression) of the lung cells to the different treatments. We observed significant increased expression of genes related to the mTOR pathway and proprotein convertase subtilisin/kexin type 9 (PCSK9) after exposure to hYTX and the laboratory-generated SSA. In contrast, we observed a significant decreased expression of the genes related to the mTOR pathway and PCSK9 after exposure to the natural SSA and the mTOR inhibitor, suggesting induction of apoptosis. These effects, observed in the natural SSA treatment, are thus induced by other marine compounds than YTXs. Our results indicate that marine compounds in SSAs interact with PCSK9 and the mTOR pathway, and that they can be further explored for potential new pharmaceutical applications. Overall, our results provide molecular evidence for potential beneficial health effects at environmental relevant concentrations of natural SSAs.

1 Introduction

The ocean contains a variety of biogenic or naturally produced compounds that become airborne via sea spray aerosolization.[218–220] In addition to bacteria, many phytoplankton species also produce a wide range of bioactive compounds such as vitamins, pigments, polyphenolics and phycotoxins.[121,221] Phycotoxins have primarily been studied in the context of harmful algal blooms (HABs), in which they can be present at detrimental concentrations.[23,121] Human intoxications with phycotoxins mainly occur via seafood consumption and more specifically via shellfish poisoning.[121,222,223] Furthermore, some of these phycotoxins can cause health effects through their presence in SSAs. This has been reported for PbTxs, i.e., a group of toxic cyclic polyethers produced by the dinoflagellate *K. brevis*.[224] Exposure to aerosolized PbTxs can lead to respiratory symptoms in humans during HAB conditions, particularly in people with asthma,[177,225] and have been well-studied and documented.[23,177,224,225]

Little attention has been given to other phycotoxins and to their potential effects at the low, environmentally relevant, concentrations in which they may be present in SSAs during regular environmental conditions.[82] In addition, some of these bioactive compounds (e.g., yessotoxins (YTXs))[145] have been targeted for their pharmaceutical or biotechnological potential.[104,226] YTXs, produced by marine dinoflagellates such as *Protoceratium reticulatum*, appear to induce apoptotic cell death through the mammalian target of rapamycin (mTOR) pathway[164,180] and seems to inhibit tumor growth.[227] Combined with other unidentified compounds in the marine environment, these known bioactive compounds could contribute to beneficial health effects in coastal environments. A number of studies highlight several health promoting pathways through which airborne microbiota and compounds from blue and green environments may have beneficial health effects.[45,46] Airborne microbiota are thought to contribute to a more effective immunoregulation once inhaled or ingested.[45] Additionally, it was suggested that inhalation of low levels of microbes and parasites reduces inflammation and improves immunoregulation.[45,46] Biogenic or natural compounds produced by plants, fungi, phytoplankton species and bacteria,[48,218,219] have been hypothesized to induce positive health effects via the interaction with specific cell signaling pathways such as the mTOR pathway.[46] This pathway is a key regulator of cell growth and cell proliferation that integrates signals from both the environment (e.g., nutrients) and internal processes (e.g., energy status, growth factors) to regulate several cell processes including autophagy and energy metabolism.[228] The link between the mTOR pathway and beneficial health effects is supported by a number of studies,[52,229–231] demonstrating that its inhibition is associated with health benefits such as anti-cancer and anti-inflammatory effects.

Here, we hypothesize that beneficial health effects of SSAs in coastal environments can be attributed to interactions between bioactive marine compounds such as yessotoxin (YTX) and the mTOR pathway. To this end, we exposed human lung cells to (1) the pure compound homoyessotoxin (hYTX), (2) the extract of a SSA generated in a marine aerosol reference tank (MART) inoculated with the hYTX producing dinoflagellate *P. reticulatum*,[232] (3) a natural SSA collected at the seashore, and (4) a chemical inhibitor of the mTOR pathway (Torkinib/PP242). In our design, we start from the simplest situation: exposure to a biogenic compound (hYTX) as a single substance, extrapolate to a more complex but characterized laboratory-generated sample and

finally to a black-box environmental mixture (i.e., natural SSA). We used RNA sequencing to characterize the molecular responses. The different treatments, including different dose levels per treatment, allowed us to study a range of conditions, from most realistic, i.e., natural SSA, to the simplest, i.e., a single marine compound (hYTX). With this experimental design, we will address the following research questions: (1) are the effects of pure hYTX similar to the effects of hYTX in a laboratory-generated SSA matrix, (2) can the effects of the extract of a laboratory-generated SSA be extrapolated to the effects of a natural collected SSA, when dosed at more environmentally realistic levels, and (3) do hYTX, the extract of a laboratory-generated SSA (containing hYTX) and the extract of a natural collected SSA interact with the mTOR pathway in human lung cells. As such, we aim to provide molecular evidence to support the hypothesis that SSAs are a source of health benefits such as anti-cancer, positive cardiovascular and anti-inflammatory effects.

2 Materials and methods

2.1 Lung cell culturing

The used lung cell culturing methods were identical as in Chapter 2 (section 2.2). In short, adenocarcinoma alveolar basal cells (A549) were grown in Dulbecco's modified eagle medium (DMEM), including phenol red, 10% heat-inactivated fetal bovine serum (FBS), 100 U mL^{-1} penicillin, and 100 µg mL^{-1} streptomycin, at 5% CO_2, 37 °C, and >95% relative humidity. Confluent cultures were sub-cultured, using 0.5% Trypsin–EDTA, and split twice a week in a 1:8 ratio or used in experiments as explained below.

2.2 Experimental procedure

Confluent cell cultures were trypsinized and transferred in 3 mL fresh DMEM to Nunc 6-well plates at a density of 320,000 cells $well^{-1}$. After seeding, cells were incubated for 10 h at 37 °C, 5% CO_2 and >95% relative humidity to stimulate growth and adherence to the surface. Then, cells were subjected to one of five treatments and incubated for another 43 h at identical conditions prior to RNA extraction. The five treatments included (1) unexposed cells as a negative control, (2) an extract of a natural SSA sample from the seashore, (3) an extract of a laboratory-generated SSA containing hYTX, (4) pure hYTX, (5) a chemical inhibitor of the mTOR pathway,

i.e., 0.3 µM Torkinib or PP242 (LC Laboratories), as a positive control. The negative control treatment also contained 2% methanol to exclude a solvent effect as all other treatments were extracted, diluted or dissolved in methanol.

SSA samples were collected on Whatman® QM-A quartz microfiber filters (Ø 47 mm), enclosed in stainless steel in-line filter holders (Pall Corporation). The laboratory-generated SSA extract containing hYTX was generated as described in Chapter 2 section 2.1. In short, SSAs were produced in a marine aerosol reference tank (MART) filled with artificial seawater (i.e., L1-medium; see Annex III section 1) and inoculated with hYTX-producing *P. reticulatum* at 10^6 cells L^{-1}. The SSAs were sampled during 16 h, and subsequently extracted and analyzed on their Na^+ and phycotoxin (i.e., hYTX) contents following the dedicated methods described in Chapter 3 (sections 2.3-2.5). This laboratory-generated SSA extract, which is hereafter referred to as the lab SSA (extract) treatment, thus contained a known hYTX concentration and a mixture of other aerosolizable compounds (with unknown concentrations). The natural SSA sample was collected at the waterline close to Ostend, Belgium (51°14′27″N, 2°56′10″E) by sampling for 46 min at a constant air flow of 10 L min^{-1} using a battery-powered Leland Legacy personal sampling pump (SKC). The sampling flow rate corresponded to the minute ventilation of an average human in rest (9–10 L min^{-1}).[233,234] During sampling, the wind direction was 0.7 ± 3.1° (North) and wind speed was 15.0 ± 0.6 m s^{-1}, indicating white cap SSA production. This natural SSA filter sample was extracted and analyzed following the dedicated methods described in Chapter 3 (sections 2.3-2.5). The filters of the natural SSA and lab SSA were thus extracted following the same methanol extraction procedures. In contrast to the Na^+ content, the phycotoxin content was not analyzed in the natural SSA sample. Based on the analysis of similar SSA samples from that time period (i.e., July 2017; see Chapter 3), however, we can conclude that no phycotoxins would have exceeded the LODs in this rather small sample. The pure hYTX was purchased as a certified reference standard (5 µM hYTX in methanol) from the National Research Council Canada.

To allow an optimal comparison between the hYTX treatment and the lab SSA treatment the dose levels were determined based on the hYTX concentrations. The pure hYTX reference material and lab SSA extract (containing hYTX) were diluted in methanol to obtain the following hYTX dose levels: 0.5 µg L^{-1} (high), 10^{-2} µg L^{-1} (mid), 10^{-5} µg L^{-1} (low). These hYTX doses were identical to the ones used in the western

blotting experiment in Chapter 2 (see Figure 2.4), where this highest dose (i.e., 0.5 µg L^{-1}) showed a significant downregulation of the mTOR pathway activity. For the natural SSA, the low, mid and high doses were determined by comparing the total alveolar surface of human lungs with the cell surface available in a single well (9.6 cm^2), and by comparing the sample collection duration (46 min) with the experimental exposure duration (43 h), as discussed in SI (Annex IV section 1). We selected a low dose that represents the same exposure as the amount of inhaled SSA during the sampling period at the seashore but extended over a 43 h exposure period and normalized to the cell surface in a single well (detailed calculations are reported in Annex IV section 1). The mid and high dose represent a 10× and 40× concentration of the low dose level. These levels were specifically chosen to adhere to environmentally realistic (background) concentrations. The mid dose level (10× concentration) was based on the hypothesis of increased minute ventilation during physical exercise which is reported to vary between 70–100 L min^{-1} for both continuous and intermittent exercise.[234–236] The high dose level (40× concentration) was selected based on the hypothesis of increased aerosolization (i.e., wind/wave action) as well as activities at the shore line or at sea (e.g., swimming, sailing, windsurfing). The detailed procedure is described in SI (Annex IV section 1). An overview of all different treatments and concentrations levels is given in Table 4.1.

Table 4.1: Overview of the different experimental treatments. Note that the [Na^+] indicate additional concentrations that were added through the SSA treatments, as the DMEM (i.e., the medium) already contained 10.7 mg Na^+ $well^{-1}$.

Treatment	Dose level	Concentration relative to low dose	[hYTX] (µg L^{-1})	[Na^+] (µg $well^{-1}$)	[methanol] (%)
Natural SSA	Low	× 1	Unkown	0.014	2
(collected at the Belgium	Mid	× 10	Unkown	0.14	2
shore - black box mixture)	High	× 40	Unkown	0.6	2
Lab SSA	Low	× 1	10^{-5}	$6 \cdot 10^{-5}$	2
(generated in the labora-	Mid	× 10^3	10^{-2}	$6 \cdot 10^{-2}$	2
tory using the MART)	High	× $5 \cdot 10^4$	0.5	2.8	2
hYTX	Low	× 1	10^{-5}	0	2
(pure single substance)	Mid	× 10^3	10^{-2}	0	2
	High	× $5 \cdot 10^4$	0.5	0	2
mTOR inhibitor/positive control *(0.3 µM Torkinib/PP242)*	/	/	0	0	2
Negative control	/	/	0	0	2

2.3 RNA extraction, library preparation and sequencing

RNA was extracted using the Qiagen RNEasy kit following the manufacturer's instructions including DNAse digestion. After RNA extraction, the concentration and quality of the total extracted RNA was checked by using the 'Quant-it ribogreen RNA assay' (Life Technologies) and the RNA 6000 nano chip (Agilent Technologies), respectively. Subsequently, 250 ng of RNA was used to perform an Illumina sequencing library preparation using the QuantSeq 3′ mRNA-Seq Library Prep Kits (Lexogen) according to manufacturer's protocol. During library preparation 14 PCR cycles were used. Libraries were quantified by qPCR, according to Illumina's protocol 'Sequencing Library qPCR Quantification protocol guide', version February 2011. A high sensitivity DNA chip (Agilent Technologies) was used to control the library's size distribution and quality. Sequencing was performed on a high throughput Illumina NextSeq500 flow cell generating 75 bp single reads.

2.4 Data analysis

Per sample, on average $7.5 \times 10^6 \pm 1.6 \times 10^6$ reads were generated. First, these reads were trimmed using cutadapt[237] version 1.15 to remove the "QuantSEQ FWD" adaptor sequence. The trimmed reads were mapped against the Homo sapiens GRCh38.89 reference genome using STAR[238] version 2.5.3a. The RSEM[239] software, version 1.3.0, was used to generate the count tables. Differential gene expression analysis between groups of samples was performed using edgeR.[240] Genes with less than 1 cpm in less than 4 samples were discarded, resulting in 16,546 quantifiable genes. Read counts were normalized using trimmed mean of M-values (TMM) followed by a pairwise comparison of treatments with the negative and positive control using an exact test.[240] Significantly differentially expressed (DE) genes were called at a false discovery rate of 0.01. Significant enrichment of KEGG pathways[241] with differentially expressed (DE) genes was done using a fisher test and called at an adjusted p-value level of 0.01. Benjamini-Hochberg adjustment was used to account for multiple testing. Gene set enrichment analysis (GSEA) was conducted to detect enrichment in hallmark gene sets and genetic and chemical perturbations gene sets of the molecular signature database.[242] Enriched gene sets were identified at a false discovery rate of 0.01. A dose response analysis was performed with the maSigPro[243] R package for each of the three phycotoxin treatments. In a first step a general linear model was built with the

3 treatments, 3 concentrations and the square of each concentration. Statistical testing was done using the log-likelihood ratio statistic. Genes with a false discovery rate (FDR) <0.05 were considered significantly differential. In a second step, for each significant differentially expressed gene, an optimized regression model was created using stepwise backward regression. Exclusion of the quadratic term from the model was performed using a regression ANOVA, testing if the regression coefficients differed from 0 at a significance level of 0.05. Afterwards the goodness of fit (i.e., R^2) of each optimized regression model was computed. Genes with a goodness of fit greater than 0.8 were used in a hierarchical cluster analysis based on the correlation between the regression models of the genes.

3 Results

We quantified the expression of 16,565 genes and observed differential expression across all treatments. The highest number of DE genes was observed in the pure hYTX treatment, hereafter referred to as hYTX. We observed a decreasing number of differentially expressed genes in the chemical mTOR inhibitor treatment, the natural SSA treatment and the lab SSA (containing hYTX) treatment. We observed significant DE genes in all treatments at the highest dose levels at false discovery rates (FDR) of 0.01 and 0.05 (Figure 4.1A). Given the small difference between the two FDRs, the most conservative FDR was selected for further analysis. We identified two DE genes shared by all high dose level treatments and the mTOR inhibitor (Figure 4.1B) and three DE genes shared by all high dose level treatments. The two DE genes shared by all (high dose level) treatments and the mTOR inhibitor (Figure 4.1B) were the small integral membrane protein 29 (SMIM 29) and proprotein convertase subtilisin/kexin type 9 (PCSK9). The three genes shared by all high dose treatments but not with the mTOR inhibitor were stearoyl-CoA desaturase (SCD), cytochrome P450 family 1 subfamily B member 1 (CYP1B1) and peptidyl arginine deiminase 3 (PADI3).

A. **Number of significant genes**

Treatment	Dose	FDR <0.01	FDR <0.05
mTOR Inhibitor		200	465
Natural SSA	Low	0	0
Natural SSA	Mid	0	0
Natural SSA	High	126	710
Lab SSA	Low	0	0
Lab SSA	Mid	0	0
Lab SSA	High	64	98
hYTX	Low	0	0
hYTX	Mid	0	2
hYTX	High	1088	1914

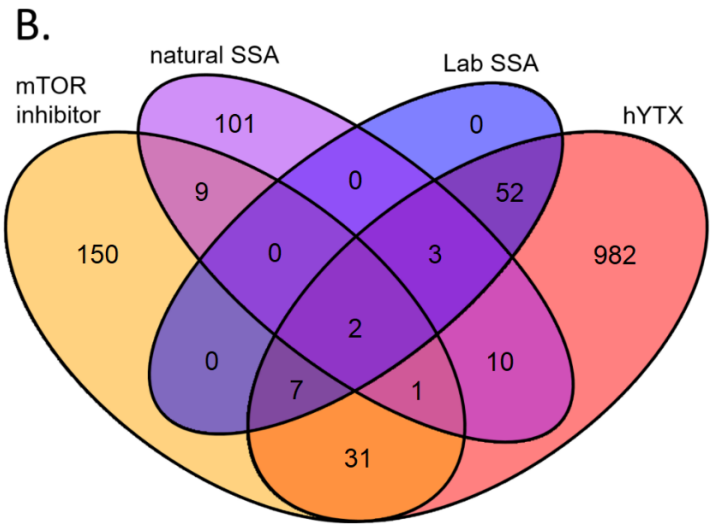

Figure 4.1: Differential gene expression across treatments. (A) Number of significant genes at different false discovery rates (FDR) for the different sea spray aerosols (SSA) treatments and homoyessotoxin (hYTX). (B) Venn diagram of shared significant genes across high dose treatments with significant genes at an FDR of 0.01.

We observed a total of 1898 genes with a significant dose response effect across the three treatments (hYTX, lab SSA and natural SSA). Based on a regression analysis and clustering, we found four clusters of dose response patterns. These clusters all showed the same trend which consists of a steep dose response curve for hYTX, while the lab SSA and the natural SSA showed a slower increase (Figure S4.1). A pathway analysis revealed four pathways that were enriched for genes with a significant dose response effect (Table S4.3). These pathways are the spliceosome, lysosome, steroid biosynthesis and glycogenesis.

3.1 Effect comparison of the hYTX and lab SSA treatments

First, we observed that all DE genes regulated by the lab SSA (containing hYTX) are a subset of the DE genes regulated by hYTX (Figure 4.1B). Second, for the five genes shared by the lab SSA, hYTX and the natural SSA (Figures 4.1B and 4.2), we saw the same dose response pattern for the hYTX and the lab SSA treatments: increasing gene expression with increasing dose. For SMIM 29, the responses to the highest dose (0.5 µg L^{-1}) of both the hYTX and lab SSA treatments were comparable to the increased expression for the mTOR inhibitor (Figure 4.2A). In contrast, PCSK9 was downregulated by the mTOR inhibitor while it was significantly upregulated at 0.5 µg L^{-1} of hYTX in both the hYTX and lab SSA treatments (Figure 4.2B). The three other genes were not significantly regulated by the mTOR inhibitor (Figure 4.2C–E).

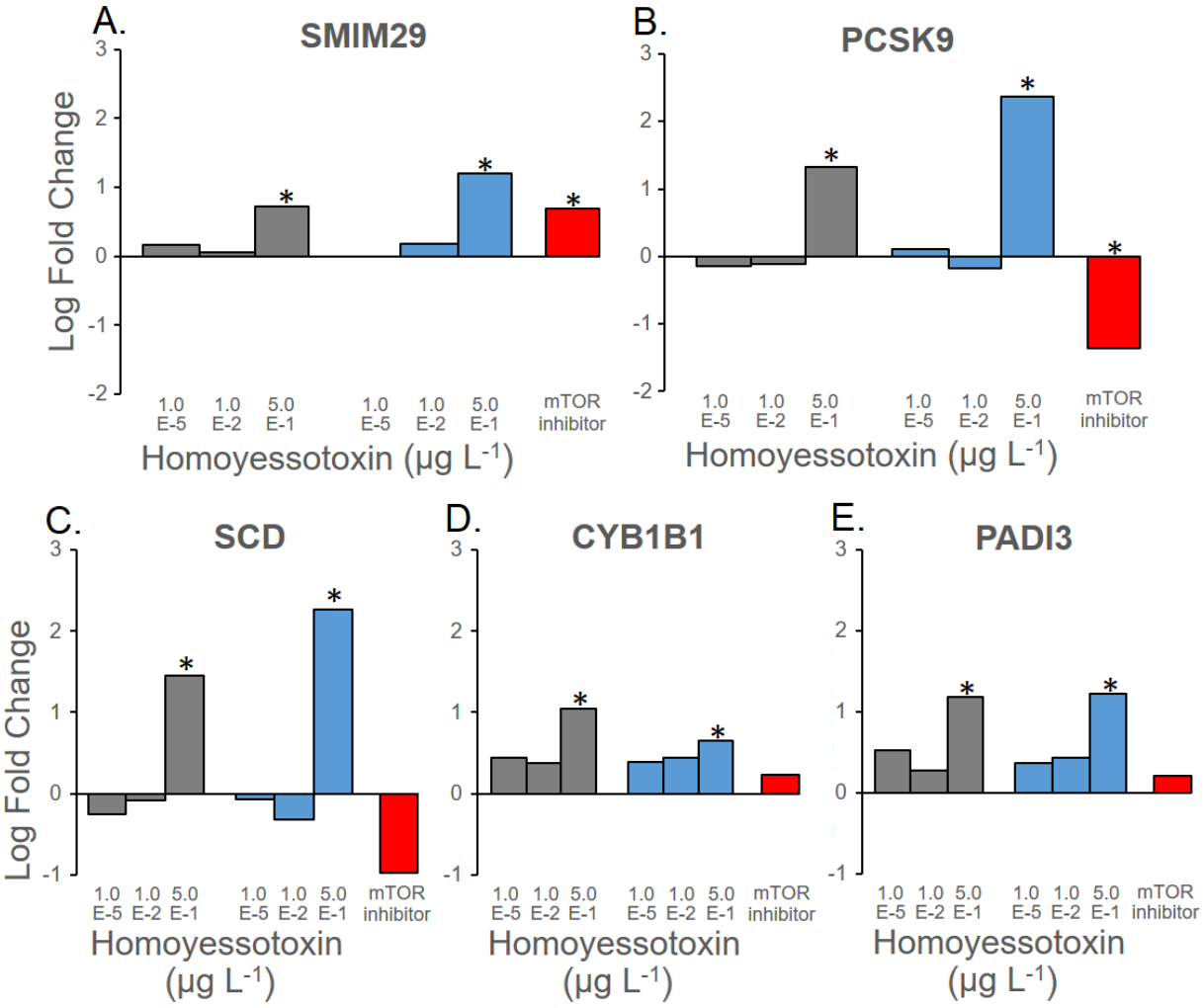

Figure 4.2: Differential gene expression in the (pure) homoyessotoxin treatment (hYTX, grey), the laboratory generated sea spray aerosol treatment (lab SSA, blue) and mTOR inhibitor treatment (red). Log fold change for (A) small integral membrane protein 29 (SMIM 29), (B) proprotein convertase subtilisin/kexin type 9 (PCSK9), (C) stearoyl-CoA desaturase (SCD), (D) cytochrome P450 family 1 subfamily B member 1 (CYP1B1) and (E) peptidyl arginine deiminase 3 (PADI3). Asterisk symbols denote significance at a false discovery rate of 0.01.

Third, at the pathway level, we observed an increase in upregulated and a decrease in downregulated genes with increasing dose levels of the hYTX treatment for all pathways (Figure 4.3). For the lab SSA, this same pattern was observed for the lysosome and steroid biosynthesis but not for the glycogenesis and the spliceosome (Figure 4.3). For the glycogenesis and the spliceosome, more upregulated genes in the highest and lowest dose treatment were observed while the mid dose treatment showed more downregulated genes (Figure 4.3A-B). For three of the four pathways, the mTOR inhibitor response was similar to the low dose of both the lab SSA and hYTX treatments (Figure 4.3A,C-D). For the spliceosome, the response differed (Figure 4.3B).

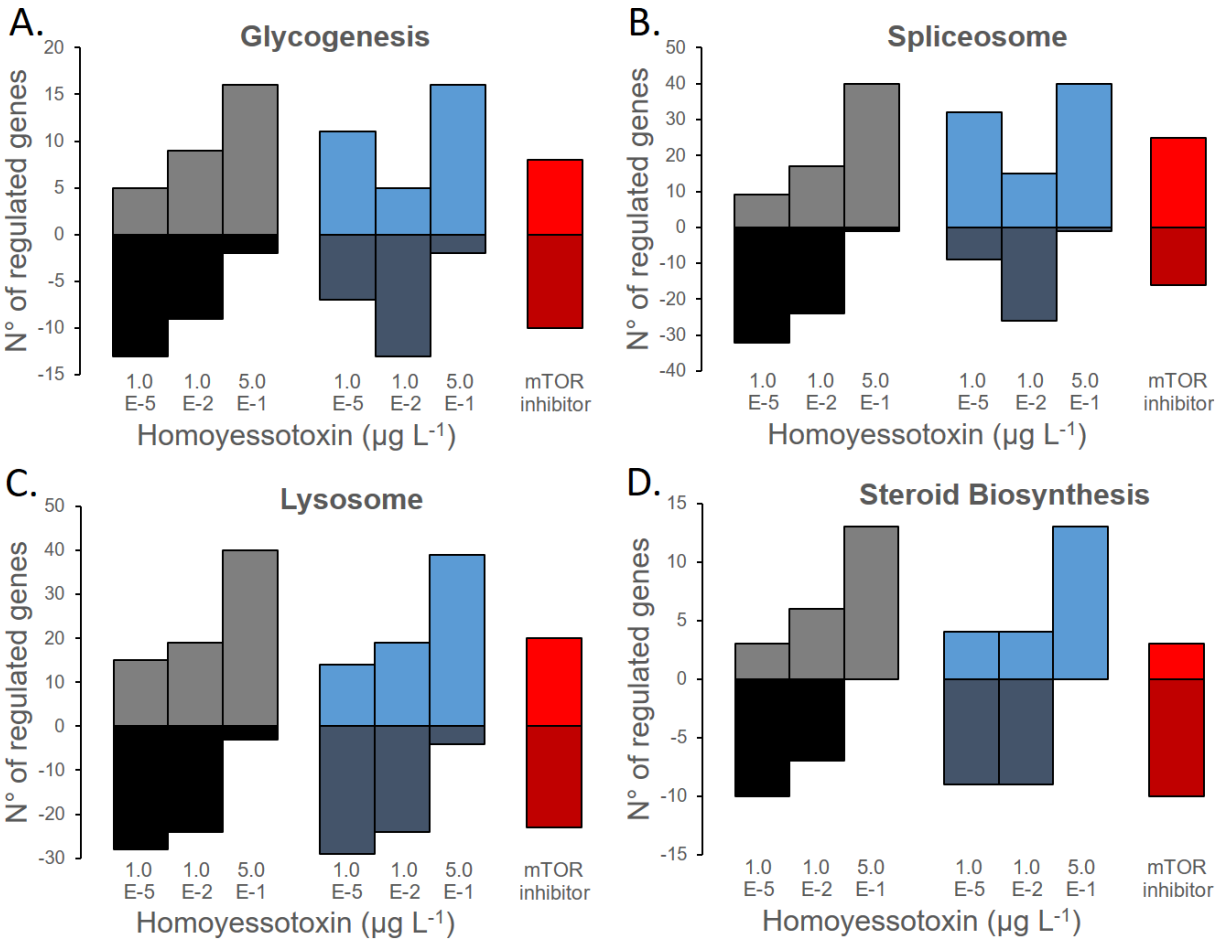

Figure 4.3: Dose response patterns in significantly affected pathways. Number of significantly upregulated (>0) or downregulated (<0) genes in (A) the glycogenesis, (B) spliceosome, (C) lysosome, (D) steroid biosynthesis for the treatments: homoyessotoxin (hYTX, grey), the lab sea spray aerosol (lab SSA, blue), and the mTOR inhibitor (red).

3.2 Effect comparison for the lab SSA and natural SSA treatments

Five DE genes that were shared between the lab SSA and the natural SSA treatments. These five genes were also shared with the hYTX treatment (Figures 4.1B and 4.4). A direct comparison between the natural and lab SSA can be made in terms of total mass of the sampled sea spray aerosol by using Na^+ as a proxy.[62] The lab SSA dose levels were 2.8, 0.06 and 0.00006 µg Na^+ $well^{-1}$ while the natural SSA dose levels, due to the smaller sample size, were 0.6, 0.14 and 0.014 µg Na^+ $well^{-1}$ (section 1.2). As such, the high dose natural SSA treatment is almost five times smaller, in terms of aerosol mass, than the high dose lab SSA treatment. This is due to the fact that the dose levels of the natural SSA were selected to represent realistic exposure scenarios whereas the lab SSA levels were selected to cover the effective range of hYTX. The low dose natural SSA can therefore be situated between the low and mid dose lab SSA, while the mid and high dose natural SSA between the mid and high dose lab SSA.

For three genes (i.e., SMIM29, CYP1B1, PADI3), the pattern was the same for both treatments with an increased gene expression with increasing dose levels (Figure 4.4A,D-E). The two other significantly affected genes (i.e., PCSK9 and SCD), showed a different pattern between these two treatments (Figure 4.4B-C). We observed an increased gene expression with increasing dose levels for the lab SSA but a decrease with increasing dose levels for the natural SSA (Figure 4.4). The mTOR inhibitor, which had a significant effect on both PCSK9 and SMIM29, showed the same response pattern as the highest dose treatment of the natural SSA (Figure 4.4A-B).

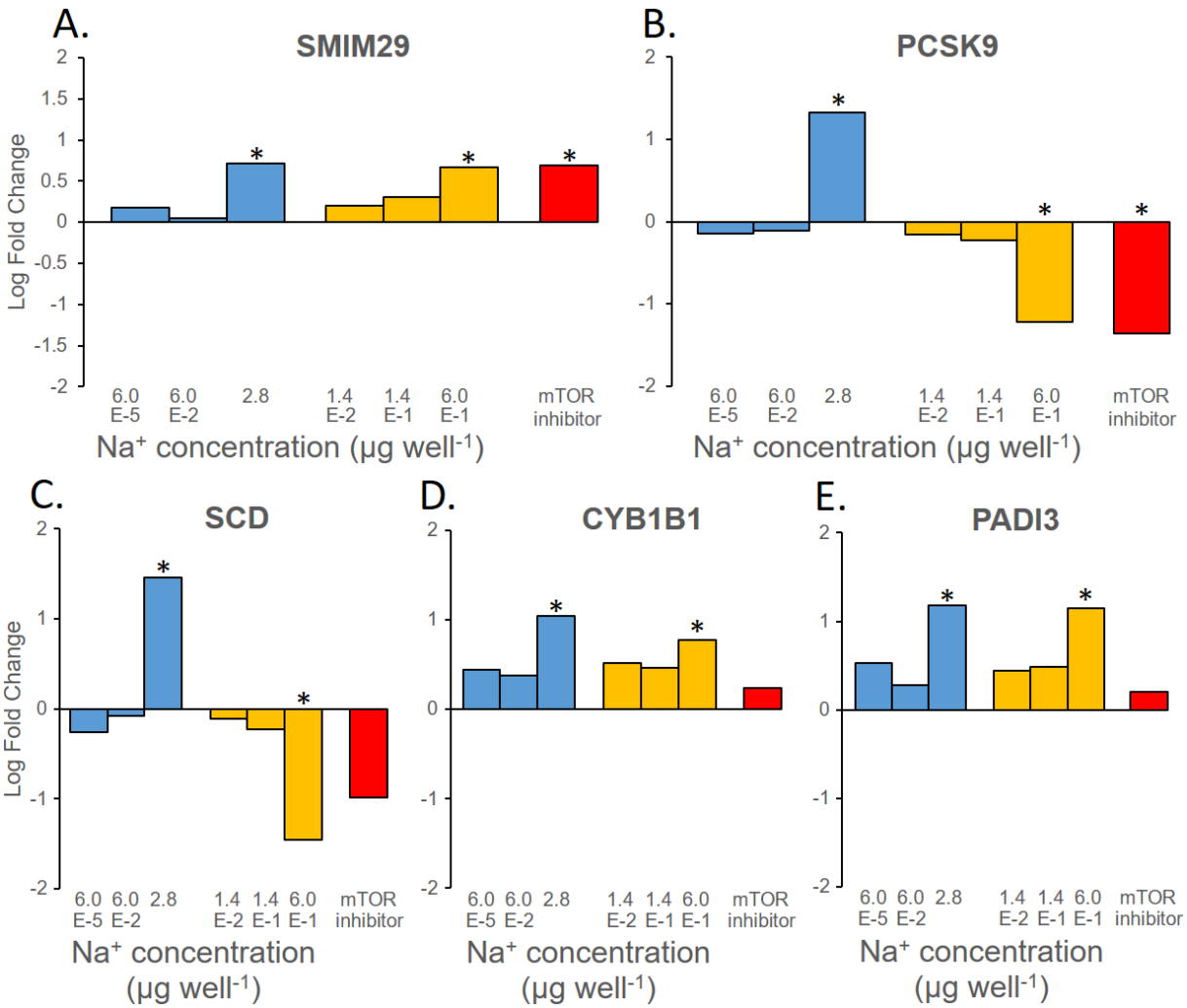

Figure 4.4: Differential gene expression in the lab SSA (blue), natural SSA (yellow) and mTOR inhibitor (red) treatments. Log fold change for (A) small integral membrane protein 29 (SMIM29), (B) proprotein convertase subtilisin/kexin type 9 (PCSK9), (C) stearoyl-CoA desaturase (SCD), (D) cytochrome P450 family 1 subfamily B member 1 (CYP1B1), and (E) peptidyl arginine deiminase 3 (PADI3). (*) denote significance at a false discovery rate of 0.01.

At the pathway level, we studied the four pathways with a significant dose response pattern: the glycogenesis, lysosome, spliceosome and steroid biosynthesis. Overall, we observed different patterns for the two treatments across the four pathways (Figure 4.5). For example, for the steroid biosynthesis, we observed more upregulation with increasing dose levels for the lab SSA treatment and more downregulation with increasing dose levels for the natural SSA treatment. In all pathways, the response of the mTOR inhibitor treatment was comparable to the response of the natural SSA treatment (Figure 4.5).

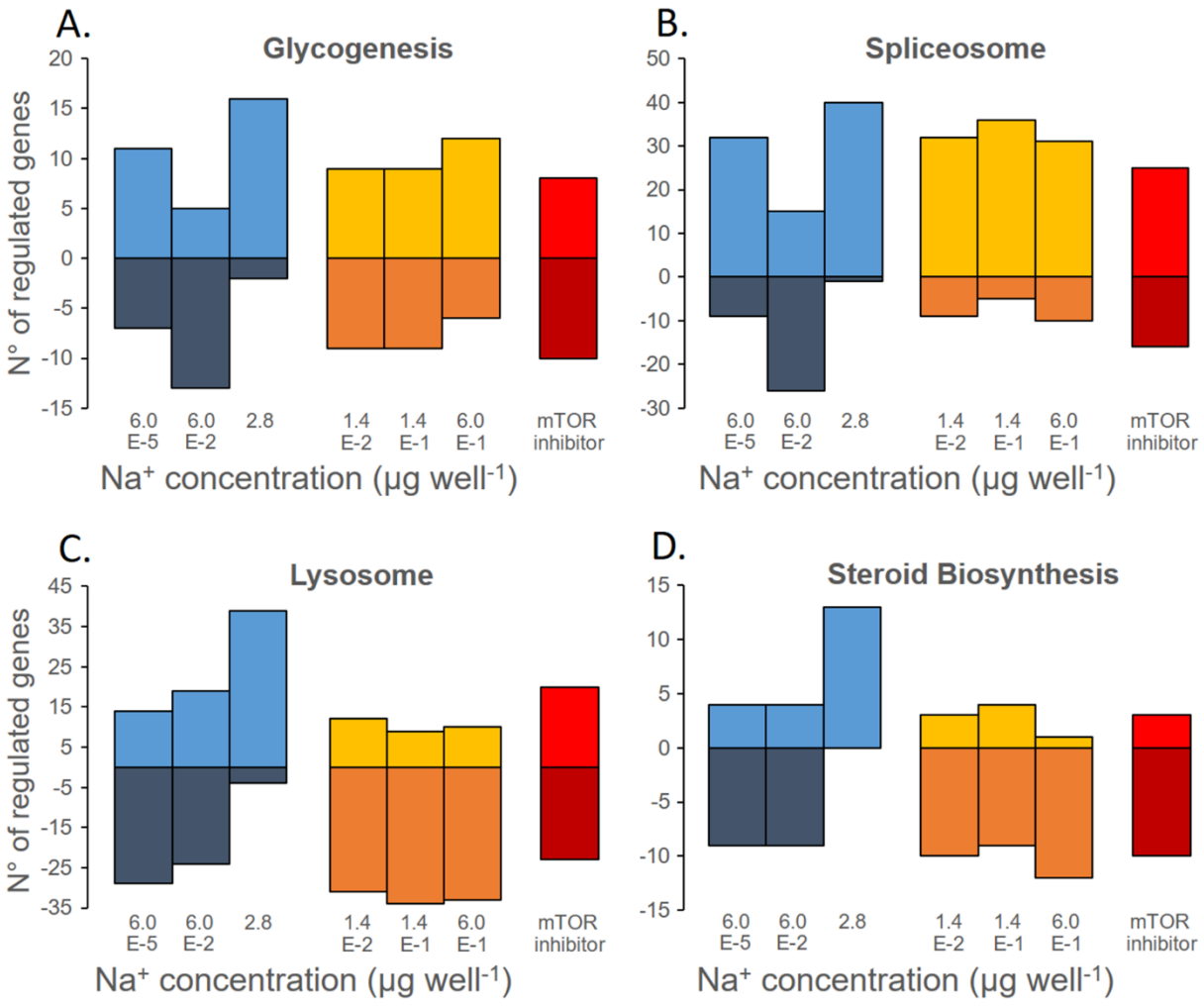

Figure 4.5: Dose response patterns in significant pathways. Number of significantly upregulated (>0) or downregulated (<0) genes in (A) the glycogenesis, (B) the spliceosome, (C) lysosome, (D) steroid biosynthesis for the treatments: lab sea spray aerosol (SSA, blue), natural SSA (yellow) and mTOR inhibitor (red).

3.3 All treatments interact with the mTOR pathway

Here, the genes of the mTOR pathway (as defined by the KEGG database)[241] and a hallmark set of genes upregulated upon activation of the mTORC1 complex (as defined by the molecular signature databases)[242] were used to evaluate potential effects of the treatments on the mTOR pathway. No enrichment of significantly expressed genes of the mTOR pathway (as defined by the KEGG database) was observed in any of the treatments. However, individual genes of the mTOR pathway (as defined by the KEGG database), were significantly regulated in different high dose treatments, with the exception of the lab SSA for which no genes were differentially expressed (Table S4.1). Taking a closer look at the hallmark mTORC1 set, we observed that the gene expression patterns differed across treatments (Figure S4.2). Hierarchical clustering of these patterns indicated that differentially expressed genes were in general regulated in the opposite direction for hYTX and the lab SSA versus the natural SSA and the chemical inhibitor (Figure S4.2). This pattern is even more prominent when focusing on the genes that contribute significantly (FDR<0.05) to the enrichment score in the hallmark set for all 4 treatments (Figure 4.6). This group of 17 genes showed completely opposite regulation patterns in the high dose hYTX and high dose lab SSA versus the high dose natural SSA and the chemical inhibitor (Figure 4.6). The first group showed increased expression or upregulation of hallmark genes, confirmed by a significant positive enrichment score of 2.14 and 1.92 for the pure hYTX and lab SSA treatments respectively (Table S4.2). In contrast, the chemical inhibitor and high dose natural SSA treatments showed an inhibition of expression or downregulation of the hallmark genes, reflected by a negative enrichment score of −2.32 and −1.24 for the mTOR inhibitor and the natural lab SSA treatment respectively (Table S4.2).

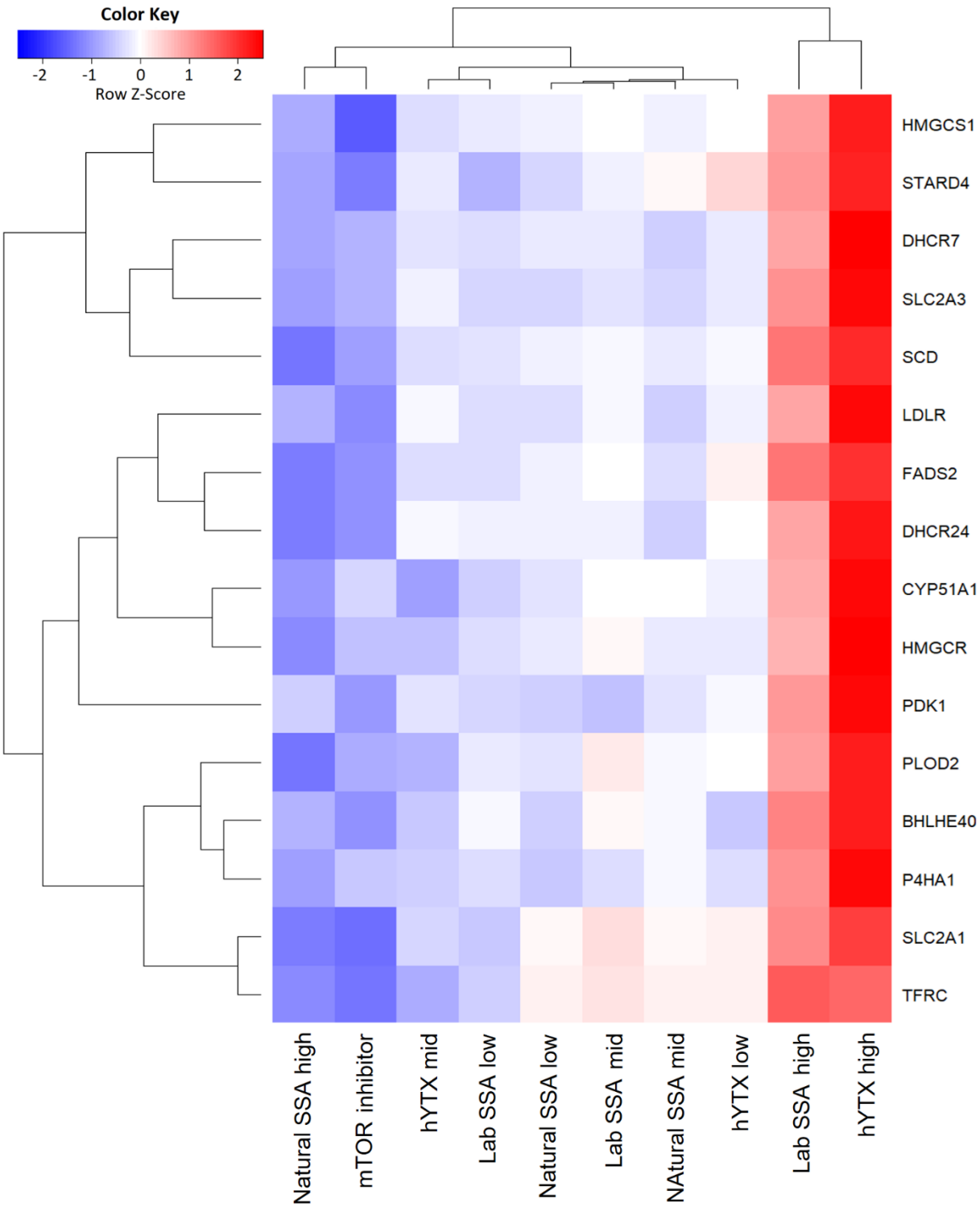

Figure 4.6: Enrichment of the mTOR Hallmark set. Heatmap for all treatments of the fold changes of genes that contribute significantly to the enrichment score for all three treatments at the highest dose and the mTOR inhibitor. Treatments: chemical mTOR inhibitor, homoyessotoxin (hYTX), lab sea spray aerosol (lab SSA) and natural sea spray aerosol (SSA) at high, mid and low doses. For hYTX and the lab SSA, hYTX levels are: 0.5 µg L^{-1} (high), 10^{-2} µg L^{-1} (mid), 10^{-5} µg L^{-1} (low). For the lab SSA, sodium levels are: 2.8 µg Na^{+} $well^{-1}$(high), $6{\cdot}10^{-2}$ µg Na^{+} $well^{-1}$(mid), and $6{\cdot}10^{-5}$ µg Na^{+} $well^{-1}$(low), and for the natural SSA, sodium levels are: 0.6 µg Na^{+} $well^{-1}$(high), 0.14 µg Na^{+} $well^{-1}$ (mid) and 1.4 µg$\cdot 10^{-2}$ Na^{+} $well^{-1}$(low).

4 Discussion

It has been postulated that marine compounds in SSAs lead to beneficial health effects in humans through interactions with the mTOR pathway.[46] This is based on the fact that the augmented activity of this kinase pathway is related to multiple pathological conditions.[49] As such, the mTOR pathway is important in the context of cancer pathogenesis. Many genes encoding proteins that lie upstream (e.g., PTEN, PI3K) and downstream (e.g., 4E-BP1 and eIF4E) of the mTOR complexes are mutated in human cancers. This often leads to oncogenic activation of the mTOR pathway inducing processes required for cancer cell growth, survival, and proliferation.[49] The fact that a carcinogenic lung cell line (i.e., A549) was used in the performed in vitro experiments is therefore most interesting. For comparison, it would have been even more interesting when a normal lung cell line was also included. Unfortunately this was not possible due to experimental limitations.

Here, we report the effects of a pure natural compound hYTX, the extract of a lab generated SSA (containing hYTX from an algal producer) and the extract of a natural SSA sampled from the environment on human lung cells. We observed a high overlap between the effects of the pure hYTX and the lab SSA treatments at the gene and pathway level. This suggests that the effects of the lab SSA are most likely comparable to effects of a diluted hYTX treatment. Or, in other words, the effects of the lab SSA containing hYTX from an algal producer are weaker than the effects of the pure hYTX treatment despite containing the same amount of hYTX. This suggests that (1) the lab SSA may have contained additional compounds which interact with hYTX leading to weaker effects or that (2) the lab SSA may have contained hYTX or YTX analogues or metabolites with potential weaker effects that competed with hYTX for molecular binding sites and uptake. In this context, Paz et al.[244] described nearly 40 YTX analogues. Both assumptions (1) and (2) suggest a lower bioavailability of pure hYTX, potentially leading to a lower actual dose.

Interestingly, the effects of the natural SSA at the gene and pathway level closely resembled the effects of the mTOR inhibitor, but contrast with the effects of hYTX and the lab SSA. The differences between these two treatment clusters highlight that while all treatments targeted the mTOR pathway, their molecular responses were opposite.

This suggests that the natural SSA is a complex mixture of marine compounds interacting with the mTOR pathway leading to different expression patterns of the same pathway than the lab SSA. Literature reports only briefly on the organic composition of SSAs, but suggests a large diversity in natural compounds (see Table S3.6). The similarities in gene regulation between the natural SSA and mTOR inhibitor suggest that natural SSAs indeed contain marine compounds that cause comparable effects as the known mTOR inhibitor and could therefore downregulate the mTOR pathway. In contrast, the pure hYTX and lab SSA treatments induced a significant increased expression of the genes related to the mTOR pathway. This does not necessarily imply that the activity of the mTOR pathway was stimulated. It does show that hYTX and the lab SSA interacted differently with the mTOR pathway and that most probably other marine chemicals (than hYTX) induced the effects observed in the natural SSA treatment. The high dose treatments for both hYTX and the lab SSA of 0.5 µg hYTX L^{-1} are however an extreme case scenario, reflecting concentrations in the sea water during harmful algal blooms (see Annex IV section 1). The environmental concentrations of hYTX in seawater and coastal air have not been previously reported but are expected to lie (for the seawater) between the low and mid dose levels based on estimates of cell counts of hYTX producers and hYTX production per cell (see Annex IV section 1). It is clear that while the exact regulation of genes and pathways differs between the lab SSA and natural SSA extracts, both samples significantly interact with the mTOR pathway. Furthermore, the effects of the natural SSA extract are similar to the effects of the chemical mTOR inhibitor suggesting beneficial health effects at environmentally relevant concentrations.

We observed two genes significantly regulated by all treatments and by the mTOR inhibitor. The first gene was the small integral membrane protein 29 (SMIM 29). Little functional information on this protein is available, although it is ubiquitously expressed in at least 25 tissues.[245] The other gene is proprotein convertase subtilisin/ kexin type 9 (PCSK9; see Figure 4.7), primarily involved in lipid homeostasis and apoptosis.[246] PCSK9 is thought to have two major functions: (1) maintenance of lipid homeostasis by the regulation of low-density lipoprotein receptors and (2) the regulation of neural apoptosis.[246] In general, the overexpression or upregulation of PCSK9 is associated with the dysregulation of pathways involved in the cell cycle, inflammation and apoptosis while the inhibition or downregulation of PCSK9 in carcinogenic lung cells

has been associated with apoptosis of these cell lines.[246] In mouse, a similar pattern has been observed.[247] Upregulation of PCSK9 was associated with multi-organ pathology and inflammation while PCSK9 downregulation was associated with protection against inflammation, organ pathology and systemic bacterial dissemation.[247] These findings in literature together with our results, (i.e., downregulation of PCSK9 in the mTOR inhibitor and the natural SSA treatments) suggest beneficial health effects of natural SSAs through the apoptosis of lung cancer cells. Based on the results provided here on PCSK9, we propose that SSAs could contain compounds with significant pharmaceutical potential in targeting PCSK9.[248] In fact, in recent years, an increasing number of natural occurring compounds and extracts have shown to inhibit PCSK9, including (marine) n-3 fatty acids.[249]

We also observed three genes that were significantly regulated by all treatments but not by the mTOR inhibitor: SCD, PADI3 and CYP1B1. The pattern of SCD was comparable to that of PCSK9 while the patterns of PADI3 and CYP1B1 were comparable to the pattern of SMIM29. This can be attributed to the functions of SCD and PCSK9, as both are involved in lipid biosynthesis. Furthermore, research has already indicated links between the mTOR pathway and the lipid homeostasis,[50] including the effects on SCD and other genes after exposure to mTOR inhibitors (see Figure 4.7).[50] Evidence points to the sterol regulatory element binding transcription factor 1 (SREBF1) through which the regulation of lipogenesis by mTOR is achieved.[50] This gene was significantly regulated by the natural SSA treatment, but not by any of the other treatments. CYP1B1 is commonly involved in the metabolism of xenobiotics and could play a role in metabolizing some of the marine compounds. Literature has also reported a relation between CYP1B1 and SCD in lipid homeostasis in liver cells,[250] (see Figure 4.7) although the extent of this relation in lung cells remains unclear. Here we observed an increase in expression of CYP1B1 in all treatments. Overexpression of CYP1B1 has also been reported in lung cell lines through the aryl hydrocarbon receptor,[251] but no significant effects for this receptor were observed in any treatment of our study (Table S4.4). This suggests that the overexpression of CYP1B1 is more likely related to the regulation of SCD. In addition, PADI3 was also upregulated in all three high dose treatments (hYTX, lab SSA and natural SSA, see Figure 4.7). PADI3 is generally not expressed in lung cells[245] and is primarily expressed in epidermis cells and keratinocytes.[252] Its function in lung cell lines remains unclear.

At the pathway level, we observed differential expression of genes linked to the mTOR pathway in all three high dose treatments (natural SSA, lab SSA, and hYTX). Our results also indicated significant effects on the mTOR pathway, but the effects and the potential beneficial health effects differ across treatments. Most likely, the effects on these genes are caused by the primary effects on the mTOR pathway. Furthermore, for three genes, these effects while linked to the mTOR pathway, are not observed with the mTOR inhibitor. This suggests that the effects of these experimental treatments (natural SSA, lab SSA, and hYTX) extend beyond the inhibition of mTOR but are related to or initiated by the effects on the mTOR pathway.

We observed four pathways that were significantly affected by the different treatments: glycogenesis, lysosome, spliceosome and steroid biosynthesis. For the steroid biosynthesis, these results are not surprising given the links that have already been discussed above between mTOR and lipid biosynthesis. In addition to steroid biosynthesis, the lysosome and glycogenesis also have links to mTOR. The inhibition of the mTOR pathway is known to activate protein degradation and autophagy through among others the lysosome (see Figure 4.7).[253,254] The spliceosome has been proposed as a therapeutic target in cancer cells to inhibit mTOR, which leads to autophagy (see Figure 4.7).[255] Specifically, depletion of small nuclear ribonucleoprotein polypeptide E (SNRPE) led to reduced cell viability in lung cancer cell lines. Here, we observed in addition to dose response effects for the spliceosome, a significant downregulation of SNRPE in the highest hYTX treatment but not in any of the other treatments (Table S4.5). Overall, the pathways with significant dose response effects can all be indirectly linked to the mTOR pathway, suggesting that the effects here are a consequence of the effects on the mTOR pathway, which most likely induces a cascade of events and interactions with other pathways.

Overall, the results at the gene level and at the pathway level highlight that the effects are primarily mediated or linked through the mTOR pathway supporting the biogenesis hypothesis postulated by Moore[46] that marine airborne compounds interact with the mTOR pathway leading to health benefits. All treatments significantly affected the mTOR pathway, but we observed differences in the direction of the regulation of this pathway (Figure 4.7). Furthermore, significant genes and enriched pathways across treatments all interact with mTOR, indicating that marine compounds trigger a cascade

of events through interaction with the mTOR pathway (Figure 4.7). Thus, the effects of marine airborne compounds are not limited to the mTOR pathway but include a cascade of genes and pathways involved in different metabolic processes (e.g., steroid biosynthesis, lysosome) with key links to mTOR (Figure 4.7).

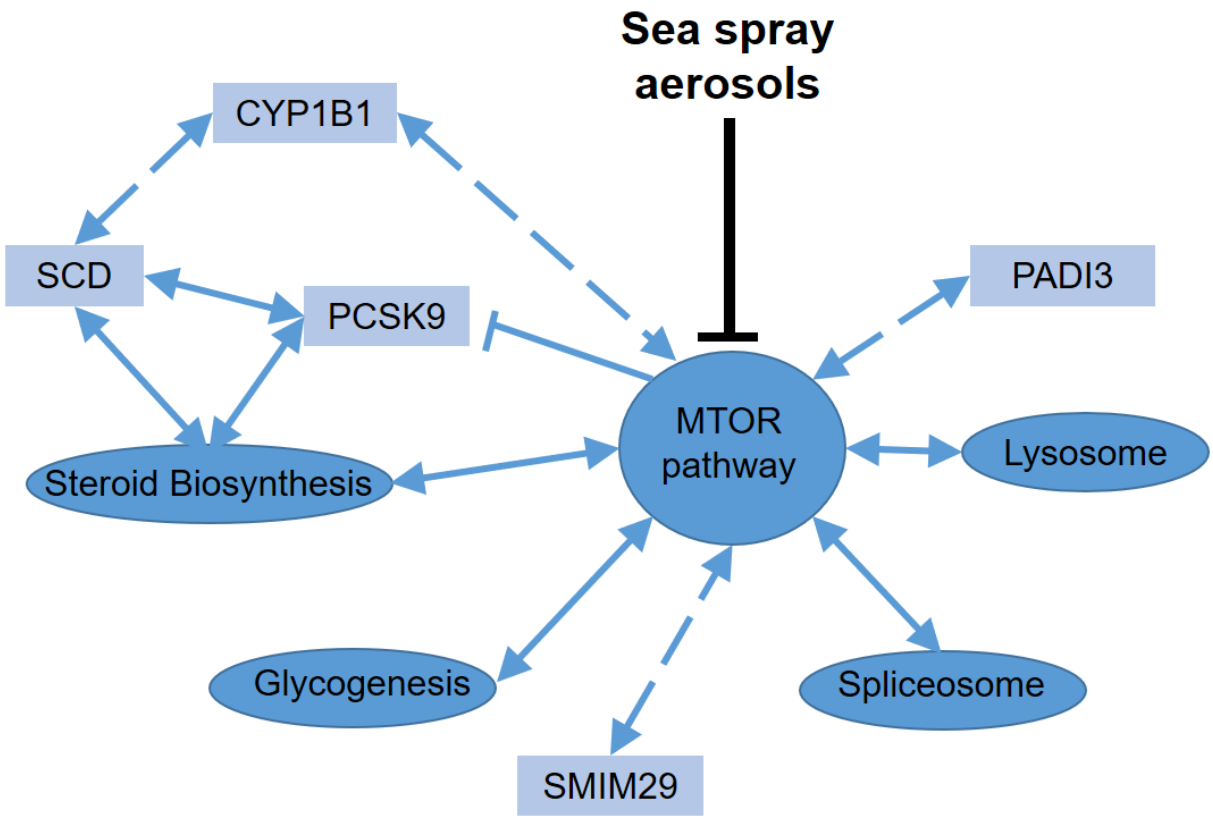

Figure 4.7: Molecular effects of marine aerosolized compounds. A schematic representation of the molecular effects of sea spray aerosols observed within this study. Pathways are represented by ellipses, genes are represented by rectangles. Solid blue arrows represent interactions with a solid evidence base, dashed arrows represent hypothetical interactions observed, ⊢ represent inhibition.

Chapter 5

Algal phospholipids in sea spray aerosols: a surprising parallel with medical aerosol therapy

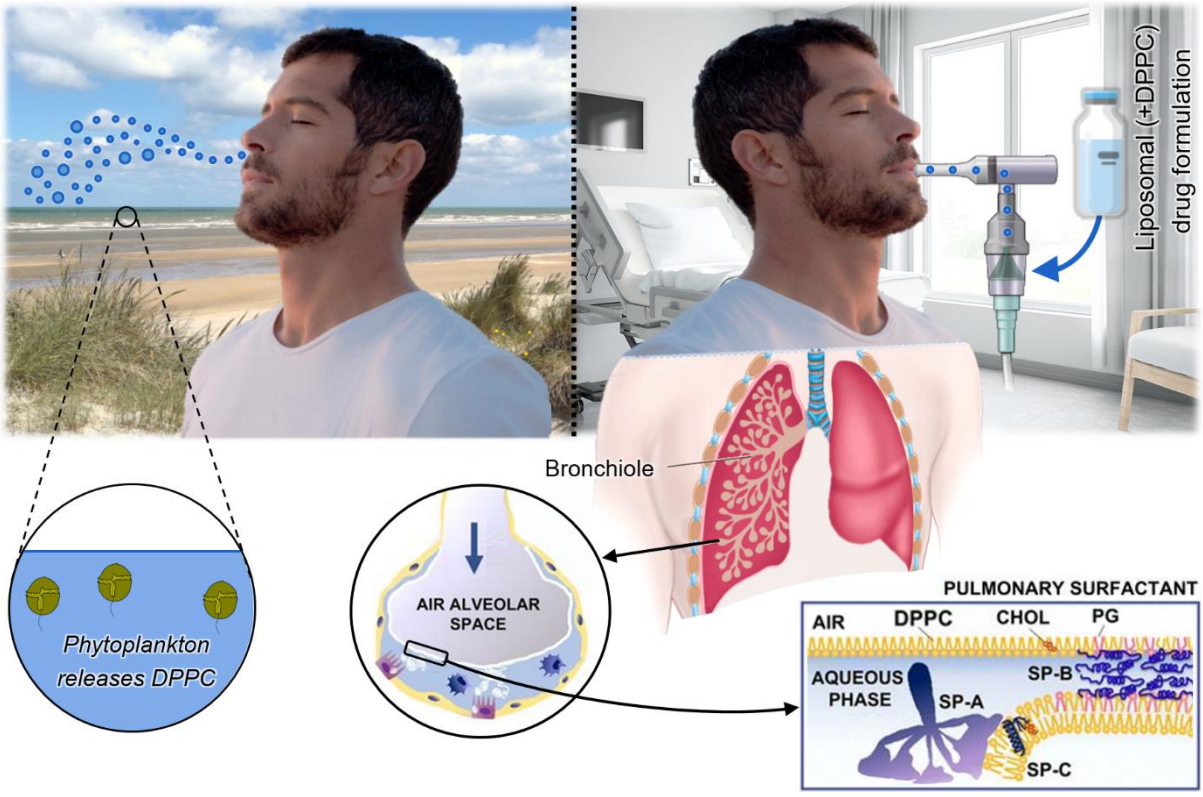

Figure adapted from Autilio et al.[256]*, © Medline Plus, and © gauzy.com*

Redrafted from:

Van Acker, E.; De Rijcke, M.; Liu, Z.; Asselman, J.; De Schamphelaere, K.; Vanhaecke, L.; Janssen, C. Algal phospholipids in sea spray aerosols: a surprising parallel with medical aerosol therapy. Submitted to Environmental Science and Technology.

Chapter contents

Abstract

It has been observed that marine phytoplankton influence the composition of sea spray aerosols (SSAs). This is among others linked to their release of natural compounds like dipalmitoylphosphatidylcholine (DPPC). As DPPC is a surfactant known to accumulate in the sea surface microlayer (SSML), it has been suggested but not confirmed that DPPC may be present in SSAs. Here we conducted a one-year SSA sampling campaign at the Belgian coast and analyzed the organic composition of the samples using ultra-high-performance liquid chromatography high-resolution Q-Orbitrap™ hybrid mass spectrometry (UHPLC-HR-Q-Orbitrap™-MS/MS). We identified and quantified DPPC in nearly all SSA samples at air concentrations ranging between <1.1 and 33 pg m^{-3}. This discovery may be of great importance for the research field that links the ocean and human health. Indeed, DPPC is used as an excipient in medical aerosol therapy to facilitate the effects of respiratory delivered drugs. Its presence in natural SSAs could thus facilitate the effects of marine bioactive compounds. By identifying and analyzing the environmental variables that determine the DPPC concentrations, using (among others) a generalized linear model (GLM), we established that wave height is the most important variable which (negatively) influences the coastal air concentrations of DPPC. We also demonstrated that the DPPC content in SSAs is positively correlated with the enriched aerosolization of Mg^{2+} and Ca^{2+}. Our findings are thus not only important from a human health point of view, they also increase our understanding of the production, composition and atmospheric behavior of SSAs.

1 Introduction

Sea spray aerosols (SSAs) are of crucial importance for diverse meteorological and climatological processes. They act as cloud condensation nuclei,[87] ice nucleating particles[87,257] and increase the albedo of the atmosphere.[258,259] Both the inorganic (i.e., Ca^{2+}, K^{+}, Mg^{2+}, trace metals)[73–75] and organic[73,184] composition of SSAs can be enriched relative to the subsurface seawater. Such enrichment processes are usually determined relative to sodium (Na^{+}), which is the most common proxy to quantify SSA densities and is considered not to be enriched during SSA formation.[62]

The presence, type and life phase of marine phytoplankton plays an important role in determining the (organic and inorganic) composition of SSAs.[73,74,184] It has, however, been suggested that phytoplankton biomass does not have a straightforward positive relation with the organic content of SSAs.[260] Indeed, recent studies demonstrated that a high organic enrichment in SSAs is rather associated with the demise of phytoplankton communities or blooms, which result in cell lysis, bacterial degradation and the release of (intracellular) biogenic compounds.[74,260–263] Especially biogenic or natural surfactants which accumulate in the sea surface microlayer (SSML) have an important effect on SSA production processes. The SSML is a thin film (20-400 µm) found at the air-water interface of the ocean surface which is chemically distinct from the subsurface water (SSW).[88,89] Surfactants decrease the surface tension at the air-water interphase and increase the bubble surface lifetime, that is, the time period an air bubble resides at the sea surface until it bursts. With an increasing surface lifetime, more seawater drains from the bubble film, it becomes thinner and eventually produces smaller film drops with a higher organic enrichment.[95,213] The phospholipid dipalmitoylphosphatidylcholine (DPPC) is one such surfactants which is excreted upon phytoplankton cell lysis[264] and is known to be abundant in the SSML.[265,266] Although it has been suggested that DPPC is likely to be found in SSAs,[267] to our knowledge it has never been quantified nor detected in these aerosols.

Despite the fact that the marine biosphere contains a large number of natural compounds with known or suspected pharmacological effects,[26,27] little research has been performed to study the potential human health effects resulting from airborne exposure to SSAs. In this context, airborne exposure to SSAs that potentially contain

DPPC can be important for human health. Indeed, DPPC is the major component (±40%) of the pulmonary surfactant in human alveoli and is essential for good lung functioning.[268,269] Conversely, lung surfactant abnormalities are associated with obstructive lung diseases (e.g., bronchiolitis, asthma).[270] DPPC and other phospholipids, however, also play an important role as potential carriers enhancing the delivery of hydrophobic and hydrophilic compounds deep into the lung.[268] Among others, they can stimulate pharmacokinetics via enhancement of the drug permeability through the lung epithelium and reduce recognition of exogenous aerosols by alveolar macrophages.[268,271] Drug formulations containing DPPC as an excipient are therefore used (and widely investigated) in medical aerosol therapies.[272–274] The potential sea spray aerosolization of DPPC is thus extremely interesting from a human health point of view.

In the current study we investigated the potential presence of DPPC in ambient SSAs and aimed to quantify its concentration in coastal air ($[DPPC]_{coastal\ air}$). To this end, a SSA sampling campaign, was conducted at the Belgian coast. Air samples were analyzed on their DPPC and inorganic (i.e., Na^+, Mg^{2+}, Ca^{2+}, K^+, trace metals) composition, allowing the quantification of the $[DPPC]_{coastal\ air}$ and the characterization of the SSA composition (relative to Na^+). Finally, by analyzing our results relative to key environmental variables, we aimed to reveal the meteorological and/or ecological processes that determine the DPPC content of SSAs.

2 Materials and methods

2.1 SSA sampling

A one-year SSA sampling campaign was conducted at the Belgium coast in Ostend from March 19th 2018 until March 19th 2019. The SSA collection system was installed at the lab facilities of the Flanders Marine Institute (VLIZ) which is situated ±300 m from the high-water mark (beach) in Ostend, Belgium (51°14’09.7”N, 2°55’42.4’’E; Figure 5.1). Every week, a new pretreated quartz fiber membrane filter (QM-A, Ø 47 mm, Whatman®) enclosed in a stainless steel in-line filter holder (Pall Corporation) was placed at a height of 10 m and connected via tubing to an Air-Cube™ HE sampler pump. This sampler pump was set at a constant air flow of 25 L min^{-1} and registered

the effective sampled air volume which was approximately 250 m^3 $week^{-1}$. The inlet of the filter holder was oriented north (i.e., towards the sea). The sampling set-up is shown in Figure S5.1 (supplementary information). To confirm the absence of contamination and account for any filter background, 10 field blank samples were taken over the course of the sampling campaign. These blank filters underwent the same manipulations as the real SSA samples but were not exposed to SSAs. As sampling was performed at ±300 m from the high-water mark, it needs to be stressed that we did not collect nascent or freshly emitted SSAs. The collected aerosol was, however, representative for the airborne SSA exposure of human coastal populations.

Figure 5.1: SSA sampling station (⊠) at the lab facilities of the Flanders Marine Institute (VLIZ), situated ±300 m from the high-water mark in Ostend, Belgium (51°14'09.7"N, 2°55'42.4"E). The inland marine water bodies (i.e., the harbor and the "spuikom") are indicated with a red dashed line. The dashed black lines at the edge of the dark blue semi-circle indicate the wind directions (°N) which were considered to be the boundary between sea and land wind. The meteorological station measuring the wind direction (▽), and the buoy measuring the wave height (▲) are also indicated on the map, together with the 7×7 km window (with its center at 51°16'2" N, 2°53'19" E) wherein the phytoplankton biomass ([PhyC]) data were selected.

2.2 Sample extractions

After deployment, quartz filters were cut in two. One half was used to analyze the inorganic content of the collected SSAs, while the other half was stored in a petri dish and stored at -20 °C until the DPPC analysis. Filter extraction for inorganic analysis was executed by eluting filters three times with 5 mL of 0.14 M HNO_3. Extracts were then filtered over 0.45 µm (Acrodisc®) and stored at 4°C until further inorganic analysis.

The DPPC extraction from the filter (halves) was performed largely according to the dedicated DPPC extraction protocol of Ullah et al.[275] In short, filters were inserted in glass tubes and spiked with 2.4 ng of dimyristoylglycerophosphocholine (DMPC; Avanti Polar Lipids) as internal standard.[276,277] The filters were subsequently eluted three times using 4 mL of methanol, a 5 min sonication and a 20 sec vortex step (per elution). The combined extracts (12 mL in total) were centrifuged (10 min, 2250 g) and the supernatant was transferred to a new pre-cleaned glass tube. Extracts were then evaporated to incipient dryness, under a gentle N_2 stream at 40 °C, reconstituted in 120 µL of 90% methanol in water containing 3.5 mM ammonium acetate and vortexed for 10 sec. After a last centrifugation step (10 min, 2500 g), the supernatant was transferred to a glass insert in a LC-MS vial prior to analysis. To avoid contamination of the samples with DPPC, the following precautionary measures were taken: (1) the extraction was performed using new glass tubes that were additionally rinsed with chloroform and methanol, (2) the other accessories (tips, beakers, Pasteur pipets) were also made of glass (or metal) and were cleaned extensively, (3) a face mask was worn by the analyst during the extraction procedure.

2.3 Chemical analysis

DPPC

The analysis of the DPPC content in the final filter extracts was performed in a targeted manner using high-performance liquid chromatography coupled to high resolution Q-Orbitrap™ hybrid mass spectrometry (UHPLC-HR-Q-Orbitrap™-MS/MS). The DPPC reference standard was purchased from Avanti Polar Lipids. Chromatographic separation was achieved on a Dionex Ultimate 3000 XRS UHPLC system (Thermo Fisher Scientific) equipped with an Acquity ethylene-bridged hybrid (BEH) phenyl column (1.7 µm, 150 × 2.1 mm; Waters). A constant flow rate of 300 $\mu L \cdot min^{-1}$ and a column oven temperature of 40 °C were applied. A C18 DGM Symmetry HPLC column

(5 µm, 150 × 2.1 mm; Waters) was used as a trapping column and installed between the LC pump and injector valve of the injector. The applied analytical method was adapted from the UHPLC-HR-Q-Orbitrap™-MS lipidomics method of Van Meulebroek et al.[278] Their UHPLC gradient elution program using a binary solvent system consisting of ultrapure water (solvent A) and methanol (solvent B), both acidified with 3.5 mM ammonium acetate, was shortened from 20 to 15 min. The following proportions (v/v) of solvent B were now used: 0−1 min at 75%, 1−2 min from 75% to 90%, 2−5 min from 90% to 98%, 5−10 min from 98% to 100%, and 10−12 min at 100%, followed by 3 min of equilibration at 75% (i.e., initial conditions). Detection was carried out by a benchtop HR-Q-Orbitrap™-MS (Thermo Fisher Scientific) preceded by heated electrospray ionization (HESI-II). The full-scan method used by Van Meulebroek et al.[278] was modified by adding a parallel reaction monitoring (PRM) approach which operated in positive ion mode and selected the precursor ion of DPPC ($[M+H]^+$; m/z of 734.56943) in an isolation window of 1 *m/z* for fragmentation. Fragmentation was performed using high energy collision dissociation (HCD), with an optimized (see Annex V section 1 and Figure S5.2) normalized collision energy (NCE) of 52 eV. Furthermore, the targeted HRMS/MS analysis used an automatic gain control (AGC) of 2×10^5 ions, a maximum injection time of 100 ms, and the mass resolution was set at 17,500 full width at half maximum (FWHM).

Data processing, including identification and quantification of DPPC, was performed using XCalibur 3.0 software (Thermo Fisher). Compound identification was realized based on the dedicated method of Ullah et al.,[275] using (1) the relative chromatographic retention time (Δ≤2.5%), i.e., the ratio of the retention time of DPPC to that of the internal standard (DMPC), (2) the accurate masses (mass extraction window of 3 ppm) of the three main fragments of DPPC, and (3) the correct product ion ratios (i.e., relative peak intensities) of these three fragments (Δ≤10%). Quantification was performed using the area ratio (i.e., ratio of the analyte and the internal standard peak areas) of the most abundant fragment of DPPC (*m/z* 86.09681; see Figure S5.2C) and a calibration curve prepared with the extracts of eight spiked filter samples (i.e., 0, 0.3, 0.6, 0.9, 1.2, 1.8 and 2.4 ng DPPC per ½ filter).

It should be noted that in our preliminary research, before the dedicated analysis of DPPC, we also screened several SSA samples for 14 other marine bioactive compounds. These compounds (Table S5.1) were targeted based on the following

selection criteria: (1) bioactivity properties, (2) occurrence in the North Sea, (3) polarity (determining EF_{SSA} potential), (4) availability of reference standards for analysis, and (5) low volatility (based on Henry constant, boiling temperature, and molecular weight).

Inorganics

For every SSA sample, half of the filter was analyzed for its inorganic content, using inductively coupled plasma-optical emission spectroscopy (ICP-OES; Thermo Scientific iCAP 7000 series). The certified reference materials Cranberry 05 and TMDA 25.5 (Environment Canada), were used to verify the calibration curves of the major (Na^+, Mg^{2+}, Ca^{2+}, K^+) and minor inorganic constituents (Cu^{2+}, Zn^{+2}, Pb^{2+}, Cd^{2+}), respectively. These majors and minors were analyzed in radial-and axial-view modus, respectively. The calibration curves ranged from 0.1 to 100 µg per mL extract.

2.4 Environmental variables

Meteorological data

To assess the quantified $[DPPC]_{coastal\ air}$, SSA densities (i.e., $[Na^+]_{coastal\ air}$), and SSA composition relative to environmental variables that influence the SSA production and enrichment of DPPC in the SSML and SSAs, we collected relevant meteorological data. As indicated on Figure 5.1, we used the wind direction data (at 10m altitude) of a meteorological station situated 330 m northwest of our sampling station and the wave height measured by a monitoring buoy situated 1 km north of our sampling station. Both the wind and wave measurements, having respective time resolutions of 10 and 30 min, were taken from the database "*Meetnet Vlaamse Banken*" of the Flemish Government.[279] For every sampling week, we calculated (1) the time during which the wind actually blew from across the sea (% $time_{seawind}$; ≤58°N and ≥235°N; Figure 5.1) and (2) the average wave height during the periods with seawind ($WH_{seawind}$).

Phytoplankton data

To investigate the influence of phytoplankton on the $[DPPC]_{coastal\ air}$, we used data of the daily phytoplankton biomass in the surface seawater (depth ≤1 m) expressed as concentrations of carbon ([PhyC], µM C). These [PhyC] data were taken from the "*ocean biogeochemistry reanalysis for the North-West European Shelf"* dataset[280] of the Copernicus-program, which were generated using the European Regional Seas

Ecosystem Model (ERSEM 15.06).[281] This model uses satellite measurements and in-situ observations, and produces data with a (horizontal) spatial resolution of 7×7 km. As depicted on Figure 5.1, the [PhyC] data of the closest geographical "point" to our sampling station was selected to perform a modelling analysis as explained below.

2.5 Aerosol source

As is common practice in SSA studies,[62] we used Na^+ as a proxy to quantify SSA densities and potential enrichment processes. To confirm that the Na^+ in our air samples indeed originated from seawater and thus from SSAs, we analyzed the correlation between the $[Na^+]_{coastal\ air}$ and the % $time_{seawind}$ using a linear regression. We also performed this exercise for the other analyzed inorganic ions (Mg^{+2}, Ca^{2+}, K^+, Cu^{2+}, Zn^{2+}, Pb^{2+}, Cd^{2+}). Next, by analyzing the Mg^{2+}/Na^+ mass ratio in our air samples, relative to this ratio in seawater (11.9%.),[204,205] we could assess the seawater and thus SSA origin[202] of Na^+ and Mg^{2+} (see results in section 3.3). While characterizing the inorganic SSA composition we also determined the SSA enrichment factor (EF_{SSA}) for the (major) inorganic ions (X) relative to the subsurface water (SSW). This was performed using their theoretical seawater ratios[205] (per Na^+) and the following equation:

$$\mathrm{EF_{SSA}} = \frac{[\mathrm{X}]_{\mathrm{SSA}} / [\mathrm{Na^+}]_{\mathrm{SSA}}}{[\mathrm{X}]_{\mathrm{SSW}} / [\mathrm{Na^+}]_{\mathrm{SSW}}} \qquad \text{(eq. 5.1)}$$

To confirm that the DPPC in our air samples originated from SSAs, and not from a terrestrial aerosol source, we performed a similar (linear regression) analysis between $[DPPC]_{coastal\ air}$ and % $time_{seawind}$. If the wind is mainly coming across land areas, the $[DPPC]_{coastal\ air}$ should be much lower than when there is a predominant seawind. It should be noted that our sampling station is, however, surrounded with "inland" marine water bodies (i.e., the harbor and the "*Spuikom*" a human made saltwater basin; see Figure 5.1) which may - to a certain extent - also produce SSAs containing DPPC.

2.6 DPPC concentration model

By exploring the relationship between the $[DPPC]_{coastal\ air}$ and other environmental variables, we aimed to reveal the most important meteorological and/or ecological processes determining the $[DPPC]_{coastal\ air}$. Literature suggests that the increase and

decrease of phytoplankton biomass are more important in determining the $[DPPC]_{coastal\ air}$, than just the biomass abundance (as such). Indeed a higher phytoplankton productivity (i.e., growth) showed to induce an increased excretion of marine surfactants,[282] while higher organic contents have been observed in SSA upon the demise of phytoplankton.[262] The latter has been linked to the lysis of phytoplankton cells.[264] It is clear that there can be a time-lag between the manifestation of phytoplankton biomass (i.e., [PhyC]) and their highest DPPC excretion/release, after which DPPC becomes available for aerosolization. This time-lag is further discussed and quantified in the results section 3.4 and was used as a time correction on the [PhyC] variable. Using the time-lag corrected [PhyC] data, we calculated the total weekly decrease ($[PhyC]_{decrease}$) and increase in phytoplankton biomass ($[PhyC]_{increase}$). To be clear, the $[PhyC]_{decrease}$ were calculated as the summation of all daily decreases in [PhyC] during each sampling week. The $[PhyC]_{increase}$ was calculated alike with all daily increases in [PhyC]. In addition, weekly mean values were also calculated ($[PhyC]_{mean}$) using the lag time corrected [PhyC] data.

A generalized linear model (GLM) was used to reveal the relations between the $[DPPC]_{coastal\ air}$ and the environmental variables. To make sure each variable in the model had a similar variance, we first transformed the $[DPPC]_{coastal\ air}$ using a natural logarithm and then performed z-transformations on all variables. These z-transformed data were subsequently used to construct the GLM. We used a full model containing all the independent variables (Table 5.1) and their interactions, then conducted stepwise regressions to select the best regression formula for the model. This stepwise regressions were based on the Akaike information criterion (AIC) and adjusted R^2 of the regressions. The final GLM (discussed below) was only retained after the following confirmatory analyses: (1) the linear model assumptions were verified using the "gvlma" R package,[283] (2) absence of multicollinearity was confirmed by calculating the variance inflation factor (VIF)[284] of each independent variable (using a <5 threshold), and (3) component residual plots[285] were used to verify that there were no significant remaining trends in the residual data. Finally, to analyze the relative importance of each independent variable to $[DPPC]_{coastal\ air}$, linear regressions were performed for each independent variable individually.

Table 5.1: Overview of the different independent variables used to model the DPPC concentrations of the sampled coastal air ($[DPPC]_{coastal\ air}$). The phytoplankton biomass data discussed here represent the time-lag corrected [PhyC] data (as discussed above).

Independent variable	Description	Variance before transformation	Covariance with $[DPPC]_{coastal\ air}$ after transformation
$WH_{seawind}$	Mean wave height of the sampling week during seawind periods	1403	-0.63
$[PhyC]_{mean}$	Mean value of [PhyC] of the sampling week	17.9	0.13
$[PhyC]_{decrease}$	Accumulated daily decreases of [PhyC] of the sampling week	5.02	0.27
$[PhyC]_{increase}$	Accumulated daily increases of [PhyC] of the sampling week	2.07	0.29

3 Results

3.1 Analytical performance

DPPC

The *m/z* and product ion ratios (i.e., relative peak intensities; Figure S5.2C) of the three main fragments of DPPC, at its respective relative retention time (Δ≤2.5%), were used for compound identification. The product ion ratios of the sampled DPPC always deviated, in comparison to the DPPC reference standard, less than the tolerance level of 10% and deviated on average less than 2.3%. As such, DPPC was successfully identified in the air samples when present at detectable concentrations. The major fragment (*m/z* 86.09681, Figure S5.2C) was used for quantification. The limits of detection (LOD) and quantification (LOQ) were determined using the standard deviation of the response, i.e., the error of estimate ($S_{y/x}$), and the slope of the calibration curve.[193,203] This calibration curve showed excellent linearity ($R^2 = 0.998$), which was confirmed with a lack-of-fit analysis (F- test, $p > 0.05$; 95% confidence level). The derived LOD and LOQ were 138 and 418 pg per ½ filter, respectively. In a 250 m^3 air sample, these values correspond to air concentrations of 1.1 and 3.3 pg m^{-3}. The field blank samples never contained detectable DPPC concentrations (≥LOD).

Inorganics

The LOD and LOQ values for the targeted inorganic constituents were determined using the standard deviation of (spiked) samples with a concentration near the LOD.[286] For the minor and major constituents the LOQs (per filter) ranged from 30 to 240 ng and from 1.5 to 3 µg, respectively. The exact LOD and LOQ values for the analysis of these inorganics can be found in Table S5.2, together with their respective background levels in the field blank samples. If relevant (>LOD) the background levels of these inorganics were accounted for in the quantification of their concentration.

3.2 Air concentrations and SSA composition

Six of the 52 samples taken during the one-year sampling campaign (52 weeks) were impaired due to various interferences (e.g., electricity interruptions, clogging of the sampling inlet) and could not be used in the final analysis. DPPC was found in detectable concentrations (>LOD) in all but one of the 46 remaining SSA samples and 38 of these samples contained quantifiable (>LOQ) concentrations. Figure 5.2A shows the DPPC and Na^+ concentrations of the sampled air ($[DPPC]_{coastal\ air}$ and $[Na^+]_{coastal\ air}$) as a function of time. In Figure 5.2B the $[DPPC]_{coastal\ air}$ are plotted together with the DPPC/Na^+ ratios. As $[Na^+]_{coastal\ air}$ are used to quantify SSA densities, these DPPC/Na^+ ratios represent the DPPC content of the sampled SSAs. In combination with Figure S5.3A, it is clear that the DPPC content of SSAs (i.e., DPPC/Na^+) determines the $[DPPC]_{coastal\ air}$ to a large extent (R^2 = 0.64, $p<0.001$; 99.9% confidence level). Conversely, the SSA density (i.e., $[Na^+]_{coastal\ air}$) has an inverse correlation with the $[DPPC]_{coastal\ air}$ (R^2 = 0.24; $p<0.001$; Figure S5.3B) and with the DPPC content of SSAs (R^2 = 0.77; $p<0.001$; Figure S5.3C). These inverse relations with the $[Na^+]_{coastal\ air}$ seem to result from the inverse relationship between the $WH_{seawind}$ and the DPPC content of SSAs (Figure S5.3D). As discussed below (in section 4.1), these data do not only represent the first measurements of DPPC in SSAs, they also contribute to our understanding of the factors that control the composition of SSAs.

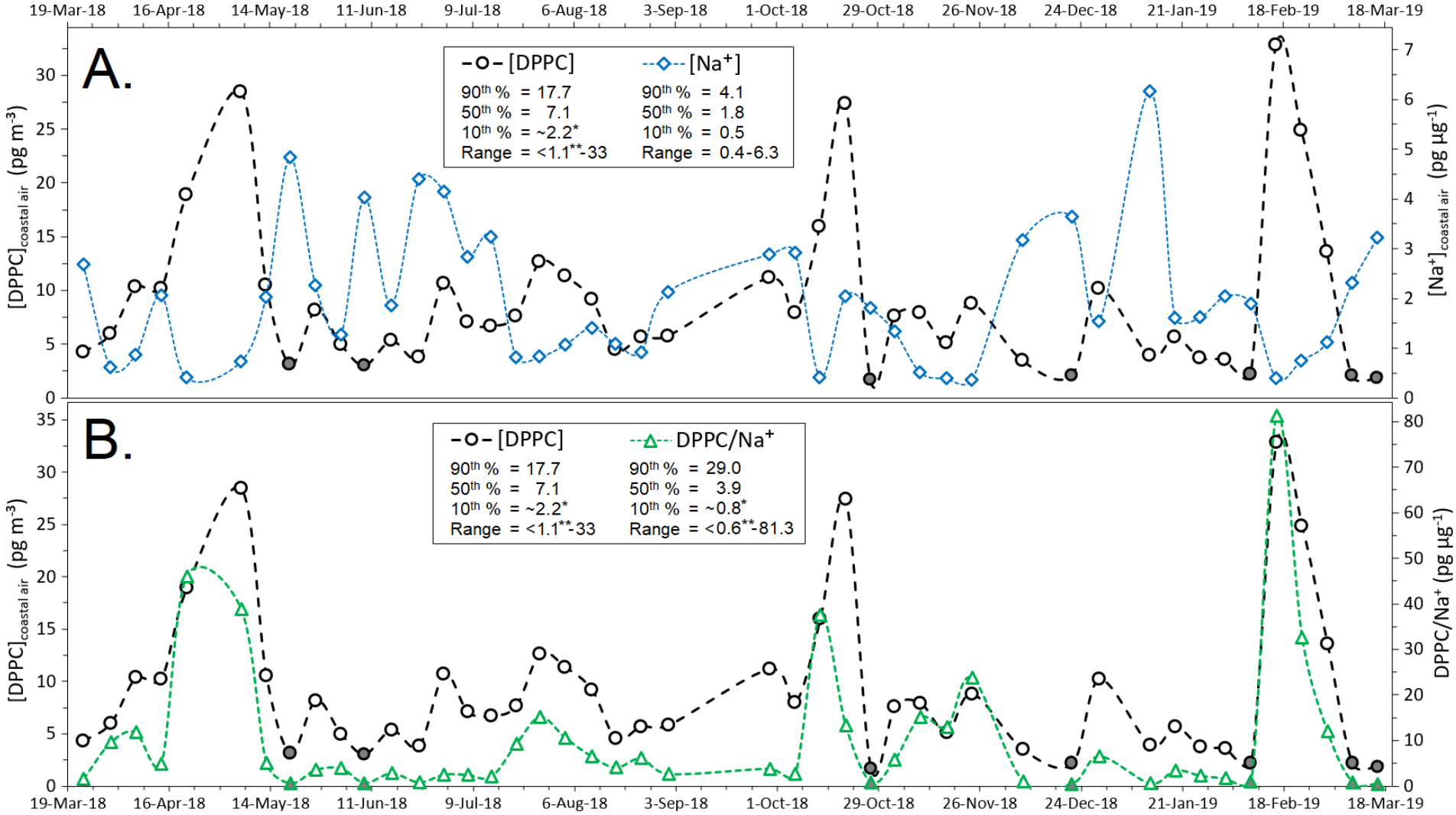

Figure 5.2: Results of the SSA sampling campaign. In (A) the DPPC and Na^+ concentrations ([DPPC], [Na^+]) of the sampled coastal air are plotted. In (B) the $[DPPC]_{coastal\ air}$ are plotted next to the corresponding DPPC/Na^+ ratios, which illustrate the DPPC content of the sampled SSAs. The filled dots (●, ▲) indicate [DPPC] < LOQ. The ranges and the 10^{th}, 50^{th}, and 90^{th} percentiles of these data are also given. The (*) and (**) indicate the values based on concentrations between the LOQ-LOQ and below the LOD, respectively.

3.3 Aerosol source

Next to $[Na^+]_{coastal\ air}$, we also analyzed the coastal air concentrations for three other major inorganic seawater constituents and four trace metals. By analyzing the correlation with the % $time_{seawind}$ (Figure S5.4), we identified their main aerosol source. All sampled trace metals (Cu^{2+}, Zn^{2+}, Pb^{2+}, Cd^{2+}) predominantly originated from a terrestrial aerosol source or from the anthropogenic activities in the harbor ($p<0.001$; 99.9% confidence level). The sampled Ca^{2+} had a weak but significant ($p<0.05$; 95% confidence level) positive correlation with the % $time_{seawind}$. It should therefore be noted, that it cannot be completely excluded that other (terrestrial) aerosol sources also influenced the $[Ca^{2+}]_{coastal\ air}$ to a certain extent. The sampled $[K^+]_{coastal\ air}$ did not have a significant correlation with the % $time_{seawind}$, implying that neither the SSA nor inland aerosol sources were dominant. Finally, Na^+ and Mg^{2+} clearly originated from the seawind ($p<0.001$). The Mg^{2+}/Na^+ mass ratios of our air samples, additionally confirmed the SSA origin of Na^+ and Mg^{2+}. Indeed, Figure S5.5 shows that at a low DPPC content ($DPPC/Na^+ < 7$ pg μg^{-1}) the sampled Mg^{2+}/Na^+ mass ratios (12.4 ± 1.4%) were consistent with that of seawater (11.9%).[204,205] At higher DPPC contents ($DPPC/Na^+ \geq 7$ pg μg^{-1}), however, an increasing Mg^{2+}/Na^+ ratio can be observed. In fact, Figure 5.3 shows that the enrichment (EF_{SSA}) of Mg^{2+} and Ca^{2+} is strongly related to the (enriched) DPPC content in SSAs. This interesting relation is further discussed in section 4.1.

Evidence demonstrating the SSA origin of the sampled DPPC is provided by the analysis of the effect of the wind direction on the sampled $[DPPC]_{coastal\ air}$ (alike this analysis for inorganics). As discussed above, the $[DPPC]_{coastal\ air}$ are largely dependent on the SSA content (i.e., $DPPC/Na^+$). The relation between $[DPPC]_{coastal\ air}$ and % $time_{seawind}$ was therefore examined in 4 different $DPPC/Na^+$ ranges (Figure S5.6). In all but one $DPPC/Na^+$ range, the % $time_{seawind}$ had a significant positive correlation with the $[DPPC]_{coastal\ air}$ ($p<0.05$). As discussed below, the SSA origin of DPPC was further supported by our final GLM and by the strong correlation of the (enriched) DPPC content in SSAs with the EF_{SSA} for Mg^{2+} and Ca^{2+} in SSAs.

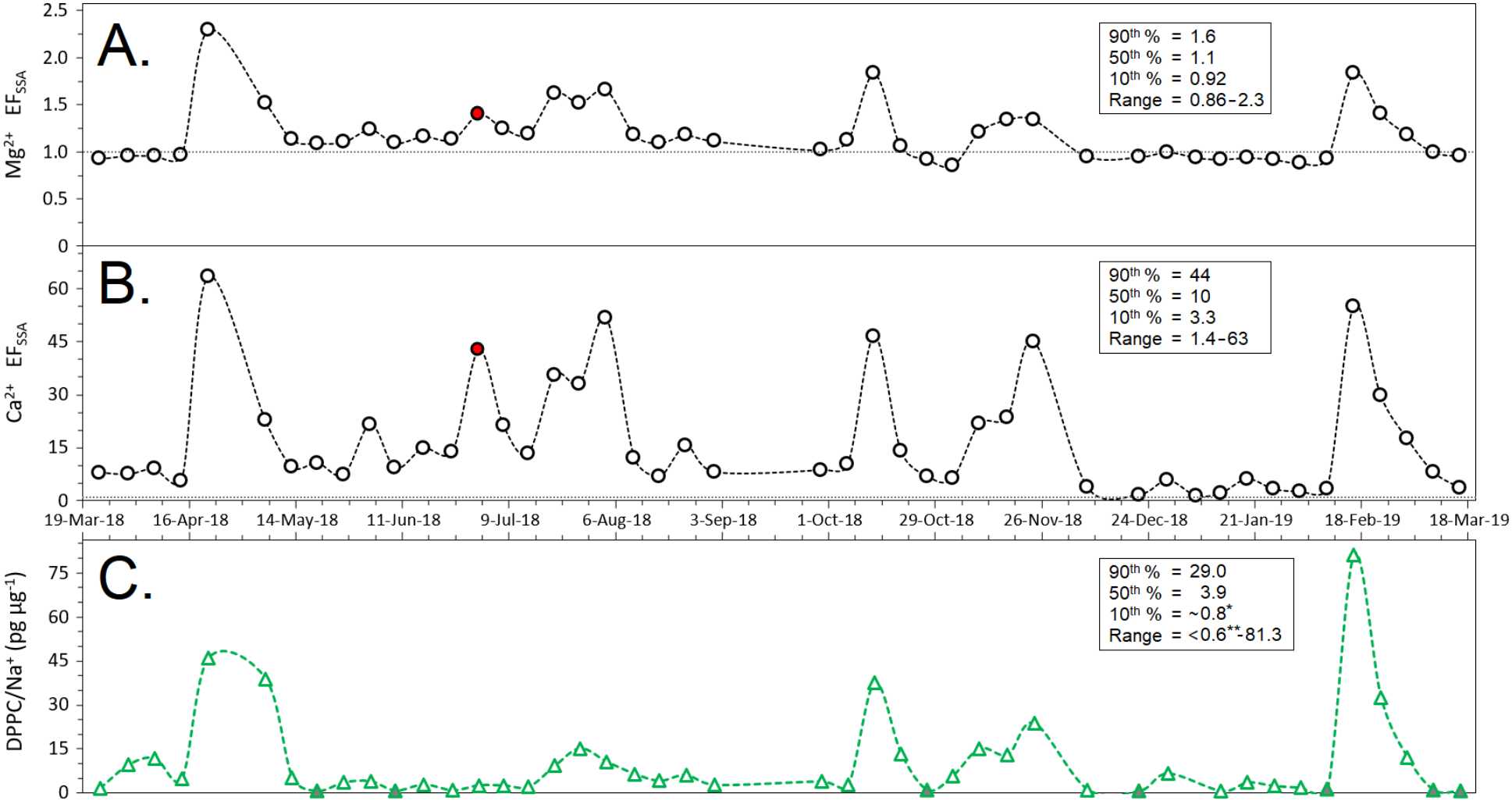

Figure 5.3: Sea spray aerosol enrichment factors (EF_{SSA}) for (A) Mg^{2+} and (B) Ca^{2+}, calculated using eq. 5.1 and the theoretical seawater ratios for Mg^{2+}/Na^+ (11.9%) and Ca^{2+}/Na^+ (3.82%).[205] In (C) the DPPC/Na^+ ratios are plotted to illustrate the correlation of the DPPC content of the sampled SSAs and their respective EF_{SSA} for Mg^{2+} and Ca^2. The ● and ▲ indicate nearby construction works (i.e., dust) and [DPPC] < LOQ, respectively. The dotted gray lines indicate the no-enrichement levels (EF_{SSA} = 1). The ranges and 10th, 50th, and 90th percentiles of these data are also given. The (*) and (**) indicate the values that are based on concentrations between the LOQ-LOQ and below the LOD, respectively.

3.4 DPPC concentration model

After comparing the model fitness for different time-lag corrections on the [PhyC] variable, the best time-lag correction showed to be 6 days. The different variables used in the final model are plotted in Figure 5.4. This final GLM achieved an adjusted R^2 of 0.529 (F-test; p <0.001) and had good accuracy, as illustrated by Figure S5.7. Our model showed that four independent variables (Table 5.2) had significant influence on the $[DPPC]_{coastal\ air}$, but no significant interactions between these variables were found. The final model equation with coefficients a, b, c, and d (see Table 5.2) is as follows:

$$\ln[\mathrm{DPPC}]_{\mathrm{coastal\ air}} = a \cdot [\mathrm{WH}]_{\mathrm{seawind}} + \mathrm{b} \cdot [\mathrm{PhyC}]_{\mathrm{mean}} + \mathrm{c} \cdot [\mathrm{PhyC}]_{\mathrm{decrease}} + \mathrm{d} \cdot [\mathrm{PhyC}]_{\mathrm{increase}} \quad \text{(eq. 5.2)}$$

The $WH_{seawind}$ had major negative influence (see Table 5.2) on the $[DPPC]_{coastal\ air}$, indicating that physical disturbances of the sea surface (microlayer) strongly reduce the $[DPPC]_{coastal\ air}$. Among the different phytoplankton variables, $[PhyC]_{mean}$ had a negative influence on the $[DPPC]_{coastal\ air}$, while the $[PhyC]_{decrease}$ and $[PhyC]_{increase}$ had positive influences (Table 5.2). The linear regressions using each independent variable individually showed similar results (Table 5.2). The adjusted R^2 for $WH_{seawind}$ was 0.382, which is much higher than for the other variables. Compared to the adjusted R^2 of our GLM, the $WH_{seawind}$ accounted for 72% of the total explained variance. Note that this model was developed to analyze the significant environmental variables determining the observed $[DPPC]_{coastal\ air}$ and not to predict actual $[DPPC]_{coastal\ air}$, as the model was not validated using an additional subset of $[DPPC]_{coastal\ air}$ data.

Table 5.2: Overview of the significant independent variables in the generalized linear model (GLM) for $[DPPC]_{coastal\ air}$. The description and details of these variables are given in Table 5.1. The adjusted R^2 results for the (simple) linear regressions performed for each independent variable individually, are also given and indicate their relative importance to $[DPPC]_{coastal\ air}$.

Independent variable	VIF	Coefficient of z-transformed variables	Standard error	P-value	Adjusted R^2 of the linear regression using only this single variable
(intercept)		<0.001	0.105	*not significant*	-
$WH_{seawind}$	1.51	-0.747	0.113	<0.001	0.382 (p <0.001)
$[PhyC]_{mean}$	2.05	-0.576	0.122	<0.001	*not significant*
$[PhyC]_{decrease}$	1.40	0.316	0.055	<0.05	0.049 (p <0.10)
$[PhyC]_{increase}$	1.51	0.319	0.067	<0.05	0.061 (p <0.10)

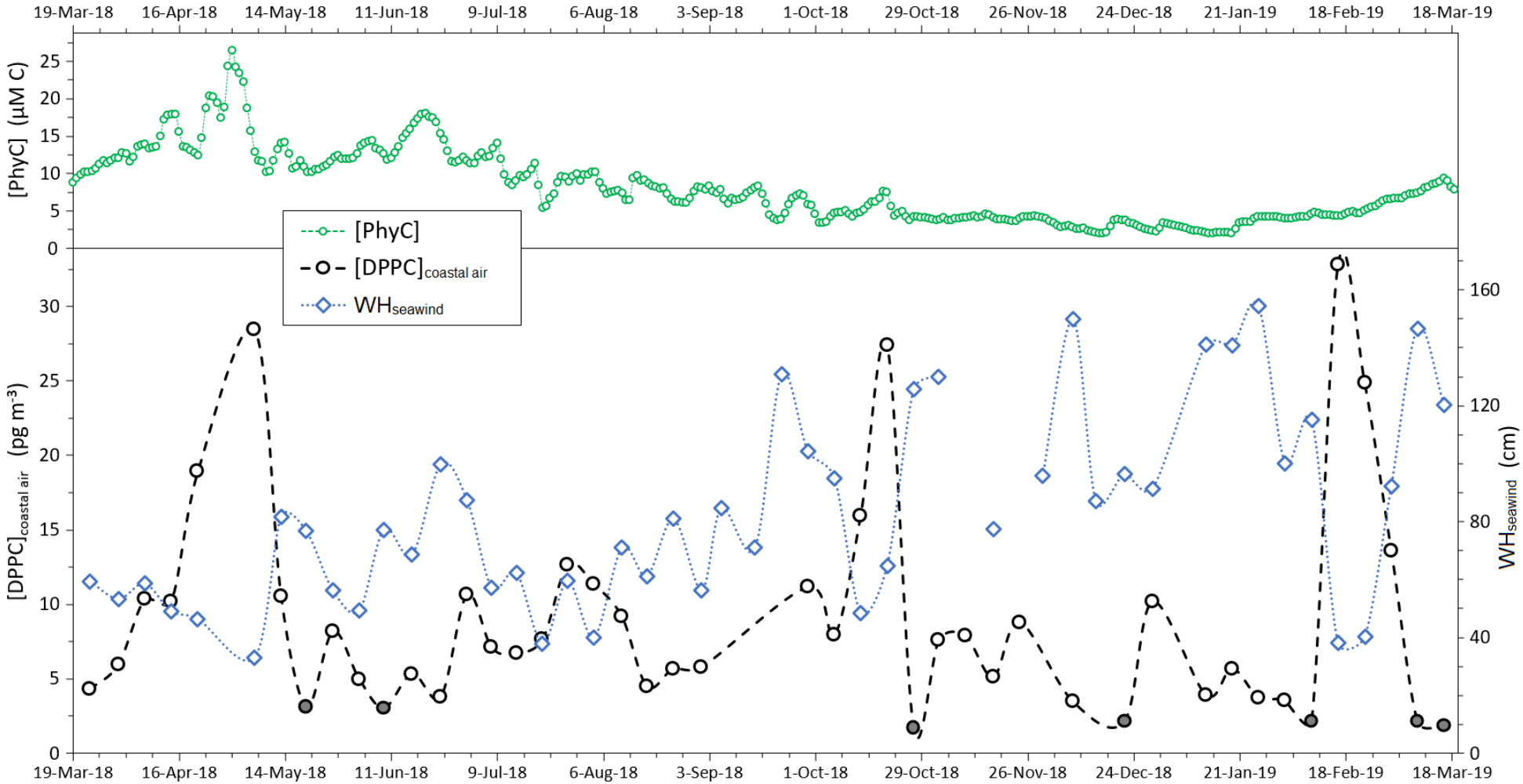

Figure 5.4: Top: The daily phytoplankton biomass expressed as concentrations of carbon ([PhyC], µM C). The [PhyC] here presented are the (6 day) time-lag corrected data. Bottom: The DPPC concentrations of the (weekly) coastal air samples ([DPPC]coastal air) and the weekly mean wave height during periods with seawind (WHseawind). The two lacking data points for the WHseawind indicate the two weeks that the wind was only coming from across land (% timeseawind = 0). The filled dots (●) indicate [DPPC] < LOQ.

4 Discussion

4.1 Source and aerosolization of DPPC

The results of our sample analyses combined with the available environmental data provide clear evidence that the sampled DPPC indeed originated from SSAs. This is based on: (1) the positive relation of $[DPPC]_{coastal\ air}$ with the $\%\ time_{seawind}$ (Figure S5.6), (2) the strong correlation of the DPPC aerosol content ($DPPC/Na^+$) with the SSA enrichment (factors) of Mg^{2+} and Ca^{2+} (Figure 5.3), and (3) the significant influences of $WH_{seawind}$ and the (changes in) phytoplankton biomass on the $[DPPC]_{coastal\ air}$, as determined by the GLM (eq. 5.2; Table 5.2). While the first argument is straightforward, the second and third are discussed in more detail hereunder.

It has long been assumed that the inorganic composition of SSAs was similar to that of seawater.[62,262] In the last two decades, however, a number of studies monitoring ambient air[287–289] or using SSA generating systems[73,74,92,218,289,290] have reported enriched SSA concentrations for Mg^{2+} and Ca^{2+} (and K^+). As reported for the SSA enrichment of organic compounds,[73,83,172,184] inorganic ions seem to be increasingly enriched with decreasing SSA sizes.[287–289] In this study SSA sampling was performed ±300 m from the high water mark. This favors smaller sized SSAs, with a higher inorganic and organic enrichment as compared to nascent SSAs. Jayarathne et al.[73] performed SSA experiments using natural coastal seawater and analyzed the EF_{SSA} for both fine (<2.5 µm) and coarser SSAs (2.5-10 µm). Their experimental results (EF_{SSA}) for the fine SSAs are comparable (1.1-2.1) to the ambient EF_{SSA} range for Mg^{2+} we observed (Figure 5.3), but are considerably lower (1.0-3.4) for Ca^{2+}. Ca^{2+} is generally found to be the most enriched inorganic constituent in SSAs.[74,92,289] The highest EF_{SSA} reported for Ca^{2+}, in very fine (0.029-0.060 µm) nascent SSAs, reaches values higher than 100.[289] The origin of the enrichment processes for Ca^{2+} and Mg^{2+} is suggested to result from the complexes they form with (surface active) biogenic organic compounds in the sea surface microlayer (SSML).[287,291–293] This cation binding effect has also been reported for DPPC in air-water interphases.[267,294] As biogenic surfactants (e.g., DPPC) are enriched in the SSML,[79,294,295] they can enhance the enrichment of Ca^{2+} and Mg^{2+} concurrently with their own enrichment in SSAs.[266] Indeed, Figure 5.3 demonstrates the strong relation between the DPPC SSA content

and the EF_{SSA} of Mg^{2+} and Ca^{2+}. As such, our study indicates that biogenic surfactants (e.g., DPPC), produced and released by marine phytoplankton, not only control the (enriched) organic[87,208] but also the (enriched) inorganic composition of SSAs.

Interestingly the $[DPPC]_{coastal\ air}$ we sampled were largely dependent on the DPPC content of SSAs (i.e., DPPC/Na^+) and much less on the SSA density (i.e., $[Na^+]_{coastal\ air}$; Figure S5.3A/B). In fact at higher SSA densities significantly lower $[DPPC]_{coastal\ air}$ and DPPC/Na^+ were encountered (Figure S5.3B/C). To explain these findings, the SSA production processes and the involvement of surfactant effects are discussed. It is clear that a lower SSA density results from a lower SSA production and thus from a lower wave action (i.e., $WH_{seawind}$, see Figure S5.3D). However, not only the SSA density but also the SSA size and content change as a function of $WH_{seawind}$. In this context, the concept of forced bubble bursting should be introduced.[95] The lifetime of air bubbles at the sea surface increases with a decreasing wind speed and wave height.[95] The bubble film thus bursts more slowly, and has more time to drain (water) and thin out.[212] As such, at lower wave heights (and wind speeds) bubbles have a lower tendency to burst and thus produce smaller and more enriched (e.g., higher DPPC/Na^+) film drop SSAs.[95] In addition, surfactants like DPPC stabilize the bubble film, increase the lifetime of air bubbles at the surface,[95,213] and increase the rate at which the film drains.[213,296] When high concentrations of DPPC are present in the seawater and SSML, the produced SSAs will thus be smaller and more enriched. Surfactants can therefore stimulate their own SSA enrichment. At a stronger wave action the SSML is, however, increasingly disturbed as breaking waves can force surfactants back down in the SSW.[89,297] As such, a strong wave action can influence the SSA size and SSA content via various mechanisms. As a consequence of the production of smaller (film drop) SSAs, the SSAs will have a longer atmospheric retention time and will transported over larger distances.[61]

The generalized linear model we developed (see section 3.4) indicates that $WH_{seawind}$ is much more important in determining the $[DPPC]_{coastal\ air}$, as compared to the (changes in) phytoplankton biomass ([PhyC]). The significant positive influences of the $[PhyC]_{decrease}$ and $[PhyC]_{increase}$ on the $[DPPC]_{coastal\ air}$ were expected, as literature indicates that phytoplankton productivity stimulates excretion of marine surfactants[282] and the demise of phytoplankton biomass increases the organic SSA content.[262] The

latter can be explained by release of DPPC upon cell lysis of phytoplankton cells.[264] The negative influence of the $[PhyC]_{mean}$, on the other hand, seems rather contradictory at first sight. A possible explanation for this can be found by looking at nutrient-phytoplankton-zooplankton-detritus (NPZD) models for the North Sea.[298,299] During winter periods (i.e., low primary productivity), the zooplankton ingests relatively less phytoplankton biomass compared to summer periods. As such, during winter, the phytoplankton could release relatively more DPPC into the seawater, instead of being taking up in the food chain. Following this theory, during spring (algal) blooms the zooplankton abundance is relatively low which should lead to increased $[DPPC]_{coastal\ air}$. This was indeed observed in the springtime periods of our SSA sampling campaign (see Figure 5.4). This potential ecological explanation of the (indirect) inverse effect of the $[PhyC]_{mean}$ on the $[DPPC]_{coastal\ air}$ can, currently not be proven or disproven and is a only introduced as a new hypothesis at this time.

This study also contributes to the knowledge on the production and behavior of SSAs in a meteorological context. Our results support that increasing surfactant concentrations and decreasing forced bubble bursting processes induce a higher surfactant SSA content and smaller SSAs.[95,213] As smaller (film drop) aerosols have a larger atmospheric retention time their meteorological influence increases. Additionally, a higher surfactant content in SSAs can enhance (hygroscopic) cloud droplet growth processes.[300] The concurrent enrichment of cations (Mg^{2+} and Ca^{2+}, Figure 5.3) with marine surfactants (DPPC) can also introduce meteorological effects. Indeed, the presence of charges on the surfaces of SSAs influence their activity as cloud condensation nuclei and play a role in lightning and thunderstorms.[66,294,301]

4.2 DPPC exposure and human health

Although DPPC has never detected in coastal air before, it had been suggested that DPPC is likely to be present in SSAs.[267] Here we quantified the range of $[DPPC]_{coastal\ air}$ (<1.1-33 pg m^{-3}; Figure 5.2) to which coastal (human) populations are exposed. As discussed above (in section 1) DPPC has a crucial role in the human respiratory system, as it is the major component (±40%) of the pulmonary surfactant present in alveoli.[268,269]

We suggest, however, that the quantified $[DPPC]_{coastal\ air}$ are too low to induce human health effects through the additional supply of pulmonary surfactant. The maximum airborne exposure via coastal air, assuming an extremely high inhalation flow rate (100 L min^{-1}),[235] equals 4.8 ng DPPC day^{-1}. Medical therapies for pulmonary surfactant related diseases use much larger doses. Respiratory distress syndrome (RDS) in preterm newborns for example is treated with (modified) animal-derived lung surfactant using doses from 50 to 200 mg of per kg bodyweight.[302] As lung surfactant contains 40% DPPC[268,269] and the preterm birth weight can range from 0.75 to 2.5 kg, the deployed DPPC doses of a treatment range from 15 to 200 mg. Such surfactant replacement therapies (SRT) have also been widely examined to treat acute respiratory distress syndrome.[303] Overall these studies use even higher surfactant doses than the ones mentioned above for the treatment of preterm newborns suffering from RDS.[303] Intubation methods for SRT are still the predominant treatment strategy but aerosol delivery systems are increasingly examined and introduced.[302,304–306] A last argument indicating that the $[DPPC]_{coastal\ air}$ we determined are not expected to have a direct health effect is given by Ullah et al.[275]. They determined that humans can exhale 20 to 700 ng DPPC m^{-3} via aerosols upon (strong) breathing. This exhaled concentration range is up to 3 orders of magnitude higher than that found in coastal air. Although that it cannot be complete excluded upon chronic exposure, it is therefore unlikely that $[DPPC]_{coastal\ air}$ will have a direct effect on human health.

There is, however, another fascinating mechanism by which DPPC can induce - indirect - health effects through airborne exposure via (sea spray) aerosols. Surfactants like fatty acids and phospholipids coat the surface of SSA droplets.[171] This SSA coating can play a facilitating role in the delivery of other marine bioactive chemicals. Indeed DPPC is one of the excipients which is currently authorized and used for medical pulmonary drug delivery via aerosol therapy.[271,273] These pulmonary drug delivery methodologies are rapidly evolving, and are indeed already used for a range of drugs (e.g., antibiotics, vaccines, peptides and chemotherapeutics).[273,307] Depending on the type of aerosol formulation (e.g., micelles; liposomes, solid particles)[271] phospholipids like DPPC may (1) improve the transport of poorly water-soluble drugs,[268,271] (2) reduce recognition of exogenous aerosols by alveolar macrophages,[271,308,309] (3) serve as a post-deposition spreading agent,[274] (4) stimulate pharmacokinetics via enhancement of the drug permeability through the lung

epithelium.[271,310] As such, the DPPC content of SSAs draws a very interesting parallel with medical aerosol therapy. It can facilitate the effects of other bioactive compounds present in SSAs. We know that the marine biosphere contains a whole spectrum of natural compounds with known or suspected pharmacological effects.[26,27] The medical/pharmaceutical research investigating the facilitating effects of DPPC and other phospholipids may thus contribute to the unraveling of mechanisms that occur upon airborne exposure to natural SSAs.

It should be noted that this facilitating effect of marine surfactants like DPPC could also hold true for toxic chemicals. It has been shown, for example, that some marine phycotoxins can be found in coastal air[22,137,311] and induce respiratory syndromes during harmful algal blooms (HABs).[17,138,312] Such harmful exposures to aerosolized phycotoxins are rather rare events, requiring a combination of favorable weather conditions for SSA production and a severe toxin-producing harmful algal bloom. Although that we cannot ignore this potential negative effect of DPPC, we do not expect it to overrule its potential positive effect. If the adverse effects of DPPC would outweigh its positive effects one would expect the health status of coastal populations to be lower than that of inland populations, and this is not the case. On the contrary, a positive coastal proximity health effect is increasingly observed in epidemiological research.[32,33,35,313] In this context, Moore[46] published his biogenics hypothesis suggesting that regular airborne exposure to aerosolized natural compounds may be health promoting via the downregulation of specific cell signaling pathways. While our previous work using in vitro studies on lung cells[179,180] supported the principles of this hypothesis, our new findings on DPPC presented here further highlight the potential health promoting effect of airborne exposure to SSAs in coastal air.

Chapter 6

General conclusions and perspectives

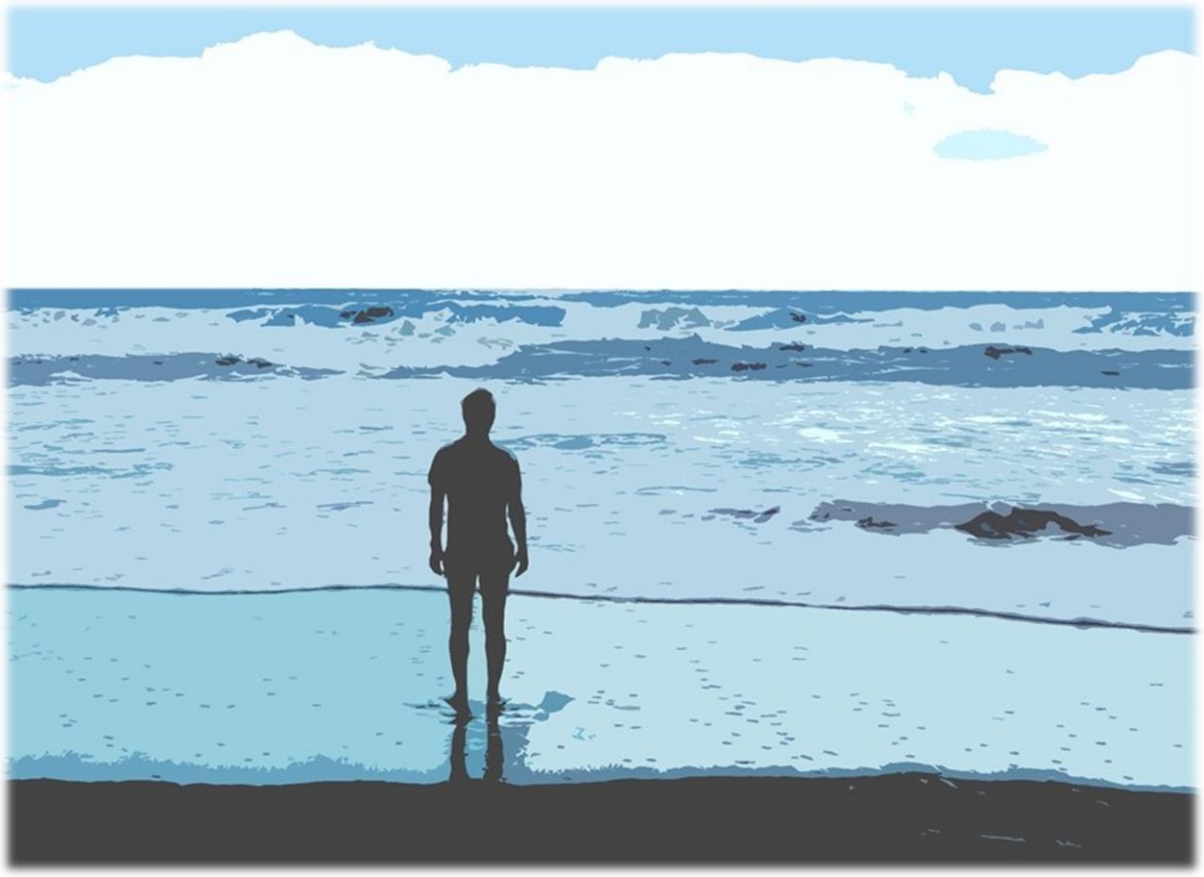

Chapter contents

1 Introduction

Despite the generally accepted believe that coastal air induces beneficial human health effects, the mechanisms by which these potential effects are induced are poorly understood. The main objective of this interdisciplinary PhD thesis was to perform an exploratory assessment of the airborne exposure to and potential health effects of marine compounds in SSAs. To this end, we combined (1) in-depth research that focused on specific bioactive compounds, and (2) exploratory research aiming to examine the entire chemical mixture of natural SSAs.

The former part (1) was targeted at understanding the potential role of marine phycotoxins, i.e., a globally occurring group of bioactive compounds. As such, we examined their potential harmful and/or beneficial (in vitro) health effects upon airborne exposure, the processes determining their sea spray aerosolization and their environmental concentrations resulting in human airborne exposure. The latter research part (2) assessed the potential health effects of natural SSAs by using natural SSA sample extracts. The bioactivity of SSA extracts was examined using the (in vitro) differential gene expression of lung cells; i.e., an endpoint giving a general overview of the (potential) effects at the molecular level. The composition of the SSA sample extracts was analyzed for marine compounds having well-known effects on the human respiratory system.

Due to the large amount of pioneering work that was performed, it was of course not possible to unravel all aspects of possible linkages between SSAs and human health. Nonetheless I believe that some major breakthroughs were made in this PhD research. To summarize the discoveries and general conclusions of this PhD study, I have attempted to answer the research questions (Q1-8) introduced in Chapter 1. Where possible an initial human health risk and/or benefit assessment was performed. Next, I will discuss the perspectives concerning (future) human health risks and opportunities linked to SSA exposure. Finally, research recommendations are formulated which will hopefully lead to the enhancement of our knowledge in this young and at the same time ancient research field.

2 General conclusions

- Q1*: Can low doses of phycotoxins induce negative health effects via SSAs?* ***(Chapter 2)***

It is clear that the two well-known cases of phycotoxins inducing respiratory syndromes via SSAs (i.e., brevetoxins (PbTxs) and ovatoxins (OVTXs)) occur during harmful algal bloom (HAB) events.[22,24] Under normal non-HAB circumstances most phycotoxins are expected to be present at much lower (background) concentrations. As such, it was important to examine which phycotoxins could induce health effects at low exposure doses. To this end, we used in vitro experiments wherein we dosed phycotoxins to lung cells and analyzed the effects on the cell viability.

The two yessotoxins (YTXs) showed to induce effects at the lowest concentrations (Figure 2.1). At first sight one could expect that YTXs are therefore more toxic than the other examined phycotoxins. As discussed under the next research question, the partial cells viability effects of YTXs are rather linked to beneficial mechanisms than to a higher toxicity. Two of the other examined phycotoxins showed to initiate mechanisms that lead to the mortality of the exposed lung cells. Based on these cell viability data (43 h EC_{50}; see Table S2.1) okadaic acid (OA), the primary phycotoxin in the North Sea,[151–153] induced these toxic effects at (on average) 43 times lower concentrations as compared to PbTx-2.

These results suggest that OA could induce negative health effects via SSA at much lower doses than the ones reported for PbTx-2. As far as we know, the lowest ambient $[PbTx]_{coastal\ air}$ inducing a respiratory syndrome were reported by Cheng et al.[314] for the upper respiratory tract (3.4 ng m^{-3} for a 6-8 h exposure) and by Fleming et al.[225] for the lower respiratory tract (57 ng m^{-3} for a 1 h exposure). The (lowest) effective air concentration reported by Cheng et al.[314] equals a total inhaled dose of 36 ng, at an respiration rate of 25 L min^{-1} (light exercise).[314] This dose can thus be considered to be the lowest observed adverse effect level (LOAEL*) for respiratory exposure to PbTx.

** In human toxicology the lowest observed adverse effect level (LOAEL) represents the lowest experimental or observed dose or concentration that induces a significant harmful effect.*

If we assume that the difference in toxicity of our in vitro model system can be extrapolated to the (in vivo) human respiratory tract, we can also estimate a LOAEL value for OA. We are aware that this extrapolation includes a large uncertainty, but as there is no other information available, it is the best method to get a first indication of the harmful dose for OA. Following this extrapolation approach, we calculated that OA could induce negative (in vivo) health effects in the upper respiratory tract at a minimal dose of 0.84 ng. The further assessment to examine whether such a OA dose could be inhaled via SSAs is performed further below (Q4).

- Q2*: Can phycotoxins induce positive health effects via the mTOR pathway, as suggested by the biogenics hypothesis? (**Chapter 2)***

The performed in vitro experiments on lung cells showed a different image for yessotoxin and homoyessotoxin as compared to the other examined phycotoxins. These YTXs only induced a partial cell viability decrease at the highest test concentrations, while the other phycotoxins induce complete cell mortality (see Figure 2.1). Growth inhibition and apoptosis, both linked to a lower mTOR pathway activity, may explain these cell viability effects of YTXs. In agreement with literature, our in vitro experiments - using western blotting methods – showed that YTXs downregulate this cell signaling pathway. Although that we only observed different effects between cancer (A549) and normal cells (BEAS-2B) in the western blotting experiments. It has been suggested that YTXs have a stronger activity in cancer cells and could therefore have potential as an anticancer drug.[162] Downregulation of the mTOR pathway is crucial in Moore's biogenics hypothesis.[46] These findings therefore support a basic principle of this hypothesis. Indeed, based on our research it can be concluded that specific marine compounds like YTXs could induce positive health effects via the mTOR pathway.

The lung cells we used in our experiments showed cell viability effects for YTXs at (on average) 1640 times lower concentrations than for PbTx-2 (based on the 43 h EC_{50} values; Table S2.1). Following the same extrapolation assumptions as in the previous research question (Q1), we calculated that a dose of 22 pg YTXs could potentially induce an in vivo downregulation of the mTOR pathway. The further assessment to examine whether such a YTXs dose could be inhaled via natural SSAs is performed further below (Q6). First the sea spray aerosolization potential of YTXs and other phycotoxins like OA are discussed in the next two research questions (Q3-4).

- Q3*: Are these phycotoxins easily aerosolized via sea spray and which factors affect these water-air transfer processes?* ***(Chapter 3)***

Via aerosolization experiments using seawater spiked with toxin-producing algae, this study provided the first (experimental) evidence and characterization of the sea spray aerosolization of OA, hYTX, and dinophysistoxin-1 (DTX-1). The potential for aerosolization of these phycotoxins was highlighted by their 78- to 1769-fold enrichment in SSAs relative to the subsurface water. The enrichment in the sea surface microlayer (SSML), only reaching enrichment factors (EFs) up to 6.4, could not explain the high SSA enrichment processes. In agreement with literature,[87] we concluded that the scavenging (enrichment) process of rising air bubbles determines the SSA enrichment (i.e., EF_{SSA}) of (dissolved) compounds like phycotoxins to a far greater extent than SSML enrichment does. This conclusion does not hold true for surface active compounds or surfactants. As further discussed below under Q8, surfactants accumulate in the SSML and have an important role in the bubble bursting processes and SSA production. Such effects of marine surfactants were also observed in the current experiments examining the aerosolization of phycotoxins. Indeed, the experiment using natural seawater showed a much higher foam stability and consequently a lower magnitude of SSA production (Figure 3.2A/B).

To obtain and support these experimental results, we first developed a method for the determination of phycotoxin concentrations in SSAs. This analytical method showed good linearity ($R^2 > 0.99$), recovery (85.3−101.8%), and precision (RSDs ≤ 17.2%). Concurrent analysis of the organic and inorganic SSA content provided crucial information to unravel specific SSA processes (e.g., magnitude, enrichment) and make extrapolation calculations as discussed (among others) in the next research question (Q4).

- Q4*: What are the phycotoxin air concentrations occurring at the Belgium coast, and do they pose a potential risk or benefit to human health?* ***(Chapter 3)***

In the SSA samples we collected on the beach, we were not able to detect any phycotoxins above the limits of detection (LODs). From these natural samples we were only able to determine the ambient SSA densities (i.e., $[Na^+]_{coastal\ air}$). Concurrently we performed aerosolization experiments using natural seawater in a marine aerosol reference tank (MART). In these experiments we detected OA in the SSAs and were

able to predict the phycotoxin composition of the nascent environmental SSAs (i.e., $[OA]_{SSA}/[Na^+]_{SSA}$). Using the combination of these environmental and experimental data (Table 3.2), we indirectly quantified the OA concentrations in the coastal air ($[OA]_{coastal\ air}$ = 0.6−51 pg m^{-3}). As such we could determine that in a worst case scenario, the inhaled dose of a person walking along the waterline during an 8 h exposure period (light exercise respiration rate of 25 L min^{-1})[314] equals 0.41 ng OA.

Performing a risk assessment, to determine whether these $[OA]_{coastal\ air}$ could pose a threat to human health, is not that straightforward. In absence of toxicological in vivo data for respiratory exposure to OA, the LOAEL can only be estimated via the extrapolation of (in vivo) effect data of ingestion exposure or in vitro cell viability data of lung cells. Using the LOAEL for ingestion exposure (50 µg OA per person),[315,316] a margin of exposure (MOE)** larger than 10^4 was calculated. Here this so-called MOE indicates the ratio between the LOAEL and the inhaled dose during the above described 8 h exposure scenario. Conversely, using the data of our lung cell in vitro experiments and the respiratory in vivo effect concentrations for PbTx, as performed above under Q1, a LOAEL of 0.84 ng was calculated. Using this LOAEL relative to the inhaled dose during the above described 8 h exposure scenario (0.41 ng OA) only results in a MOE of 2.

While the first human risk assessment approach predicted a safe situation (MOE >10^4), the latter approach predicted a situation that is far from protective (MOE of 2). It needs to be stressed that both the performed exposure and effects assessments used extrapolations with high uncertainties. It is therefore clear that due to the shortage of data, a robust risk assessment for the airborne exposure to OA via SSAs is currently not possible and too arbitrary to be trustworthy. To date, there have been no reported (medical) cases of respiratory syndromes upon airborne exposure to SSAs, during HABs of OA-producing algae. It therefore seems rather unlikely that the current $[OA]_{coastal\ air}$ could induce any negative health effects.

*** The MOE is commonly used in human health risk assessment and represents the ratio of the no-observed-adverse-effect level (NOAEL) or LOAEL to the predicted, or estimated human exposure level or dose. Generally a MOE ≥ 100 is considered to be protective. When the LOAEL is used instead of the NOAEL, or when carcinogenic or genotoxic compounds are considered, the MOE needs to be ≥ 10^4 to have an protective exposure scenario.*

- Q5*: Which effects, after respiratory exposure, can marine compounds in SSAs have at the molecular level?* ***(Chapter 4)***

Using in vitro experiments with lung cells we compared the molecular effects (i.e., differential gene expression) of a natural SSA sample extract with those of a chemical mTOR inhibitor. At a high but realistic dose this natural SSA extract induced effects at the gene and pathway level in close resemblance to the known mTOR inhibitor. The similarities in regulation of the genes related to the mTOR pathway (Figure 4.6) suggest that natural SSAs indeed contain natural compounds that cause similar effects on the mTOR pathway as the known mTOR inhibitor. The effects extended even further as four additional pathways, linked to the mTOR pathway (i.e., glycogenesis, spliceosome, lysosome, steroid biosynthesis), were also significantly influenced. An important gene that was downregulated by both the mTOR inhibitor and the natural SSA treatment was PCSK9. Upregulation of this gene is associated with multi-organ pathology and inflammation, while PCSK9 downregulation is associated with protection against inflammation, organ pathology and systemic bacterial dissemation.[247] It has been shown that PCSK9 induces secretion of pro- inflammatory cytokines,[317] and that its inhibition may reduce the binding of bacterial endotoxin to Toll-like receptors by improving the hepatic clearance of circulating endotoxin.[247] Overall these results provide molecular evidence for potential beneficial health effects of exposure to bioactive compounds in SSAs, as hypothesized by Moore.[46]

- Q6*: How do these effects of natural SSAs, at a molecular level, relate to the effects induced by specific phycotoxins?* ***(Chapter 4)***

The examined hYTX treatments (i.e., pure hYTX and lab SSA, see Chapter 4) also had a significant effect on PCSK9 and the mTOR pathway. The concentrations inducing these different gene expression effects were consistent with the hYTX concentrations inducing inhibition effects on the cell viability (e.g., growth inhibition and apoptosis) and the activity of the mTOR pathway, as observed in Chapter 2 and discussed under Q2. This additionally confirmed that YTXs indeed influence the mTOR pathway. In the current in vitro experiment (Chapter 4), the hYTX treatments did however show an upregulated expression of the PCSK9 gene and the genes of the mTOR pathway. This was unlike the natural SSA and mTOR inhibitor treatments, which showed a downregulated expression of these genes. The effects observed in the natural SSA treatment should thus be induced by other marine compounds than YTXs.

The question whether sea spray aerosolized YTXs could reach effective concentrations however still remains. Under Q2 we calculated that a minimal dose of 22 pg YTXs could potentially induce an in vivo downregulation of the mTOR pathway. For an exposure to such a dose during an 8 h period, at an (light exercise) respiration rate of 25 L min^{-1},[314] a minimal $[YTXs]_{coastal\ air}$ of 1.8 pg m^{-3} should be inhaled. YTXs have, however, never been measured in ambient coastal air, also not in our study.

In Chapter 3, we did show that YTXs can be easily aerosolized and strongly enriched in SSAs. To estimate the maximum potential $[YTXs]_{coastal\ air}$, to which people can be exposed near the waterline, we can extrapolate the results obtained in our MART aerosolization experiments. In the MART experiment using natural seawater (Figure 3.2B) a *Protoceratium reticulatum* density of 500 000 cells L^{-1} was used and YTXs air concentrations of 0.8 ng m^{-3} were measured. In comparison, *P. reticulatum* blooms in natural marine environments reach peak densities which are about 1000 times lower (400-700 cells L^{-1}).[196,197] Following the proposed extrapolation, the maximum potential $[YTXs]_{coastal\ air}$ are calculated to be 1000 times lower than in our MART experiment and are equal to 0.8 pg m^{-3}. These extrapolation calculations thus predict a MOE of 2.3 and suggest that the $[YTXs]_{coastal\ air}$ cannot reach effective concentrations. It should be noted, however, that the uncertainty on these extrapolations are too high to formulate solid conclusions.

- Q7*: Which marine bioactive compounds are present in SSAs at concentrations that can influence human health?* ***(Chapter 5)***

Via the chemical analysis of the SSA samples of a one-year campaign at the Belgium coast, we detected and quantified the coastal air concentrations of dipalmitoylphosphatidylcholine (DPPC) for the first time. It is clear that the bioactivity and airborne exposure of DPPC can be related to human health. Indeed, DPPC is the major component (±40%) of the pulmonary surfactant in human alveoli and essential for good lung functioning.[268,269] Conversely, lung surfactant abnormalities are associated with obstructive lung diseases (e.g., bronchiolitis, asthma).[270] In Chapter 5 section 4.2, we discussed that the quantified $[DPPC]_{coastal\ air}$ (<1.1-33 pg m^{-3}) are probably too low to directly induce human health effects through the additional supply of pulmonary surfactant.

We suggest however, that DPPC in SSAs can induce human health in an indirect way. Together with other marine surfactants DPPC will form a coating on the surface of SSA droplets.[171] This (surface–active) property of DPPC is one of the essential reasons why it is used as an excipients for medical pulmonary drug delivery via aerosol therapy.[271,273] Depending on the type of aerosol formulation (e.g., micelles; liposomes, solid particles)[271] phospholipids like DPPC may (1) improve the transport of poorly water-soluble drugs,[268,271] (2) reduce the recognition of the exogenous aerosol nature by alveolar macrophages,[271,308,309] (3) serve as a post-deposition spreading agent,[274] (4) stimulate pharmacokinetics via enhancement of the drug permeability through the lung epithelium.[271,310] In summary this discovery of DPPC in SSAs draws a very interesting parallel with medical aerosol therapy, as it can facilitate the effects of other bioactive compounds present in the inhaled sea spray aerosols.

- Q8: *Are the coastal air concentrations of these compounds related to the ecological and/or meteorological state of the marine environment?* ***(Chapter 5)***

Interestingly the $[DPPC]_{coastal\ air}$ we sampled were largely dependent on the DPPC content of the SSAs ($DPPC/Na^+$) and much less on the SSA density (i.e., $[Na^+]_{coastal\ air}$). In fact at higher SSA densities significantly lower $[DPPC]_{coastal\ air}$ and DPPC contents in SSAs were observed. Consequently we found that the DPPC content of SSAs was strongly dependent on the wave height. The generalized linear model we developed indeed showed that wave height had a major negative effect on the $[DPPC]_{coastal\ air}$. This important negative relation with wave height can be attributed to two mechanisms. As discussed in more detail in Chapter 5 section 4.1, an increased wave action reduces the surface lifetime of air bubbles, which consequently leads to larger and less enriched SSAs that have a shorter atmospheric retention time. Secondly, a strong wave action disrupts the sea surface microlayer (SSML).[297] The SSML is known to have high DPPC concentrations,[265,266] and is assumed to stimulate the aerosolization of its compounds. Increased wave action however pushes surfactants from the SSML back in to the subsurface water (SSW).[297]

Our model also suggested that the available concentration of DPPC in the seawater is not the main driver of the $[DPPC]_{coastal\ air}$. Seawater concentrations of marine surfactants, like DPPC, are mainly linked to a high primary productivity[282] and phytoplankton cell lysis.[264] Both increases and decreases in phytoplankton biomass

([PhyC]) should thus promote the $[DPPC]_{coastal\ air.}$ The generalized linear model we developed indeed confirmed this hypothesis. The (weekly) $[PhyC]_{increase}$ and $[PhyC]_{decrease}$ had significant positive effects on the $[DPPC]_{coastal\ air}$. Conversely, the $[PhyC]_{mean}$ had a significant negative effect. Still these effects of the (changes in) [PhyC] were of lower importance than the wave action, as the latter accounted for 72% of the total explained variance of our model.

3 Perspectives

3.1 Opportunities and risks

Since the Industrial Revolution, anthropogenic activities have increasingly impacted the biotic and abiotic state of marine environments.[318] Disturbances of marine ecosystems do, however, not only affect the organisms living in the seawater. The marine sphere influences much more. The health of human coastal populations is among others interconnected with the (health) state of the ocean.[29,319] The SSA relationship between the ocean and human health (OHH), which was investigated in this PhD thesis, creates both opportunities and risks for coastal populations. Indeed SSAs can deliver natural marine compounds with a beneficial pharmacological[26,27] or potent toxic activity,[20–22,138] but also pollutants that are released to the seawater through human activities.

Despite the historical believe that coastal air induces beneficial human health effects, little to no scientific studies have investigated the potential beneficial effects of SSAs before this PhD research. The fact that we started to examine the basic principles of the biogenics hypothesis and have demonstrated in this PhD research that natural SSA extracts have positive effects on important cellular pathways, may be the start of further discoveries in this OHH research field. I hope that this will stimulate more research that will eventually lead to a more comprehensive evidence base demonstrating the beneficial health effects of SSAs. I believe that, the medical, economic and ecological opportunities linked to natural SSAs exposure are enormous. Indeed, it is argued that the opportunities and benefits related to a healthy ocean (e.g., healthy SSAs) are more convincing than the risks of an unhealthy or polluted ocean to additionally safeguard marine ecosystems.

Marine environments host a whole range of undiscovered natural compounds, all of which may have a pharmacological, nutritional, agricultural and/or industrial use. The improvements of the strategies to identify new bioactive compounds, such as new genome mining approaches (see Chapter 1 section 4.1) are accelerating the discovery of marine drugs and the production of new marine pharmaceuticals.[109] An important message and opportunity is that by protecting the high biodiversity of marine ecosystems, we safeguard a treasure of undiscovered marine bioactive compounds. At the same time, medical aerosol therapy is increasingly being investigated and ameliorated. In this study we discovered the presence of DPPC for the first time in SSAs. As in medical aerosol therapy where this compound is added as an excipient to facilitate the effects of the deployed drugs, DPPC could also stimulate the health effects of beneficial marine compounds in natural SSAs. Future research into the surfactant composition and effects of natural SSAs will render important new insights. This can create interesting opportunities to extent and improve medical aerosol therapies with new (marine) pharmaceuticals and excipient combinations.

Conversely, it may also be hypothesized that DPPC present in natural SSAs could also facilitate the adverse health effects of natural toxins and/or pollutants. The human health risks or toxicity of these compounds in SSAs would then not only be dependent on their coastal air concentrations, but also on the surfactant composition of the natural SSAs. As DPPC is an ubiquitous natural compound, the only possibility to limit the potential risks related to toxic chemicals in SSAs is by reducing their emission (for pollutants) or production (for toxins) in seawater. Although the range of pollutants is very broad (e.g., industrial chemicals, wide dispersive use chemicals, radioisotopes) it is clear that reducing their emission is more straightforward than that of naturally produced toxins.

Algal toxins or phycotoxins are by far the most important group of naturally produced toxins in the marine environment. In this study we showed for the first time that, next to PbTxs and OVTXs, other globally occurring phycotoxins like OA can also be found in SSAs at enriched concentrations (i.e., relative to the subsurface seawater). The production of phycotoxins is often linked to nutrient pollution of coastal waters (i.e., eutrophication), which could in theory also be remediated if and where needed. In the past decades, there has however been (scientific) discussion on whether the increase

in reported HAB events could be alternatively explained by heightened monitoring and scientific awareness.[320] Recently Hallegraef et al.[129] reported that, over the period 1985–2018, no evidence can be found to support a general global increase in HAB events. Significant increases (and decreases) of HABs have still been observed on local and regional scales.[129] New emerging cases of toxin-producing HABs that introduce harmful concentrations of phycotoxin in SSAs can thus not be excluded.[129] The benthic dinoflagellate *Ostreopsis ovata* producing OVTXs is one HAB species that is spreading into new areas (e.g., Mediterranean Sea) and introduces harmful phycotoxins in SSAs.[129,321] As the control and prediction of such HAB events are very difficult, the health risks for coastal populations can be controlled by good monitoring programs and by taking measures. The latter can include the closure of beaches when a toxic HAB event is occurring. Such harmful exposures to aerosolized phycotoxins are however rare events. At the Belgium coast no such harmful cases have been reported so far. During our study we determined that OA is the only phycotoxin present at (indirectly) detectable air concentrations at the Belgian coast. We also determined that it is rather unlikely that these $[OA]_{coastal\ air}$ could induce any negative health effects. The current human health risks related to SSA exposure are therefore assessed to be low at the Belgian coast. Also, phycotoxins do not necessarily induce negative health effects. As demonstrated in our in vitro studies and as demonstrated by others,[145,162,178] the bioactivity of YTXs can be linked to positive therapeutic effects and is as such an interesting compound to investigate the marine biogenics hypothesis.

3.2 Future research

In the second section of this chapter, I have showed that the shortage of exposure and in vivo effect data makes it difficult to confidently perform unambiguous human risk and benefit assessments. To improve these assessments and to build further on the work performed in this PhD research, recommendations for future research are formulated in this section.

A first major recommendation is to improve our knowledge on the different processes influencing the sea spray aerosolization of marine compounds. These processes determine the air concentrations, aerosol size, atmospheric retention time and eventually human exposure to these compounds. As such, a better understanding of these processes will make it possible to model the human exposure to specific

compounds (e.g., phycotoxins, DPPC) based on meteorological and ecological data or predictions. One of these SSA processes which is of major importance is the SSA enrichment. In this PhD for example we found that the SSML is of lesser importance for the SSA enrichment of phycotoxins, while it seemed to be of major importance for the aerosolization of the surfactant DPPC. As applied in this thesis, a combination of environmental SSA sampling campaigns and aerosolization experiments is needed and recommended to increase our knowledge on SSA processes in the best way possible. In continuous environmental sampling campaigns all possible variations of the different (meteorological, ecological and physicochemical) variables determining the SSA processes are monitored. Using this type of data it will be possible to determine the ambient SSA processes and bio-compound specific concentrations in SSA and the (coastal) air.

The above research recommendation can be performed for marine compounds known to be found in SSAs. A major challenge is, however, to discover and quantify the sea spray aerosolization and (coastal) air concentrations for other marine compounds. In this PhD research we always used chemical analysis methods targeting specific compounds. For the discovery of new compounds in SSAs untargeted analytical methods can prove to be even more useful. As such the principal components (i.e., compounds) of natural SSA samples can be determined. From our point of view, the presence of marine compounds in SSAs is only important if they have a bioactivity at ambient concentrations. To this end, the activity-guided approach displayed in Figure 1.10A using fractionated extracts of natural SSA extracts is a perfect strategy. As such, in vitro experiments using endpoints like differential gene expression, which give a general overview of the induced effects, can be combined with a final untargeted chemical analysis. This approach represents a major research recommendation, as it suggests a method to discover new bioactive compounds in SSAs (if present).

The current set-up of our in vitro experiments included a maximum exposure period of about two to three days. After this exposure period the cells cultures reach a confluent state. In order to test more chronic and thus longer exposures, experiments can be prolonged by splitting or sub culturing the cells cultures during the experiments and by restoring the test concentrations in the medium upon every translocation.[322] Another way to increase the realism of our in vitro models, instead of using 2D classic

monocultures, is to grow 3D cell cultures and/or to combine different cell lines in a so called co-cultures. Both 3D and co-culture cell cultures more closely resemble in vivo tissue in terms of cellular communication and the development of extracellular matrices.[323] The most advanced development in terms of realistic in vitro lung cell models for this kind of research is the lung-on-a-chip.[324] This type of organ-on-a-chip or organoid consists of organ-specific multicellular 3D cell cultures that recapitulate some of the critical structural and functional properties of the corresponding organ.[325] They are constructed (see Figure 6.1) as a microfluidic device for cell culture which is comprised of continuously perfused channels populated by living cells.[324,325]

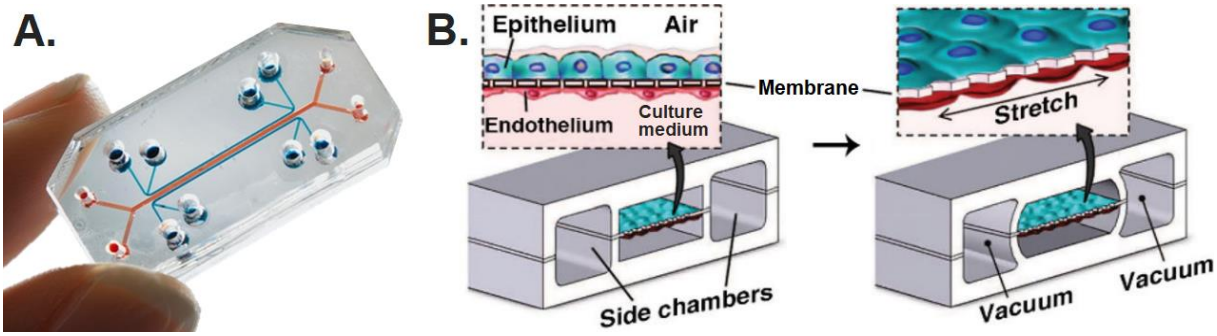

Figure 6.1: (A) real life version of a lung-on-a-chip, © Wyss institute, (B) illustration of the detailed composition of a lung-on-a-chip: the upper alveolar channel is lined by alveolar epithelial cells, and the lower vascular channel is lined with pulmonary vascular endothelial cells. It replicates the physiological breathing pattern by mechanical stretching of the membrane by using vacuum chambers alongside the cell culture channels. This illustration is adapted from Shrestha et al.[324]

A quite specific research recommendation concerning the sampling and analysis of organic compounds in SSAs, is to include a precombustion step (2-4 h at 450-550°C) in the pretreatment of new (quartz fiber) filters. By doing so, any (background) compounds (e.g., fatty acids) present on the filter will be largely degraded. As such, the risk for interference of the filter matrix/background is much lower. Here, except for SPX-1, we did not encounter any background issues for the compounds we targeted.

It is clear that our discovery of DPPC in SSAs opens a range of research perspectives and opportunities. The medical/pharmaceutical research investigating the facilitating effects of phospholipids (e.g., DPPC) can now be viewed from another perspective and should aim to also unravel the mechanisms that occur upon airborne exposure to natural SSAs. Our research showed that the DPPC content in SSAs was (concurrently)

enriched with major inorganic ions and can thus be linked to the electrification of the atmosphere and biogeochemical cycles. DPPC has also potential effects on the atmospheric retention time (i.e., SSA size) and meteorological (e.g., hygroscopic) behavior of SSAs. All these aspects should be examined in detail to elucidate their specific effects.

Our final research recommendation is to perform both specific and broad epidemiological studies. The more we examine the composition of SSAs, the more bioactive marine compounds that will be discovered. In vitro experiments or even in vivo experiments on test organisms can be performed to investigate the potential health effects of these compounds. These experiments can, however, never determine the exact health effects on the exposed coastal populations. To this end, long term sampling campaigns in combination with specific epidemiological studies should be performed. These specific (bottom-up) epidemiological studies should evaluate the effects and pathologies which are to be expected upon long term airborne exposure to specific bioactive compounds in SSAs. Broad epidemiological studies on the other hand should follow a more top-down approach by investigating the differences in human health between coastal and inland populations. As medical files of patients are increasingly well-documented, such epidemiological studies have (in theory) growing and improving datasets at their disposal. Under strict privacy conditions, this medical information could serve as a massive tool to reveal additional coastal proximity health effects and to verify diverse beneficial health hypotheses linked to coastal environments. Once (and if) differences concerning specific pathologies are found between coastal and inland populations, one can investigate if its origin could be attributed to marine compounds that have already been quantified in SSAs or are potentially present in SSAs.

I hope this PhD thesis opened new frontiers for understanding the positive relationship between the ocean and human health. Better knowledge of how we impact the ocean's health status and vice versa will contribute to a better management of marine ecosystems. This will create many opportunities that will also teach us to live in harmony with nature. It has been long clear that the ocean will almost certainly survive the Anthropocene … it is also obvious that the human species on the contrary cannot survive without a healthy ocean!

Annex I

Supportive information Chapter 1

Annex contents

1 Supportive figures

A.

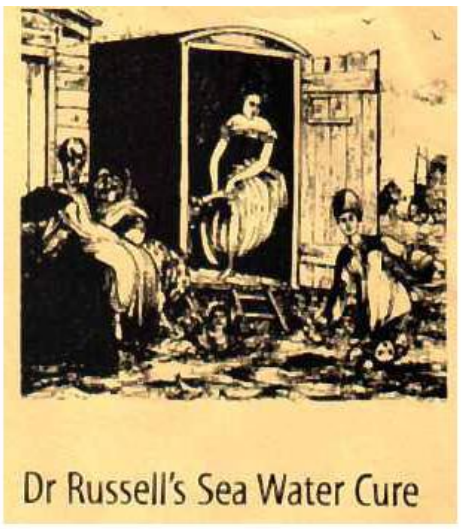

B.

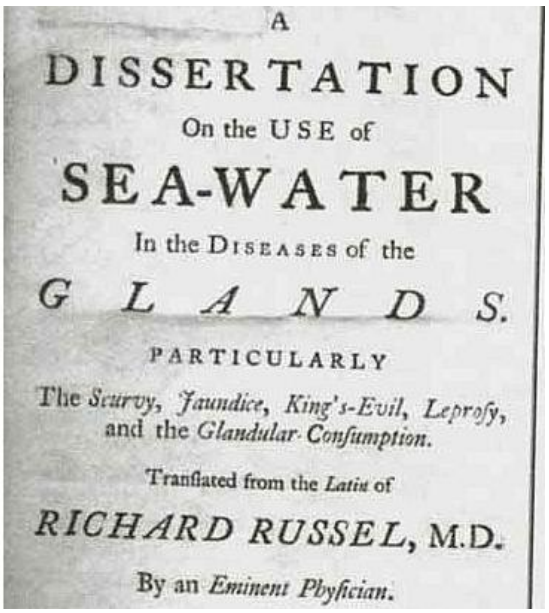

Figure S1.1: Documents showing the interest in Thalassotherapy in 18th century England.

Figure S1.2: Marine sanatorium in Gorliz, Spain. © bancodeimagenesmedicina.com

Figure S1.3: Marine sanatorium in Roscoff, France. © Association HeSCO.

GREEN-BLUE SPACE effect	Psychological Hypothesis	Immunoregulation Hypothesis	Biogenics Hypothesis
Walking and recreation in green-blue space	Evolutionarily determined psychological need (habitat selection?)	Evolutionarily determined need for diverse microbial input to immune system	Evolutionarily determined need for diverse exposure to biogenics
Social interactions	Build social capital	Exchange of microbiota	Exchange of microbiota-associated biogenics
Sport & exercise	"Hunter-gatherer" activity; health benefit; weight loss	Exchange of microbiota; more Treg*; immunoregulation;	Exchange of microbiota-associated biogenics; increased inhalation/ingestion of biogenics; hypoxia and ROS induced mTOR-inhibition mediated autophagy
Sunlight	Combat Seasonal Affective Disorder (SAD)	Vitamin D and nitric oxide (NO) improve immunoregulation	Enhanced vitamin D; vitamin D receptor (VDR) induced autophagy
CLINICAL OUTCOME		↓	↓
Fewer deaths, less cardiovascular disease, less neurodegeneration, less cancers ?, increased longevity?	Relaxation and exercise?	Low CRP; low inflamation	Inhibition of PI3K/Akt/mTOR; activation of PTEN; reduced ROS; enhanced cellular housekeeping (autophagy); improved innate immunity; Treg* immunoregulation; low inflammation ; enhanced brain function; anti-cancer; anti-ageing effects; more stress resilience
Less depression	Relaxation; restoration; social capital?	Lower cytokine response to stress; more stress resilience	Inhibition of PI3K/Akt/mTOR; low inflammation; more stress resilience

Figure S1.4: Summary diagram of the psychological, immunoregulation and biogenics hypotheses explaining the human health benefits arising from exposure to coastal (and rural) environments (Green-Blue Space). From Moore.[46]

2 Supportive tables

Table S1.1: Overview of the 21 marketed drugs (up to December 2020) that are directly or indirectly derived from marine compounds. Information from Jaspars et al.[108], Gerwick[106] and Barreca et al.[326]

Drug	Pharmacological activity	Biological origin	Relation to the marine compound(s)
Fludarabine phosphate	Cancer - Leukemia	*Tectitethya crypta*	Analogue
Nelarabine	Cancer - T-cell acute lymphoblastic leukemia	*Tectitethya crypta*	Analogue
Cytarabine	Cancer - Leukemia and Lymphomas	*Tectitethya crypta*	Analogue
Vidarabine	Antiviral - ocular	*Tectitethya crypta*	Analogue
Prialt	Painkiller	*Conus magus*	Identical
Plitidepsin	Cancer - Multiple myeloma	*Aplidium albicans*	Identical
Lovaza Omtryg Vascepa Epanova	Hyperlipidemia	Fishoil	Derived mixture
Propylene glycol alginate sulfate sodium	Cardiovascular, Hyperlipidemia	Brown algae	Derivate
Iota-carrageenan	Nasal spray - Reduce duration of vial colds	*Eucheuma denticulatum*	Identical
Brentuximab vedotin Polatuzumab vedotin Enfortumab vendotin Belantamab mafodotin	Lymphoma/Carcinoma	*Dolabella auricularia*	Identical drug, antibody-drug conjugate
Protamine sulfate	Diabetes & heparin overdose	Salmon sperm	Identical
Hemocyanin KLH	Immune stimulation with cancer vaccines	*Megathura crenulata*	Identical
Trabectedin Lurbinectedin	Cancer - Sarcomas	*Ecteinascidia turbinata*	Identical
Erubulin	Cancer - Breast carcinoma	*Halichondria okadai*	Analogue

Annex II

Supportive information Chapter 2

Annex contents

1 SDS-PAGE and western blotting procedures

Following the 43 h exposure period, the medium was removed and the cell monolayer was washed with ice cold D-PBS (137 mM NaCl; 8.1 mM Na_2HPO_4; 2.6 mM KCl; 1.5 mM KH_2PO_4). Cells were scraped from the surface, resuspended in D-PBS and transferred to a sterile Eppendorf tube. A second and third washing step was performed using 1 mL ice cold D-PBS and centrifugation (4°C at 300 g), at every turn. The cell pellet was subsequently resuspended in 100 µL lysis buffer and put on ice for 15 min. The lysis buffer consisted out of 99% Totex buffer (20 mM HEPES/KOH pH 7.9; 0.35 M NaCl; 1 mM $MgCl_2$; 20% glycerol; 1% Triton X-100; 0.5 mM EDTA; 0.1 mM EGTA) and 1% protease & phosphatase inhibitor cocktail (Halt, Thermo Fisher Scientific). Cell lysates were clarified by centrifugation for 15 min at 20,000 g and 4°C. Protein concentrations were subsequently determined using Bradford analysis. Related samples were diluted to the same protein concentration, using additional 1× Laemmli on top of the 4× Laemmli loading buffer (250 mM Tris/HCl pH 6.8; 8% SDS; 40% Glycerol; 0.008% Bromophenol blue; 20% mercaptoethanol). Samples with a considerable lower protein concentration as compared to the average, were taken out of consideration for the normalisation of the protein concentrations.

2 Data transformation to finally produce cell viability dose response curve models

Using the DRC package 3.0-1[327] in RStudio software, a 4-parametric log logistic dose response curve (DRC) model was first fitted to the absorbance data. If the highest concentration treatments induced complete cell mortality, based on microscopic observations and the absorbance data, the upper (i.e., 100% viability) and lower limits (i.e., 0% viability) of these first DRC model fits were used to transform the absorbance data to relative (%) cell viability values. In the cases where the highest concentration treatments only showed partial mortality effects, the positive control treatment was used instead as a lower normalisation limit (i.e., 0% viability). With this transformed data the final cell viability DRC models were made using 2- or 3-parametric log logistic models. Consequently, effect concentrations for 10% (EC_{10}) and 50% (EC_{50}) decrease in cell viability were derived from the final DRC models.

3 Calculating the highest potential YTX water concentration

Currently, literature reports YTX concentrations in shellfish and other marine organisms but not in water nor SSAs. Therefore, we calculated the highest potential YTX water concentration. The cell densities of *Protoceratium reticulatum* during a bloom in the marine environment can rise up to 400–700 cells L^{-1}.[196,197] The reported YTX production for *P. reticulatum* strains can reach up to 28.6-33.6 pg $cell^{-1}$.[142,143] Finally, up to 38% of the produced YTXs are found extracellular and dissolved in the surrounding water.[142] By combining these data we calculated a maximum potential water concentration for YTXs of 8.9 ng L^{-1} (= 700 cell L^{-1} × 33.6 pg $cell^{-1}$ × 38%).

4 Importance of lower respiratory system for SSA exposure

Cheng et al.[156] determined the SSA deposition in the upper (75–84%) and lower respiratory tract (2–6%) based on the size distribution of SSAs and the ICRP 66 lung model. Based on these deposition rates, one could ask the question why not to examine effects on cell lines from the upper airways (i.e., extrathoracic region) instead of the lower airways (i.e., tracheobronchial and pulmonary region). A large fraction of the (solid) particles that are deposited in the upper airways associate with the mucus membranes, are transported to the laryngopharynx and become ingested.[46] The human health effects of SSA exposure by gastrointestinal uptake would make an interesting topic in itself, but is outside the scope of this study. A small SSA fraction (2–6%) is deposited in the lower airways. According to Thompson,[328] the clearance for the small particles penetrating in the lower airways is much slower and soluble chemicals can dissolve in the epithelial lining fluid. Despite low deposition rates of SSAs in lower airways, harmful marine compounds are able to induce lower airway symptoms (e.g., cough, wheezing, chest tightness upon PbTx exposure), illustrating their potential for significant human health effects. Further evidence for the penetration of small sized aerosols into the lower airways can be found in the medical world. There are numerous medical therapies using aerosol devices to deliver miscellaneous drugs to treat both pulmonary and non-pulmonary diseases.[329] This drug delivery is also an attractive route to treat non-pulmonary diseases due to fast absorption by the massive alveolar surface area, the abundant vasculature and thin air–blood barrier.[329] Regarding the above, the importance of SSA exposure in the lower airways is much larger than one would expect from the deposited SSA fraction (2–6%).[156]

5 Supportive Figures

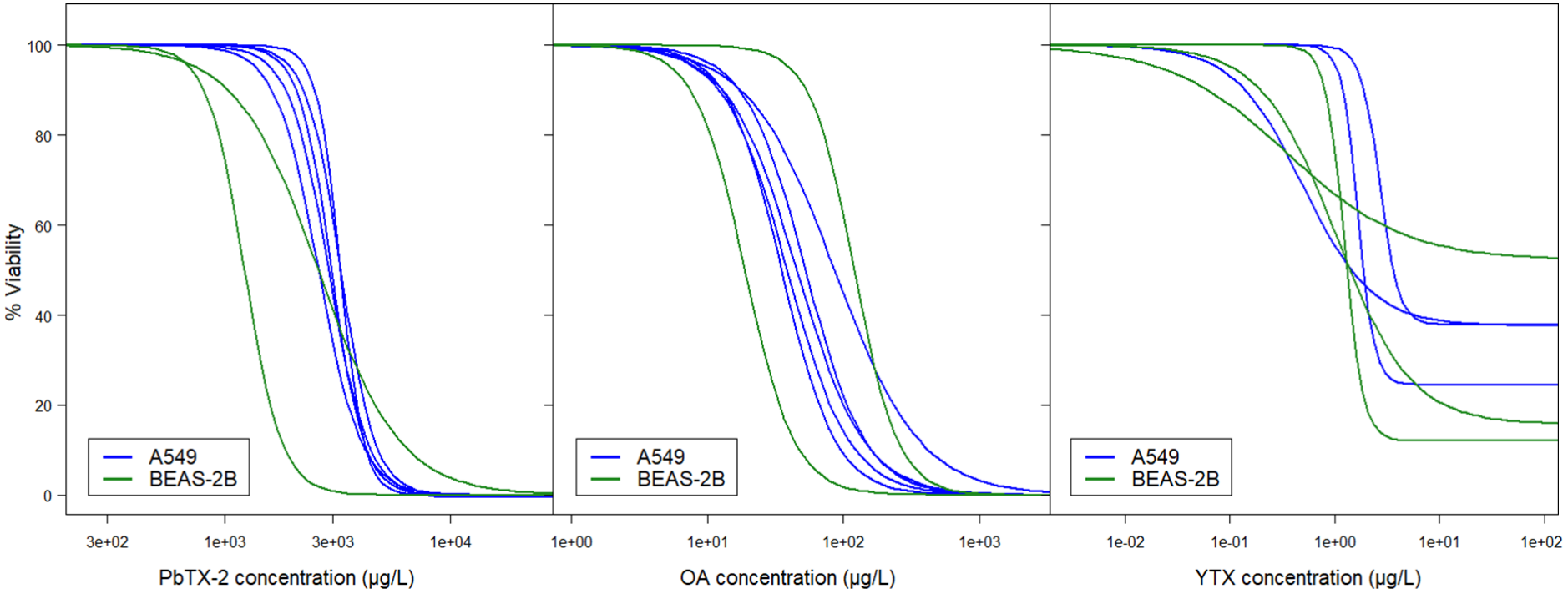

Figure S2.1: Comparison of the cell viability effects on two different types of epithelial lung cells (i.e., A549 and BEAS-2B) using the dose response model fits of multiple experiments. The 3 different phycotoxins tested, shown from left to right, are brevetoxin-2 (PbTx-2), okadaic acid (OA) and yessotoxin (YTX). These MTT assays were performed over an exposure period of 43 h with a start cell density of 3000 cells well^{-1} for all experiments shown here, except for the experiments on YTX for which 8000 cells well^{-1} were used. Note that the DRC models were fitted using all test concentrations, including lower concentrations than the range shown here.

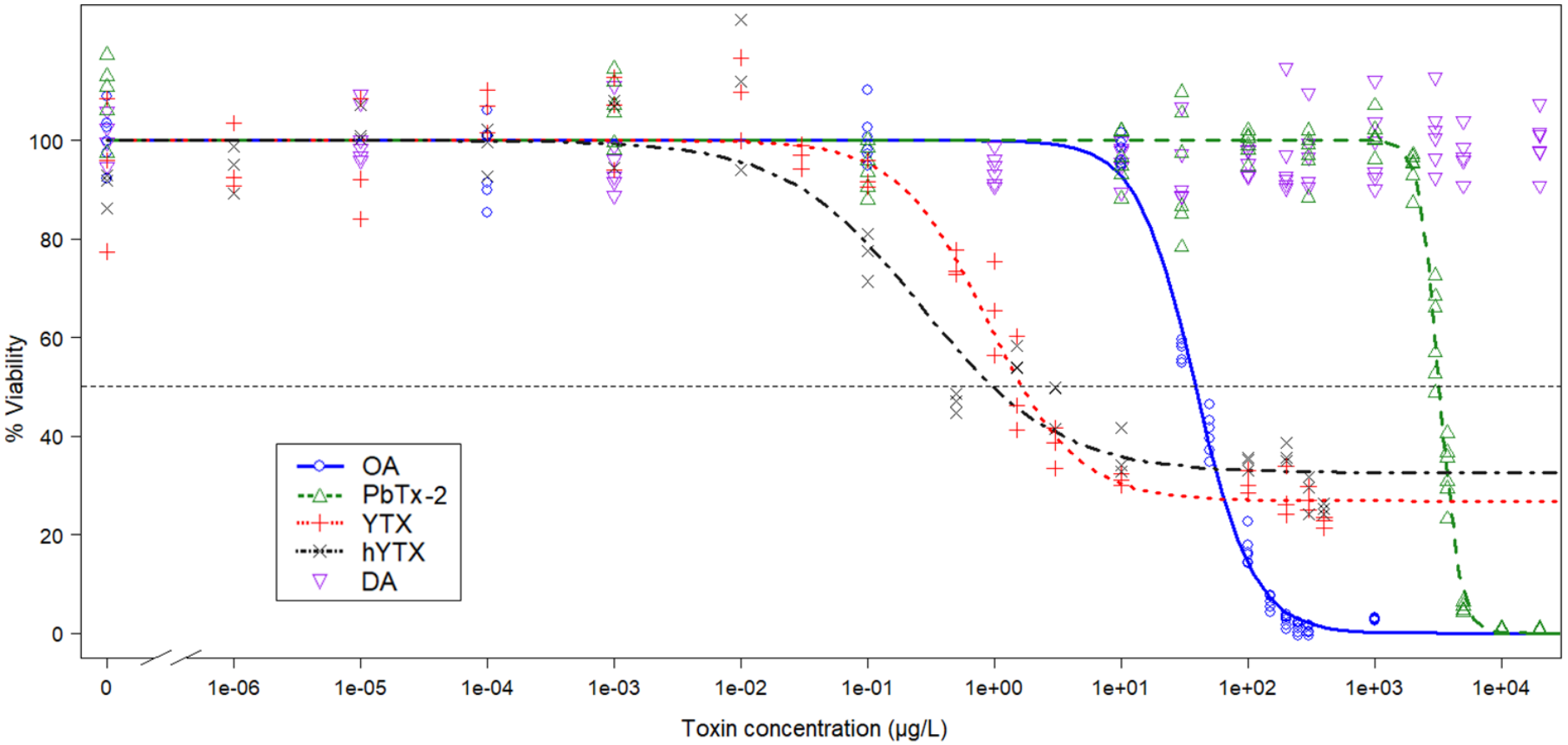

Figure S2.2: Log-logistic dose response curve (DRC) models fitted to the experimental data of MTT cell viability assays performed on A549 cells over a exposure period of 43 h. The five different phycotoxins tested are okadaic acid (OA), brevetoxin-2 (PbTx-2), yessotoxin (YTX), homoyessotoxin (hYTX) and domoic acid (DA). The start cell density was 3000 cells well^{-1} for all experiments. The parameter estimates (i.e., estimate ± SE) for all dose response model fits shown here are available in Table S2.1 under experiment 3-A549 and 9-A549. For DA the data points are shown without a DRC as there were no effects observed at the highest possible test concentrations.

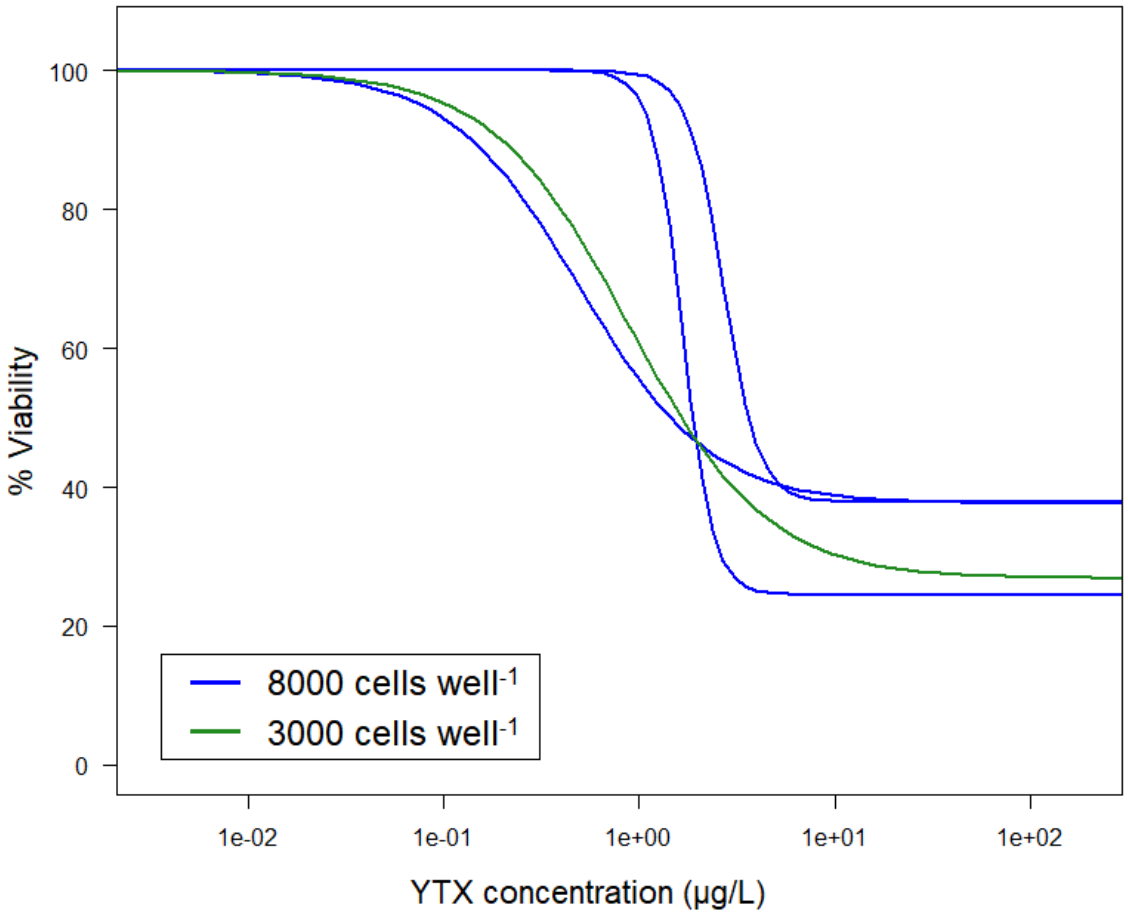

Figure S2.3: Comparison of the cell viability effects of yessotoxin (YTX) at different start cell densities of 3000 and 8000 cells well^{-1}, using the log-logistic dose response model fits of multiple experiments. These MTT assays were performed on A549 cells over a exposure period of 43 h. The parameter estimates (i.e., estimate ± SE) for all model fits shown here are available in Table S2.1 under experiment 6. A549, 7. A549, 8. A549 and 9. A549.

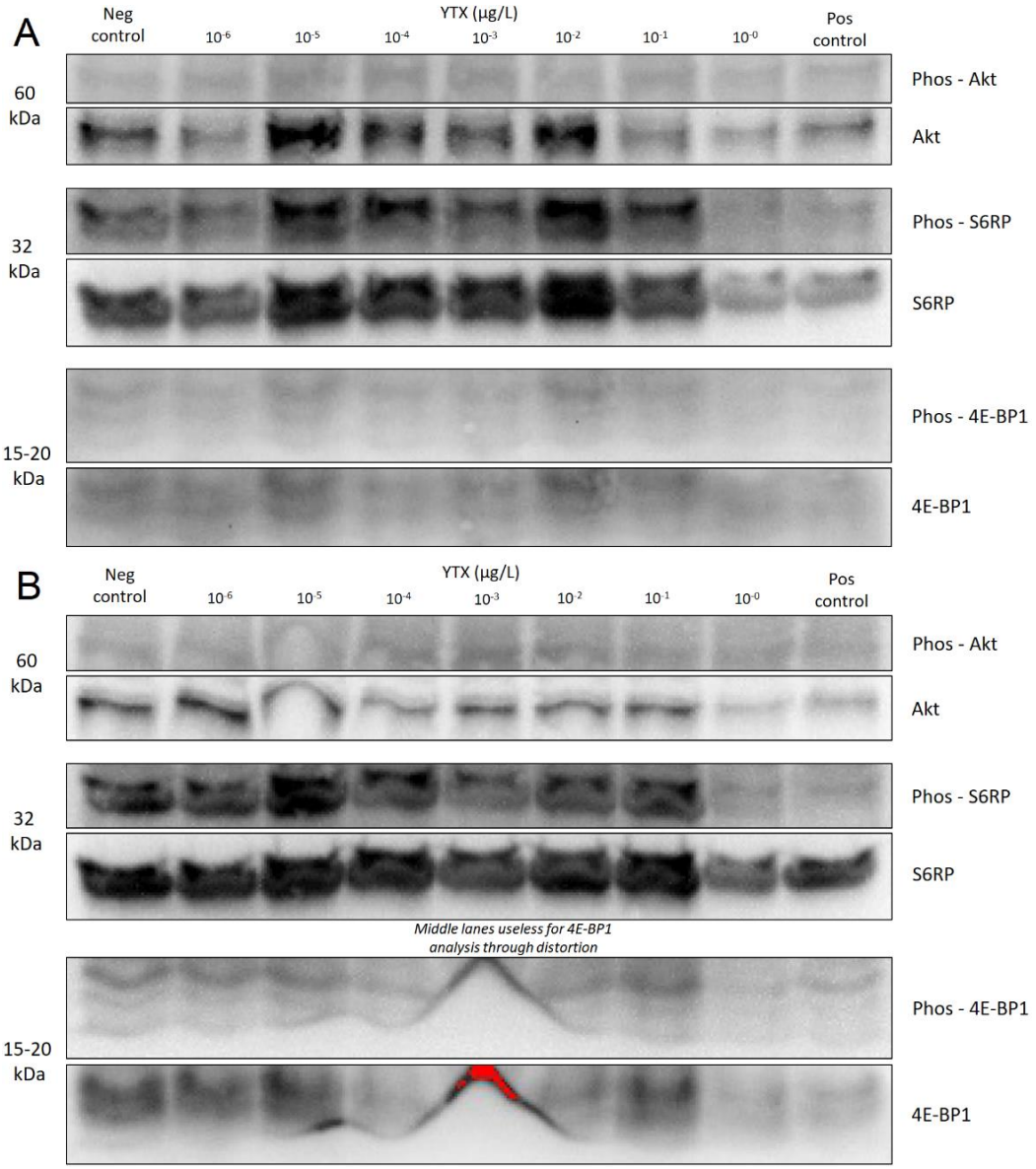

Figure S2.4: Cropped, non-edited versions of blots related to the experiment shown in Figure 2.3. For both (A) the A549 and (B) BEAS-2B cell line, a representative example of one of the blots is shown. A darker band indicates a stronger chemiluminescent signal.

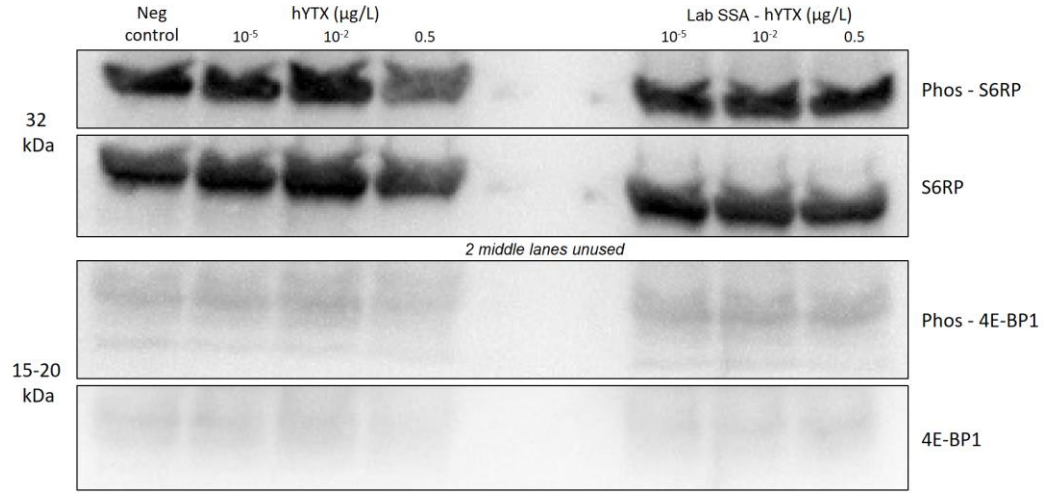

Figure S2.5: Cropped, non-edited versions of a representative blot for the experiment shown in Figure 2.4. A darker band indicates a stronger chemiluminescent signal.

6 Supportive Tables

Table S2.1: Summary of the effect concentrations and log-logistic dose response models parameter estimates for all performed MTT cell viability experiments. 10% and 50% effect concentrations are reported as 43 h EC_{10} and 43 h EC_{50} values. The results shown here are for two different types of epithelial lung cell lines (i.e., A549 and BEAS-2B cells), for two starting cell densities and for four different phycotoxins. The four different phycotoxins are okadaic acid (OA), brevetoxin-2 (PbTx-2), yessotoxin (YTX), and homoyessotoxin (hYTX). Since the exposure to domoic acid (DA) induced no viability effects, no data of these experiments are shown. The minimum estimate values for OA and PbTx-2 are not relevant (NR) as the these are all 0%. Only in experiment 9, the effect of hYTX was tested. For other experiments no data is available (NA) for hYTX.

Experiment & cell type	Cell density ($well^{-1}$)	43 h EC_{10} ($\mu g\ L^{-1}$)		43 h EC_{50} ($\mu g\ L^{-1}$)		Inflection point ($\mu g\ L^{-1}$)		Slope		Minimum (%)	
		OA	PbTx-2	OA	PbTx-2	OA	PbTx-2	OA	PbTx-2	OA	PbTx-2
1. A549	3000	17.2 ± 1.1	1889 ± 167	52.8 ± 1.6	2884 ± 64	Equal to EC_{50} values		1.96 ± 0.10	5.19 ± 0.91	NR	NR
2. A549	3000	12.9 ± 1.4	2069 ± 96	45.6 ± 2.2	2966 ± 55			1.75 ± 0.12	6.10 ± 0.64	NR	NR
3. A549	3000	12.1 ± 1.4	2227 ± 94	38.7 ± 2.1	3259 ± 59			1.90 ± 0.17	5.76 ± 0.58	NR	NR
4. A549	3000	17.7 ± 1.6	1612 ± 54	86.5 ± 4.5	2598 ± 41			1.38 ± 0.08	4.61 ± 0.28	NR	NR
4. BEAS-2B	3000	53.5 ± 3.2	1032 ± 54	121 ± 4.5	2591 ± 71			2.70 ± 0.23	2.39 ± 0.14	NR	NR
5. A549	3000	12.9 ± 1.2	2499 ± 76	35.2 ± 1.3	3247 ± 36			2.18 ± 0.17	8.40 ± 0.87	NR	NR
5. BEAS-2B	3000	7.5 ± 0.7	805 ± 35	18.9 ± 0.9	1221 ± 36			2.37 ± 0.17	5.28 ± 0.65	NR	NR
		YTX	hYTX	YTX	hYTX	YTX	hYTX	YTX	hYTX	YTX	hYTX
6. A549	8000	1.49 ± 0.40	NA	3.87 ± 0.63	NA	2.49 ± 0.26	NA	3.23 ± 1.30	NA	38.0 ± 2.5	NA
6. BEAS-2B	8000	0.19 ± 0.13	NA	1.40 ± 0.23	NA	1.03 ± 0.18	NA	1.19 ± 0.41	NA	15.5 ± 3.7	NA
7. A549	8000	1.19 ± 0.20	NA	1.88 ± 0.14	NA	1.67 ± 0.13	NA	5.55 ± 2.07	NA	24.6 ± 3.2	NA
7. BEAS-2B	8000	0.81 ± 0.10	NA	1.31 ± 0.11	NA	1.24 ± 0.09	NA	4.88 ± 1.63	NA	12.0 ± 3.1	NA
8. A549	8000	0.14 ± 0.02	NA	1.45 ± 0.22	NA	0.50 ± 0.04	NA	1.31 ± 0.13	NA	37.6 ± 1.4	NA
8. BEAS-2B	8000	0.06 ± 0.02	NA	NR (see Min.)	NA	0.35 ± 0.06	NA	0.77 ± 0.12	NA	52.2 ± 1.9	NA
9. A549	3000	0.20 ± 0.06	0.03 ± 0.01	1.65 ± 0.25	0.98 ± 0.38	0.88 ± 0.11	0.27 ± 0.07	1.24 ± 0.22	0.81 ± 0.13	26.8 ± 2.0	32.5 ± 2.3

Annex III

Supportive information Chapter 3

Annex contents

1 Culturing of algae

Prorocentrum lima and Protoceratium reticulatum were grown as single strain cultures in 250 mL Erlenmeyer flasks containing 50 mL of L1 medium (Figure S3.11). L1 medium[330] is a general-purpose growth-medium for (coastal) algae and was prepared with sterilized, filtered (0.2 µm) Instant Ocean^{TM} (Belcopet) artificial seawater of 32 ppt and pH 8.0. Algae were grown at 20°C with a light-dark cycle (300-600 µmol m^{-2} s^{-1}) of 12 h, and 90% of the culture medium was replaced every 3 weeks. To culture larger quantities of algae, 5 L Erlenmeyer flasks were filled with 2.5 L of L1 medium and inoculated with two 50 mL algal cultures. Cell counts were determined prior to each experiment using a Sedgewick Rafter counting chamber (SPI supplies).

2 MART set-up and settings

The marine aerosol reference tank (MART) used in this study was constructed (Figure S3.1) as described by Stokes *et al*.[90] A control valve regulated by a timer (Solid-state Timer, Omron H3BF) directed the water intermittently to a central spillway slot of 20 cm long and 6 mm wide. In this way, 4-second plunging sheets of 4.08 ± 0.05L were generated, with an intermediate rest phase of 8 seconds. The MART's bubble plume size distribution (Figure S3.13) was verified following photographic procedures described by Callaghan *et al*.[93]

3 Experimental filter choice

To determine which membrane filter was best suited to retain and analyze aerosolized phycotoxins and Na^+ (i.e., proxy for the collected SSA quantity), three selected filter types were tested using MART experiments. These experiments were performed by introducing artificial seawater (i.e., L1-medium; Annex III section 1) and toxin-producing algae (*P. lima* and *P. reticulatum*) in the MART. Three experiments were performed using algal densities of 10, 100 and 1000 cells mL^{-1}, respectively. The MART was activated and SSA sampling was performed during 1.5 h, using the three filter types in parallel. To verify that the obtained differences between the three filter types could not be explained by a potential difference in sampling position, as there were three different MART air sampling outlets, a nearly identical follow-up experiment was performed using 1000 cells mL^{-1}. In this experiment only quartz filters were used. The three replicate samples showed a relative standard deviation (RSD) below 10%.

The highest phycotoxin yields were obtained with the quartz and glass fiber filters (Figure S3.3). To test the suitability of these filters towards aerosolized Na^+, MART experiments were performed using pure artificial seawater (i.e., L1-medium), i.e., without deliberate introduction of toxin-producing algae. The MART was activated and SSA sampling was performed using these two filter types during periods of 1 to 16 h.

4 Experimental SSA sampling optimization

Following the selection of the quartz filter as the most suited filter type the SSA sampling methods were further optimized. This was performed using MART experiments with pure artificial seawater (i.e., L1-medium; see Annex III section 1) and a combination of different set-ups and modifications. The effects of all these potential modifications were examined through the analysis of the subsequent Na^+ extract (i.e., proxy for the collected SSA quantity). First, the effect of a filter pretreatment was examined. Filters were rinsed twice with 0.14 M HNO_3, twice with H_2O and were subsequently dried at 30-40°C. Pretreated filters should have a lower background content of Na^+ and could therefore results in less variable results. Multiple MART experiments (ranging from 2 to 16 h) were performed using pretreated and non-pretreated filters in triplicate. Secondly, a modification to the filter and filter holder set-

up was examined in 8 h MART experiments. The filter holder's frontal support screen (shown in Figure S3.7) was considered non-essential and its removal could lead to a higher SSA collection efficiency for the filter. As such, the different components of the filter and filter holder set-up were analyzed on their Na^+ content (i.e., proxy for the collected SSA quantity) in both the presence and absence of the frontal support screen. Finally the MART set-up was further examined by (1) adding a perforated plate in the MART's headspace which could potentially improve the airflow and as such increase the SSA density in the sampled air, and by (2) deploying only one or two sampling pumps simultaneously instead of three (i.e., our standard set-up). The latter tests if the SSA production and the SSA density in the MART headspace was respectively fast and large enough to deploy three SSA sampling pumps simultaneously. Likewise, we examined if the deployment of one or two simultaneous sampling pumps gave a higher Na^+ filter content as compared to the simultaneous deployment of three pumps (i.e., our standard set-up). The combination of both experimental MART setups (i.e., (1) and (2)) is shown in Figure S3.14.

The results of the experiments examining the filter pretreatment and the removal of the frontal support screen are described the results section of the main paper. The results of (1) the addition of the perforated plate in the MART headspace and (2) the deployment of a different number of sampling pump are summarized in Figure S3.15. These confirm that (1) the airflow in the standard MART-set-up was adequate and that no shortcut airflow existed between the air inlet valve and the sampling pumps, and (2) that the SSA production and SSA density in the MART headspace were large enough to deploy three SSA sampling set-ups simultaneously.

5 Production of SSA loaded filters & examination of salt effect on the analysis

Using the MART, filled with pure artificial seawater (i.e., L1-medium; see Annex III section 1), we produced SSA loaded (15.3 ± 5.3 µg Na^+) quartz filters over a course of 4 h. These SSA loaded filters were used (1) to test if the salt content of deployed filters did not affect the extraction and analysis efficiency of the targeted phycotoxins and (2) as true blanks to examine the specificity of the method as part of the validation (as described in the results section of Chapter 3).

Environmental SSA samples will, depending on the ambient conditions, contain a variable salt content. Prior to the actual method validation, we examined if this salt content did not interfere significantly with the phycotoxin extraction and analysis. We spiked both blank and SSA loaded filters with the seven targeted phycotoxin standards in triplicate. This was performed at a low and mid-level concentration, i.e., representing 1 and 5 ng mL^{-1} in the final 250 µL extract. The salt effect on the surface area response was tested using a two-way anova. It was confirmed that the salt interference could only be minor, as not a single phycotoxin showed a significant effect ($p>0.05$; 95% confidence level). The results of this experiments are shown in Figure S3.16.

6 Extraction procedures for the different water (size) phases

In the MART experiments using artificial and natural seawater, 10 mL samples of each water layer (i.e., bottom, SSW and SSML) were analyzed in triplicate. Apart from the total concentration, the phycotoxin distribution over the different size fractions is an important factor determining the sea spray aerosolization. We therefore determined the phycotoxin concentrations in the dissolved (<0.2 µm), small particulate (0.2-5 µm) and large particulate (>5 µm) fractions. The 10 mL samples were first filtered over 5.0 µm (Durapore®). As the residue (>5 µm) mainly containing algal cells (i.e., intracellular phycotoxins) and larger particulate material, the dedicated and validated method of Orellana et al.[132] was used for phycotoxin analysis. The filtrate (<5 µm) was subsequently filtered over 0.2 µm (Supor®). As no specific method existed for this small particulate residue fraction (0.2-5 µm), the same methodology as for the large particulate phase (>5 µm) was used. The final filtrate (<0.2 µm), containing the dissolved phycotoxin fraction, was subsequently extracted using a three-fold scaled up version of the validated SPE method of Gerssen et al.[185] with Strata-X columns (Phenomenex). The two filter residues (i.e., >5 µm and 0.2-5 µm) and the final filtrate (<0.2 µm) were spiked with 5 ng eprinomectin as an internal standard (IS) as suggested by Rubies et al.[134] This IS was also tested for the phycotoxin SSA filter analysis but was not retained as all validation criteria indicated a (slightly) lesser quality analysis using the IS normalized data. Identical as for SSA sample extract, the above described (water phase) extracts were filtered over 0.2 µm, dried until last drop, and reconstituted in 50 µL acetonitrile and 200 µL H_2O (both containing 6.7 mM NH_4OH). After a purification centrifugation step (5 min, 7200 g), the supernatant was transferred

to a glass insert in a LC-MS vial prior to analysis. The LOD and LOQ values (Table S3.7) for phycotoxins analysis in the different seawater matrices (i.e., size fractions) were determined as described in the manuscript (i.e., using the standard deviation of the response and the slope of their respective calibration curves).[193,203]

The Na^+ concentrations in the different water phases were determined via salinity measurements. The ratios of the major inorganic constituents (e.g., Mg^{2+}, Na^+) of seawater are very constant and can be correctly determined from the salinity.[204,205]

7 Testing SSA filter collection efficiency

The two MART experiments, using artificial and natural seawater (Figure 3.2A/B), were also used to test the collection efficiency of the quartz filters for aerosolized phycotoxins and Na^+. The air passing through the filter was therefore subjected to another SSA sampling technique, based on the methods described by Tsunogai *et al*.[201] The sampled air was subsequently drawn in small bubbles through 250 mL of pure water in a 500 mL Duran bottle via a perforated Teflon tube as shown in Figure S3.17. Half of this 250 mL solution was dried, reconstituted in 10 mL of 0.14 M HNO_3 and analyzed for its Na^+ content. The other half was analyzed on its phycotoxin content using the same SPE method[185] as for the dissolved (<0.2 µm) phycotoxin fraction of the MART water samples (see Annex III section 5).

These additional control (air purged) water samples of the Duran bottles generally confirmed the good collection efficiency of the membrane filters. Only one out of six samples showed a significant breakthrough of Na^+ (i.e., representing 40% of the total sampled Na^+ content). This sample was the only one wherein all three phycotoxin were found (i.e., representing 43 ± 23% of the total sampled contents). Only one other sample showed a minor phycotoxin content (i.e., detection of 2 phycotoxins at 12 ± 4% of the total sampled content). As only one sampling set-up (out of six) showed a major and one a minor breakthrough of the sampled SSAs, we can conclude that there was only low breakthrough and thus a good filter collection efficiency. The cases were there was some breakthrough are most probably due to a small filter artefact (e.g., incidental wetting of the filter). This does, however, stress the importance of the usage of multiple replicate samples and the careful handling of membrane filters.

8 Supportive Figures

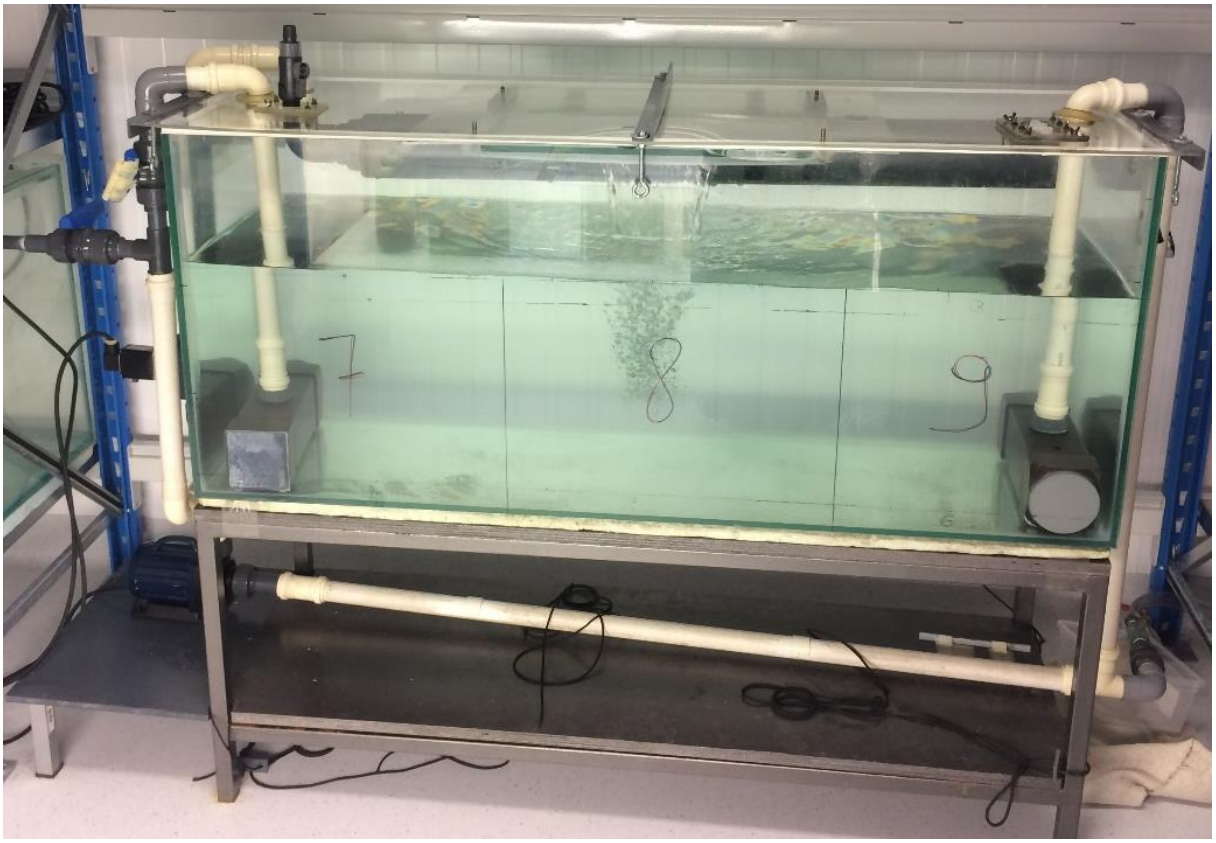

Figure S3.1: Marine aerosol reference tank (MART) which was constructed following the descriptions of Stokes et al.[90]

Figure S3.2: Lifeguard chair which was used, as a mobile sampling station, to take additional SSA samples close to the water line using mobile sampling pumps.

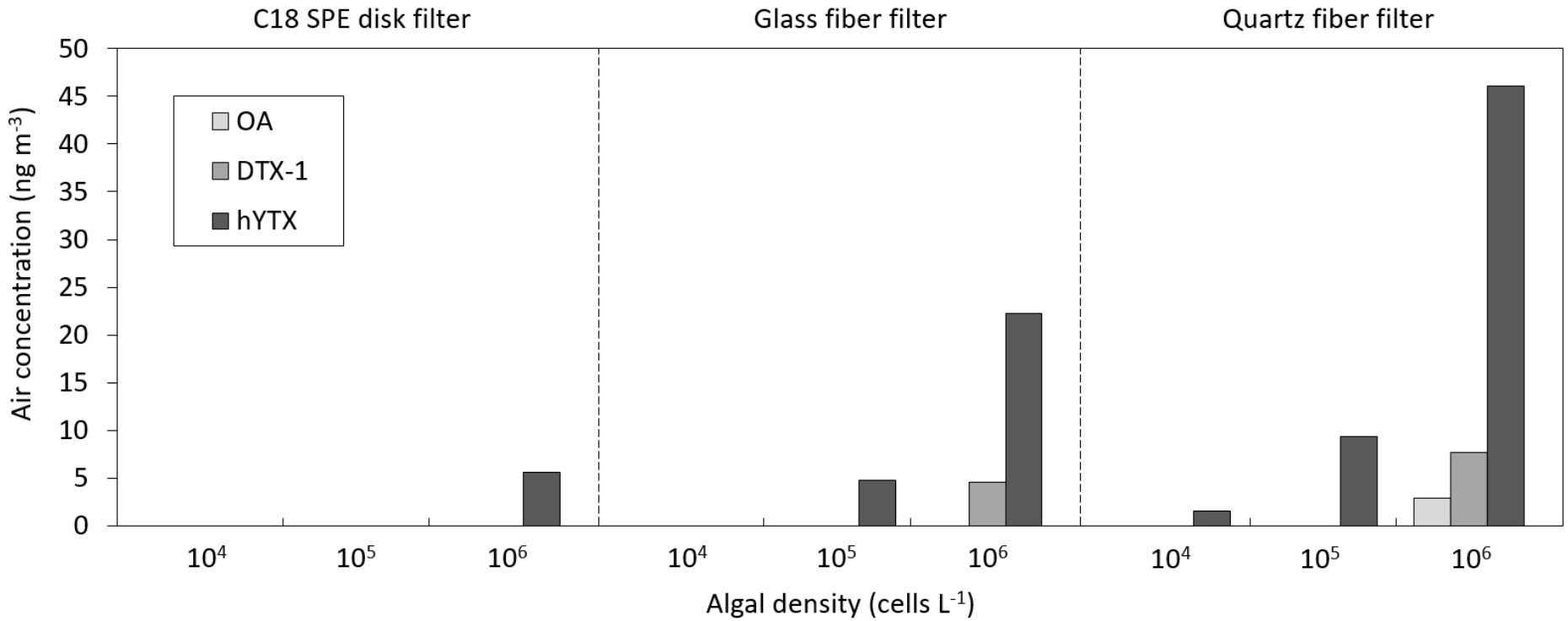

Figure S3.3: Results of a series MART experiments where three different membrane filters were deployed simultaneously, to compare their efficiency for the collection, extraction and analysis of aerosolized phycotoxins and SSAs as a whole. The air concentrations for okadaic acid (OA), diniphysistoxin-1 (DTX-1) and homoyessotoxin (hYTX) are shown for each evaluated filter type (Ø 47mm) and for each of the examined algal densities. The selected membrane filters were (1) an octadecyl (C18) bonded silica solid phase extraction disk (3M Empore™), (2) a pure borosilicate glass fiber filter (EPM2000, Whatman®) (GE Healthcare Life Sciences), and (3) a high purity quartz microfiber filter (QM-A grade, Whatman®) (GE Healthcare Life Sciences).

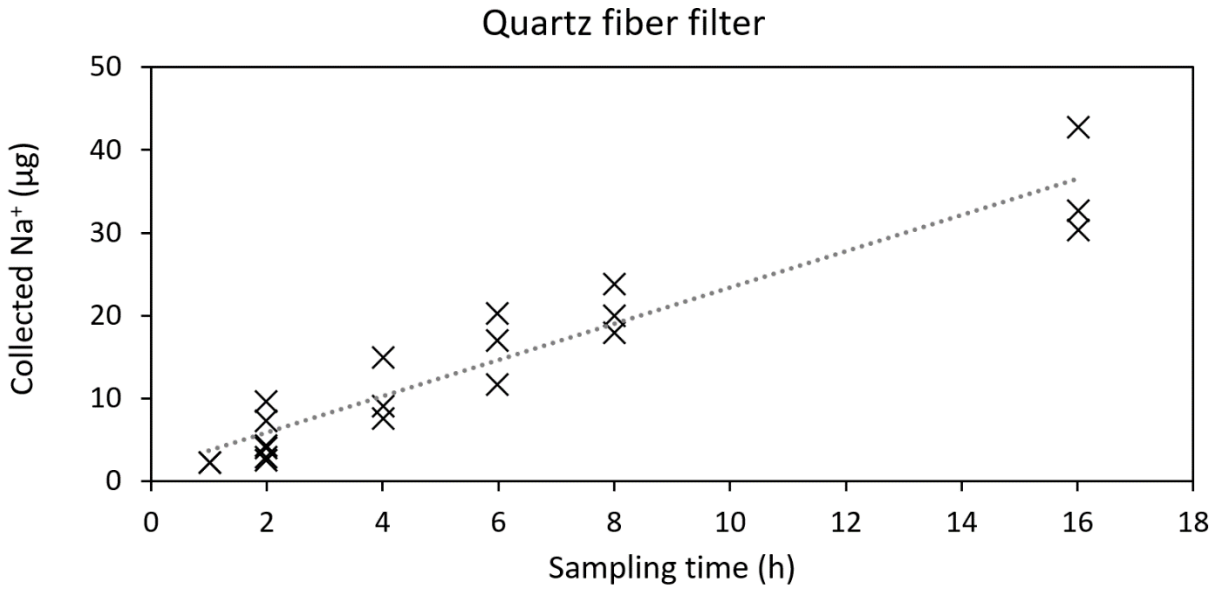

Figure S3.4: Collected Na^+ content on quartz filters as a function of the sampling time in a marine aerosol reference tank (MART). The regression (y = 2.2 x + 1.5) showed a significant slope (p<0.001; confidence level of 99.9%), an insignificant intercept (p>0.05; 95% confidence level) and a good linearity (R^2 = 0.902). As such, a good filter suitability was shown for the collection, extraction and quantification of aerosolized Na^+, and SSAs as a whole. The depicted data points have already been accounted for the background Na^+ content (19.9 ± 0.85 µg Na^+) present in blank quartz filters (without pretreatment).

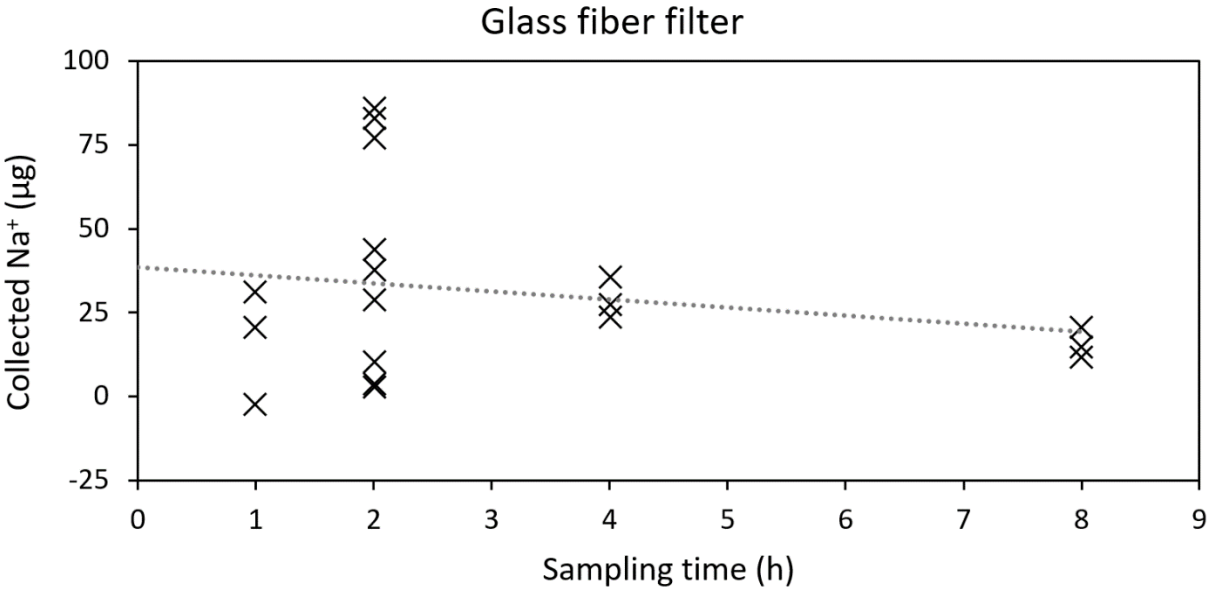

Figure S3.5: Collected Na^+ content on glass fiber filters as a function of the sampling time in a marine aerosol reference tank (MART). The regression (y = -2.4 x + 38.5) showed a very bad linearity (R^2 = 0.0474) and thus that this filter type is unsuitability for the collection, extraction and quantification of aerosolized Na^+, and SSAs as a whole. The depicted data points have already been accounted for the background Na^+ content (480 ± 11 µg Na^+) present in blank glass fiber filters.

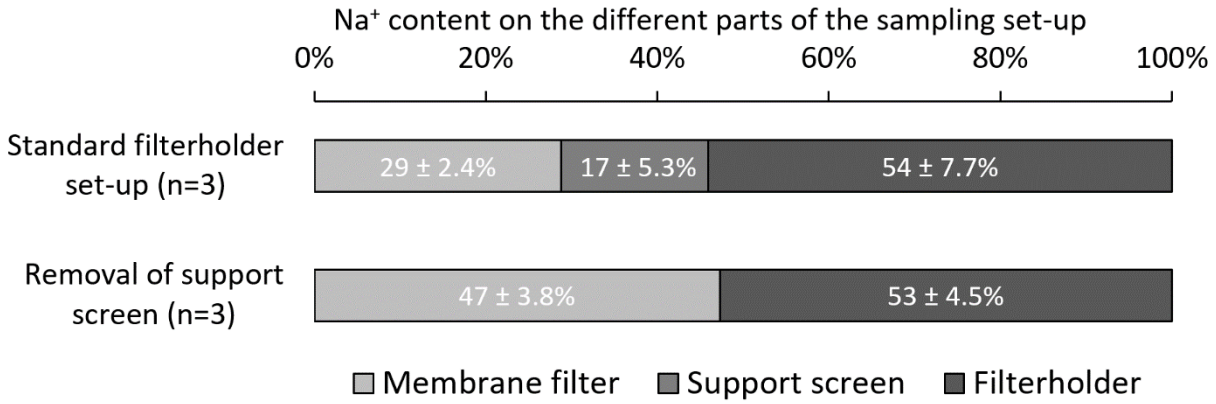

Figure S3.6: Results of the MART experiments examining the Na^+ content, and thus SSA collection, of the different components of the filter and filter holder set-up as shown in Figure S3.7. The results for the filter holder represent the Na^+ content on its frontal half, as no significant Na^+ content was ever found on the rear half of the filter holder.

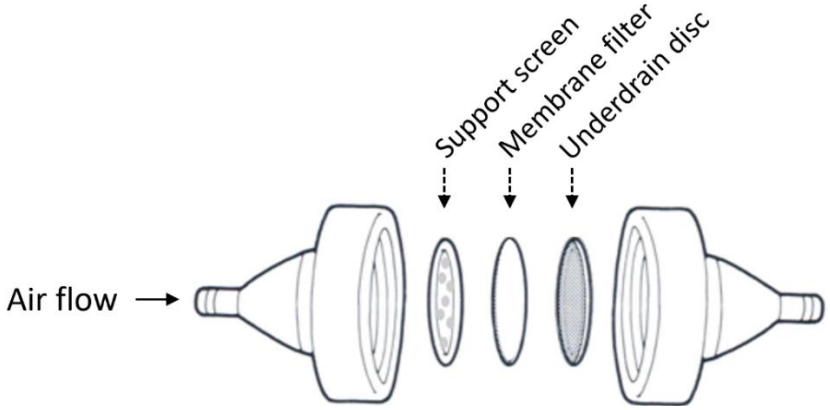

Figure S3.7: Filter and filter holder set-up used to sample artificial and natural SSAs. The frontal support screen in the filter holder was found to be non-essential and was removed to receive a higher SSA collection efficiency for the filter (Figure S3.6).

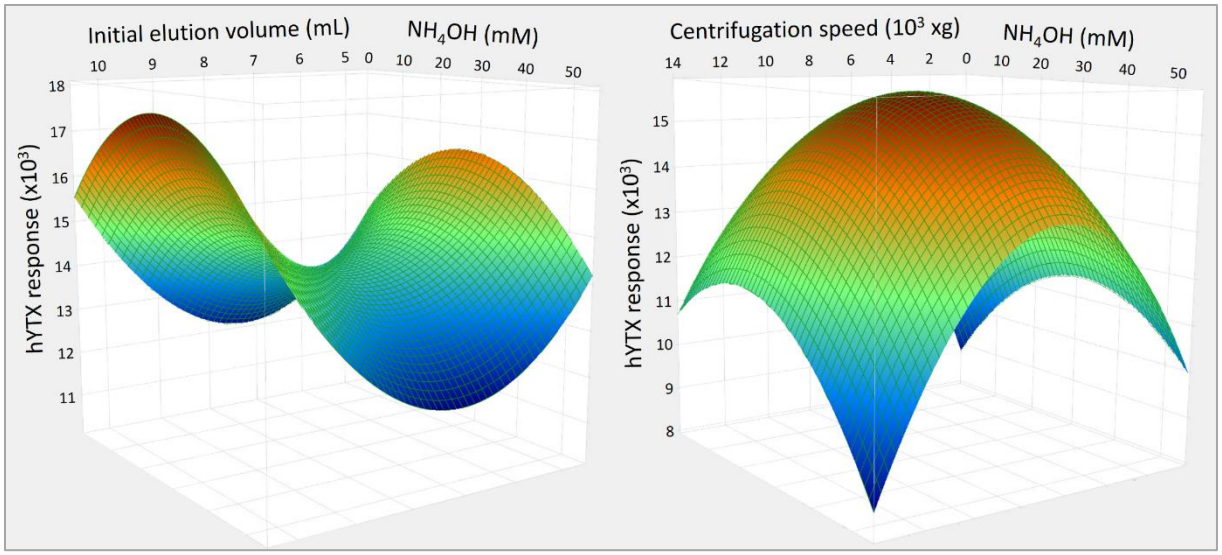

Figure S3.8: Response Surface Model (RSM) plot for the response area of homoyessotoxin (hYTX) as a function of the optimized quantitative variables.

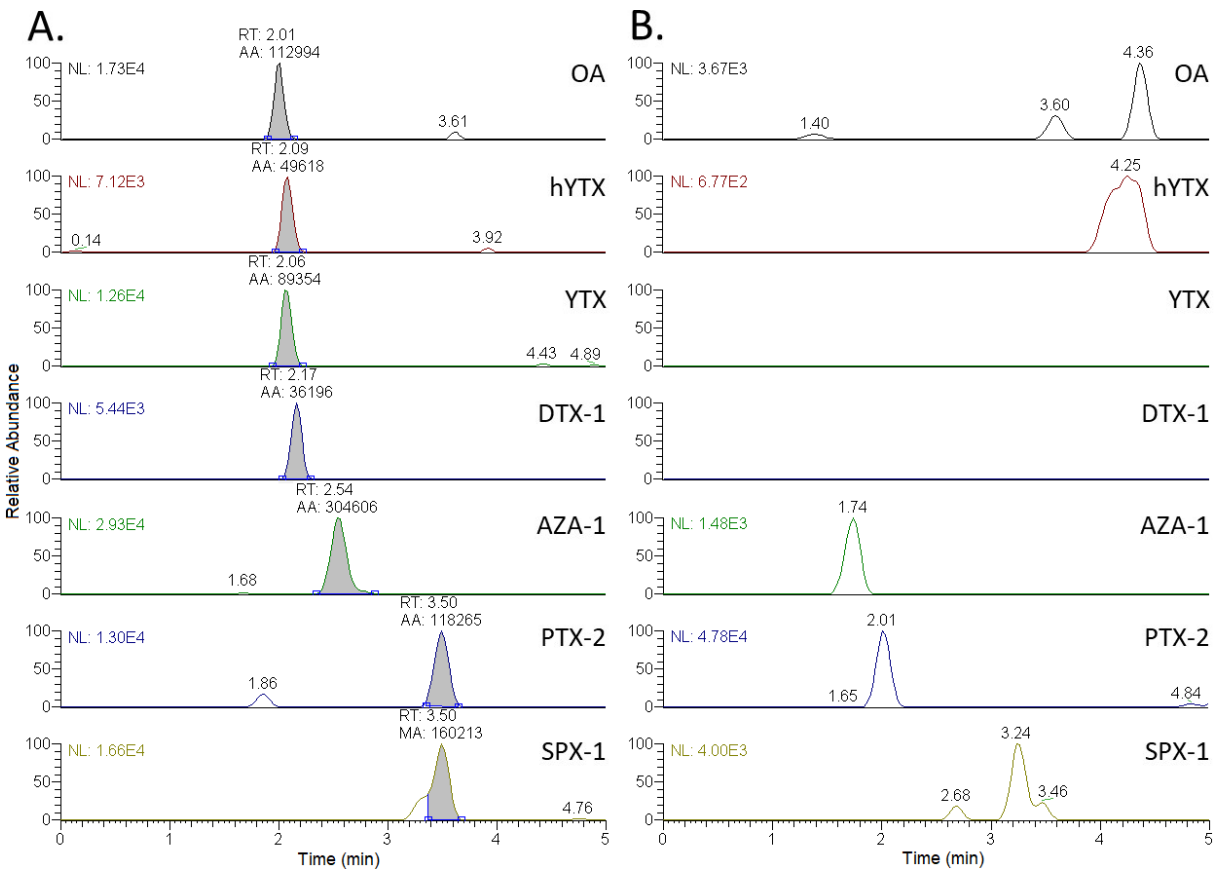

Figure S3.9: Representative chromatograms for the extracts of (A) a quartz filter spiked with all 7 phycotoxins at the low level concentration of 1.5x LOQ (i.e., 1.5 ng mL^{-1}), and (B) a SSA loaded quartz filter (i.e., true blank), produced using blank artificial seawater in the MART set-up. The accurate mass (m/z) for each compound was set at the values reported in Table S3.4 and the mass extraction window was set at 5 ppm. Both the retention time (RT) and the automatic (AA) or manual (MA) integrated peak areas are shown for every peak, together with the normalized intensity level per chromatogram.

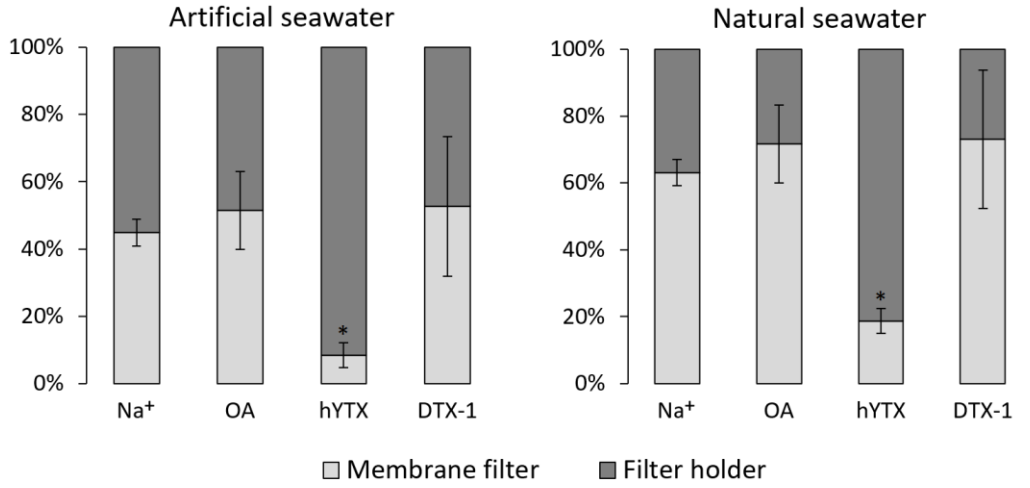

Figure S3.10: Fraction (%) of the total amount of aerosolized sodium (Na^+), okadaic acid (OA), homoyessotoxin (hYTX), and dinophysistoxin-1 (DTX-1), analyzed on the (quartz) membrane filter and its corresponding filter holder. Error bars represent the standard deviations (n=3). Significant different distributions ($p<0.05$; 95% confidence level) are indicated with an (*). These data are from the MART experiments shown in Figure 3.2.

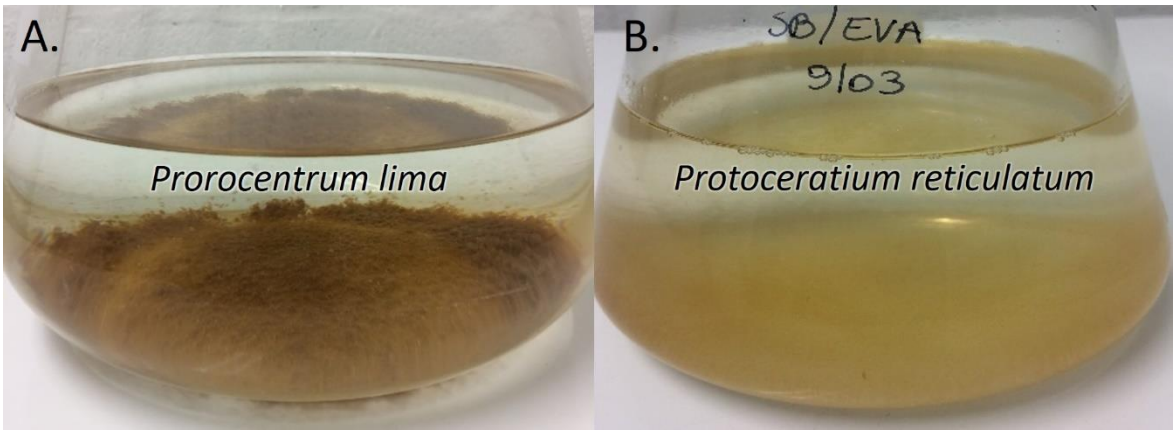

Figure S3.11: Algal cultures in 250 mL Erlenmeyer flasks containing 50 mL of L1 medium of (A) the benthic Prorocentrum lima and (B) the pelagic Protoceratium reticulatum algae which tended to accumulate in the SSML.

Figure S3.12: Pictures showing the high foam stability of the natural water used the MART experiment (see Figure 3.2B). The foam is shown on (A) the glass plate for SSML sampling, (B) the water surface in the MART, and (C) at the sampling location.

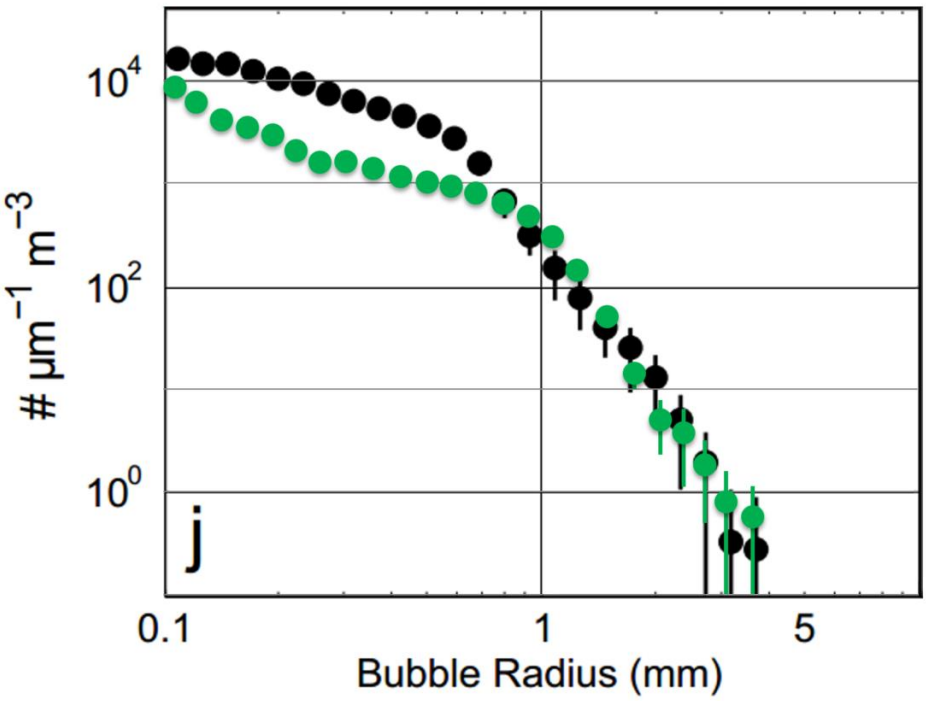

Figure S3.13: The bubble plume size distribution of our MART (in green) is plotted on the graph presenting (in black) the bubble plume size distribution of the original MART system used by Callaghan et al.[93] *Error bars represent the standard error (n=5).*

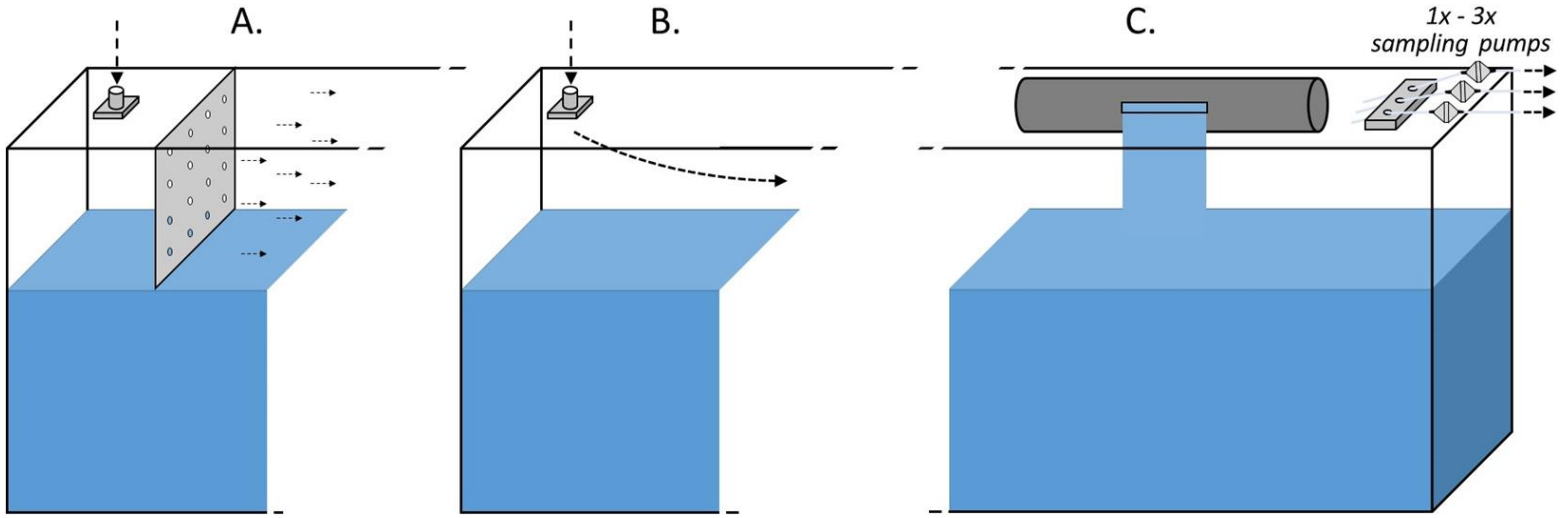

Figure S3.14: combination of 2 MART set-ups to examine (A. vs B.) the addition of a perforated plate in the MART headspace to potentially improve the airflow and as such increase the SSA density in the sampled air, and (C.) the deployment of only one or two sampling pumps simultaneously instead of three pumps (i.e., our standard set-up). The latter tests if the SSA production and the SSA density in the MART headspace was fast and large enough, respectively, to deploy three SSA sampling pumps simultaneously.

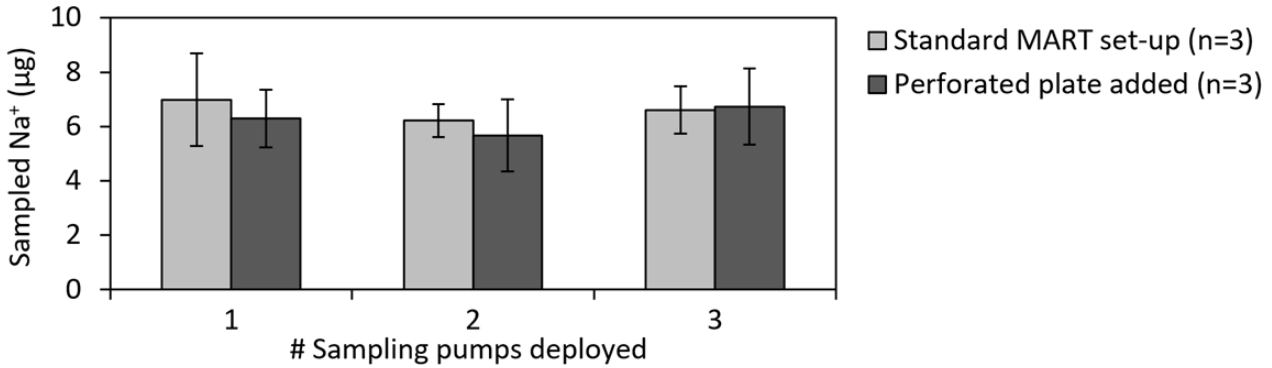

Figure S3.15: Results of the MART experiments examining the addition of a perforated plate in the MART headspace and the deployment of a different number of sampling pumps.

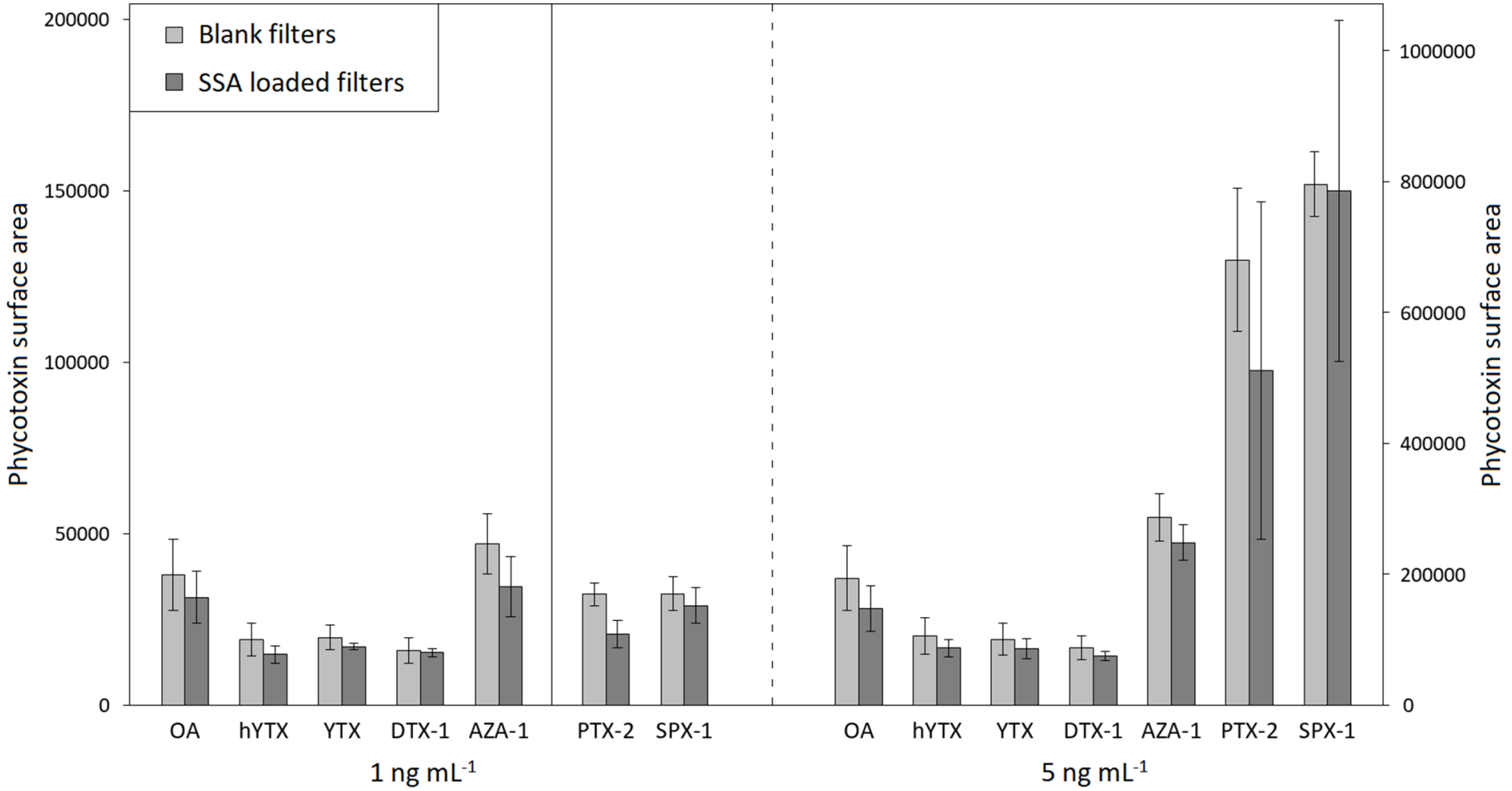

Figure S3.16: Results of the experiment examining the potential effect of the salt content of SSA loaded filters on the extraction efficiency and analysis of phycotoxins. As different SSA filter samples have a different salt content. These salts cannot interfere with the phycotoxin extraction and analysis to ensure a good quality and repeatable analysis. Both blank filters and SSA loaded filters were spiked with seven phycotoxins at a low and mid-level concentration (i.e., representing 1 and 5 ng mL^{-1} in the final 250 µL extract). As only the relative difference between the blank and SSA loaded filters was important. the raw response values (i.e., phycotoxin surface area) are shown on the y-axis. Error bars present the standard deviation (n = 3).

Figure S3.17: The additional SSA sampling technique used in natural and artificial seawater MART experiments to control the collection efficiency. The air passing through the quartz filters was drawn (in small bubbles) through pure water following the sampling method described by Tsunogai et al.[201]

9 Supportive Tables

Table S3.1: Plackett-Burman design of 24 experimental runs used to evaluate the effect of 11 factors on the extraction efficiency of 7 phycotoxins. Each of these factors was evaluated at two levels, being [No] or [Yes] for qualitative factors and a low or high value for qualitative factors.

Run	2 Level pattern	Cutting filter in pieces prior to the elution	Initial elution volume (mL)	NH_4OH in eluent (mM)	Steps during the elution			Extra elution steps (with 3 mL)	Rinse collection tube & PTFE filter (with 1 mL)	Vortex during evaporation		Centrifugation as a last purification step (5 min, 12000 g)
					Vortex (20 sec)	Sonication (5 min)	Centrifugation (5min, 6000 g)			at 5 mL	at 0.3 mL	
1	+−+−+−−++−+	Yes	5	50	No	Yes	No	1	Yes	Yes	No	Yes
2	−−++−−++−++	No	5	50	Yes	No	No	2	Yes	No	Yes	Yes
3	−++−++−+−+−	No	8	50	No	Yes	Yes	1	Yes	No	Yes	No
4	−+−+−++−−+−	No	8	0	Yes	No	Yes	2	No	No	Yes	No
5	+−−−++−−++	Yes	5	0	No	Yes	Yes	2	No	No	Yes	Yes
6	+−+++−−−+−	Yes	5	50	Yes	Yes	No	1	No	No	Yes	No
7	++−++−++−−−	Yes	8	0	Yes	Yes	No	2	Yes	No	No	No
8	−−−−−−−−−−	No	5	0	No	No	No	1	No	No	No	No
9	−−−−+−++++−	No	5	0	No	Yes	No	2	Yes	Yes	Yes	No
10	+++−−−+−++−	Yes	8	50	No	No	No	2	No	Yes	Yes	No
11	++++−+−−−+	Yes	8	50	Yes	No	Yes	1	No	No	No	Yes
12	−+−++−−−+++	No	8	0	Yes	Yes	No	1	No	Yes	Yes	Yes
13	−−−+++−+−−+	No	5	0	Yes	Yes	Yes	1	Yes	No	No	Yes
14	−+−−−++++−+	No	8	0	No	No	Yes	2	Yes	Yes	No	Yes
15	−+++−−−++−−	No	8	50	Yes	No	No	1	Yes	Yes	No	No
16	++++++++++	Yes	8	50	Yes	Yes	Yes	2	Yes	Yes	Yes	Yes
17	−−+−−+−−+++	No	5	50	No	No	Yes	1	No	Yes	Yes	Yes
18	−++−+−+−−−+	No	8	50	No	Yes	No	2	No	No	No	Yes
19	−−++++−+−−	No	5	50	Yes	Yes	Yes	2	No	Yes	No	No
20	+−−+−−+−+−+	Yes	5	0	Yes	No	No	2	No	Yes	No	Yes
21	++−−++−−+−−	Yes	8	0	No	Yes	Yes	1	No	Yes	No	No
22	+−+−−+++−−−	Yes	5	50	No	No	Yes	2	Yes	No	No	No
23	+−−+−+−+++−	Yes	5	0	Yes	No	Yes	1	Yes	Yes	Yes	No
24	++−−−−−+−++	Yes	8	0	No	No	No	1	Yes	No	Yes	Yes

Table S3.2: Box-Behnken design used to further optimize three significant quantitative factors via response surface modelling. Each of these factors was evaluated at three levels, being a low, mid and high value.

Run	3 Level pattern	NH_4OH in eluent (mM)	Initial extraction volume (mL)	Centrifugation speed of last purification step (g)
1	+ 0 −	50	7.5	0
2	− 0 −	0	7.5	0
3	+ 0 +	50	7.5	12000
4	0	25	7.5	6000
5	− 0 +	0	7.5	12000
6	0 − −	25	5	0
7	0 + −	25	10	0
8	0	25	7.5	6000
9	0	25	7.5	6000
10	− − 0	0	5	6000
11	0 + +	25	10	12000
12	− + 0	0	10	6000
13	+ + 0	50	10	6000
14	0 − +	25	5	12000
15	+ − 0	50	5	6000

*Table S3.3: Summary of the response surface modelling (RSM) results, giving the optimum level for each quantitative extraction parameter or factor that significantly influenced the extraction efficiency ($p<0.1$; 90% confidence level) for at least one phycotoxin. This RSM was performed using a Box-Behnken design. These results indicate the levels at which each phycotoxin reaches a maximum extraction efficiency. The overall optimum levels were determined based on the levels of the phycotoxins for which these factors were significant (indicated in bold with an *).*

	OA	hYTX	YTX	DTX-1	AZA-1	PTX-2	SPX-1	Overall optimum level
Initial elution volume (mL)	10	**10***	10	6.87	8.35	5	5	10
NH_4OH in eluent (mM)	15.3	**27.8***	**24.3***	16.2	20.6	0	0	26
Centrifugation (purification) (g)	**7304***	**6062***	6940	7133	**8331***	4687	12000	7200

Table S3.4: Instrumental performance for the pure certified reference standards of the 7 target compounds using the UHPLC-HR-Orbitrap MS method developed by Orellana et al.[132] The empirical mass (m-z) of the below described diagnostic ions was in all cases higher than the theoretical mass (m-z). This difference is reported as the mass accuracy (Δppm). The empirical data is based on the average results of the consecutive analysis of five independent pure (multi-)standards (i.e., without matrix) with a concentration of 1, 2, 3, 4 and 5 ng mL^{-1}, respectively. Next to the mass accuracies, the reported retention time (RT) and the empirical ^{13}C-^{12}C ratio are also based on these analyses.

				Diagnostic quantification ion		Diagnostic ^{13}C-isotope ion for confirmation			
Compound	Elemental formula	RT (min)	Adduct ion	Theoretical mass (*m-z*)	Mass accuracy (Δppm)	Theoretical mass (*m-z*)	Mass accuracy (Δppm)	Theoretical ^{13}C-^{12}C ratio	Empirical ^{13}C-^{12}C ratio
Okadaic acid (OA)	$C_{44}H_{68}O_{13}$	2.00 ± 0.01	$[M - H]^-$	803.45872	1.40 ± 0.17	804.46207	1.36 ± 0.15	47.6%	45.6 ± 2.5%
Homoyessotoxin (hYTX)	$C_{56}H_{84}O_{21}S_2$	2.07 ± 0.01	$[M - 2H]^{2-}$	577.24005	0.46 ± 0.06	577.74173	0.34 ± 0.20	60.6%	62.6 ± 3.6%
Yessotoxin (YTX)	$C_{55}H_{82}O_{21}S_2$	2.07 ± 0.01	$[M - 2H]^{2-}$	570.23222	0.52 ± 0.36	570.73390	0.58 ± 0.13	59.5%	59.7 ± 3.4%
Dinophysistoxin-1 (DTX-1)	$C_{45}H_{70}O_{13}$	2.16 ± 0.02	$[M - H]^-$	817.47437	1.63 ± 0.26	818.47772	1.74 ± 0.25	48.7%	47.7 ± 2.4%
Azaspiracid-1 (AZA-1)	$C_{47}H_{71}NO_{12}$	2.52 ± 0.01	$[M + H]^+$	842.50490	0.21 ± 0.11	843.50826	0.38 ± 0.14	50.8%	48.9 ± 2.3%
Pectenotoxin-2 (PTX-2)	$C_{47}H_{70}O_{14}$	3.51 ± 0.01	$[M + NH_4]^+$	876.51038	0.26 ± 0.09	877.51374	0.40 ± 0.12	50.8%	52.9 ± 2.0%
13-desmethyl spirolide C (SPX-1)	$C_{42}H_{61}NO_7$	3.52 ± 0.01	$[M + H]^+$	692.45208	0.25 ± 0.08	693.45543	0.27 ± 0.09	45.4%	46.1 ± 1.0%

Table S3.5: Summary of the validation data (n=24) concerning the deviations of the four identification criteria at the lowest concentration level (1.5x LOQ), relative to the empirical data of the pure standards (i.e., without matrix) as reported in Table S3.4.

			Deviation from the accurate mass for the diagnostic ion for quantification		Deviation from the accurate mass for the ^{13}C-isotope for confirmation			
Compound	Average RT (min)	Maximum deviation RT (min)	Average (Δppm)	Max. (Δppm)	Average (Δppm)	Max. (Δppm)	Average ^{13}C-^{12}C ratio	Deviation from the ^{13}C-^{12}C ratio
OA	2.01 ± 0.01	0.03	0.53 ± 0.42	1.35	0.83 ± 0.38	1.42	45.7 ± 2.5 %	0.12%
hYTX	2.09 ± 0.02	0.06	0.72 ± 0.29	1.23	0.64 ± 0.51	1.74	63.1 ± 4.8 %	0.47%
YTX	2.09 ± 0.02	0.06	0.66 ± 0.37	1.28	0.59 ± 0.31	1.29	61.1 ± 4.5 %	1.41%
DTX-1	2.18 ± 0.01	0.05	0.72 ± 0.30	1.31	0.96 ± 0.33	1.61	46.4 ± 3.9 %	1.31%
AZA-1	2.57 ± 0.02	0.09	0.32 ± 0.31	1.06	0.46 ± 0.41	1.32	50.9 ± 4.7 %	1.95%
PTX-2	3.49 ± 0.02	0.06	0.38 ± 0.36	1.46	0.63 ± 0.51	1.49	52.5 ± 4.7 %	0.45%
SPX-1	3.50 ± 0.02	0.06	0.38 ± 0.34	1.10	0.58 ± 0.26	1.23	47.3 ± 7.3 %	1.17 %

Table S3.6: Overview of the compounds, chemical classes or total organic carbon (OC) for which enrichment processes have been quantified (i.e., EF_{SSA} & EF_{SSML}). Cells with an (-), denote unavailable data. This table was partly based on Quinn et al.[87]

Product	EF_{SSA} (-)			EF_{SSML} (-)	Origin of data
Prokaryotes (e.g., bacteria)	10-20			1-6	Experimental aerosols using water spiked with bacteria,[331] and environmental samples.[76,86,297]
	± 30 *(<1.2 µm)*	± 3 *(>1.2 µm)*		-	Experimental SSAs using natural seawater.[83]
Virus-like particles	± 2 · 10^2 *(<1.2 µm)*	10 *(<10 µm)*		1.5-7	Environmental samples[76,86] and experimental SSAs using natural seawater.[83]
Saccharides	14-1314 *(<2.5 µm)*	3-138 *(2.5 – 10 µm)*		1-16.2	Experimental SSAs using natural seawater.[73]
	± 10^5	± 10^4		-	Experimental SSAs using natural seawater.[83]
DNA	± 2 · 10^4	± 10^4			
Lipids	± 10^5	± 10^4			
Proteinaceous matter	± 10^5 *(<1.2 µm)*	± 10^4 *(>1.2 µm)*			
	1.2-20			1.9	Environmental samples.[76,86]
Total OC	10^4-10^5 *(<0.25 µm)*	10^3-10^4 *(<1 µm)*	± 10^2 *(<20 µm)*	1-2	Environmental samples[172,184] and experimental SSAs using natural water.[92,208]
Brevetoxins	5-50			-	Experimental SSAs using a *Karenia brevis* culture.[206]
OA, hYTX and DTX-1	480-1800			2.9-5.7	Experimental SSAs using artificial seawater spiked with toxin-producing algae (this study).
	78-520			1.3-6.4	Experimental SSAs using natural seawater spiked with toxin-producing algae (this study).

Table S3.7: Limits of detection (LODs) and quantification (LOQs) for the different phycotoxins we quantified in the different size fractions of the seawater (for the MART experiments shown in Figure 3.2). Conversely to the LOD and LOQ values reported in Table 3.1, the reported values here represent seawater concentrations instead of concentrations in the final extract.

	> 5 µm (large particulate)		0.2 - 5 µm (small particulate)		< 0.2 µm (dissolved)	
Compound	LOD (ng mL^{-1})	LOQ (ng mL^{-1})	LOD (ng mL^{-1})	LOQ (ng mL^{-1})	LOD (ng mL^{-1})	LOQ (ng mL^{-1})
OA	0.011	0.032	0.012	0.037	0.015	0.046
hYTX	0.024	0.072	0.028	0.083	0.035	0.104
DTX-1	0.027	0.080	0.031	0.092	0.038	0.115

Annex IV

Supportive information Chapter 4

Annex contents

1 Determination of dose levels for different treatments

For the natural SSA sample, we aimed at selecting environmentally relevant doses. Hence, we sampled for 45 minutes at the sea shore on a windy day at a volume of 10 L min^{-1}, equivalent to the minute ventilation in rest for an average person.[233,234] Given that the multiwell plates only have a surface of 9.6 cm^2 whereas the total lung surface is reported to be between 35-140 m^2 depending on body size, measurement technique and inhalation or expiration.[332] Given the variation in reported size for the total lung surface, we selected 40 m^2 as average epithelial alveolar surface. We needed to account for the reduction in surface size as otherwise the amount of aerosols per surface would be larger than in reality. In addition, we also accounted for the exposure duration. As a result, during our sampling, we collected 460L of air, which would theoretically be taken up by the entire alveolar surface (40 m^2). Hence, we calculated the amount of air taken up by 9.6 cm^2 cells, which is 0.011 L. This amount of air is inhaled in a period of 46 min, while the experimental exposure will last 43 h. Hence, we calculated the amount of air that would hypothetically be inhaled in a 43 h exposure period, which is 0.619 L. As such, this is relatively 0.26% of the filter extract. This level was selected as the low dose level. We then determined the mid and high dose treatment by using a factor 10 (2.6%) and 40 (10.8%) relative to the low dose. The factor 10 accounts for increased breathing during exercise and activity while the factor 40 additionally accounts for variation in weather conditions (e.g., more favorable aerosolization conditions due to subsequent windy days, giving higher waves and a subsequent higher SSA production).

Currently, literature reports homoyessotoxin (hYTX) concentrations in shellfish and other marine organisms but not in seawater nor in SSAs. The (maximum) reported cell densities of *Protoceratium reticulatum* range between 400-700 cells L^{-1} in the marine

environment.[196,197] Second, the maximum reported homoyessotoxin concentrations range between 28.6 to 33.6 pg per cell of *P. reticulatum*.[142,143] Based on these reports, we estimated a high seawater concentration to be equal to 0.01 µg L^{-1}. As such, 0.5 µg L^{-1} (×50) reflect an extreme case scenario and 10^{-5} µg L^{-1} (1/1000) a background seawater concentration with low algal cell densities reported as at most 10 cells L^{-1}.[196]

2 Supportive Figures

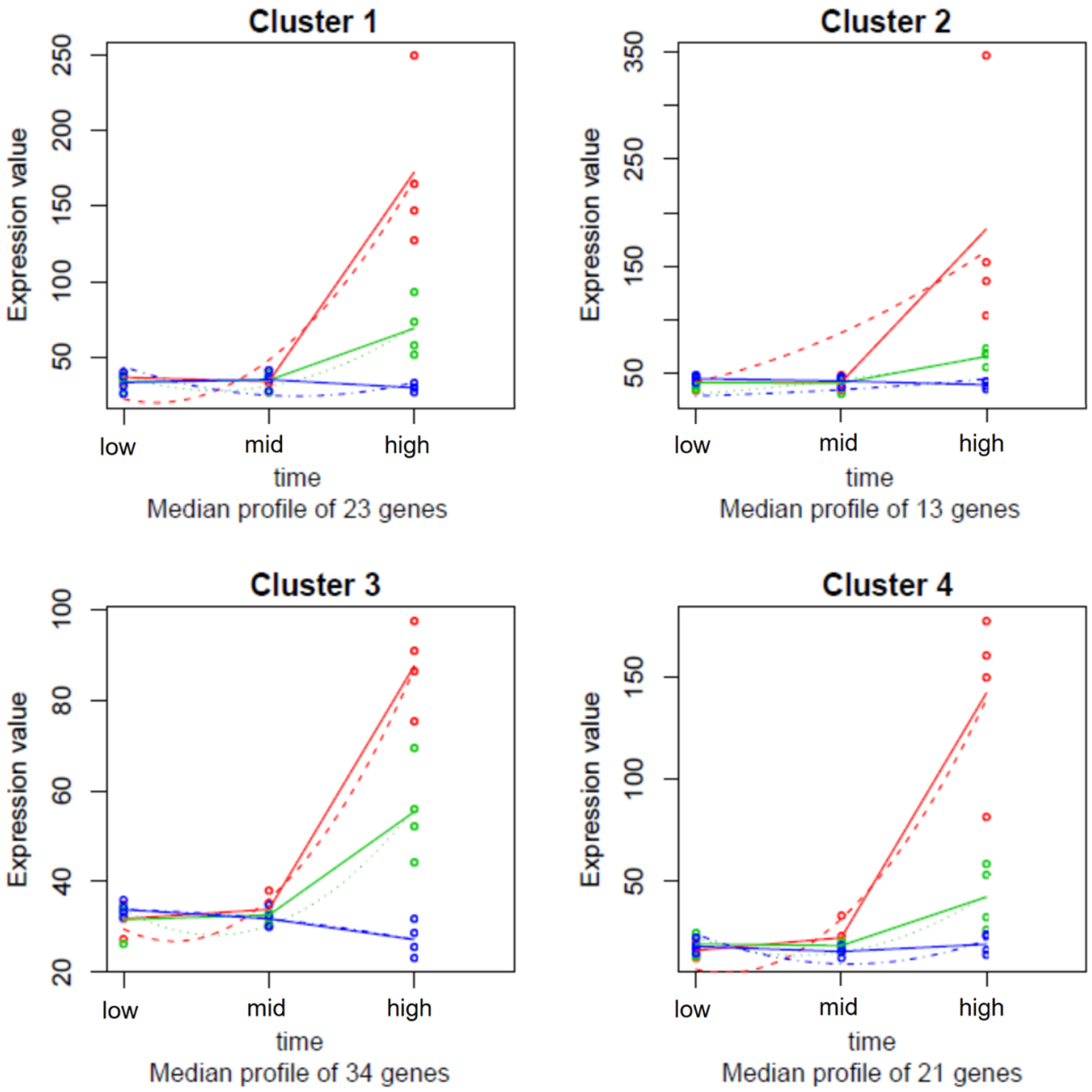

Figure S4.1: Median gene expression profiles for the different clusters plotted per treatment. Red represents the homoyessotoxin treatment, green represents the lab sea spray aerosol treatment and blue represents the natural sea spray aerosol treatments. Points are median values connected by solid lines, dotted lines are the regression models. Expression values were normalized counts.

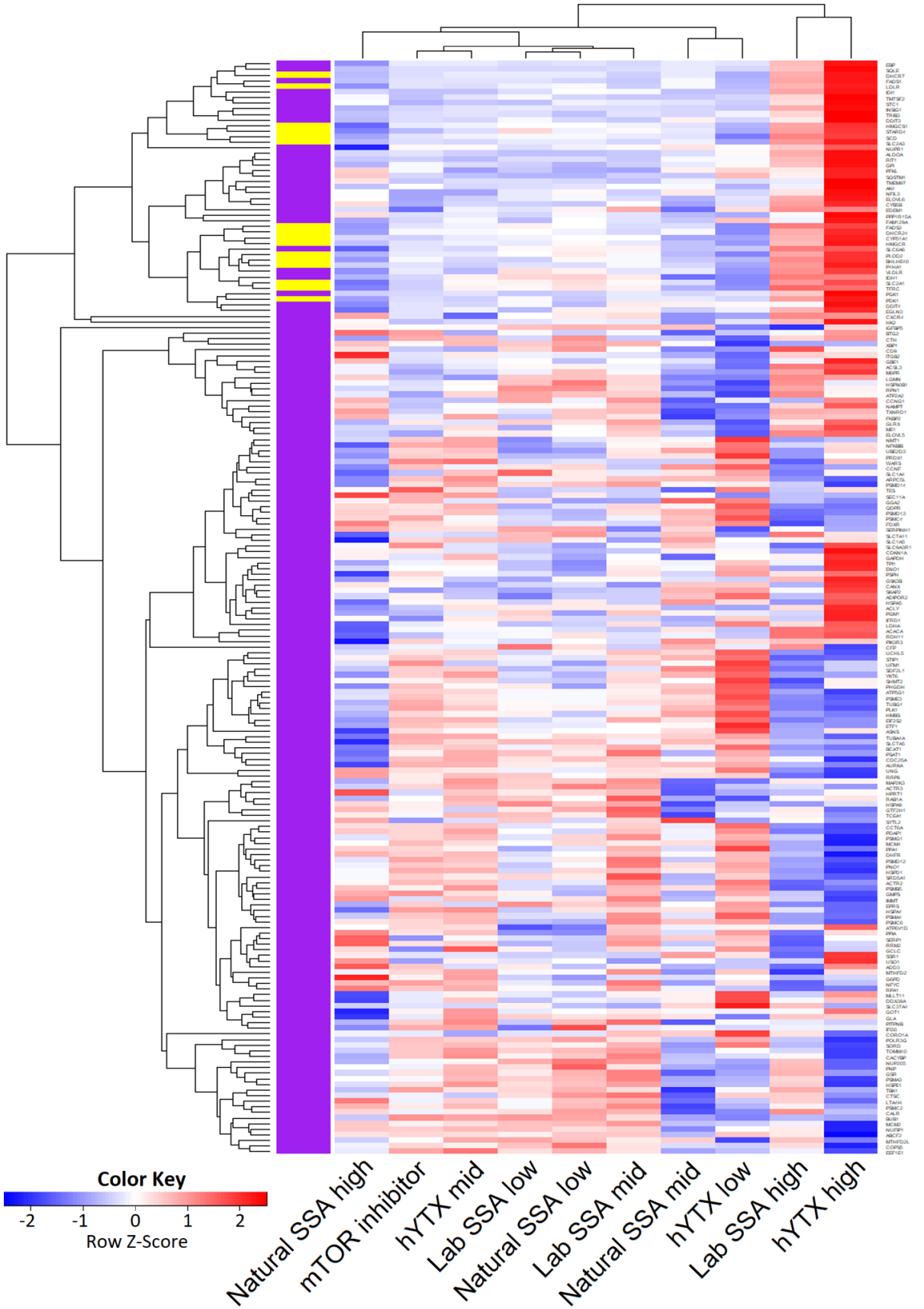

Figure S4.2: Heatmap of the mTOR Hallmark set for all treatments (the natural and laboratory sea spray aerosol (SSA), homoyessotoxin (hYTX)) for all dose levels and the chemical inhibitor. Yellow band distinguishes genes enriched in all three high dose treatments and the chemical inhibitor from the other hallmark genes (purple).

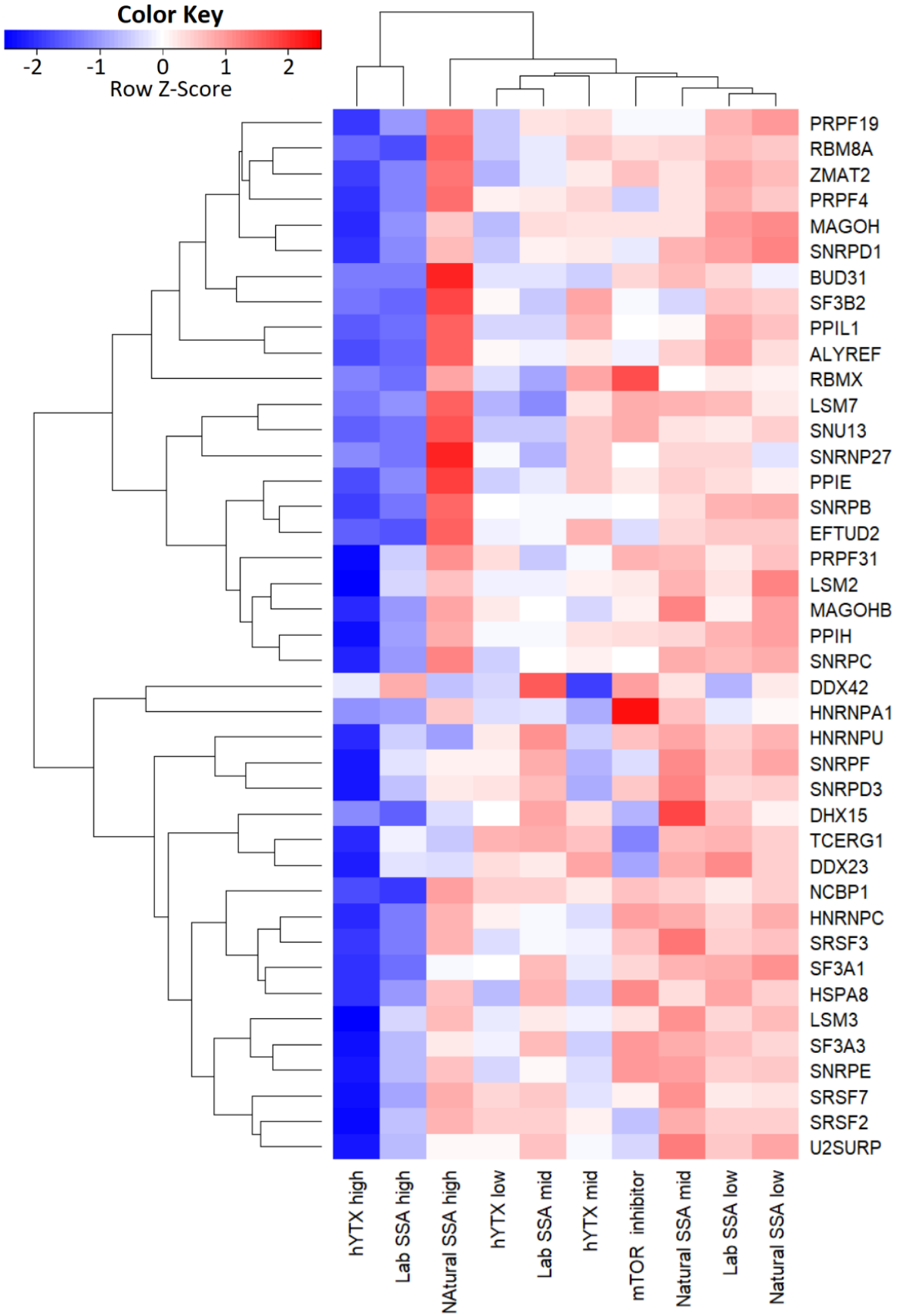

Figure S4.3: Heatmap of all genes with a significant dose response (FDR<0.01) effect in the spliceosome for all treatments and all dose levels (natural sea spray aerosol: natural SSA, laboratory sea spray aerosol: lab SSA, homoyessotoxin: hYTX, mTOR inhibitor).

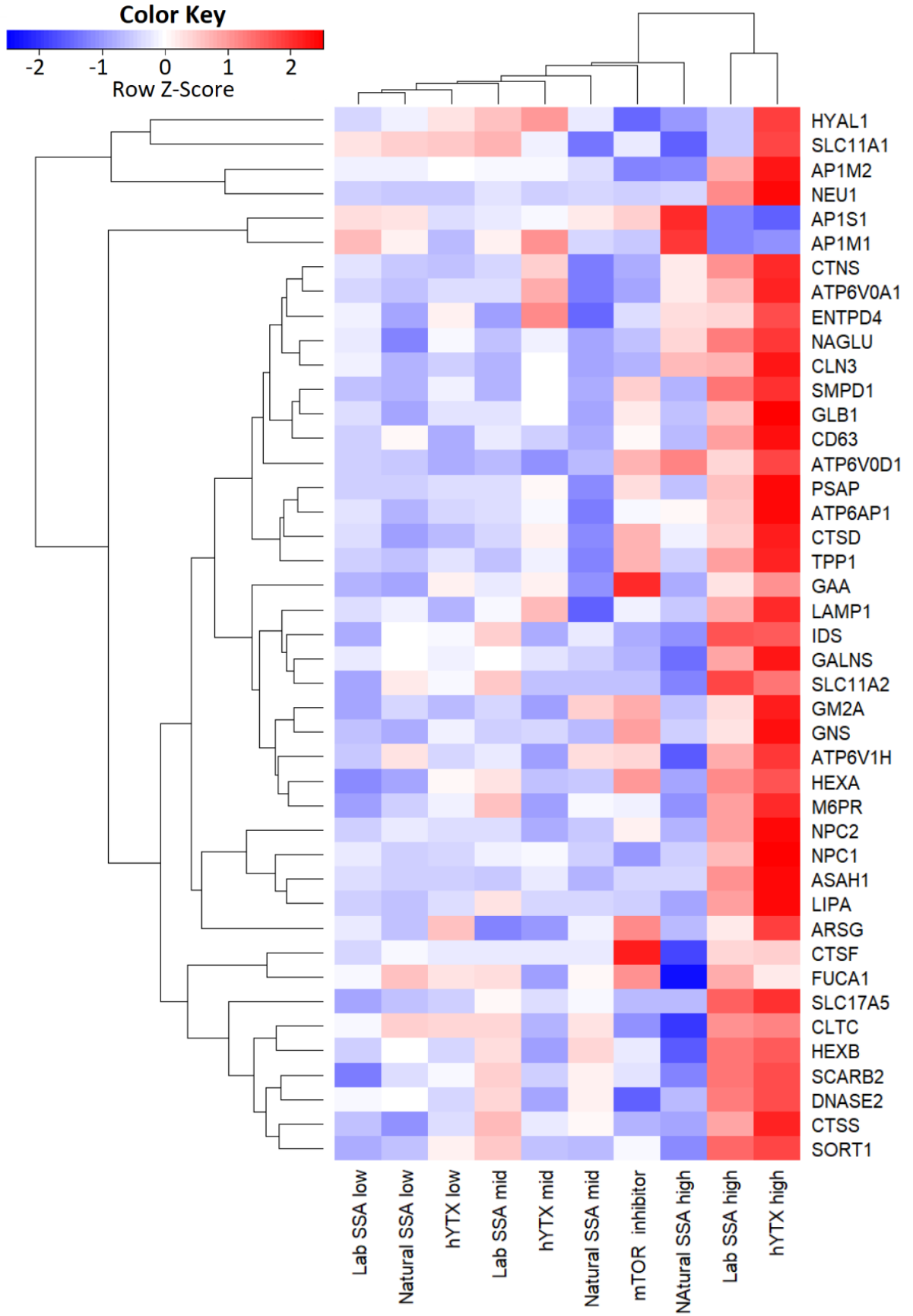

Figure S4.4: Heatmap of all genes with a significant dose response (FDR<0.01) effect in the lysosome for all treatments and all dose levels (natural sea spray aerosol: natural SSA, laboratory sea spray aerosol: lab SSA, homoyessotoxin: hYTX, mTOR inhibitor).

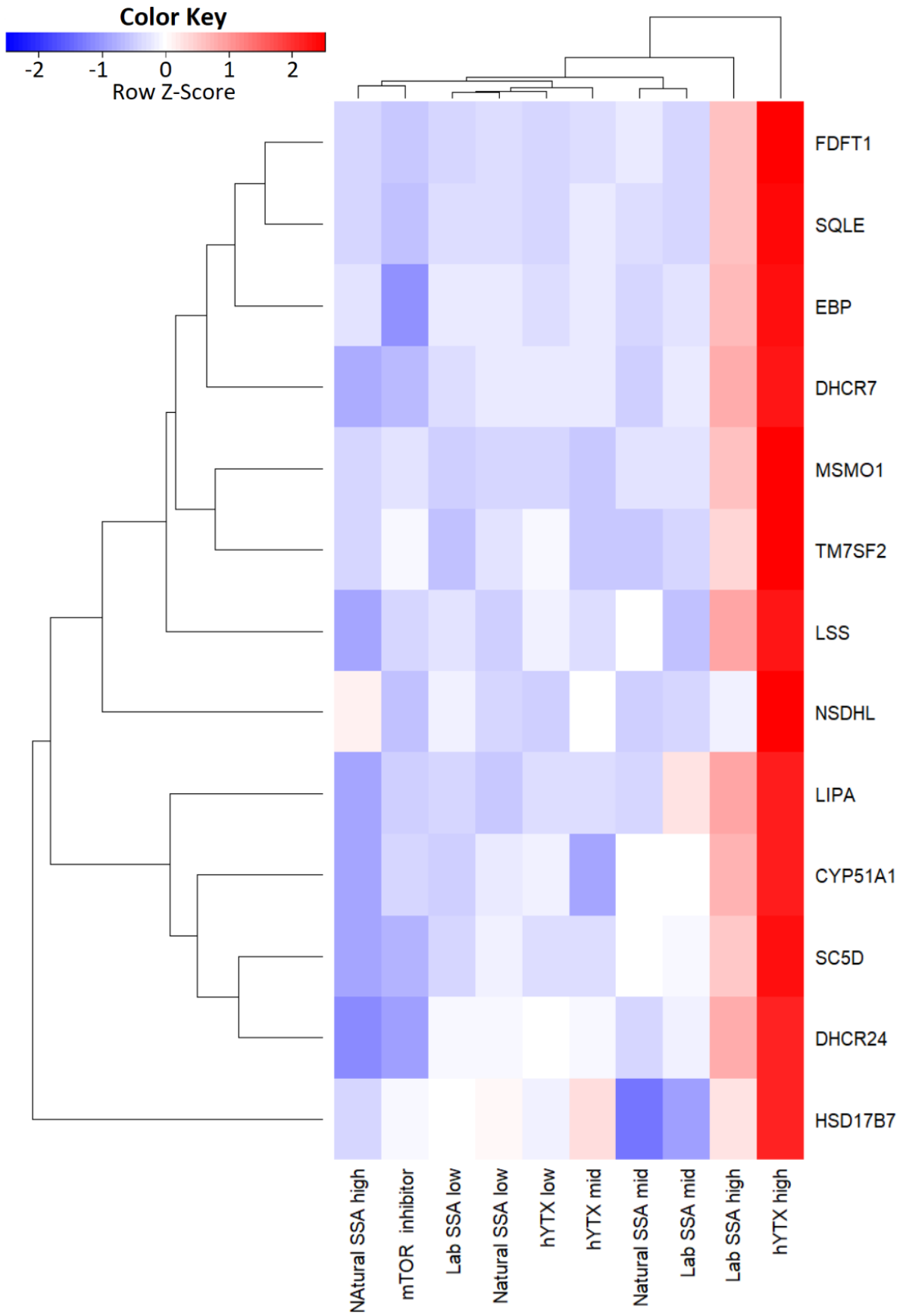

Figure S4.5: Heatmap of all genes with a significant dose response (FDR<0.01) effect in the steroid biosynthesis for all treatments and all dose levels (natural sea spray aerosol: natural SSA, laboratory sea spray aerosol: lab SSA, homoyessotoxin: hYTX, mTOR inhibitor)

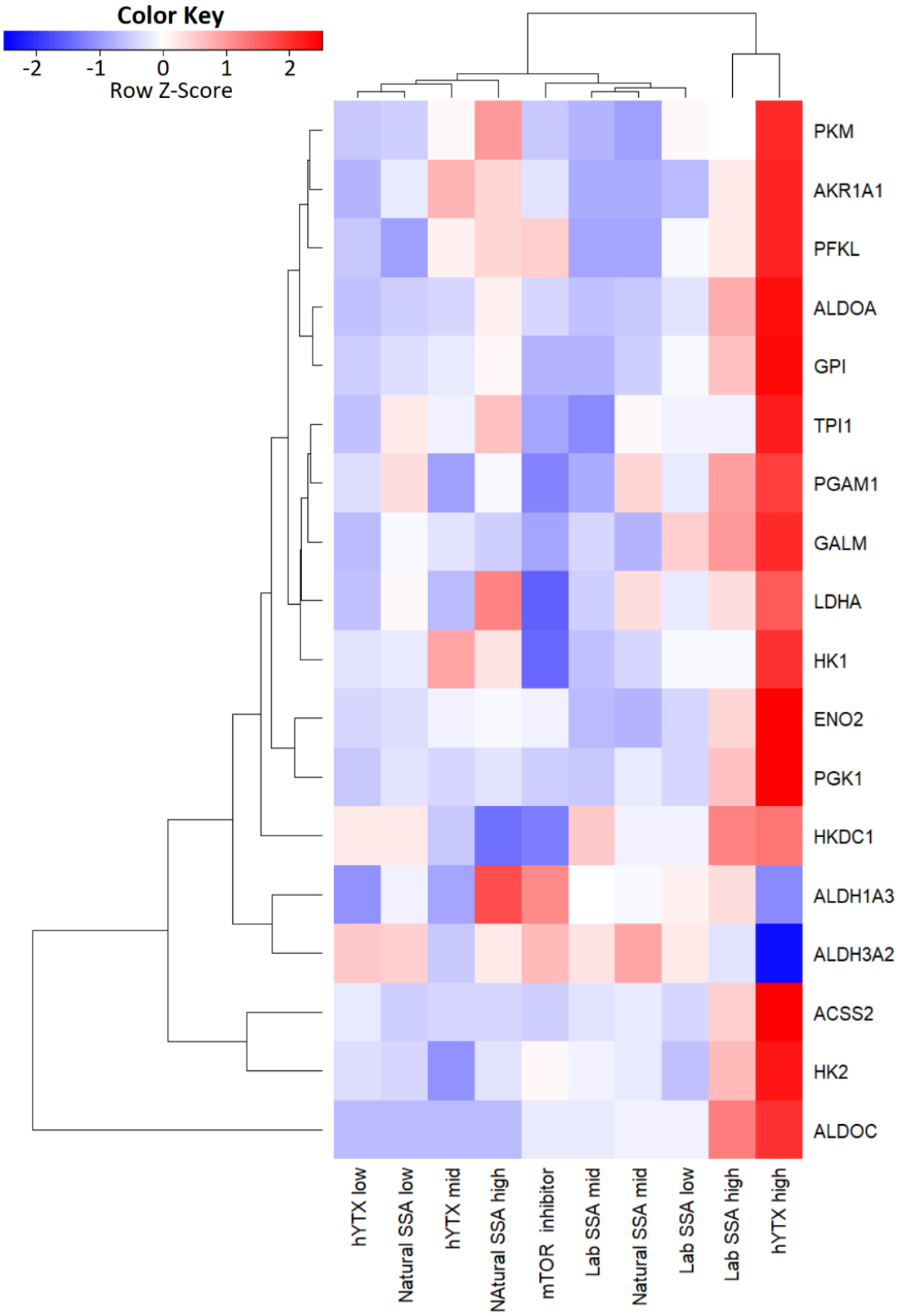

Figure S4.6: Heatmap of all genes with a significant dose response (FDR<0.01) effect in the glycogenesis for all treatments and all dose levels (natural sea spray aerosol: natural SSA, laboratory sea spray aerosol: lab SSA, homoyessotoxin: hYTX, mTOR inhibitor).

3 Supportive Tables

Table S4.1: Enrichment scores (ES), normalized enrichment scores (NES) and the false discovery rate (FDR) for gene set enrichment analysis of the mTOR hallmark gene set for all treatments.

	Natural sea spray aerosol			Lab sea spray aerosol			Homoyessotoxin			mTOR
	High	Mid	Low	High	Mid	Low	High	Mid	Low	inhibitor
ES	-0.25	0.31	0.16	0.39	-0.18	-0.2	0.46	-0.35	-0.26	-0.48
NES	-1.24	1.48	0.83	1.92	-0.83	-0.92	2.14	-1.7	-1.2	-2.32
FDR	0.2	0.04	1	0.001	1	0.9	0	0.006	0.38	0

Table S4.2: Genes, assigned to the mTOR pathway based on KEGG pathway annotations, with a false discovery rate (FDR) <0.01 in at least 1 treatment. The false discovery rates and log2 fold changes are reported for all high dose treatments (the natural and laboratory sea spray aerosol (SSA), homoyessotoxin (hYTX) and the mTOR inhibitor. Significances are highlighted in bold.

Ensembl Gene ID	Natural SSA		Lab SSA		hYTX		mTOR inhibitor	
	FC	FDR	FC	FDR	FC	FDR	FC	FDR
ENSG00000167965	**0.85**	**7.73 e-03**	0.29	0.78	0.29	0.78	0.1	0.53
ENSG00000168209	-0.20	0.70	-0.28	0.84	**1.19**	**4.49 e-06**	**-0.96**	**7.24 e-03**
ENSG00000173511	0.16	0.71	0.34	0.7	**0.98**	**2.85 e-05**	0.24	0.64
ENSG00000171608	0.23	0.40	0.03	1	**0.58**	**2.95 e-03**	-0.07	0.94
ENSG00000063046	0.25	0.40	0.04	0.94	-0.07	0.94	**0.88**	**4.61 e-05**
ENSG00000117461	0.12	0.80	0.25	0.84	0.21	0.61	**-1.21**	**1.14 e-04**

Table S4.3: Kegg pathways and their corresponding adjusted p-value for Fisher enrichment test of genes with a significant dose response effect (false discovery rate (FDR) <0.01)).

Kegg pathway name	p.adjusted	Genes with FDR	
		<0.01	>0.01
Lysosome	**7.09E-06**	**43**	**69**
Steroid biosynth.	**3.26E-05**	**13**	**5**
Spliceosome	**8.29E-04**	**41**	**85**
Glycolysis / Gluconeogenesis	**4.84E-03**	**18**	**25**
Chagas disease (American trypanosomiasis)	6.57E-02	3	68
Glycosaminoglycan degradation	6.57E-02	8	8
Metabolic pathways	6.57E-02	181	699
Regulation of actin cytoskeleton	6.57E-02	13	147
Terpenoid backbone biosynth.	6.57E-02	7	6
Arginine and proline metabolism	8.17E-02	15	29
Galactose metabolism	8.17E-02	9	12
Phagosome	8.17E-02	28	71
Neomycin, kanamycin and gentamicin biosynth.	8.18E-02	3	0
DNA replication	8.65E-02	13	23
Basal transcription factors	9.42E-02	0	31
GnRH signaling pathway	9.42E-02	4	70
TGF-beta signaling pathway	9.42E-02	3	62
Amino sugar and nucleotide sugar metabolism	0.13	14	28
Ribosome biogenesis in eukaryotes	0.13	21	52
Cell cycle	0.13	30	85
RNA transport	0.13	35	106
Biosynth. of unsaturated fatty acids	0.16	8	13
Tight junction	0.2	8	91
Fructose and mannose metabolism	0.25	10	21
Neurotrophin signaling pathway	0.25	10	100
PPAR signaling pathway	0.25	12	27
Glycosphingolipid biosynth. - ganglio series	0.3	5	7
Nicotinate and nicotinamide metabolism	0.3	0	21
Starch and sucrose metabolism	0.31	9	19
Alanine, aspartate and glutamate metabolism	0.36	8	16
Fat digestion and absorption	0.36	6	11
Shigellosis	0.36	4	53
Type I diabetes mellitus	0.36	5	8
Glycosphingolipid biosynth. - globo and isoglobo series	0.45	4	6
Leukocyte transendothelial migration	0.45	7	72
MAPK signaling pathway	0.45	24	177
Acute myeloid leukemia	0.45	3	44
Osteoclast differentiation	0.45	8	76
Retinol metabolism	0.45	7	15
Vasopressin-regulated water reabsorption	0.45	2	35
Antigen processing and presentation	0.48	11	29
Fc gamma R-mediated phagocytosis	0.48	7	68
Nitrogen metabolism	0.48	5	10
Toll-like receptor signaling pathway	0.52	6	60
Fatty acid degradation	0.53	9	24

Bile secretion	0.57	10	27
Ribosome	0.57	21	69
African trypanosomiasis	0.57	4	8
Carbohydrate digestion and absorption	0.57	6	14
Propanoate metabolism	0.57	8	20
RIG-I-like receptor signaling pathway	0.57	4	45
Apoptosis	0.58	7	65
Calcium signaling pathway	0.58	11	89
Colorectal cancer	0.58	5	52
Cytokine-cytokine receptor interaction	0.58	12	94
Fatty acid elongation	0.58	3	5
Focal adhesion	0.58	18	131
Graft-versus-host disease	0.58	3	5
Natural killer cell mediated cytotoxicity	0.58	16	53
Toxoplasmosis	0.58	9	78
Taste transduction	0.58	0	15
Protein processing in endoplasmic reticulum	0.58	19	135
Endometrial cancer	0.6	4	42
Other glycan degradation	0.6	5	11
Allograft rejection	0.62	3	6
Autoimmune thyroid disease	0.62	3	6
Aldosterone-regulated sodium reabsorption	0.62	7	19
Cyanoamino acid metabolism	0.65	2	3
Fatty acid biosynth.	0.65	2	3
Valine, leucine and isoleucine degradation	0.65	10	30
Huntingtons disease	0.65	21	142
Parkinsons disease	0.65	14	101
Small cell lung cancer	0.65	8	67
Vascular smooth muscle contraction	0.65	8	67
Glycerophospholipid metabolism	0.66	6	54
Long-term depression	0.66	4	39
Type II diabetes mellitus	0.66	8	23
Lysine biosynth.	0.67	12	89
Ether lipid metabolism	0.67	1	20
Rheumatoid arthritis	0.67	11	36
Ubiquitin mediated proteolysis	0.67	16	111
Chemokine signaling pathway	0.7	14	99
Phenylalanine metabolism	0.7	4	9
Pyruvate metabolism	0.7	8	26
Peroxisome	0.71	8	62
Arachidonic acid metabolism	0.72	6	18
Aminoacyl-tRNA biosynth.	0.77	4	37
Citrate cycle (TCA cycle)	0.77	2	25
Thyroid cancer	0.77	2	24
Porphyrin and chlorophyll metabolism	0.77	7	21
Nucleotide excision repair	0.77	10	34
Pathways in cancer	0.78	37	222
Glycosaminoglycan biosynth. - heparan sulfate / heparin	0.79	1	16
Glyoxylate and dicarboxylate metabolism	0.79	1	16

Table S4.3 continued

Kegg pathway name	p.adjusted	Genes with FDR	
		<0.01	>0.01
Phosphatidylinositol signaling system	0.79	8	60
Renin-angiotensin system	0.79	2	5
Synthesis and degradation of ketone bodies	0.79	2	5
Taurine and hypotaurine metabolism	0.79	2	5
Butanoate metabolism	0.79	5	15
Collecting duct acid secretion	0.79	5	15
Glycerolipid metabolism	0.79	8	27
mRNA surveillance pathway	0.79	15	58
Pentose phosphate pathway	0.79	5	15
T cell receptor signaling pathway	0.79	9	65
Jak-STAT signaling pathway	0.8	10	70
VEGF signaling pathway	0.8	12	45
Leishmaniasis	0.83	4	34
Proteasome	0.84	9	32
Adipocytokine signaling pathway	0.84	6	45
Arrhythmogenic right ventricular cardiomyopathy (ARVC)	0.84	6	44
Ascorbate and aldarate metabolism	0.84	3	9
Asthma	0.84	1	2
Drug metabolism - other enzymes	0.84	6	22
Glioma	0.84	11	43
Homologous recombination	0.84	3	26
Inositol phosphate metabolism	0.84	6	44
Lipoic acid metabolism	0.84	1	2
Melanogenesis	0.84	9	63
NOD-like receptor signaling pathway	0.84	5	40
Pancreatic secretion	0.84	6	46
Phenylalanine, tyrosine and tryptophan biosynth.	0.84	1	2
Protein export	0.84	2	21
Systemic lupus erythematosus	0.84	10	39
Vibrio cholerae infection	0.84	10	38
Vitamin digestion and absorption	0.84	3	10
Wnt signaling pathway	0.84	23	98
Dilated cardiomyopathy (DCM)	0.86	7	50
Purine metabolism	0.86	25	108
Pancreatic cancer	0.87	8	55
Selenocompound metabolism	0.87	1	15
beta-Alanine metabolism	0.88	4	13
Bladder cancer	0.88	8	30
One carbon pool by folate	0.88	4	13
Pathogenic Escherichia coli infection	0.93	9	36
Melanoma	0.94	6	42
Salivary secretion	0.94	6	43
Alzheimers disease	0.95	22	127
Bacterial invasion of epithelial cells	0.95	8	53
Drug metabolism - cytochrome P450	0.95	3	24
ECM-receptor interaction	0.95	7	46

Endocytosis	0.95	25	144
Epithelial cell signaling in Helicobacter pylori infection	0.95	8	53
Glycosylphosphatidylinositol (GPI)-anchor biosynth.	0.95	5	20
Linoleic acid metabolism	0.95	0	7
Riboflavin metabolism	0.95	0	6
Steroid hormone biosynth.	0.95	5	18
Ubiquinone and other terpenoid-quinone biosynth.	0.95	0	6
ErbB signaling pathway	0.98	10	63
ABC transporters	1	5	22
Adherens junction	1	9	55
alpha-Linolenic acid metabolism	1	1	7
Amoebiasis	1	9	55
Amyotrophic lateral sclerosis (ALS)	1	6	33
Autophagy - animal	1	3	16
Axon guidance	1	0	2
B cell receptor signaling pathway	1	8	50
Basal cell carcinoma	1	6	35
Base excision repair	1	5	28
Biotin metabolism	1	0	2
Caffeine metabolism	1	0	2
Cardiac muscle contraction	1	7	43
Cell adhesion molecules (CAMs)	1	9	54
Chronic myeloid leukemia	1	11	55
Circadian rhythm	1	3	17
Complement and coagulation cascades	1	6	31
Cysteine and methionine metabolism	1	5	23
Cytosolic DNA-sensing pathway	1	4	26
D-Glutamine and D-glutamate metabolism	1	0	3
Dorso-ventral axis formation	1	2	17
Fc epsilon RI signaling pathway	1	7	45
Folate biosynth.	1	1	6
Gap junction	1	9	55
Gastric acid secretion	1	6	39
Glutathione metabolism	1	7	30
Glycine, serine and threonine metabolism	1	3	19
Glycosaminoglycan biosynth. - chondroitin/dermatan sulfate	1	3	16
Glycosaminoglycan biosynth. - keratan sulfate	1	2	12
Glycosphingolipid biosynth. - lacto and neolacto series	1	2	14
Hedgehog signaling pathway	1	6	31
Hematopoietic cell lineage	1	5	26
Hepatitis C	1	15	86
Histidine metabolism	1	3	18
Hypertrophic cardiomyopathy (HCM)	1	7	45
Insulin signaling pathway	1	19	95
Intestinal immune network for IgA production	1	2	12
Long-term potentiation	1	8	44
Lysine degradation	1	6	33
Malaria	1	3	15
Maturity onset diabetes of the young	1	2	8

Table S4.3 continued

Kegg pathway name	p.adjusted	Genes with FDR	
		<0.01	>0.01
Metabolism of xenobiotics by cytochrome P450	1	5	25
Mismatch repair	1	4	19
mTOR signaling pathway	1	6	39
Mucin type O-glycan biosynth.	1	4	20
N-Glycan biosynth.	1	8	38
Neuroactive ligand-receptor interaction	1	12	69
Non-homologous end-joining	1	1	11
Non-small cell lung cancer	1	8	40
Notch signaling pathway	1	6	35
Olfactory transduction	1	2	15
Oocyte meiosis	1	16	78
Other types of O-glycan biosynth.	1	5	25
Oxidative phosphorylation	1	19	102
p53 signaling pathway	1	10	50
Pantothenate and CoA biosynth.	1	2	9
Pentose and glucuronate interconversions	1	3	14
Phototransduction	1	1	11
Primary bile acid biosynth.	1	1	8
Primary immunodeficiency	1	2	11
Prion diseases	1	3	17
Progesterone-mediated oocyte maturation	1	11	61
Prostate cancer	1	14	64
Protein digestion and absorption	1	7	32
Proximal tubule bicarbonate reclamation	1	2	10
Pyrimidine metabolism	1	16	71
Renal cell carcinoma	1	9	54
RNA degradation	1	11	55
RNA polymerase	1	5	22
SNARE interactions in vesicular transport	1	5	28
Sphingolipid metabolism	1	5	30
Staphylococcus aureus infection	1	2	14
Sulfur metabolism	1	2	10
Sulfur relay system	1	1	9
Thiamine metabolism	1	0	3
Tryptophan metabolism	1	5	22
Tyrosine metabolism	1	5	21
Valine, leucine and isoleucine biosynth.	1	1	9
Viral myocarditis	1	7	30
Vitamin B6 metabolism	1	1	5

Table S4.4: Log2 Fold change (FC) and false discovery rates (FDR) for the aryl hydrocarbon receptor (AHR) in all treatments. Significances are highlighted in bold.

Treatment	Dose	FC	FDR
Natural sea spray aerosol	Low	-0.19	1.00
Natural sea spray aerosol	Mid	-0.18	1.00
Natural sea spray aerosol	High	-0.13	0.86
Laboratory sea spray aerosol	Low	-0.06	1.00
Laboratory sea spray aerosol	Mid	0.16	1.00
Laboratory sea spray aerosol	High	-0.65	0.55
Homoyessotoxin	Low	0.11	1.00
Homoyessotoxin	Mid	-0.17	0.89
Homoyessotoxin	High	0.25	0.67
mTOR inhibitor	-	0.17	0.88

Table S4.5: Log2 Fold change (FC) and false discovery rates (FDR) for the small nuclear ribonucleoprotein polypeptide E (SNRPE) in all treatments. Significances are indicated in bold.

Treatment	Dose	FC	FDR
Natural sea spray aerosol	Low	0.01	1.00
Natural sea spray aerosol	Mid	0.12	1.00
Natural sea spray aerosol	High	0.01	1.00
Laboratory sea spray aerosol	Low	-0.03	0.90
Laboratory sea spray aerosol	Mid	-0.13	1.00
Laboratory sea spray aerosol	High	-0.35	0.57
Homoyessotoxin	Low	-0.27	1.00
Homoyessotoxin	Mid	-0.25	0.54
Homoyessotoxin	High	-0.83	**4.58E-05**
mTOR inhibitor	-	0.14	0.76

Annex V

Supportive information Chapter 5

Annex contents

1 Fragmentation collision energy

The normalized collision energy (NCE) used for the fragmentation of DPPC was optimized to receive three main fragments for identification of which one could be used for quantification. 10 different collision energies between 20 eV and 80 eV were tested. At the lowest collision energy (i.e., 20 eV) the precursor ion of DPPC ($[M+H]^+$; m/z of 734.56943) was still detectable, but no there was only one main fragment (Figure S5.2A). At a collision energy of 33 eV, an intermediate scenario was found where two smaller fragments started to appear (Figure S5.2B). Fragmentation using a collision energy of 52 eV was found to give the best balance between identification and quantification of DPPC. Three main fragments could be used for identification and one fragment was dominant and could be used for quantification purposes (Figure S5.2C). The fragments with a m/z of 86 and 184 were also found and used by Ullah et al.[275] to identify and quantify DPPC. According Ullah et al.[275] the formation of these ions originate from the polar headgroup of choline and the phosphocholine headgroup, respectively.

2 Supportive Figures

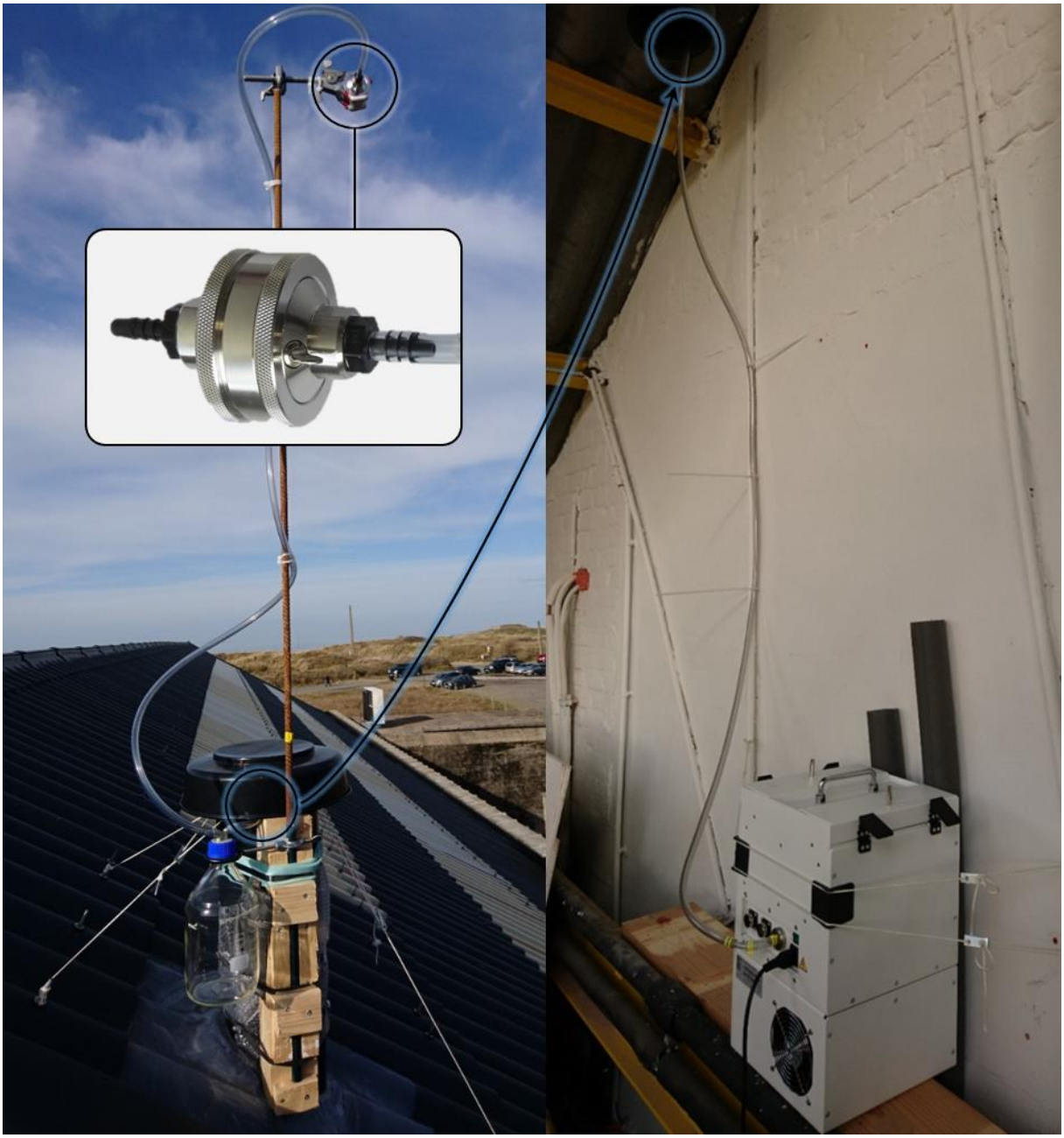

Figure S5.1: SSA sampling set-up on the roof (10m above ground level) of the lab facilities of the Flanders Marine institute (VLIZ) at 300 m from the high water mark. The filter holder containing the quartz fiber membrane filter is connected via tubing to the sampling pump, which was placed inside the building (close to the roof). Halfway the tubing connection we inserted a glass bottle to protect the pump against any liquid (i.e., condensation or potential rain intake).

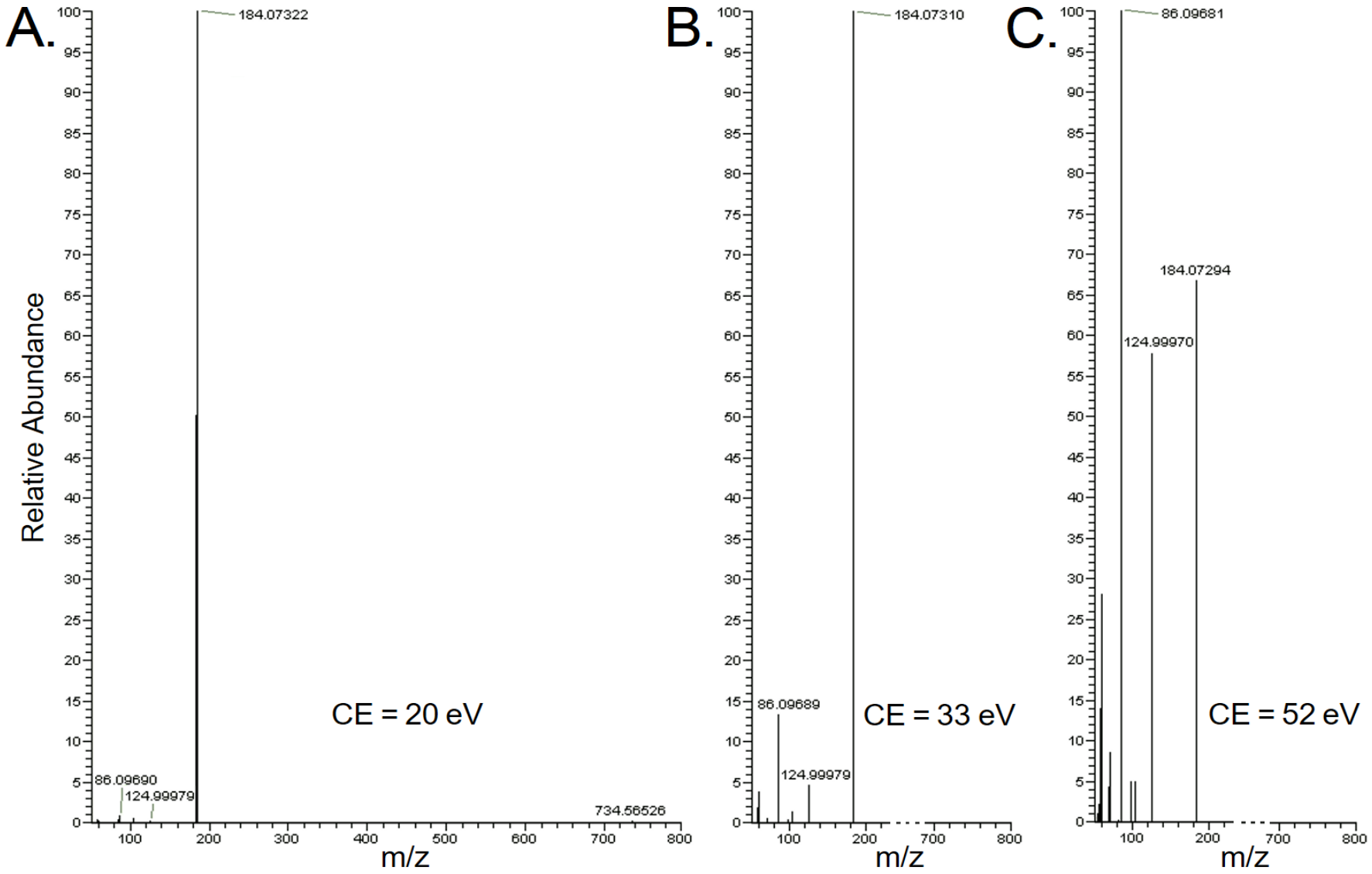

Figure S5.2: Fragmentation spectra of dipalmitoylphosphatidylcholine (DPPC) at different collision energies (CE). At the lowest CE the parent ion (m/z 734.56526) is still detectable.

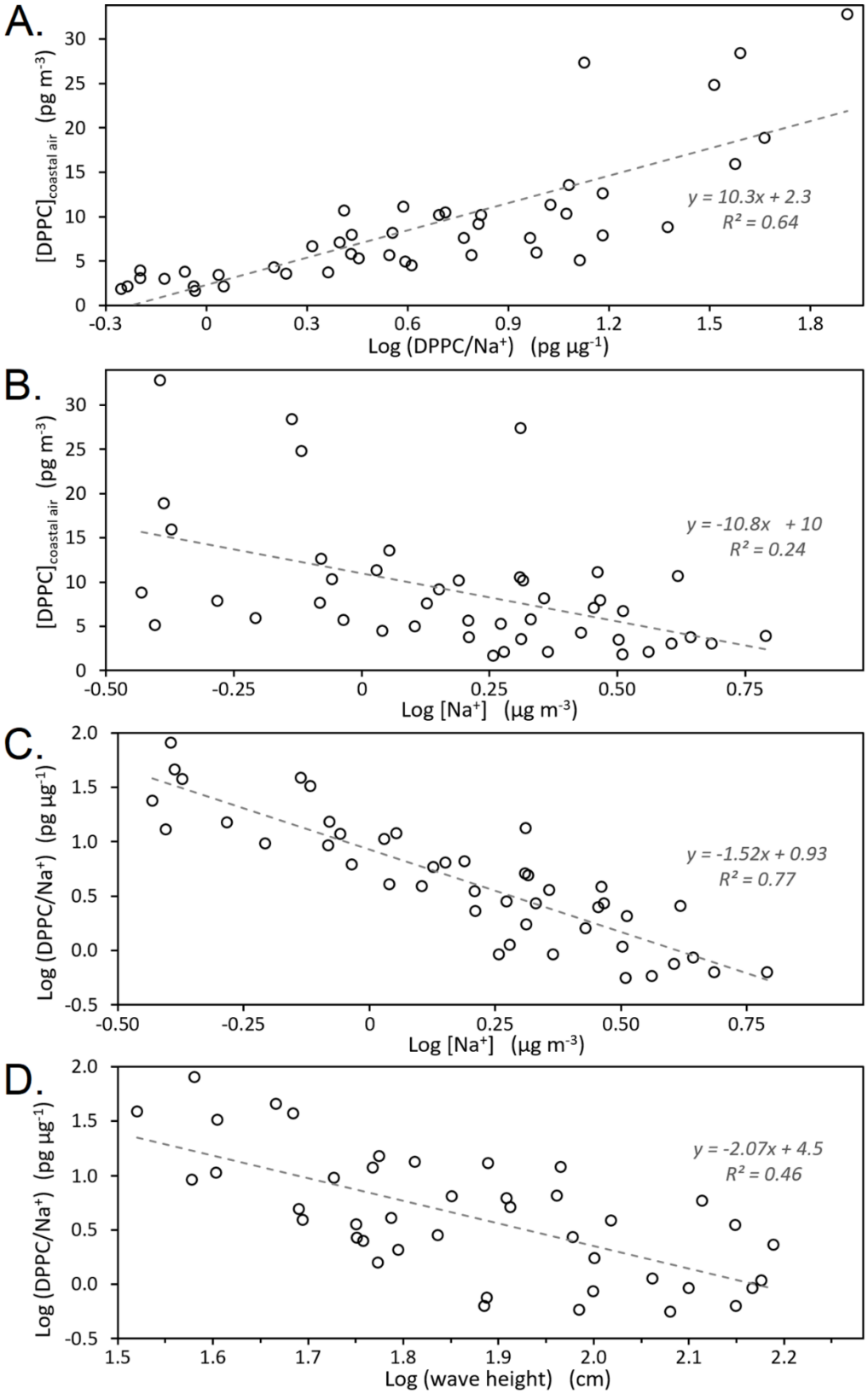

Figure S5.3: Significant correlations ($p<0.001$; 99.9% confidence level) between (A) the DPPC and (log-transformed) Na^+ concentrations ([DPPC], $[Na^+]$) of the sampled coastal air, (B) the $[DPPC]_{coastal\ air}$ and (log-transformed) DPPC/Na^+ ratio of the SSA samples, (C) the (log-transformed) DPPC/Na^+ ratio and (log-transformed) $[Na^+]_{coastal\ air}$, and (D) the (log-transformed) DPPC/Na^+ ratio and (log-transformed) $WH_{seawind}$. The gray dashed trendlines illustrate the linear regressions, of which the equations and coefficients of determination (R^2) are given.

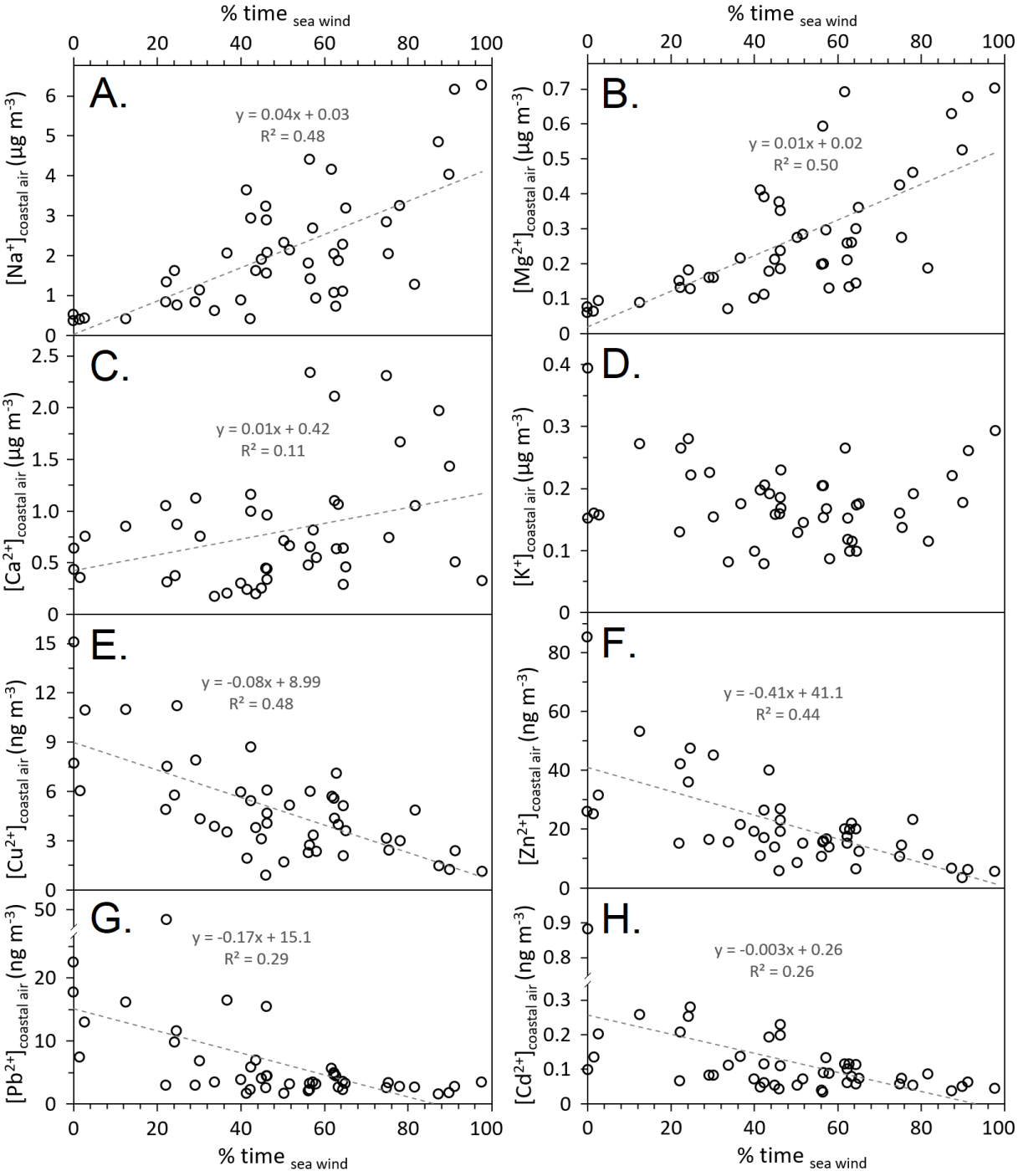

Figure S5.4: Sampled air concentrations of the diverse analyzed inorganic ions as a function of the % time with seawind. The gray (linear) trendlines illustrate the significant correlations between the two variables ($p<0.05$ for (C) and $p<0.001$ for (A), (B), (E), (F), (G), (H)). The equations and coefficients of determination (R^2) for these linear models are also given in the graphs.

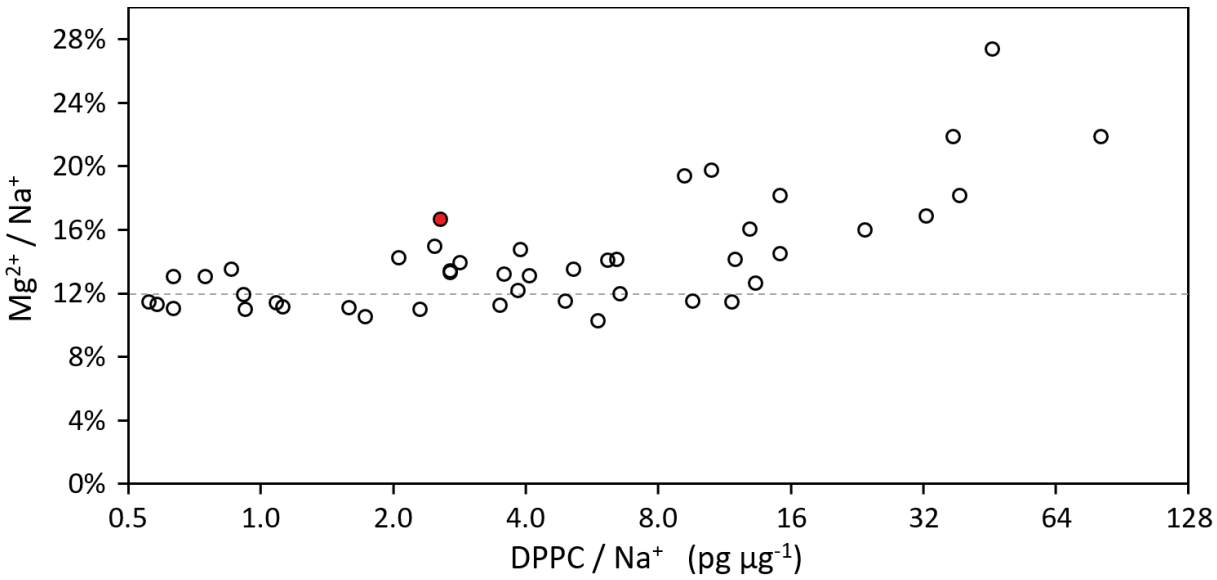

Figure S5.5: Mg^{2+}/Na^{+} ratio (µg µg^{-1}) as a function of the DPPC/Na^{+} ratio (DPPC SSA content) of the sampled SSAs. The red filled dot (●) indicates nearby construction works (i.e., dust production), and the dashed gray lines indicates the theoretical Mg^{2+}/Na^{+} mass ratio in seawater (11.9%).[205]

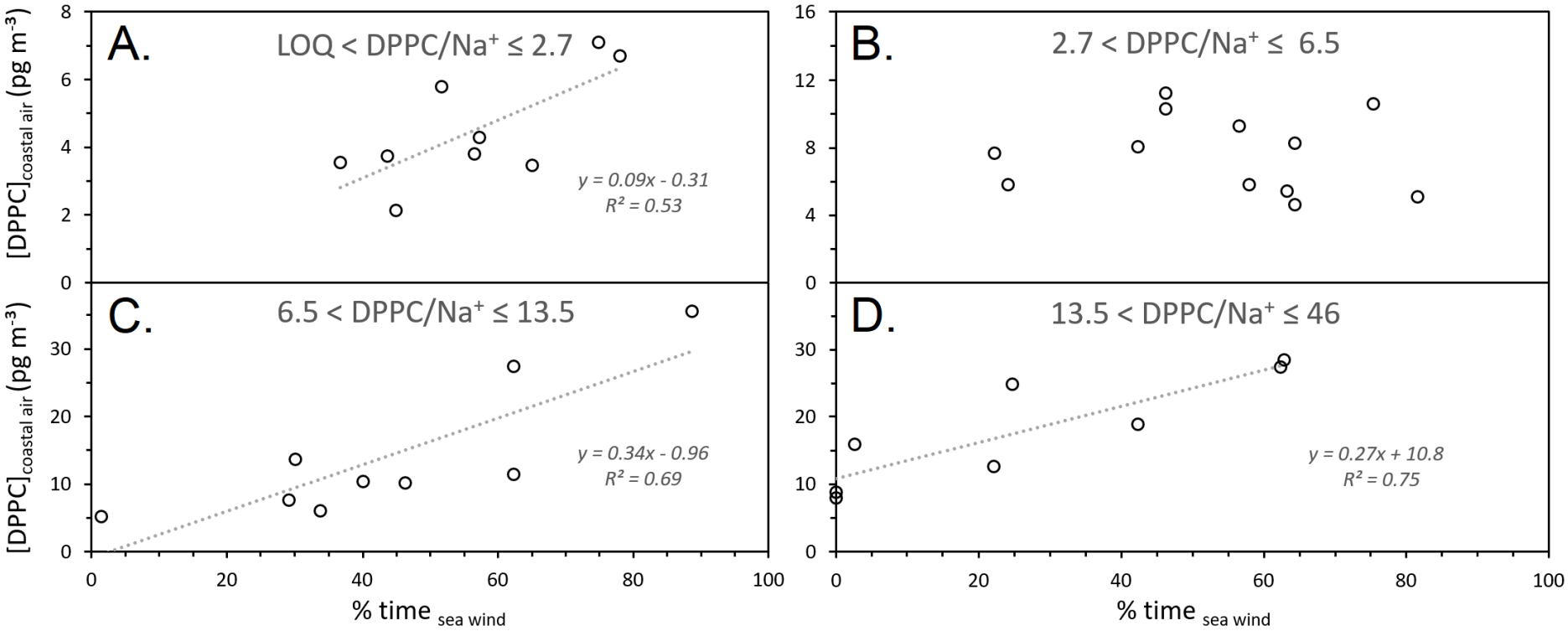

Figure S5.6: DPPC concentration of the sampled coastal air ($[DPPC]_{coastal\ air}$) as a function of the % time with seawind (Figure 5.1). Because the $[DPPC]_{coastal\ air}$ is largely dependent on the aerosol content ($DPPC/Na^+$; see Figures S5.3 and 5.2), we examined this relation in different classes of $DPPC/Na^+$, ranging over (A) ≤2.7, (B) 2.7 – 6.5, (C) 6.5 – 13.5, and (D) 13.5 – 46. The gray (linear) trendlines illustrate the significant positive correlations between the two variables ($p<0.05$; 95% confidence level). The equations and coefficients of determination (R^2) for the linear models are also given in the graphs.

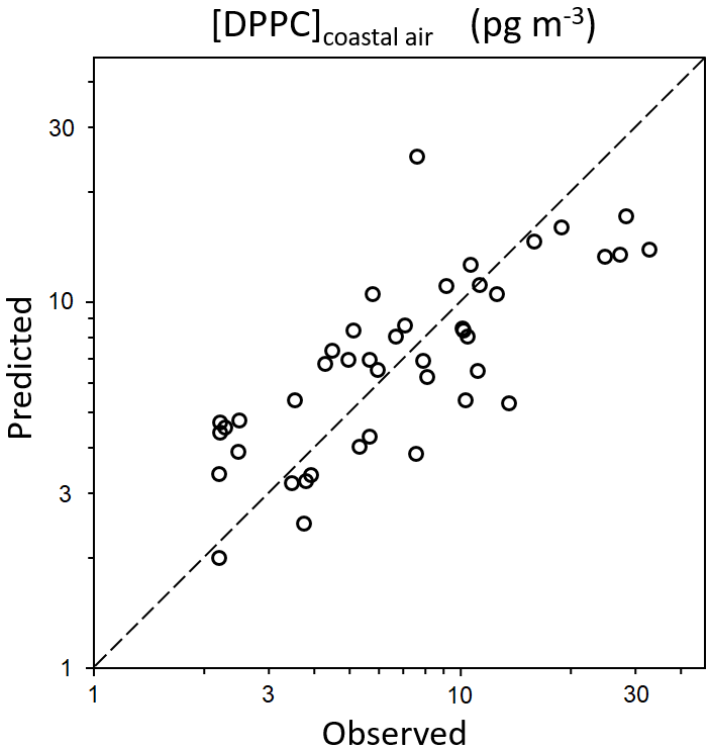

Figure S5.7: Scatter plot of the observed vs the predicted (modeled) values for the DPPC concentration of the sampled coastal air ($[DPPC]_{coastal\ air}$). The dashed line indicates the 1:1 line.

3 Supportive Tables

Table S5.1: Overview of the other 14 marine compounds that were screened in natural SSAs, next to DPPC. They were selected based on their bioactivity, potential occurrence in the North Sea, polarity (i.e., Kow), the availability of analytical reference material (RM), and low volatility. The latter was based on their molecular weight (Mw; g mol^{-1}), and Henry constant (H; atm m^3 mol^{-1}). Values for the log Kow, Mw and H originate from Pubchem and the US Environmental Protection Agency.

Compound	Elemental formula	Bioactivity	Biological source	log Kow	RM available	Mw	H
Cholesterol	$C_{27}H_{46}O$	Component of the human pulmonary surfactant.[270]	Red algae[27]	8.7	Yes	386.7	10^{-8}
Fucoxanthin	$C_{42}H_{58}O_6$	Antioxidant, anticancer, anti-inflammatory, anti-obese, antidiabetic, antimalarial.[333]	Brown algae, and diatoms.[333]	8.1	Yes	658.9	/
Violacein	$C_{20}H_{13}N_3O_3$	Antiviral, antibacterial, anti-tumor, antiparasitic, antiprotozoal.[334]	Bacteria[334]	1.9	Yes	343.3	/
Retinol (Vitamin A)	$C_{20}H_{30}O$	Antiaging of skin[335]	Cyanobacteria[336]	5.7	Yes	286.5	10^{-4}
Eicosapentaenoic acid (EPA)	$C_{20}H_{30}O_2$	Reduces among other cardiovascular disorders, and various mental illnesses.[115]	Fish/fishoil[115]	6.42	Yes	302.5	10^{-8}
Catechin	$C_{15}H_{14}O_6$	Antioxidant, anticancer, anti-inflammatory, antiviral.[337]	Macroalgae[337]	0.4	Yes	290.3	10^{-10}
Tetrabromo-hydroquinione	$C_6H_2Br_4O_2$	Anticancer[338]	Hemichordate (e.g. Phycodera flava laysanica)[339]	4	Yes	425.7	/

Table S5.1 (continued).

Compound	Elemental formula	Bioactivity	Biological source	log Kow	RM available	Mw	H
Ergosterol	$C_{28}H_{44}O$	Anticancer and antiproliferative.[340]	Green algae[341]	7.4	Yes	396.7	10^{-8}
2,4,6-Tribromo-phenol	$C_6H_3Br_3O$	Antibiotic.[339]	Marine worms (e.g. *Phoronopsis viridis*)[339]	4.4	Yes	330.8	10^{-7}
Phloroglucinol	$C_6H_6O_3$	*(Phloroglucinol is the basic structure of phlorotannins)* Antioxidant, anti-inflammatory, radioprotective, antibacterial.[342]	Brown algae[342]	0.2	Yes	126.1	10^{-8}
Prodigiosin	$C_{20}H_{25}N_3O$	Antibacterial, antifungal, antimalarial, antibiotic, anticancer, immunosuppressive. [343]	Bacteria[343]	4	Yes	323.4	/
Pheophorbide A	$C_{35}H_{36}N_4O_5$	Antimutagenic, antitumor.[344]	Green algae[344]	5.2	Yes	592.7	/
Fucosterol	$C_{29}H_{48}O$	Anticancer, antidiabetic, antioxidant, hepatoprotective, antihyperlipidemic, antifungal.[345]	Brown algae and diatoms[345]	8.9	Yes	412.7	/

Table S5.2: The limit of detection (LOD), limit of quantification (LOQ), and the background levels (in field blank samples; n=10) for the various analyzed major and minor inorganic ions. The filter content of the field blanks is reported as the mean content and standard deviation (n=10).

	Na^+ (µg)	Mg^{2+} (µg)	Ca^{2+} (µg)	K^+ (µg)	Cu^{2+} (ng)	Zn^{2+} (ng)	Pb^{2+} (ng)	Cd^{2+} (ng)
LOD (per filter)	0.9	0.45	0.45	0.9	60	15	75	9
LOQ (per filter)	3.0	1.5	1.5	3.0	150	60	240	30
Mean content field blanks	22 ± 8	0.48 ± 0.30	6.1 ± 3.6	< LOQ	< LOQ	383 ± 151	< LOD	< LOD

References

(1) Gianfaldoni, S.; Tchernev, G.; Wollina, U.; Roccia, M. G.; Fioranelli, M.; Gianfaldoni, R.; Lotti, T. History of the Baths and Thermal Medicine. **2017**, *5* (4), 566–568.
(2) Charlier, R. H.; Chaineux, M.-C. P. Health Tourism: Tool for Development: Thalassotherapy. In *Using today's scientific knowledge for the Black Sea area's development tomorrow: Proceedings of the IOI-BSOC Leadership Seminar*; Bologa, A. S., Ed.; Mamaia, Romania, 2000; pp 147–165.
(3) Tountas, Y. The Historical Origins of the Basic Concepts of Health Promotion and Education : The Role of Ancient Greek Philosophy and Medicine. **2009**, *24* (2), 185–192.
(4) Wormer, E. J. A taste for salt in the history of medicine http://www.tribunes.com/tribune/sel/worm.htm.
(5) Gotoh, H.; Takezawa, M.; Maeno, Y.; Maezawa, M. Current Status of Marine Leisure Activities in Japan. *WIT Trans. Ecol. Environ.* **2008**, *115*, 23–33.
(6) Casteur, G. Het Belgisch Zee Instituut Voor Orthopedie (BZIO) En de Familie Delcroix Dames. 2004, p 2.
(7) La Bonnardiere, J. Introduction à La Thalassothérapie, Montpellier, 1865.
(8) Verhaeghe, L. *Les Bain de Mer d'ostende, Leurs Effets Physiologiques et Thérapeutiques*; J. Elleboudt: Ostend, Belgium, 1843.
(9) Roubardi. Sur La Non-Existance de l'acide Hydrochlorique Ou d'hydrochlorated Dans l'atmosphere Près de La Mer Ou Sur La Mer Même. *Journ. de Pharm.* **1833**, *November*.
(10) Charlier, R. H.; Chaineux, M.-C. P. The Healing Sea: A Sustainable Coastal Ocean Resource: Thalassotherapy. *J. Coast. Res.* **2009**, *254* (254), 838–856.
(11) Moyers, J. L.; Duce, R. A. Gaseous and Particulate Iodine in the Marine Atmosphere. *J. Geophys. Res.* **1972**, *77* (27), 5330–5338.
(12) Saiz-Lopez, A.; Fernandez, R. P.; Ordóñez, C.; Kinnison, D. E.; Martín, J. C. G.; Lamarque, J. F.; Tilmes, S. Iodine Chemistry in the Troposphere and Its Effect on Ozone. *Atmos. Chem. Phys.* **2014**, *14* (23), 13119–13143.
(13) Zimmermann, M. B.; Jooste, P. L.; Pandav, C. S. Iodine-Deficiency Disorders. *Lancet* **2008**, *372* (9645), 1251–1262.
(14) Smyth, P. P. A.; Burns, R.; Huang, R. J.; Hoffman, T.; Mullan, K.; Graham, U.; Seitz, K.; Platt, U.; O'Dowd, C. Does Iodine Gas Released from Seaweed Contribute to Dietary Iodine Intake? *Environ. Geochem. Health* **2011**, *33* (4), 389–397.
(15) Woodcock, A. H. Note Concerning Human Respiratory Irritation Associated with High Concentrations of Plankton and Mass Mortality of Marine Organisms. *J. Mar. Res.* **1948**, *7*, 56–62.
(16) Glibert, P. M.; Anderson, D. M.; Gentien, P.; Granéli, E.; Sellner, K. G. The Global Complex Phenomena of Harmful Algal Blooms. *Oceanography* **2005**, *18* (2), 136–147.
(17) Fleming, L. E.; Kirkpatrick, B.; Backer, L. C.; Walsh, C. J.; Nierenberg, K.; Clark, J.; Reich, A.; Hollenbeck, J.; Benson, J.; Cheng, Y. S.; Naar, J.; Pierce, R.; Bourdelais, A. J.; Abraham, W. M.; Kirkpatrick, G.; Zaias, J.; Wanner, A.; Mendes, E.; Shalat, S.; Hoagland, P.; Stephan, W.; Bean, J.; Watkins, S.; Clarke, T.; Byrne, M.; Baden, D. G. Review of Florida Red Tide and Human Health Effects. *Harmful Algae* **2011**, *10* (2), 224–233.
(18) Taylor, H. F. Mortality of Fishes on the West Coast of Florida, Rep. U.S.A. *Commun. Fish. Doc. 848* **1917**, 24.

(19) Magaña, H. A.; Contreras, C.; Villareal, T. A. A Historical Assessment of Karenia Brevis in the Western Gulf of Mexico. *Harmful Algae* **2003**, *2* (3), 163–171.
(20) Pierce, R. H. Red Tide (Ptychodiscus Brevis) Toxin Aerosols: A Review. *Toxicon* **1986**, *24* (10), 955–965.
(21) Fleming, L. E.; Backer, L. C.; Baden, D. G. Overview of Aerosolized Florida Red Tide Toxins: Exposures and Effects. *Environ. Health Perspect.* **2005**, *113* (5), 618–620.
(22) Ciminiello, P.; Dell'aversano, C.; Iacovo, E. Dello; Fattorusso, E.; Forino, M.; Tartaglione, L.; Benedettini, G.; Onorari, M.; Serena, F.; Battocchi, C.; Casabianca, S.; Penna, A. First Finding of Ostreopsis Cf. Ovata Toxins in Marine Aerosols. *Environ. Sci. Technol.* **2014**, *48* (6), 3532–3540.
(23) Cheng, Y. S.; Zhou, Y.; Irvin, C. M.; Pierce, R. H.; Naar, J.; Backer, L. C.; Fleming, L. E.; Kirkpatrick, B.; Baden, D. G. Characterization of Marine Aerosol for Assessment of Human Exposure to Brevetoxins. *Environ. Health Perspect.* **2005**, *113* (5), 638–643.
(24) Pierce, R. H.; Henry, M. S.; Blum, P. C.; Hamel, S. L.; Kirkpatrick, B.; Cheng, Y. S.; Zhou, Y.; Irvin, C. M.; Naar, J.; Weidner, A.; Fleming, L. E.; Backer, L. C.; Baden, D. G. Brevetoxin Composition in Water and Marine Aerosol along a Florida Beach: Assessing Potential Human Exposure to Marine Biotoxins. *Harmful Algae* **2005**, *4* (6), 965–972.
(25) Medina-Pérez, N. I.; Osto, M. D.; Decesari, S.; Paglione, M.; Berdalet, E. Aerosol Toxins Emitted by Harmful Algal Blooms Susceptible to Complex Air − Sea Interactions. *Environ. Sci. Technol.* **2020**, *55* (1), 468–477.
(26) Arrieta, J. M.; Arnaud-Haond, S.; Duarte, C. M. What Lies underneath: Conserving the Oceans' Genetic Resources. *Proc. Natl. Acad. Sci. U. S. A.* **2010**, *107* (43), 18318–18324.
(27) Hamed, I.; Özogul, F.; Özogul, Y.; Regenstein, J. M. Marine Bioactive Compounds and Their Health Benefits: A Review. *Compr. Rev. Food Sci. Food Saf.* **2015**, *14* (4), 446–465.
(28) *UN Environment Programme 2007 Annual Report*; United Nations, 2007.
(29) Moore, M. N.; Owen, R.; Depledge, M. H. Scientific Challenges and Policy Needs. In *Marine Pollution and Human Health*; Hester, R. E., Harrison, R. M., Eds.; RSC Publishing, 2011; pp 128–163.
(30) Moore, M. N.; Depledge, M. H.; Fleming, L.; Hess, P.; Lees, D.; Leonard, P.; Madsen, L.; Owen, R.; Pirlet, H.; Seys, J.; Vasconcelos, V.; Viarengo, A. Oceans and Human Health (OHH): A European Perspective from the Marine Board of the European Science Foundation (Marine Board-ESF). *Microb. Ecol.* **2013**, *65* (4), 889–900.
(31) H2020 SOPHIE Consortium. *A Strategic Research Agenda for Oceans and Human Health in Europe. H2020 SOPHIE Project*; Ostend, Belgium, 2020.
(32) Brereton, F.; Clinch, J. P.; Ferreira, S. Happiness, Geography and the Environment. *Ecol. Econ.* **2008**, *65* (2), 386–396.
(33) Wheeler, B. W.; White, M.; Stahl-Timmins, W.; Depledge, M. H. Does Living by the Coast Improve Health and Wellbeing. *Heal. Place* **2012**, *18* (5), 1198–1201.
(34) White, M. P.; Pahl, S.; Ashbullby, K.; Herbert, S.; Depledge, M. H. Feelings of Restoration from Recent Nature Visits. *J. Environ. Psychol.* **2013**, *35*, 40–51.
(35) Hooyberg, A.; Roose, H.; Grellier, J.; Elliott, L. R.; Lonneville, B.; White, M. P.; Michels, N.; De Henauw, S.; Vandegehuchte, M.; Everaert, G. General Health and Residential Proximity to the Coast in Belgium: Results from a Cross-Sectional Health Survey. *Environ. Res.* **2020**, *184*, 1–10.

(36) White, M. P.; Elliott, L. R.; Grellier, J.; Economou, T.; Bell, S.; Bratman, G. N.; Cirach, M.; Gascon, M.; Lima, M. L. Associations between Green / Blue Spaces and Mental Health across 18 Countries. *Sci. Rep.* **2021**, 1–12.
(37) Plutchik, R. A Psychoevolutionary Theory of Emotions. *Soc. Sci. Inf.* **1982**, *21* (4–5), 529–553.
(38) Hartig, T.; Mitchell, R.; de Vries, S.; Frumkin, H. Nature and Health. *Annu. Rev. Public Health* **2014**, *35* (1), 207–228.
(39) Depledge, M. H.; Bird, W. J. The Blue Gym: Health and Wellbeing from Our Coasts. *Mar. Pollut. Bull.* **2009**, *58* (7), 947–948.
(40) Garrett, J. K.; Clitherow, T. J.; White, M. P.; Wheeler, B. W.; Fleming, L. E. Coastal Proximity and Mental Health among Urban Adults in England: The Moderating Effect of Household Income. *Heal. Place* **2019**, *59* (August), 102200.
(41) Bauman, A.; Smith, B.; Stoker, L.; Bellew, B.; Booth, M. Participation : Evidence of a ' Coastal Effect .' **1999**, *23* (3), 322–324.
(42) Witten, K.; Hiscock, R.; Pearce, J.; Blakely, T. Neighbourhood Access to Open Spaces and the Physical Activity of Residents: A National Study. *Prev. Med. (Baltim).* **2008**, *47* (3), 299–303.
(43) White, M. P.; Wheeler, B. W.; Herbert, S.; Alcock, I.; Depledge, M. H. Coastal Proximity and Physical Activity: Is the Coast an under-Appreciated Public Health Resource? *Prev. Med. (Baltim).* **2014**, *69*, 135–140.
(44) Pasanen, T. P.; White, M. P.; Wheeler, B. W.; Garrett, J. K.; Elliott, L. R. Neighbourhood Blue Space , Health and Wellbeing: The Mediating Role of Different Types of Physical Activity. *Environ. Int.* **2019**, *131* (July), 105016.
(45) Rook, G. A. Regulation of the Immune System by Biodiversity from the Natural Environment: An Ecosystem Service Essential to Health. *Proc Natl Acad Sci USA* **2013**, *110* (46), 18360–18367.
(46) Moore, M. N. Do Airborne Biogenic Chemicals Interact with the PI3K/Akt/MTOR Cell Signalling Pathway to Benefit Human Health and Wellbeing in Rural and Coastal Environments? *Environ. Res.* **2015**, *140*, 65–75.
(47) Rook, G. A. W.; Lowry, C. A.; Raison, C. L. Microbial "Old Friends", Immunoregulation and Stress Resilience. *Evol. Med. Public Heal.* **2013**, *2013* (1), 46–64.
(48) Després, V. R.; Alex Huffman, J.; Burrows, S. M.; Hoose, C.; Safatov, A. S.; Buryak, G.; Fröhlich-Nowoisky, J.; Elbert, W.; Andreae, M. O.; Pöschl, U.; Jaenicke, R. Primary Biological Aerosol Particles in the Atmosphere: A Review. *Tellus, Ser. B Chem. Phys. Meteorol.* **2012**, *64* (1), 1–57.
(49) Laplante, M.; Sabatini, D. M. MTOR Signaling in Growth Control and Disease. *Cell* **2012**, *149* (2), 274–293.
(50) Laplante, M.; Sabatini, D. M. An Emerging Role of MTOR in Lipid Biosynthesis. *Curr Biol.* **2009**, *19* (22), R1046–R1052.
(51) Liu, T.; Zhang, L.; Joo, D.; Sun, S. NF- KB Signaling in Inflammation. *Signal Transduct. Target. Ther.* **2017**, *2*.
(52) Sabatini, D. M. MTOR and Cancer: Insights into a Complex Relationship. *Nat. Rev. Cancer* **2006**, *6* (9), 729–734.
(53) Massel, S. R. *Ocean Waves Breaking and Marine Aerosol Fluxes*; Mysak, L., Hamilton, K., Eds.; Springer, 2007.
(54) Lu, S.; Ren, J.; Hao, X.; Liu, D.; Zhang, R.; Wu, M.; Yi, F.; Lin, J.; Shinich, Y.; Wang, Q. Characterization of Protein Expression of Platanus Pollen Following Exposure to Gaseous Pollutants and Vehicle Exhaust Particles. *Aerobiologia (Bologna).* **2014**, *30*, 281–291.

(55) Sedghy, F.; Varasteh, A.; Sankian, M.; Moghadam, M. Interaction Between Air Pollutants and Pollen Grains: The Role on the Rising Trend in Allergy. *Reports Biochem. Mol. Biol.* **2018**, *6* (2), 219–224.
(56) D'Amato, G.; Cecchi, L.; D'Amato, M.; Liccardi, G. Urban Air Pollution and Climate Change as Environmental Risk Factors of Respiratory Allergy: An Update. *J. Investig. Allergol. Clin. Immunol.* **2010**, *20* (2), 95–102.
(57) Okuyama, Y.; Matsumoto, K.; Okochi, H.; Igawa, M. Adsorption of Air Pollutants on the Grain Surface of Japanese Cedar Pollen. *Atmos. Environ.* **2007**, *41* (2), 253–260.
(58) Parnia, S.; Brown, J. L.; Frew, A. J. The Role of Pollutants in Allergic Sensitization and the Development of Asthma. *Allergy Eur. J. Allergy Clin. Immunol.* **2002**, *57* (12), 1111–1117.
(59) Veron, F. Ocean Spray. *Annu. Rev. Fluid Mech.* **2015**, *47*, 507–538.
(60) Andreae, M. O.; Rosenfeld, D. Aerosol-Cloud-Precipitation Interactions. Part 1. The Nature and Sources of Cloud-Active Aerosols. *Earth-Science Rev.* **2008**, *89* (1–2), 13–41.
(61) Saltzman, E. S. Marine Aerosols. *Geophys. Monogr. Ser.* **2009**, *187*, 17–35.
(62) Lewis, E. R.; Schwartz, S. E. *Sea Salt Aerosol Production: Mechanisms, Methods, Measurements and Models - A Critical Review*; American Geophysical Union: Washington, 2004.
(63) Deane, G. B.; Stokes, M. D. Scale Dependence of Bubble Creation Mechanisms in Breaking Waves. *Nature* **2002**, *418* (6900), 839–844.
(64) Mårtensson, E. M.; Nilsson, E. D.; de Leeuw, G.; Cohen, L. H.; Hansson, H.-C. Laboratory Simulations and Parameterization of the Primary Marine Aerosol Production. *J. Geophys. Res.* **2003**, *108*, 1–12.
(65) Blanchard, D. C.; Woodcock, A. H. Bubble Formation and Modification in the Sea and Its Meteorological Significance. *Tellus IX* **1957**, *9* (2), 145–158.
(66) Blanchard, D. C.; Keith, C. The Electrification of the Atmosphere by Particles from Bubbles in the Sea. *Prog. Oceanogr.* **1963**, 73–202.
(67) Richter, D. H.; Veron, F. Ocean Spray: An Outsized Influence on Weather and Climate. *Phys. Today* **2016**, *69* (11), 34–39.
(68) Monahan, E. C.; Fairall, C. W.; Davidson, K. L.; Boyle, P. J. Observed Inter-Relations between 10m Winds, Ocean Whitecaps and Marine Aerosols. *Q. J. R. Meteorol. Soc.* **1983**, *109* (460), 379–392.
(69) Grammatika, M.; Zimmerman, W. B. Microhydrodynamics of Flotation Processes in the Sea Surface Layer. *Dyn. Atmos. Ocean.* **2001**, *34* (2–4), 327–348.
(70) Kiger, K. T.; Duncan, J. H. Air-Entrainment Mechanisms in Plunging Jets and Breaking Waves. *Annu. Rev. Fluid Mech.* **2011**, *44* (December 2011), 563–596.
(71) Ardon-Dryer, K.; Huang, Y. W.; Cziczo, D. J. Laboratory Studies of Collection Efficiency of Sub-Micrometer Aerosol Particles by Cloud Droplets on a Single-Droplet Basis. *Atmos. Chem. Phys.* **2015**, *15* (16), 9159–9171.
(72) Leelőssy, Á.; Molnár, F.; Izsák, F.; Havasi, Á.; Lagzi, I.; Mészáros, R. Dispersion Modeling of Air Pollutants in the Atmosphere: A Review. *Cent. Eur. J. Geosci.* **2014**, *6* (3), 257–278.
(73) Jayarathne, T.; Sultana, C. M.; Lee, C.; Malfatti, F.; Cox, J. L.; Pendergraft, M. A.; Moore, K. A.; Azam, F.; Tivanski, A. V.; Cappa, C. D.; Bertram, T. H.; Grassian, V. H.; Prather, K. A.; Stone, E. A. Enrichment of Saccharides and Divalent Cations in Sea Spray Aerosol during Two Phytoplankton Blooms. *Environ. Sci. Technol.* **2016**, *50* (21), 11511–11520.

(74) Schwier, A. N.; Sellegri, K.; Mas, S.; Charrière, B.; Pey, J.; Rose, C.; Temime-roussel, B.; Jaffrezo, J.-L.; Parin, D.; Picard, D.; Ribeiro, M.; Roberts, G.; Sempéré, R.; Marchand, N.; D'Anna, B. Primary Marine Aerosol Physical Flux and Chemical Composition during a Nutrient Enrichment Experiment in Mesocosms in the Mediterranean Sea. *Atmos. Chem. Phys.* **2017**, *17*, 14645–14660.
(75) Witt, M. L. I.; Mather, T. A.; Baker, A. R.; De Hoog, J. C. M.; Pyle, D. M. Atmospheric Trace Metals over the South-West Indian Ocean: Total Gaseous Mercury, Aerosol Trace Metal Concentrations and Lead Isotope Ratios. *Mar. Chem.* **2010**, *121* (1–4), 2–16.
(76) Kuznetsova, M.; Lee, C.; Aller, J. Characterization of the Proteinaceous Matter in Marine Aerosols. *Mar. Chem.* **2005**, *96*, 359–377.
(77) Kuznetsova, M.; Lee, C.; Aller, J.; Frew, N. Enrichment of Amino Acids in the Sea Surface Microlayer at Coastal and Open Ocean Sites in the North Atlantic Ocean. *Limnol. Oceanogr.* **2004**, *49* (5), 1605–1619.
(78) Barbier, M.; D., T.; Marty, J. C.; Saliot, A. Sterols in Aerosols, Surface Microlayer and Subsurface Water in the North-Eastern Tropical Atlantic. *Oceanol. Acta* **1981**, *4* (1), 77–84.
(79) Marty, J. C.; Saliot, A.; Buat-Ménard, P.; Chesselet, R.; Hunter, K. A. Relationship between the Lipid Compositions of Marine Aerosols, the Sea Surface Microlayer, and Subsurface Water. *J. Geophys. Res.* **1979**, *84*, 5707–5716.
(80) Lewandowska, A. U.; Śliwinska-Wilczewska, S.; Wozniczka, D. Identification of Cyanobacteria and Microalgae in Aerosols of Various Sizes in the Air over the Southern Baltic Sea. *Mar. Pollut. Bull. J.* **2017**, *125*, 30–38.
(81) Genitsaris, S.; Kormas, K. A.; Moustaka-Gouni, M. Airborne Algae and Cyanobacteria: Occurrence and Related Health Effects. *Front. Biosci.* **2011**, *3* (2), 772–787.
(82) Després, V. R.; Huffman, J. A.; Burrows, S. M.; Hoose, C.; Safatov, A. S.; Buryak, G.; Fröhlich-Nowoisky, J.; Elbert, W.; Andreae, M. O.; Pöschl, U.; Jaenicke, R. Primary Biological Aerosol Particles in the Atmosphere: A Review. *Tellus Ser. B Chem. Phys. Meteorol.* **2012**, *64*, 1–58.
(83) Rastelli, E.; Corinaldesi, C.; Dell'anno, A.; Lo Martire, M.; Greco, S.; Cristina Facchini, M.; Rinaldi, M.; O'Dowd, C.; Ceburnis, D.; Danovaro, R. Transfer of Labile Organic Matter and Microbes from the Ocean Surface to the Marine Aerosol: An Experimental Approach. *Sci. Rep.* **2017**, *7* (1), 1–10.
(84) Lee, C.; Sultana, C. M.; Collins, D. B.; Santander, M. V.; Axson, J. L.; Malfatti, F.; Cornwell, G. C.; Grandquist, J. R.; Deane, G. B.; Stokes, M. D.; Azam, F.; Grassian, V. H.; Prather, K. A. Advancing Model Systems for Fundamental Laboratory Studies of Sea Spray Aerosol Using the Microbial Loop. *J. Phys. Chem. A* **2015**, *119* (33), 8860–8870.
(85) Quinn, J. A.; Steinbrook, R. A.; Anderson, J. L. Breaking Bubbles and the Water-to-Air Transport of Particulate Matter. *Chem. Eng. Sci.* **1975**, *30* (9), 1177–1184.
(86) Aller, J. Y.; Kuznetsova, M. R.; Jahns, C. J.; Kemp, P. F. The Sea Surface Microlayer as a Source of Viral and Bacterial Enrichment in Marine Aerosols. *J. Aerosol Sci.* **2005**, *36* (5–6), 801–812.
(87) Quinn, P. K.; Collins, D. B.; Grassian, V. H.; Prather, K. A.; Bates, T. S. Chemistry and Related Properties of Freshly Emitted Sea Spray Aerosol. *Chem. Rev.* **2015**, *115* (10), 4383–4399.

(88) Burrows, S. M.; Ogunro, O.; Frossard, A. A.; Russell, L. M.; Rasch, P. J.; Elliott, S. M. A Physically Based Framework for Modeling the Organic Fractionation of Sea Spray Aerosol from Bubble Film Langmuir Equilibria. *Atmos. Chem. Phys.* **2014**, *14* (24), 13601–13629.
(89) Hardy, J. T. The Sea Surface Microlayer: Biology, Chemistry and Anthropogenic Enrichment. *Prog. Oceanogr.* **1982**, *11* (4), 307–328.
(90) Stokes, M. D.; Deane, G. B.; Prather, K.; Bertram, T. H.; Ruppel, M. J.; Ryder, O. S.; Brady, J. M.; Zhao, D. A Marine Aerosol Reference Tank System as a Breaking Wave Analogue for the Production of Foam and Sea-Spray Aerosols. *Atmos. Meas. Tech.* **2013**, *6* (4), 1085–1094.
(91) King, S. M.; Butcher, A. C.; Rosenoern, T.; Coz, E.; Lieke, K. I.; De Leeuw, G.; Nilsson, E. D.; Bilde, M. Investigating Primary Marine Aerosol Properties: CCN Activity of Sea Salt and Mixed Inorganic-Organic Particles. *Environ. Sci. Technol.* **2012**, *46* (19), 10405–10412.
(92) Keene, W. C.; Maring, H.; Maben, J. R.; Kieber, D. J.; Pszenny, A. A. P.; Dahl, E. E.; Izaguirre, M. A.; Davis, A. J.; Long, M. S.; Zhou, X.; Smoydzin, L.; Sander, R. Chemical and Physical Characteristics of Nascent Aerosols Produced by Bursting Bubbles at a Model Air-Sea Interface. *J. Geophys. Res. Atmos.* **2007**, *112* (21), 1–16.
(93) Callaghan, A. H.; Stokes, M. D.; Deane, G. B. The Effect of Water Temperature on Air Entrainment, Bubble Plumes, and Surface Foam in a Laboratory Breaking-Wave Analog. *J. Geophys. Res. Atmos.* **2014**, *119*, 7463–7482.
(94) TSI Incorporated. Instruction Manual Model 3076 Constant Output Atomizer. 2005, p 63.
(95) Sellegri, K.; O'Dowd, C. D.; Yoon, Y. J.; Jennings, S. G.; de Leeuw, G. Surfactants and Submicron Sea Spray Generation. *J. Geophys. Res. Atmos.* **2006**, *111* (22), 1–12.
(96) Fuentes, E.; Coe, H.; Green, D.; McFiggans, G. Laboratory-Generated Primary Marine Aerosol via Bubble-Bursting and Atomization. *Atmos. Meas. Tech. Discuss.* **2010**, *3*, 141–162.
(97) Guaadaoui, A.; Benaicha, S.; Elmajdoub, N.; Bellaoui, M.; Hamal, A. What Is a Bioactive Compound? A Combined Definition for a Preliminary Consensus. *Int. J. Food Sci. Nutr.* **2014**, *3* (3), 17–179.
(98) Martins, A.; Vieira, H.; Gaspar, H.; Santos, S. Marketed Marine Natural Products in the Pharmaceutical and Cosmeceutical Industries: Tips for Success. *Mar. Drugs* **2014**, *12* (2), 1066–1101.
(99) Vignesh, S.; Raja, A.; Arthur James, R. Marine Drugs: Implications and Future Studies. *Int. J. Pharmacol.* **2011**, *7*, 22–30.
(100) Blunt, J. W.; Copp, B. R.; Keyzers, R. A.; Munro, M. H. G.; Prinsep, M. R. Marine Natural Products. *Nat. Prod. Rep.* **2015**, *32* (2), 116–211.
(101) Wiens, J. J. Faster Diversification on Land than Sea Helps Explain Global Biodiversity Patterns among Habitats and Animal Phyla. *Ecol. Lett.* **2015**, *18* (11), 1234–1241.
(102) Farmilo, C. G.; Rhodes, H. L. J.; Hart, H. R. L.; Taylor, H. Detection of Morphine in Papaver Setigerum DC. *Bull. Narcotics* **1953**, *1*, 26–31.
(103) Fleming, A. On the Antibacterial Action of Cultures of a Penicillium, with Special Reference to Their Use in the Isolation of B. Influenzæ. *Br. J. Exp. Pathol.* **1929**, *10* (3), 226–236.
(104) Fenical, W. New Pharmaceuticals from Marine Organisms. *Trends Biotechnol.* **1997**, *15* (9), 339–341.

(105) Blasiak, R.; Jouffray, J. B.; Wabnitz, C. C. C.; Österblom, H. Scientists Should Disclose Origin in Marine Gene Patents. *Trends Ecol. Evol.* **2019**, *34* (5), 392–395.
(106) Gerwick, W. The Ocean, a Reservoir of Active Bio-Molecules. Internation Symposium on Human Health & the Ocean in a Changing World; Monaco, 2020.
(107) Newman, D. J.; Cragg, G. M. Drugs and Drug Candidates from Marine Sources: An Assessment of the Current “State of Play.” *Planta Med.* **2016**, *82* (9–10), 775–789.
(108) Jaspars, M.; De Pascale, D.; Andersen, J. H.; Reyes, F.; Crawford, A. D.; Ianora, A. The Marine Biodiscovery Pipeline and Ocean Medicines of Tomorrow. *J. Mar. Biol. Assoc. United Kingdom* **2016**, *96* (1), 151–158.
(109) Yan, Y.; Liu, N.; Tang, Y. Recent Developments in Self-Resistance Gene Directed Natural Product Discovery. *Nat. Prod. Rep.* **2020**, *37* (7), 879–892.
(110) Nützmann, H. W.; Huang, A.; Osbourn, A. Plant Metabolic Clusters – from Genetics to Genomics. *New Phytol.* **2016**, *211* (3), 771–789.
(111) UN Environment Programme. The Nagoya Protocol.
(112) Blasiak, R.; Jouffray, J. B.; Wabnitz, C. C. C.; Sundström, E.; Osterblom, H. Corporate Control and Global Governance of Marine Genetic Resources. *Sci. Adv.* **2018**, *4* (6).
(113) Cremers, K.; Wright, G.; Rochette, J. UN discussions on marine genetic resources shape the future of marine biotechnology https://www.iddri.org/en/publications-and-events/blog-post/un-discussions-marine-genetic-resources-shape-future-marine.
(114) United Nations. *Draft Text of an Agreement under the United Nations Convention on the Law of the Sea on the Conservation and Sustainable Use of Marine Biological Diversity of Areas beyond National Jurisdiction*; New York, 2019.
(115) Shahidi, F.; Ambigaipalan, P. Omega-3 Polyunsaturated Fatty Acids and Their Health Benefits. *Annu. Rev. ofFood Sci. Technol.* **2018**, *9*, 345–381.
(116) Aung, T.; Halsey, J.; Kromhout, D.; Gerstein, H. C.; Marchioli, R.; Tavazzi, L.; Geleijnse, J. M.; Rauch, B.; Ness, A.; Galan, P.; Chew, E. Y.; Bosch, J.; Collins, R.; Lewington, S.; Armitage, J.; Clarke, R. Associations of Omega-3 Fatty Acid Supplement Use with Cardiovascular Disease Risks Meta-Analysis of 10 Trials Involving 77 917 Individuals. *JAMA Cardiol.* **2018**, *3* (3), 225–234.
(117) Rizos, E. C.; Elisaf, M. S. Does Supplementation with Omega-3 PUFAs Add to the Prevention of Cardiovascular Disease? *Curr. Cardiol. Rep.* **2017**, *19* (6).
(118) Mozaffarian, D.; Rimm, E. B. Fish Intake, Contaminants, and Human Health. *Clin. Rev.* **2020**, *296* (15), 1885–1900.
(119) Hallegraeff, G. M.; Anderson, D. M.; Cembella, A. D. *Manual on Harmful Marine Microalgae*; UNESCO: Paris, France, 2003.
(120) Botana, L. M. *Seafood and Freshwater Toxins: Pharmacology, Physiology and Detection*; Marcel Dekker: New York - Basel, 2000.
(121) Van Dolah, F. M. Marine Algal Toxins: Origins, Health Effects, and Their Increased Occurrence. *Environ. Health Perspect.* **2000**, *108*, 133–141.
(122) Hallegraeff, G. M. A Review of Harmful Algal Blooms and Their Apparent Global Increase. *Phycologia* **1993**, *32* (2), 79–99.
(123) Heisler, J.; Glibert, P. M.; Burkholder, J. M.; Anderson, D. M.; Cochlan, W.; Dennison, W. C.; Dortch, Q.; Gobler, C. J.; Heil, C. A.; Humphries, E.; Lewitus, A.; Magnien, R.; Marshall, H. G.; Sellner, K.; Stockwell, D. A.; Stoecker, D. K.; Suddleson, M. Eutrophication and Harmful Algal Blooms: A Scientific Consensus. *Harmful Algae* **2008**, *8*, 3–13.

(124) FAO. *The State of World Fisheries and Aquaculture*; Food and Agriculture Organization of the United Nations: Rome, 2016.
(125) Anderson, D. M.; Cembella, A. D.; Hallegraeff, G. M. Progress in Understanding Harmful Algal Blooms: Paradigm Shifts and New Technologies for Research, Monitoring, and Management. *Annu. Rev. Mar. Sci* **2012**, *4*, 143–176.
(126) Smayda, T. J. Reflections on the Ballast Water Dispersal-Harmful Algal Bloom Paradigm. *Harmful Algae* **2007**, *6*, 601–622.
(127) Anderson, D. M.; Glibert, P. M.; Burkholder, J. M. Harmful Algal Blooms and Eutrophication: Nutrient Sources, Composition, and Consequences. *Estuaries* **2002**, *25* (4), 704–726.
(128) Davidson, K.; Gowen, R. J.; Harrison, P. J.; Fleming, L. E.; Hoagland, P.; Moschonas, G. Anthropogenic Nutrients and Harmful Algae in Coastal Waters. *J. Environ. Manage.* **2014**, *146*, 206–216.
(129) Hallegraeff, G.; Enevoldsen, H.; Zingone, A. Global Harmful Algal Bloom Status Reporting. *Harmful Algae* **2021**, *102*.
(130) Wells, M. L.; Trainer, V. L.; Smayda, T. J.; Karlson, B. S. O.; Trick, C. G.; Kudela, R. M.; Ishikawa, A.; Bernard, S.; Wulff, A.; Anderson, D. M.; Cochlan, W. P. Harmful Algal Blooms and Climate Change: Learning from the Past and Present to Forecast the Future. *Harmful Algae* **2015**, *49*, 68–93.
(131) Zendong, Z.; McCarron, P.; Herrenknecht, C.; Sibat, M.; Amzil, Z.; Cole, R. B.; Hess, P. High Resolution Mass Spectrometry for Quantitative Analysis and Untargeted Screening of Algal Toxins in Mussels and Passive Samplers. *J. Chromatogr. A* **2015**, *1416*, 10–21.
(132) Orellana, G.; Van Meulebroek, L.; Van Vooren, S.; De Rijcke, M.; Vandegehuchte, M.; Janssen, C. R.; Vanhaecke, L. Quantification and Profiling of Lipophilic Marine Toxins in Microalgae by UHPLC Coupled to High-Resolution Orbitrap Mass Spectrometry. *Anal. Bioanal. Chem.* **2015**, *407* (21), 6345–6356.
(133) Orellana, G.; Vanden Bussche, J.; Van Meulebroek, L.; Vandegehuchte, M.; Janssen, C.; Vanhaecke, L. Validation of a Confirmatory Method for Lipophilic Marine Toxins in Shellfish Using UHPLC-HR-Orbitrap MS. *Anal. Bioanal. Chem.* **2014**, *406* (22), 5303–5312.
(134) Rubies, A.; Munoz, E.; Gibert, D.; Cortés-Francisco, N.; Granados, M.; Caixach, J.; Centrich, F. New Method for the Analysis of Lipophilic Marine Biotoxins in Fresh and Canned Bivalves by Liquid Chromatography Coupled to High Resolution Mass Spectrometry: A Quick, Easy, Cheap, Efficient, Rugged, Safe Approach. *J. Chromatogr. A* **2015**, *1386* (853), 62–73.
(135) Panda, D.; Dash, B. P.; Manickam, S.; Boczkaj, G. Recent Advancements in LC-MS Based Analysis of Biotoxins: Present and Future Challenges. *Mass Spectrom. Rev.* **2021**, No. October 2020, 1–38.
(136) Kirkpatrick, B.; Fleming, L. E.; Squicciarini, D.; Backer, L. C.; Clark, R.; Abraham, W.; Benson, J.; Cheng, Y. S.; Johnson, D.; Pierce, R.; Zaias, J.; Bossart, G. D.; Baden, D. G. Literature Review of Florida Red Tide: Implications for Human Health Effects. *Harmful Algae* **2004**, *3* (2), 99–115.
(137) Pierce, R. H.; Henry, M. S.; Blum, P. C.; Hamel, S. L.; Kirkpatrick, B.; Cheng, Y. S.; Zhou, Y.; Irvin, C. M.; Naar, J.; Weidner, A.; Fleming, L. E.; Backer, L. C.; Baden, D. G. Brevetoxin Composition in Water and Marine Aerosol along a Florida Beach: Assessing Potential Human Exposure to Marine Biotoxins. *Harmful Algae* **2005**, *4* (6), 965–972.

(138) Vila, M.; Abós-Herràndiz, R.; Isern-Fontanet, J.; Àlvarez, J.; Berdalet, E. Establishing the Link between Ostreopsis Cf. Ovata Blooms and Human Health Impacts Using Ecology and Epidemiology. *Sci. Mar.* **2016**, *80*, 107–115.
(139) Tubaro, A.; Durando, P.; Del Favero, G.; Ansaldi, F.; Icardi, G.; Deeds, J. R.; Sosa, S. Case Definitions for Human Poisonings Postulated to Palytoxins Exposure. *Toxicon* **2011**, *57* (3), 478–495.
(140) Landsberg, J. H. The Effects of Harmful Algal Blooms on Aquatic Organisms. *Fish. Sci.* **2002**, *10* (2), 113–390.
(141) Vanucci, S.; Guerrini, F.; Milandri, A.; Pistocchi, R. Effects of Different Levels of N- and P-Deficiency on Cell Yield, Okadaic Acid, DTX-1, Protein and Carbohydrate Dynamics in the Benthic Dinoflagellate Prorocentrum Lima. *Harmful Algae* **2010**, *9* (6), 590–599.
(142) Paz, B.; Riobó, P.; Ramilo, I.; Franco, J. M. Yessotoxins Profile in Strains of Protoceratium Reticulatum from Spain and USA. *Toxicon* **2007**, *50*, 1–17.
(143) Riccardi, M.; Guerrini, F.; Roncarati, F.; Milandri, A.; Cangini, M.; Pigozzi, S.; Riccardi, E.; Ceredi, A.; Ciminiello, P.; Dell'Aversano, C.; Fattorusso, E.; Forino, M.; Tartaglione, L.; Pistocchi, R. Gonyaulax Spinifera from the Adriatic Sea: Toxin Production and Phylogenetic Analysis. *Harmful Algae* **2009**, *8* (2), 279–290.
(144) Pierce, R. H.; Henry, M. S.; Blum, P. C.; Lyons, J.; Cheng, Y. S.; Yazzie, D.; Zhou, Y. Brevetoxin Concentrations in Marine Aerosol: Human Exposure Levels During a Karenia Brevis Harmful Algal Bloom. *Bull. Environ. Contam. Toxicol.* **2003**, *70* (1), 161–165.
(145) Alfonso, A.; Vieytes, M.; Botana, L. Yessotoxin, a Promising Therapeutic Tool. *Mar. Drugs* **2016**, *14* (2), 1–14.
(146) Botana, L. M.; Vilariño, N.; Alfonso, A.; Vale, C.; Louzao, C.; Elliott, C. T.; Campbell, K.; Botana, A. M. The Problem of Toxicity Equivalent Factors in Developing Alternative Methods to Animal Bioassays for Marine-Toxin Detection. *TrAC - Trends Anal. Chem.* **2010**, *29* (11), 1316–1325.
(147) De Rijcke, M. The Current and Future Risk of Harmful Algal Blooms in the North Sea, 2017.
(148) Minns, A. B.; Matteucci, M. J.; Ly, B. T.; Clark, R. F. Seafood Toxidromes https://aneskey.com/seafood-toxidromes/.
(149) Gopalakrishnakone, P.; Haddad, V. J.; Tubaro, A.; Kim, E.; Kem, W. R. *Marine and Freshwater Toxins*; 2016; Vol. 89.
(150) Guéret, S. M.; Brimble, M. A. Spiroimine Shellfish Poisoning (SSP) and the Spirolide Family of Shellfish Toxins: Isolation, Structure, Biological Activity and Synthesis. *Nat. Prod. Rep.* **2010**, *27* (9), 1350–1366.
(151) Orellana, G.; Van Meulebroek, L.; De Rijcke, M.; Janssen, C. R.; Vanhaecke, L. High Resolution Mass Spectrometry-Based Screening Reveals Lipophilic Toxins in Multiple Trophic Levels from the North Sea. *Harmful Algae* **2017**, *64*, 30–41.
(152) Persson, M.; Karlson, B.; Zuberovic Muratovic, A.; Simonsson, M.; Bergkvist, P.; Renborg, E. *Kontrollprogrammet För Tvåskaliga Blötdjur, Årsrapport 2014-2019*; Uppsala, 2020.
(153) van der Fels-Klerx, H. J.; Adamse, P.; Goedhart, P. W.; Poelman, M.; Pol-Hofstad, I. E.; van Egmond, H.; Gerssen, A. Monitoring Phytoplankton and Marine Biotoxins in Production Waters of the Netherlands: Results after One Decade. *Food Addit. Contam. Part A* **2012**, *29* (10), 1616–1629.

(154) Krock, B.; Tillmann, U.; John, U.; Cembella, A. D. Characterization of Azaspiracids in Plankton Size-Fractions and Isolation of an Azaspiracid-Producing Dinoflagellate from the North Sea. *Harmful Algae* **2009**, *8* (2), 254–263.
(155) Delegrange, A.; Lefebvre, A.; Gohin, F.; Courcot, L.; Vincent, D. Pseudo-Nitzschia Sp. Diversity and Seasonality in the Southern North Sea, Domoic Acid Levels and Associated Phytoplankton Communities. *Estuar. Coast. Shelf Sci.* **2018**, *214* (April), 194–206.
(156) Cheng, Y. S.; McDonald, J. D.; Kracko, D.; Irvin, C. M.; Zhou, Y.; Pierce, R. H.; Henry, M. S.; Bourdelaisa, A.; Naar, J.; Baden, D. G. Concentration and Particle Size of Airborne Toxic Algae (Brevetoxin) Derived from Ocean Red Tide Events. *Environ. Sci. Technol.* **2005**, *39* (10), 3443–3449.
(157) Riquelme, G.; Sepúlveda, J. M.; Al Ghumgham, Z.; del Campo, M.; Montero, C.; Lagos, N. Neosaxitoxin, a Paralytic Shellfish Poison Toxin, Effectively Manages Bucked Shins Pain, as a Local Long-Acting Pain Blocker in an Equine Model. *Toxicon* **2018**, *141*, 15–17.
(158) Lucchetta, M.; Monaco, G.; Valenzi, V.; Russo, M.; Campanella, J.; Nocchi, S.; Mennuni, G.; Fraioli, A. The Historical-Scientific Foundations of Thalassotherapy: State of the Art. *Clin. Ther.* **2007**, *158* (6), 533–541.
(159) Korets, S. B.; Musa, F.; Curtin, J.; Blank, S. V.; Schneider, R. J. Dual MTORC1/2 Inhibition in a Preclinical Xenograft Tumor Model of Endometrial Cancer. *Gynecol. Oncol.* **2014**, *132* (2), 468–473.
(160) Walsh, C. J.; Leggett, S. R.; Strohbehn, K.; Pierce, R. H.; Sleasman, J. W. Effects of in Vitro Brevetoxin Exposure on Apoptosis and Cellular Metabolism in a Leukemic T Cell Line (Jurkat). *Mar. Drugs* **2008**, *6*, 291–307.
(161) Wang, R.; Lv, L.; Zhao, Y.; Yang, N. Okadaic Acid Inhibits Cell Multiplication and Induces Apoptosis in A549 Cells, a Human Lung Adenocarcinoma Cell Line. *Int. J. Clin. Exp. Med.* **2014**, *7* (8), 2025–2030.
(162) Botana, L. M.; Alfonso, A.; Vale, C.; Vilarino, N.; Rubiolo, J.; Alonso, E.; Cagide, E. The Mechanistic Complexities of Phycotoxins: Toxicology of Azaspiracids and Yessotoxins. In *Advances in Molecular Toxicology Volume 8*; Fishbein, J. C., Heilman, J. M., Eds.; Elsevier: Amsterdam, 2014; pp 1–33.
(163) Alexander, J.; Benford, D.; Boobis, A.; Ceccatelli, S.; Cravedi, J.; Di Domenico, A.; Doerge, D.; Dogliotti, E.; Edler, L.; Farmer, P.; Fink-gremmels, J.; Fürst, P.; Guerin, T.; Knutsen, H. K.; Livesey, C.; Machala, M.; Mutti, A.; Schlatter, J.; van Leeuwen, R. Marine Biotoxins in Shellfish - Yessotoxin Group. *EFSA J.* **2008**, 1–61.
(164) Rubiolo, J. A.; López-Alonso, H.; Martínez, P.; Millán, A.; Cagide, E.; Vieytes, M. R.; Vega, F. V.; Botana, L. M. Yessotoxin Induces ER-Stress Followed by Autophagic Cell Death in Glioma Cells Mediated by MTOR and BNIP3. *Cell. Signal.* **2014**, *26* (2), 419–432.
(165) Ikenoue, T.; Hong, S.; Inoki, K. *Chapter 11 Monitoring Mammalian Target of Rapamycin (MTOR) Activity*, 1st ed.; Elsevier Inc., 2009; Vol. 451.
(166) O'Reilly, K. E.; Rojo, F.; She, Q.; Solit, D.; Mills, G. B.; Smith, D.; Lane, H.; Hofmann, F.; Hicklin, D. J.; Ludwig, D. L.; Baselga, J.; Rosen, N. MTOR Inhibition Induces Upstream Receptor Tyrosine Kinase Signaling and Activates Akt. *Cancer Res.* **2006**, *66* (3), 1500–1508.

(167) Carracedo, A.; Ma, L.; Teruya-feldstein, J.; Rojo, F.; Salmena, L.; Alimonti, A.; Egia, A.; Sasaki, A. T.; Thomas, G.; Kozma, S. C.; Papa, A.; Nardella, C.; Cantley, L. C.; Baselga, J.; Pandolfi, P. P. Inhibition of MTORC1 Leads to MAPK Pathway Activation through a PI3K-Dependent Feedback Loop in Human Cancer. *J. Clin. Invest.* **2008**, *118* (9), 3065–3074.
(168) Pierce, R. H.; Henry, M. S.; Blum, P. C.; Lyons, J.; Cheng, Y. S.; Yazzie, D.; Zhou, Y. Brevetoxin Concentrations in Marine Aerosol: Human Exposure Levels during a Karenia Brevis Harmful Algal Bloom. *Bull Env. Contam Toxicol* **2003**, *70* (1), 161–165.
(169) Hoang, B.; Benavides, A.; Shi, Y.; Yang, Y.; Frost, P.; Gera, J.; Lichtenstein, A. The PP242 Mammalian Target of Rapamycin (MTOR) Inhibitor Activates Extracellular Signal-Regulated Kinase (ERK) in Multiple Myeloma Cells via a Target of Rapamycin Complex 1 (TORC1)/ Eukaryotic Translation Initiation Factor 4E (EIF-4E)/RAF Pathway and Acti. *J. Biol. Chem.* **2012**, *287* (26), 21796–21805.
(170) Nadon, A. M.; Perez, M. J.; Hernandez-Saavedra, D.; Smith, L. P.; Yang, Y.; Sanders, L. a.; Gandjeva, A.; Chabon, J.; Koyanagi, D. E.; Graham, B. B.; Tuder, R. M.; Schmidt, E. P. Rtp801 Suppression of Epithelial MTORC1 Augments Endotoxin-Induced Lung Inflammation. *Am. J. Pathol.* **2014**, *184* (9), 2382–2389.
(171) Schiffer, J. M.; Mael, L. E.; Prather, K. A.; Amaro, R. E.; Grassian, V. H. Sea Spray Aerosol: Where Marine Biology Meets Atmospheric Chemistry. *ACS Cent. Sci.* **2018**, *4* (12), 1617–1623.
(172) Facchini, M. C.; Rinaldi, M.; Decesari, S.; Carbone, C.; Finessi, E.; Mircea, M.; Fuzzi, S.; Ceburnis, D.; Flanagan, R.; Nilsson, E. D.; de Leeuw, G.; Martino, M.; Woeltjen, J.; O'Dowd, C. D. Primary Submicron Marine Aerosol Dominated by Insoluble Organic Colloids and Aggregates. *Geophys. Res. Lett.* **2008**, *35* (17), 1–5.
(173) Duarte, C. M. Global Change and the Future Ocean: A Grand Challenge for Marine Sciences. *Front. Mar. Sci.* **2014**, *1*, 1–16.
(174) Steffen, W.; Sanderson, R. A.; Tyson, P. D.; Jäger, J.; Matson, P. A.; Moore, B.; Oldfield, F.; Richardson, K.; Schellnhuber, H. J.; Turner, B. L.; Wasson, R. J. *Global Change and the Earth System: A Planet Under Pressure*; Springer, 2004.
(175) Granéli, E.; Turner, J. T. *Ecology of Harmful Algae*; Springer: Berlin Heidelberg, Germany, 2006.
(176) Botana, L. M. *Seafood and Freshwater Toxins: Pharmacology, Physiology, and Detection, Third Edition*; Crc Press: Boca Raton, 2014.
(177) Fleming, L. E.; Kirkpatrick, B.; Backer, L. C.; Bean, J. A.; Wanner, A.; Reich, A.; Zaias, J.; Cheng, Y. S.; Pierce, R.; Naar, J.; Abraham, W. M.; Baden, D. G. Aerosolized Red-Tide Toxins (Brevetoxins) and Asthma. *Chest* **2007**, *131* (1), 187–194.
(178) Alfonso, A.; Alfonso, C. Pharmacology of Yessotoxin. In *Phycotoxins: Chemistry and Biochemistry*; Botana, L. M., Ed.; Blackwell Publishing: Ames, 2007; pp 203–209.
(179) Asselman, J.; Van Acker, E.; De Rijcke, M.; Tilleman, L.; Van Nieuwerburgh, F.; Mees, J.; De Schamphelaere, K. A. C.; Janssen, C. R. Marine Biogenics in Sea Spray Aerosols Interact with the MTOR Signaling Pathway. *Sci. Rep.* **2019**, *9*, 1–10.

(180) Van Acker, E.; De Rijcke, M.; Asselman, J.; Beck, I. M.; Huysman, S.; Vanhaecke, L.; De Schamphelaere, K. A. C.; Janssen, C. R. Aerosolizable Marine Phycotoxins and Human Health Effects: In Vitro Support for the Biogenics Hypothesis. *Mar. Drugs* **2020**, *18*, 1–13.
(181) Visciano, P.; Schirone, M.; Berti, M.; Milandri, A.; Tofalo, R.; Suzzi, G. Marine Biotoxins: Occurrence, Toxicity, Regulatory Limits and Reference Methods. *Front. Microbiol.* **2016**, *7*, 1–10.
(182) Gerssen, A.; Pol-Hofstad, I. E.; Poelman, M.; Mulder, P. P. J.; van den Top, H. J.; de Boer, J. Marine Toxins: Chemistry, Toxicity, Occurrence and Detection, with Special Reference to the Dutch Situation. *Toxins (Basel).* **2010**, *2* (4), 878–904.
(183) Gerssen, A.; Mulder, P. P. J.; McElhinney, M.; de Boer, J. Liquid Chromatography-Tandem Mass Spectrometry Method for the Detection of Marine Lipophilic Toxins under Alkaline Conditions. *J. Chromatogr. A* **2009**, *1216* (9), 1421–1430.
(184) Quinn, P. K.; Bates, T. S.; Schulz, K. S.; Coffman, D. J.; Frossard, A. A.; Russell, L. M.; Keene, W. C.; Kieber, D. J. Contribution of Sea Surface Carbon Pool to Organic Matter Enrichment in Sea Spray Aerosol. *Nat. Geosci.* **2014**, *7* (3), 228–232.
(185) Gerssen, A.; McElhinney, M. A.; Mulder, P. P. J.; Bire, R.; Hess, P.; de Boer, J. Solid Phase Extraction for Removal of Matrix Effects in Lipophilic Marine Toxin Analysis by Liquid Chromatography-Tandem Mass Spectrometry. *Anal. Bioanal. Chem.* **2009**, *394* (4), 1213–1226.
(186) Gerssen, A.; Van Olst, E. H. W.; Mulder, P. P. J.; de Boer, J. In-House Validation of a Liquid Chromatography Tandem Mass Spectrometry Method for the Analysis of Lipophilic Marine Toxins in Shellfish Using Matrix-Matched Calibration. *Anal. Bioanal. Chem.* **2010**, *397* (7), 3079–3088.
(187) Domènech, A.; Cortés-Francisco, N.; Palacios, O.; Franco, J. M.; Riobó, P.; Llerena, J. J.; Vichi, S.; Caixach, J. Determination of Lipophilic Marine Toxins in Mussels. Quantification and Confirmation Criteria Using High Resolution Mass Spectrometry. *J. Chromatogr. A* **2014**, *1328*, 16–25.
(188) Blay, P.; Hui, J. P. M.; Chang, J.; Melanson, J. E. Screening for Multiple Classes of Marine Biotoxins by Liquid Chromatography-High-Resolution Mass Spectrometry. *Anal. Bioanal. Chem.* **2011**, *400* (2), 577–585.
(189) Plackett, R. L.; Burman, J. P. The Design of Optimum Multifactorial Experiments. *Biometrika* **1946**, *33* (4), 305–325.
(190) Box, G. E. P.; Behnken, D. W. Some New Three Level Designs for the Study of Quantitative Variables. *Technometrics* **1960**, *2* (4), 455–475.
(191) Magnusson, B.; Örnemark, U. *Eurachem Guide: The Fitness for Purpose of Analytical Methods – A Laboratory Guide to Method Validation and Related Topics, (2nd Ed.)*; Eurachem: Teddington, 2014.
(192) The European Parliament and the Council of the European Union. Commission Decision 2002/657/EC Implementing Council Directive 96/23/EC Concerning the Performance of Analytical Methods and the Interpretation of Results. *Off. J. Eur. communities* **2002**.
(193) Kruve, A.; Rebane, R.; Kipper, K.; Oldekop, M. L.; Evard, H.; Herodes, K.; Ravio, P.; Leito, I. Tutorial Review on Validation of Liquid Chromatography-Mass Spectrometry Methods: Part I. *Anal. Chim. Acta* **2015**, *870* (1), 29–44.

(194) Kruve, A.; Rebane, R.; Kipper, K.; Oldekop, M. L.; Evard, H.; Herodes, K.; Ravio, P.; Leito, I. Tutorial Review on Validation of Liquid Chromatography-Mass Spectrometry Methods: Part II. *Anal. Chim. Acta* **2015**, *870* (1), 8–28.
(195) Aissaoui, A.; Armi, Z.; Akrout, F.; Ben Hassine, O. K. Environmental Factors and Seasonal Dynamics of Prorocentrum Lima Population in Coastal Waters of the Gulf of Tunis, South Mediterranean. *Water Environ. Res.* **2014**, *86* (12), 2256–2270.
(196) Koike, K.; Horie, Y.; Suzuki, T.; Kobiyama, A.; Kurihara, K.; Takagi, K.; Kaga, S. N.; Oshima, Y. Protoceratium Reticulatum in Northern Japan: Environmental Factors Associated with Seasonal Occurrence and Related Contamination of Yessotoxin in Scallops. *J. Plankton Res.* **2006**, *28* (1), 103–112.
(197) Akselman, R.; Krock, B.; Alpermann, T. J.; Tillmann, U.; Almandoz, O.; Ferrario, M. E.; Borel, C. M. Protoceratium Reticulatum (Dinophyceae) in the Austral Southwestern Atlantic and the First Report on YTX-Production in Shelf Waters of Argentina. *Harmful Algae* **2015**, *45*, 40–52.
(198) Turkoglu, M. First Harmful Algal Bloom Record of Tycoplanktonic Dinoflagellate Prorocentrum Lima (Ehrenberg) F. Stein, 1878 in the Dardanelles (Turkish Straits System, Turkey). *J. Coast. Life Med.* **2016**, *4* (10), 765–774.
(199) Harvey, G. W.; Burzell, L. A. A Simple Microlayer Method for Small Samples. *Ocean. Inst. Contrib.* **1972**, *85*, 156–157.
(200) Després, V. R.; Alex Huffman, J.; Burrows, S. M.; Hoose, C.; Safatov, A. S.; Buryak, G.; Fröhlich-Nowoisky, J.; Elbert, W.; Andreae, M. O.; Pöschl, U.; Jaenicke, R. Primary Biological Aerosol Particles in the Atmosphere: A Review. *Tellus, Ser. B Chem. Phys. Meteorol.* **2012**, *64*, 1–58.
(201) Tsunogai, S.; Saito, O.; Yamada, K.; Nakaya, S. Chemical Composition of Oceanic Aerosol. *J. Geophys. Res.* **1972**, *77* (27), 5283–5292.
(202) May, N. W.; Gunsch, M. J.; Olson, N. E.; Bondy, A. L.; Kirpes, R. M.; Bertman, S. B.; China, S.; Laskin, A.; Hopke, P. K.; Ault, A. P.; Pratt, K. A. Unexpected Contributions of Sea Spray and Lake Spray Aerosol to Inland Particulate Matter. *Environ. Sci. Technol. Lett.* **2018**, *5* (7), 405–412.
(203) *ICH Harmonized Tripartite Guideline: Validation of Analytical Procedures: Text and Methodology Q2(R1)*; International Conference of harmonization of technical requirements for registration of pharmaceuticals for human use: Genève, 2005.
(204) DOE. *Handbook of Methods for the Analysis of the Various Parameters of the Carbon Dioxide System in Sea Water*; Dickson, A. G., Goyet, C., Eds.; 1994.
(205) Pilson, M. E. Q. Major Constituents of Seawater. In *An Introduction to the Chemistry of the Sea*; 2012; pp 66–73.
(206) Pierce, R. H.; Henry, M. S.; Proffitt, L. S.; Hasbrouck, P. A. Red Tide Toxin (Brevetoxin) Enrichment in Marine Aerosol. In *4th International Conference on Toxic Marine Phytoplankton*; Graneli, E., Sundstron, S., Elder, L., Anderson, D. M., Eds.; 1990; pp 397–402.
(207) Olson, N. E.; Cooke, M. E.; Shi, J. H.; Birbeck, J. A.; Westrick, J. A.; Ault, A. P. Harmful Algal Bloom Toxins in Aerosol Generated from Inland Lake Water. *Environ. Sci. Technol.* **2020**, *54* (8), 4769–4780.
(208) Hoffman, E. J.; Duce, R. A. Factors Influencing the Organic Carbon Content of Marine Aerosols: A Laboratory Study. *J Geophys Res* **1976**, *81* (21), 3667–3670.
(209) Blanchard, D. C. Bubble Scavenging and the Water-to-Air Transfer of Organic Material in the Sea. *Appl. Chem. Protein Interfaces* **1975**, *145*, 18–360.

(210) Stefan, R. L.; Szeri, A. J. Surfactant Scavenging and Surface Deposition by Rising Bubbles. *J. Colloid Interface Sci.* **1999**, *212*, 1–13.
(211) Lindsley, W. G. Filter Pore Size and Aerosol Sample Collection. In *NIOSH Manual of Analytical Methods*; Ashely, K., O'Connor, P. F., Eds.; National Institute for Occupational Safety and Health, 2016; p 14.
(212) Blanchard, D. C. The Electrification of the Atmosphere by Particles from Bubbles in the Sea. *Prog. Oceanogr.* **1963**, *1* (1254), 73–202.
(213) Modini, R. L.; Russell, L. M.; Deane, G. B.; Stokes, M. D. Effect of Soluble Surfactant on Bubble Persistence and Bubble-Produced Aerosol Particles. *J. Geophys. Res. Atmos.* **2013**, *118* (3), 1388–1400.
(214) Backer, L. C.; McNeel, S. V.; Barber, T.; Kirkpatrick, B.; Williams, C.; Irvin, M.; Zhou, Y.; Johnson, T. B.; Nierenberg, K.; Aubel, M.; LePrell, R.; Chapman, A.; Foss, A.; Corum, S.; Hill, V. R.; Kieszak, S. M.; Cheng, Y. S. Recreational Exposure to Microcystins during Algal Blooms in Two California Lakes. *Toxicon* **2010**, *55* (5), 909–921.
(215) May, N. W.; Olson, N. E.; Panas, M. G.; Axson, J. L.; Tirella, P. S.; Kirpes, R. M.; Craig, R. L.; Gunsch, M. J.; China, S.; Laskin, A.; Ault, A. P.; Pratt, K. A. Aerosol Emissions from Great Lakes Harmful Algal Blooms. *Environ. Sci. Technol.* **2017**, *52* (2), 397−405.
(216) Codd, G.; Bell, S.; Kaya, K.; Ward, C.; Beattie, K.; Metcalf, J. Cyanobacterial Toxins, Exposure Routes and Human Health. *Eur. J. Phycol.* **1999**, *34*, 405−415.
(217) Fitzgeorge, R. B.; Clark, S. A.; Keevil, C. W. Routes of Intoxication. In *Detection Methods for Cyanobacterial Toxins*; Elsevier: Amsterdam, 1994; pp 69–74.
(218) Prather, K. a; Bertram, T. H.; Grassian, V. H.; Deane, G. B.; Stokes, M. D.; Demott, P. J.; Aluwihare, L. I.; Palenik, B. P.; Azam, F.; Seinfeld, J. H.; Moffet, R. C.; Molina, M. J.; Cappa, C. D.; Geiger, F. M.; Roberts, G. C.; Russell, L. M.; Ault, A. P.; Baltrusaitis, J.; Collins, D. B.; Corrigan, C. E.; Cuadra-Rodriguez, L. a; Ebben, C. J.; Forestieri, S. D.; Guasco, T. L.; Hersey, S. P.; Kim, M. J.; Lambert, W. F.; Modini, R. L.; Mui, W.; Pedler, B. E.; Ruppel, M. J.; Ryder, O. S.; Schoepp, N. G.; Sullivan, R. C.; Zhao, D. Bringing the Ocean into the Laboratory to Probe the Chemical Complexity of Sea Spray Aerosol. *Proc. Natl. Acad. Sci. U. S. A.* **2013**, *110* (19), 7550–7555.
(219) Leck, C.; Bigg, E. K. Source and Evolution of the Marine Aerosol - A New Perspective. *Geophys. Res. Lett.* **2005**, *32* (19), 1–4.
(220) Leck, C.; Bigg, E. K. Biogenic Particles in the Surface Microlayer and Overlaying Atmosphere in the Central Arctic Ocean during Summer. *Tellus B Chem. Phys. Meteorol.* **2005**, *57* (4), 305–316.
(221) Greque de Morais, M.; da Silva Vaz, B.; Greque de Morais, E.; Vieira Costa, J. A. Biologically Active Metabolites Synthesized by Microalgae. *Biomed Res. Int.* **2015**.
(222) Berdalet, E.; Fleming, L. E.; Gowen, R.; Davidson, K.; Hess, P.; Backer, L. C.; Moore, S. K.; Hoagland, P.; Enevoldsen, H. Marine Harmful Algal Blooms, Human Health and Wellbeing: Challenges and Opportunities in the 21st Century. *J. Mar. Biol. Assoc. U.K.*. **2016**, *2015* (01), 61–91.
(223) James, K. J.; Carey, B.; O'Halloran, J.; Van Pelt, F. N. A. M.; Škrabáková, Z. Shellfish Toxicity: Human Health Implications of Marine Algal Toxins. *Epidemiol. Infect.* **2010**, *138* (7), 927–940.
(224) Baden, D. G.; Bourdelais, A. J.; Jacocks, H.; Michelliza, S.; Naar, J. Natural and Derivative Brevetoxins: Historical Background, Multiplicity, and Effects. *Environ. Health Perspect.* **2005**, *113* (5), 621–625.

(225) Fleming, L. E.; Bean, J. A.; Kirkpatrick, B.; Cheng, Y. S.; Pierce, R.; Naar, J.; Nierenberg, K.; Backer, L. C.; Wanner, A.; Reich, A.; Zhou, Y.; Watkins, S.; Henry, M.; Zaias, J.; Abraham, W. M.; Benson, J.; Cassedy, A.; Hollenbeck, J.; Kirkpatrick, G.; Clake, T.; Baden, D. G. Exposure and Effect Assessment of Aerosolized Red Tide Toxins (Brevetoxins) and Asthma. *Environ. Health Perspect.* **2009**, *117* (7), 1095–1100.
(226) Imhoff, J. F.; Labes, A.; Wiese, J. Bio-Mining the Microbial Treasures of the Ocean: New Natural Products. *Biotechnol. Adv.* **2011**, *29* (5), 468–482.
(227) Tobío, A.; Alfonso, A.; Madera-Salcedo, I.; Botana, L. M.; Blank, U. Yessotoxin, a Marine Toxin, Exhibits Anti- Allergic and Anti-Tumoural Activities Inhibiting Melanoma Tumour Growth in a Preclinical Model. *PLoS One* **2016**, *11* (12), 1–14.
(228) Sarbassov, D. D.; Ali, S. M.; Sabatini, D. M. Growing Roles for the MTOR Pathway. *Curr. Opin. Cell Biol.* **2005**, *17* (6), 596–603.
(229) Lamming, D. W.; Ye, L.; Sabatini, D. M.; Baur, J. A. Rapalogs and MTOR Inhibitors as Anti-Aging Therapeutics. *J. Clin. Invest.* **2013**, *123* (3), 980–989.
(230) Lamming, D. W.; Sabatini, D. M. A Central Role for MTOR in Lipid Homeostasis. *Cell Metab.* **2013**, *18* (4), 1–8.
(231) Corradetti, M. N.; Guan, K. L. Upstream of the Mammalian Target of Rapamycin: Do All Roads Pass through MTOR? *Oncogene* **2006**, *25* (48), 6347–6360.
(232) Zingone, A.; Oksfeldt Enevoldsen, H. The Diversity of Harmful Algal Blooms: A Challenge for Science and Management. *Ocean Coast. Manag.* **2000**, *43*, 725–748.
(233) Daigle, C. C.; Chalupa, D. C.; Gibb, F. R.; Morrow, P. E.; Oberdörster, G.; Utell, M. J.; Frampton, M. W. Ultrafine Particle Deposition in Humans during Rest and Exercise. *Inhal. Toxicol.* **2003**, *15*, 539–552.
(234) Henke, K. G.; Sharratt, M.; Pegelow, D.; Dempsey, J. A. Regulation of End-Expiratory Lung Volume during Exercise. *J. Appl. Physiol.* **1988**, *64* (1), 135–146.
(235) Clarenbach, C. F.; Senn, O.; Brack, T.; Kohler, M.; Bloch, K. E. Monitoring of Ventilation during Exercise by a Portable Respiratory Inductive Plethysmograph. *Chest* **2005**, *128* (3), 1282–1290.
(236) Drust, B.; Reilly, T.; Cable, N. T. Physiological Responses to Laboratory-Based Soccer-Specific Intermittent and Continuous Exercise. *J. Sports Sci.* **2000**, *18* (11), 885–892.
(237) Martin, M. Cutadapt Removes Adapter Sequences from High-Throughput Sequencing Reads. *EMBnet.journal* **2011**, *17*.
(238) Dobin, A.; Davis, C. A.; Schlesinger, F.; Drenkow, J.; Zaleski, C.; Jha, S.; Batut, P.; Chaisson, M.; Gingeras, T. R. STAR: Ultrafast Universal RNA-Seq Aligner. *Bioinformatics* **2013**, *29* (1), 15–21.
(239) Li, B.; Dewey, C. N. RSEM: Accurate Transcript Quantification from RNA-Seq Data with or without a Reference Genome. *BMC Bioinformatics* **2011**, *12* (323).
(240) Robinson, M. D.; McCarthy, D. J.; Smyth, G. K. EdgeR: A Bioconductor Package for Differential Expression Analysis of Digital Gene Expression Data. *Bioinformatics* **2010**, *26* (1), 139–140.
(241) Kanehisa, M.; Susumu, G. KEGG: Kyoto Encyclopedia of Genes and Genomes. *Nucleic Acids Res.* **2000**, *28* (1), 27–30.

(242) Subramanian, A.; Tamayo, P.; Mootha, V. K.; Mukherjee, S.; Ebert, B. L.; Gillette, M. A.; Paulovich, A.; Pomeroy, S. L.; Golub, T. R.; Lander, E. S.; Mesirov, J. P. Gene Set Enrichment Analysis: A Knowledge-Based Approach for Interpreting Genome-Wide Expression Profiles. *Proc. Natl. Acad. Sci.* **2005**, *102* (43), 15545–15550.

(243) Nueda, M. J.; Tarazona, S.; Conesa, A. Next MaSigPro: Updating MaSigPro Bioconductor Package for RNA-Seq Time Series. *Bioinformatics* **2014**, *30* (18), 2598–2602.

(244) Paz, B.; Daranas, A. H.; Norte, M.; Riobo, P.; Franco, J. M.; J., F. J. Yessotoxins, a Group of Marine Polyether Toxins: An Overview. *Mar. Drugs* **2008**, *6* (2), 73–102.

(245) Fagerberg, L.; Hallstrom, B. M.; Oksvold, P.; Kampf, C.; Djureinovic, D.; Odeberg, J.; Habuka, M.; Tahmasebpoor, S.; Danielsson, A.; Edlund, K.; Asplund, A.; Sjostedt, E.; Lundberg, E.; Szigyarto, C. A. K.; Skogs, M.; Ottosson Takanen, J.; Berling, H.; Tegel, H.; Mulder, J.; Nilsson, P.; Schwenk, J. M.; Lindskog, C.; Danielsson, F.; Mardinoglu, A.; Sivertsson, A.; Von Feilitzen, K.; Forsberg, M.; Zwahlen, M.; Olsson, I.; Navani, S.; Huss, M.; Nielsen, J.; Ponten, F.; Uhlen, M. Analysis of the Human Tissue-Specific Expression by Genome-Wide Integration of Transcriptomics and Antibody-Based Proteomics. *Mol. Cell. Proteomics* **2014**, *13* (2), 397–406.

(246) Xu, X.; Cui, Y.; Cao, L. E. I.; Zhang, Y. E.; Yin, Y. A. N.; Hu, X. U. E. PCSK9 Regulates Apoptosis in Human Lung Adenocarcinoma A549 Cells via Endoplasmic Reticulum Stress and Mitochondrial Signaling Pathways. **2017**, 1993–1999.

(247) Dwivedi, D.; Grin, P.; Khan, M.; Prat, A.; Zhou, J.; Fox-Robichaud, A.; Seidah, N.; Liaw, P. Differential Expression of PCSK9 Modulates Infection, Inflammation, and Coagulation in a Murine Model of Sepsis. *Shock* **2016**, *46*, 672–680.

(248) Hazen, S. L. New Lipid and Lipoprotein Targets for the Treatment of Cardiometabolic Diseases. *J. Lipid Res.* **2012**, *53*, 1719–1721.

(249) Adorni, M. P.; Zimetti, F.; Lupo, M. G.; Ruscica, M.; Ferri, N. Naturally Occurring PCSK9 Inhibitors. *Nutrients* **2020**, *12*, 1–30.

(250) Li, F.; Jiang, C.; Larsen, M. C.; Bushkofsky, J.; Krausz, K. W.; Wang, T.; Jefcoate, C. R.; Gonzalez, F. J. Lipidomics Reveals a Link between CYP1B1 and SCD1 in Promoting Obesity. *J. Proteome Res.* **2014**, *13* (5), 2679–2687.

(251) Chang, J. T.; Chang, H.; Chen, P. H.; Lin, S. L.; Lin, P. Requirement of Aryl Hydrocarbon Receptor Overexpression for CYP1B1 Up-Regulation and Cell Growth in Human Lung Adenocarcinomas. *Clin. Cancer Res.* **2007**, *13* (1), 38–45.

(252) Dong, S.; Kanno, T.; Yamaki, A.; Kojima, T.; Shiraiwa, M.; Kawada, A.; Méchin, M. C.; Chavanas, S.; Serre, G.; Simon, M.; Takahara, H. NF-Y and Sp1/Sp3 Are Involved in the Transcriptional Regulation of the Peptidylarginine Deiminase Type III Gene (PADI3) in Human Keratinocytes. *Biochem. J.* **2006**, *397* (3), 449–459.

(253) Settembre, C.; Zoncu, R.; Medina, D. L.; Vetrini, F.; Erdin, S.; Erdin, S.; Huynh, T.; Ferron, M.; Karsenty, G.; Vellard, M. C.; Facchinetti, V.; Sabatini, D. M.; Ballabio, A. A Lysosome-to-Nucleus Signalling Mechanism Senses and Regulates the Lysosome via MTOR and TFEB. *EMBO J.* **2012**, *31* (5), 1095–1108.

(254) Zhao, J.; Zhai, B.; Gygi, S. P.; Goldberg, A. L. MTOR Inhibition Activates Overall Protein Degradation by the Ubiquitin Proteasome System as Well as by Autophagy. *Proc. Natl. Acad. Sci.* **2015**, *112* (52), 15790–15797.
(255) Quidville, V.; Alsafadi, S.; Goubar, A.; Commo, F.; Scott, V.; Pioche-Durieu, C.; Girault, I.; Baconnais, S.; Le Cam, E.; Lazar, V.; Delaloge, S.; Saghatchian, M.; Pautier, P.; Morice, P.; Dessen, P.; Vagner, S.; Andre, F. Targeting the Deregulated Spliceosome Core Machinery in Cancer Cells Triggers MTOR Blockade and Autophagy. *Cancer Res.* **2013**, *73* (7), 2247–2258.
(256) Autilio, C.; Pérez-Gil, J. Understanding the Principle Biophysics Concepts of Pulmonary Surfactant in Health and Disease. *Arch. Dis. Child. Fetal Neonatal Ed.* **2019**, *104* (4), F443–F451.
(257) Wilson, T. W.; Ladino, L. A.; Alpert, P. A.; Breckels, M. N.; Brooks, I. M.; Browse, J.; Burrows, S. M.; Carslaw, K. S.; Huffman, J. A.; Judd, C.; Kilthau, W. P.; Mason, R. H.; McFiggans, G.; Miller, L. A.; Najera, J. J.; Polishchuk, E.; Rae, S.; Schiller, C. L.; Si, M.; Temprado, J. V.; Whale, T. F.; Wong, J. P. S.; Wurl, O.; Yakobi-Hancock, J. D.; Abbatt, J. P. D.; Aller, J. Y.; Bertram, A. K.; Knopf, D. A.; Murray, B. J. A Marine Biogenic Source of Atmospheric Ice-Nucleating Particles. *Nature* **2015**, *525* (7568), 234–238.
(258) Li, Y.; Ezell, M. J.; Finlayson-Pitts, B. J. The Impact of Organic Coatings on Light Scattering by Sodium Chloride Particles. *Atmos. Environ.* **2011**, *45* (25), 4123–4132.
(259) Finlayson-Pitts, B. J.; Pitts, J. N. J. *Chemistry of the Upper and Lower Atmosphere*; Academic Press: San Diego, 2000.
(260) Wang, X.; Sultana, C. M.; Trueblood, J.; Hill, T. C. J.; Malfatti, F.; Lee, C.; Laskina, O.; Moore, K. A.; Beall, C. M.; McCluskey, C. S.; Cornwell, G. C.; Zhou, Y.; Cox, J. L.; Pendergraft, M. A.; Santander, M. V.; Bertram, T. H.; Cappa, C. D.; Azam, F.; DeMott, P. J.; Grassian, V. H.; Prather, K. A. Microbial Control of Sea Spray Aerosol Composition: A Tale of Two Blooms. *ACS Cent. Sci.* **2015**, *1* (3), 124–131.
(261) O'Dowd, C.; Ceburnis, D.; Ovadnevaite, J.; Bialek, J.; Stengel, D. B.; Zacharias, M.; Nitschke, U.; Connan, S.; Rinaldi, M.; Fuzzi, S.; Decesari, S.; Facchini, M. C.; Marullo, S.; Santoleri, R.; Anno, A. D.; Corinaldesi, C.; Tangherlini, M.; Danovaro, R. Connecting Marine Productivity to Sea-Spray via Nanoscale Biological Processes : Phytoplankton Dance or Death Disco ? *Sci. Rep.* **2015**, No. May, 1–11.
(262) Cravigan, L. T.; Mallet, M. D.; Vaattovaara, P.; Harvey, M. J.; Law, C. S.; Modini, R. L.; Russell, L. M.; Stelcer, E.; Cohen, D. D.; Olsen, G.; Safi, K.; Burrell, T. J.; Ristovski, Z. Sea Spray Aerosol Organic Enrichment, Water Uptake and Surface Tension Effects. *Atmos. Chem. Phys. Discuss.* **2019**, *20*, 1–35.
(263) Rinaldi, M.; Fuzzi, S.; Decesari, S.; Marullo, S.; Santoleri, R.; Provenzale, A.; Von Hardenberg, J.; Ceburnis, D.; Vaishya, A.; O'Dowd, C. D.; Facchini, M. C. Is Chlorophyll-a the Best Surrogate for Organic Matter Enrichment in Submicron Primary Marine Aerosol? *J. Geophys. Res. Atmos.* **2013**, *118* (10), 4964–4973.
(264) Li, S.; Du, L.; Tsona, N. T.; Wang, W. The Interaction of Trace Heavy Metal with Lipid Monolayer in the Sea Surface Microlayer. *Chemosphere* **2018**, *196*, 323–330.
(265) Hayakawa, K.; Handa, N.; Kawanobe, K.; Wong, C. S. Factors Controlling the Temporal Variation of Fatty Acids in Piculate Matter during a Phytoplankton Bloom in a Marine Mesocosm. **1996**, *52*, 233–244.

(266) Cochran, R. E.; Laskina, O.; Jayarathne, T.; Laskin, A.; Laskin, J.; Lin, P.; Sultana, C.; Lee, C.; Moore, K. A.; Cappa, C. D.; Bertram, T. H.; Prather, K. A.; Grassian, V. H.; Stone, E. A. Analysis of Organic Anionic Surfactants in Fine and Coarse Fractions of Freshly Emitted Sea Spray Aerosol. *Environ. Sci. Technol.* **2016**, *50*, 2477−2486.
(267) Adams, E. M.; Casper, C. B.; Allen, H. C. Effect of Cation Enrichment on Dipalmitoylphosphatidylcholine (DPPC) Monolayers at the Air-Water Interface. *J. Colloid Interface Sci.* **2016**, *478*, 353–364.
(268) Hidalgo, A.; Cruz, A.; Pérez-Gil, J. Barrier or Carrier? Pulmonary Surfactant and Drug Delivery. *Eur. J. Pharm. Biopharm.* **2015**, *95*, 117–127.
(269) Orgeig, S.; Daniels, C. B. The Roles of Cholesterol in Pulmonary Surfactant : Insights from Comparative and Evolutionary Studies. *Comp. Biochem. Physiol.* **2001**, *129*, 75–89.
(270) Griese, M. Pulmonary Surfactant in Health and Human Lung Diseases : State of the Art. **1999**.
(271) Wauthoz, N.; Amighi, K. Phospholipids in Pulmonary Drug Delivery. *Eur. J. Lipid Sci. Technol.* **2014**, *116* (9), 1114–1128.
(272) Ghadiri, M.; Young, P. M.; Traini, D. Strategies to Enhance Drug Absorption via Nasal and Pulmonary Routes. *Pharmaceutics* **2019**, *11* (3), 1–20.
(273) Velino, C.; Carella, F.; Adamiano, A.; Sanguinetti, M.; Vitali, A.; Catalucci, D.; Bugli, F.; Iafisco, M. Nanomedicine Approaches for the Pulmonary Treatment of Cystic Fibrosis. *Front. Bioeng. Biotechnol.* **2019**, *7* (December).
(274) Iasella, S. V.; Stetten, A. Z.; Corcoran, T. E.; Garoff, S.; Przybycien, T. M.; Tilton, R. D. Aerosolizing Lipid Dispersions Enables Antibiotic Transport Across Mimics of the Lung Airway Surface Even in the Presence of Pre-Existing Lipid Monolayers. *J. Aerosol Med. Pulm. Drug Deliv.* **2018**, *31* (4), 212–220.
(275) Ullah, S.; Sandqvist, S.; Beck, O. Measurement of Lung Phosphatidylcholines in Exhaled Breath Particles Using a Convenient Collection Procedure. *Anal. Chem.* **2015**, *87* (22), 11553–11560.
(276) Panda, A. K.; Nag, K.; Harbottle, R. R.; Possmayer, F.; Petersen, N. O. Thermodynamic Studies on Mixed Molecular Langmuir Films Part 2. Mutual Mixing of DPPC and Bovine Lung Surfactant Extract with Long-Chain Fatty Acids. *Colloids Surfaces A Physicochem. Eng. Asp.* **2004**, *247*, 9–17.
(277) Colantonio, S.; Simpson, J. T.; Fisher, R. J.; Yavlovich, A.; Belanger, J. M.; Puri, A.; Blumenthal, R. Quantitative Analysis of Phospholipids Using Nanostructured Laser Desorption Ionization Targets. *Lipids* **2012**, *46* (5), 469–477.
(278) Van Meulebroek, L.; De Paepe, E.; Vercruysse, V.; Pomian, B.; Bos, S.; Lapauw, B.; Vanhaecke, L. Holistic Lipidomics of the Human Gut Phenotype Using Validated Ultra-High-Performance Liquid Chromatography Coupled to Hybrid Orbitrap Mass Spectrometry. *Anal. Chem.* **2017**, *89*, 12502–12510.
(279) Flemisch Government. Meetnet Vlaamse Banken https://meetnetvlaamsebanken.be/.
(280) Ciavatta, S.; Brewin, R. J. W.; Skákala, J.; Polimene, L.; de Mora, L.; Artioli, Y.; Allen, J. I. Assimilation of Ocean-Color Plankton Functional Types to Improve Marine Ecosystem Simulations. *J. Geophys. Res. Ocean.* **2018**, *123* (2), 834–854.

(281) Butenschön, M.; Clark, J.; Aldridge, J. N.; Icarus Allen, J.; Artioli, Y.; Blackford, J.; Bruggeman, J.; Cazenave, P.; Ciavatta, S.; Kay, S.; Lessin, G.; Van Leeuwen, S.; Van Der Molen, J.; De Mora, L.; Polimene, L.; Sailley, S.; Stephens, N.; Torres, R. ERSEM 15.06: A Generic Model for Marine Biogeochemistry and the Ecosystem Dynamics of the Lower Trophic Levels. *Geosci. Model Dev.* **2016**, *9* (4), 1293–1339.
(282) Long, M. S.; Keene, W. C.; Kieber, D. J.; Frossard, A. A.; Russell, L. M.; Maben, J. R.; Kinsey, J. D.; Quinn, P. K.; Bates, T. S. Light-Enhanced Primary Marine Aerosol Production from Biologically Productive Seawater. *Geophys. Res. Lett.* **2014**, *41*, 2661–2670.
(283) Peña, E. A.; Slate, E. H. Global Validation of Linear Model Assumptions. *J. Am. Stat. Assoc.* **2006**, *101* (473), 341–354.
(284) Fox, J.; Monette, G. Generalized Collinearity Diagnostics. *J. Am. Stat. Assoc.* **1992**, *87* (417).
(285) Fox, J.; Weisberg, S. *An R Companion to Applied Regression*; Sage: Thousand Oaks, CA, 2019.
(286) Clesceri, L. S.; Greenberg, A. E.; Eaton, A. D. *Standard Methods for the Examination of Water and Wastewater - 20th Edition*; American Public Health Association: Washington, 1998.
(287) Leck, C.; Svensson, E. Importance of Aerosol Composition and Mixing State for Cloud Droplet Activation over the Arctic Pack Ice in Summer. *Atmos. Chem. Phys.* **2015**, *15*, 2545–2568.
(288) Sievering, H.; Cainey, J.; Harvey, M.; McGregor, J.; Nichol, S.; Quinn, P. Aerosol Non-Sea-Salt Sulfate in the Remote Marine Boundary Layer under Clear-Sky and Normal Cloudiness Conditions : Ocean-Derived Biogenic Alkalinity Enhances Sea-Salt Sulfate Production by Ozone Oxidation. *J. Geophys. Res.* **2004**, *109*, 1–12.
(289) Salter, M. E.; Leck, C.; Werner, J.; Johnson, C. M.; Riipinen, I.; Nilsson, E. D.; Zieger, P. Calcium Enrichment in Sea Spray Aerosol Particles. *Geophys. Res. Lett.* **2016**, *43*, 8277–8285.
(290) Ault, A. P.; Zhao, D.; Ebben, C. J.; Tauber, M. J.; Geiger, F. M.; Prather, K. A.; Grassian, V. H. Raman Microspectroscopy and Vibrational Sum Frequency Generation Spectroscopy as Probes of the Bulk and Surface Compositions of Size-Resolved Sea Spray Aerosol Particles. *Phys. Chem. Chem. Phys.* **2013**, *15* (207890), 6206–6214.
(291) Nielsen, L. S.; Bilde, M. Exploring Controlling Factors for Sea Spray Aerosol Production: Temperature, Inorganic Ions and Organic Surfactants. *Tellus, Ser. B Chem. Phys. Meteorol.* **2020**, *72* (1), 1–10.
(292) Verdugo, P. Marine Microgels. *Ann. Rev. Mar. Sci.* **2012**, *4*, 375–400.
(293) Casillas-Ituarte, N. N.; Callahan, K. M.; Tang, C. Y.; Chen, X.; Roeselová, M.; Tobias, D. J.; Allen, H. C. Surface Organization of Aqueous MgCl2 and Application to Atmospheric Marine Aerosol Chemistry. *Proc. Natl. Acad. Sci. U. S. A.* **2010**, *107* (15), 6616–6621.
(294) Casper, C. B.; Verreault, D.; Adams, E. M.; Hua, W.; Allen, H. C. Surface Potential of DPPC Monolayers on Concentrated Aqueous Salt Solutions. *J. Phys. Chem. B* **2016**, *120*, 2043–2052.
(295) Gasparovic, B.; Frka, S.; Kozarac, Z.; Nelson, A. A Method for Characterization of Sea Surface Microlayer Based on Monolayer Properties in Presence and Absence of Phospholipids. *Anal. Chim. Acta* **2008**, *620*, 64–72.

(296) Mysels, K. J.; Shinoda, K.; Frankel, S. *Soap Films: Studies of Their Thinning and a Bibliography*; Pergamon Press: London, 1959.
(297) Cunliffe, M.; Upstill-Goddard, R. C.; Murrell, J. C. Microbiology of Aquatic Surface Microlayers. *FEMS Microbiol. Rev.* **2011**, *35* (2), 233–246.
(298) Daewel, U.; Schrum, C. Simulating Long-Term Dynamics of the Coupled North Sea and Baltic Sea Ecosystem with ECOSMO II: Model Description and Validation. *J. Mar. Syst.* **2013**, *119–120*, 30–49.
(299) Daewel, U.; Schrum, C.; MacDonald, J. I. Towards End-to-End (E2E) Modelling in a Consistent NPZD-F Modelling Framework (ECOSMO E2E-v1.0): Application to the North Sea and Baltic Sea. *Geosci. Model Dev.* **2019**, *12* (5), 1765–1789.
(300) Frossard, A. A.; Li, W.; Gérard, V.; Nozière, B.; Ronald, C. Influence of Surfactants on Growth of Individual Aqueous Coarse Mode Aerosol Particles Mode Aerosol Particles. *Aerosol Sci. Technol.* **2018**, *6826* (52), 459–469.
(301) Jungwirth, P.; Rosenfeld, D.; Buch, V. A Possible New Molecular Mechanism of Thundercloud Electrification. *Atmos. Res.* **2005**, *76* (1–4), 190–205.
(302) Hentschel, R. Surfactant Replacement Therapy : From Biological Basis to Current Clinical Practice. *Pediatr. Res.* **2020**, *88* (December 2019), 176–183.
(303) Meng, S.; Chang, W.; Lu, Z.; Xie, J.; Qiu, H.; Yang, Y.; Guo, F. Effect of Surfactant Administration on Outcomes of Adult Patients in Acute Respiratory Distress Syndrome: A Meta- Analysis of Randomized Controlled Trials. *BMC Pulm. Med.* **2019**, *19* (9), 1–11.
(304) Samsudin, D. D. Current Issues and Challenges in the Use of Aerosolized Surfactant for Respiratory Distress Syndrome in the Newborns. *Indones Biomed J.* **2013**, *5*, 91–100.
(305) Syedain, Z. H.; Naqwi, A. A.; Dolovich, M.; Somani, A. In Vitro Evaluation of a Device for Intra-Pulmonary Aerosol Generation and Delivery. *Aerosol Sci Technol..* **2015**, *49* (9), 747–752.
(306) Heching, M.; Lev, S.; Shitenberg, D.; Dicker, D.; Kramer, M. R. Surfactant for the Treatment of ARDS in a Patient With Coronavirus Disease 2019. *Chest* **2021**, No. March, 4–7.
(307) Muralidharan, P.; Malapit, M.; Mallory, E.; Hayes, D.; Mansour, H. M. Inhalable Nanoparticulate Powders for Respiratory Delivery. *Nanomedicine Nanotechnology, Biol. Med.* **2015**, *11* (5), 1189–1199.
(308) Poelma, D. L.; Ju, M. R.; Bakker, S. C.; Zimmermann, L. J.; Lachmann, B. F.; Van Iwaarden, J. F. A Common Pathway for the Uptake of Surfactant Lipids by Alveolar Cells. *Am. J. Respir. Cell Mol. Biol.* **2004**, *30* (5), 751–758.
(309) Hadinoto, K.; Phanapavudhikul, P.; Kewu, Z.; Tan, R. B. H. Dry Powder Aerosol Delivery of Large Hollow Nanoparticulate Aggregates as Prospective Carriers of Nanoparticulate Drugs: Effects of Phospholipids. *Int. J. Pharm.* **2007**, *333* (1–2), 187–198.
(310) Chono, S.; Fukuchi, R.; Seki, T.; Morimoto, K. Aerosolized Liposomes with Dipalmitoyl Phosphatidylcholine Enhance Pulmonary Insulin Delivery. *J. Control. Release* **2009**, *137* (2), 104–109.
(311) Van Acker, E.; Huysman, S.; De Rijcke, M.; Asselman, J.; De Schamphelaere, K. A. C.; Vanhaecke, L.; Janssen, C. R. Phycotoxin-Enriched Sea Spray Aerosols: Methods, Mechanisms, and Human Exposure. *Environ. Sci. Technol.* **2021**, *55*, 6184–6196.

(312) Poli, M.; Ruiz-Olvera, P.; Nalca, A.; Ruiz, S.; Livingston, V.; Frick, O.; Dyer, D.; Schellhase, C.; Raymond, J.; Kulis, D.; Anderson, D.; McGrath, S.; Deeds, J. Toxicity and Pathophysiology of Palytoxin Congeners after Intraperitoneal and Aerosol Administration in Rats. *Toxicon* **2018**, *150* (June), 235–250.
(313) White, M. P.; Alcock, I.; Wheeler, B. W.; Depledge, M. H. Coastal Proximity, Health and Well-Being: Results from a Longitudinal Panel Survey. *Heal. Place* **2013**, *23*, 97–103.
(314) Cheng, Y. S.; Villareal, T. A.; Zhou, Y.; Gao, J.; Pierce, R. H.; Wetzel, D.; Naar, J.; Baden, D. G. Characterization of Red Tide Aerosol on the Texas Coast. *Harmful Algae* **2005**, *4* (1), 87–94.
(315) EFSA. Marine Biotoxins in Shellfish - Okadaic Acid and Analogies - Scientific Opinion of the Panel on Contaminants in the Food Chain. *EFSA J.* **2008**, *589*, 1–62.
(316) Valdiglesias, V.; Prego-Faraldo, M. V.; Paśaro, E.; Meńdez, J.; Laffon, B. Okadaic Acid: More than a Diarrheic Toxin. *Mar. Drugs* **2013**, *11* (11), 4328–4349.
(317) Ding, Z.; Pothineni, N. V. K.; Goel, A.; Luscher, T. F.; Mehta, J. L. PCSK9 and Inflammation: Role of Shear Stress, pro-Inflammatory Cytokines, and LOX-1. *Cardiovasc. Res.* **2020**, *116*, 908–915.
(318) Rockström, J. A Safe Operating Space for Humanity Identifying. *Nature* **2009**, *461* (24), 472–475.
(319) Moore, M. N.; Baker-Austin, C.; Depledge, M. H.; Fleming, L.; Hess, P.; Lees, D.; Leonard, P.; Madsen, L.; Owen, R.; Pirlet, H.; White, M.; Vasconcelos, V.; Boase, N.; Osborne, N.; Viarengo, A. Linking Oceans and Human Health: A Strategic Research Priority for Europe. 2013, p 112.
(320) Anderson, D. M. Toxic Algal Blooms and Red Tides: A Global Perspective. *Red tides Biol. Environ. Sci. Toxicol.* **1989**, 11–16.
(321) Pavaux, A. S.; Berdalet, E.; Lemée, R. Chemical Ecology of the Benthic Dinoflagellate Genus Ostreopsis: Review of Progress and Future Directions. *Front. Mar. Sci.* **2020**, *7* (July), 1–28.
(322) Armand, L.; Tarantini, A.; Beal, D.; Biola-Clier, M.; Bobyk, L.; Sorieul, S.; Pernet-gallay, K.; Desvergne, C.; Lynch, I.; Herlin-Boime, N.; Carriere, M. Long-Term Exposure of A549 Cells to Titanium Dioxide Nanoparticles Induces DNA Damage and Sensitizes Cells towards Genotoxic Agents. *Nanotoxicology* **2016**, *10*, 913–923.
(323) Fröhlich, E. Comparison of Conventional and Advanced in Vitro Models in the Toxicity Testing of Nanoparticles. *Artif. Cells, Nanomedicine Biotechnol.* **2018**, *46*, 1091–1107.
(324) Shrestha, J.; Bazaz, S. R.; Es, H. A.; Azari, D. Y.; Thierry, B.; Warkiani, M. E.; Ghadiri, M. Lung-on-a-Chip: The Future of Respiratory Disease Models and Pharmacological Studies. *Crit. Rev. Biotechnol.* **2020**, 1–18.
(325) Wu, Q.; Liu, J.; Wang, X.; Feng, L.; Wu, J.; Zhu, X.; Wen, W.; Gong, X. Organ-on-a-Chip: Recent Breakthroughs and Future Prospects. *Biomed. Eng. Online* **2020**, *19* (1), 1–19.
(326) Barreca, M.; Spanò, V.; Montalbano, A.; Cueto, M.; Díaz Marrero, A. R.; Deniz, I.; Erdoğan, A.; Bilela, L. L.; Moulin, C.; Taffin-De-Givenchy, E.; Spriano, F.; Perale, G.; Mehiri, M.; Rotter, A.; Thomas, O. P.; Barraja, P.; Gaudêncio, S. P.; Bertoni, F. Marine Anticancer Agents: An Overview with a Particular Focus on Their Chemical Classes. *Mar. Drugs* **2020**, *18* (12).

(327) Ritz, C.; Baty, F.; Streibig, J. C.; Gerhard, D. *Dose-Response Analysis Using R*; 2015; Vol. 10.
(328) Thompson, J. Airborne Particulate Matter: Human Exposure & Health Effects. *J. Occup. Environ. Med.* **2018**, *60* (5), 329–423.
(329) Ibrahim, M.; Verma, R.; Garcia-contreras, L. Inhalation Drug Delivery Devices: Technology Update. *Med. Devices Evid. Res.* **2015**, *8*, 131–139.
(330) Guillard, R. R. L.; Hargraves, P. E. Stichochrysis Immobilis Is a Diatom, Not a Chrysophyte. *Phycologia* **1993**, *32*, 234–236.
(331) Blanchard, D. C.; Syzdek, L. D. Water-to-Air Transfer and Enrichment of Bacteria in Drops from Bursting Bubbles. *Appl. Environ. Microbiol.* **1982**, *43* (5), 1001–1005.
(332) Fröhlich, E.; Mercuri, A.; Wu, S.; Salar-behzadi, S. Measurements of Deposition, Lung Surface Area and Lung Fluid for Simulation of Inhaled Compounds. *Front. Pharmacol.* **2016**, *7* (June), 1–10.
(333) Peng, J.; Yuan, J.; Wu, C.; Wang, J. Fucoxanthin, a Marine Carotenoid Present in Brown Seaweeds and Diatoms : Metabolism and Bioactivities Relevant to Human Health. *Mar. Drugs* **2011**, *9*, 1806–1828.
(334) Thøgersen, M. S.; Delpin, M. W.; Melchiorsen, J.; Kilstrup, M. Production of the Bioactive Compounds Violacein and Indolmycin Is Conditional in a MaeA Mutant of Pseudoalteromonas Luteoviolacea S4054 Lacking the Malic Enzyme. *Front. Microbiol.* **2016**, *7*, 1–11.
(335) Bellemère, G.; Stamatas, G. N.; Bruère, V.; Bertin, C.; Issachar, N.; Oddos, T. Antiaging Action of Retinol: From Molecular to Clinical. *Ski. Pharmacol. Phsiology* **2009**, *22*, 200–209.
(336) Jonas, A.; Buranova, V.; Scholz, S.; Fetter, E.; Novakova, K.; Kohoutek, J.; Hilscherova, K. Retinoid-like Activity and Teratogenic Effects of Cyanobacterial Exudates. *Aquat. Toxicol.* **2014**, *155*, 283–290.
(337) Sithranga Boopathy, N.; Kathiresan, K. Anticancer Drugs from Marine Flora: An Overview. *J. Oncol.* **2010**, *2010*.
(338) Abdel-rahman, M. A.; Al-abd, A. M. Thermoresponsive Dendrimers Based on Oligoethylene Glycols: Design , Synthesis and Cytotoxic Activity against MCF-7 Breast Cancer Cells. *Eur. J. Med. Chem.* **2013**, *69*, 848–854.
(339) Doshi, G. M.; Aggarwal, G. V; Martis, E. A.; Shanbhag, P. P. Novel Antibiotics from Marine Sources. **2011**, 1446–1462.
(340) Slominski, A.; Semak, I.; Zjawiony, J.; Wortsman, J.; Gandy, M. N.; Li, J.; Zbytek, B.; Li, W.; Tuckey, R. C. Enzymatic Metabolism of Ergosterol by Cytochrome P450scc to Biologically Active 17, 24-Dihydroxyergosterol. *Chem. Biol.* **2005**, *12*, 931–939.
(341) Blunt, J. W.; Copp, B. R.; Keyzers, R. A.; Munro, M. H. G.; Prinsep, M. R. Marine Natural Products. *Nat. Prod. Rep.* **2014**, *31*, 160–258.
(342) Li, Y. X.; Wijesekara, I.; Li, Y.; Kim, S. K. Phlorotannins as Bioactive Agents from Brown Algae. *Process Biochem.* **2011**, *46* (12), 2219–2224.
(343) Enomoto, K. Violacein and Prodiginines from Marine Bacteria. In *Marine biotechnology*; Kim, S., Ed.; 2020.
(344) Chernomorsky, S.; Segelman, A.; Poretz, R. D. Effect of Dietary Chlorophyll Derivatives on Mutagenesis and Tumor Cell Growth. *Teratog. Carcinog. Mutagen.* **1999**, *19*, 313–322.
(345) Abdul, Q. A.; Choi, R. J.; Jung, H. A.; Choi, J. S. Health Benefit of Fucosterol from Marine Algae: A Review. *J. Sci. Food Agric.* **2016**, *96* (6), 1856–1866.

Summaries

Summary

World-wide, coastal regions are by far the most densely populated areas. Most people are not aware of or do not understand how we impact marine environments and vice versa. However, it recently becomes increasingly apparent that (changes in) marine ecosystems can have direct and indirect impacts on human health. The increasing awareness of this high interconnectivity has resulted in a new inter-disciplinary research field that links the '**ocean and human health' (OHH).** Despite the fact that coastal environments have been considered health promoting throughout human history, epidemiological studies only started to reveal improved health and happiness in coastal populations during the last decade. Several hypotheses have been proposed to explain why coastal residents are – on average – healthier. Moore's **biogenics hypothesis** for example suggests that this **beneficial coastal health effect** is caused by the regular exposure to marine compounds in sea spray aerosols (SSAs). These marine compounds would have an (inhibiting) effect on cell signaling pathways like the mechanistic target of rapamycin (mTOR) pathway. This hypothesis, which until now was supported by little to no evidence, is based on the fact that the augmented mTOR pathway activity is related to multiple pathological conditions while the pathway's downregulation has been associated with anti-cancer therapies and positive health effects. Conversely the inhalation of SSAs during toxin-producing harmful algal blooms (HABs) of *Karenia brevis* and *Ostreopsis ovata* has induced respiratory syndromes among others. The airborne exposure to such marine phycotoxins is of increasing concern, as some toxic HAB species are spreading into new areas. To date, **phycotoxins** are the only group of marine compounds that are known to induce **harmful health effects** via SSAs.

SSAs have mainly been investigated in a meteorological, climatological or biogeochemical context. Few studies have examined the role of SSAs on human health. As such, the **main objective of this PhD thesis** was to perform an exploratory assessment of the human airborne exposure to and potential health effects of marine compounds present in SSAs. **Beneficial effects** of SSAs were initially investigated in the context of the above mentioned biogenics hypothesis, while **harmful effects** of SSAs were considered via the assessment of phycotoxins. We assessed the potential health effects using **in vitro studies** with lung cells as a model for the human

respiratory system. To investigate aerosolization processes and human's exposure we constructed a **SSA generator**. This marine aerosol reference tank (MART) was used to produce environmentally realistic SSAs. Using both these effect and exposure model systems, in combination with existing and newly developed methodologies, we aimed to address some important knowledge gaps in the OHH research field.

Chapter 2 describes the first research phase of this doctoral thesis. Via an explorative in vitro study both health-affecting and potential health-promoting mechanisms of airborne phycotoxin exposure were investigated. Cell viability effects were analyzed via cytotoxicity assays and effects on the mTOR pathway via western blotting methods. Two different lung cell lines were exposed to increasing concentrations of (1) pure phycotoxins and (2) the extract of a laboratory-generated SSA containing homoyessotoxin (hYTX). Unlike the other phycotoxins, the examined yessotoxins (YTXs) initiated mechanisms which did not lead to direct cell mortality. The observed partial effects of YTXs on the cell viability can be attributed to the inhibition of cell growth and induction of apoptosis, both protective cell mechanisms that are linked to a downregulated activity of the mTOR pathway. Indeed, we showed that YTXs can downregulate the mTOR pathway and could therefore, in the light of the biogenics hypothesis, induce positive instead of negative health effects. Conversely, we found that okadaic acid (OA) and brevetoxin-2 (PbTx-2) initiated mechanisms that lead to the direct mortality of the exposed lung cells. PbTx-2 is the main phycotoxin produced by HABs of *Karenia brevis*, known to induce a respiratory syndrome via SSA. This algae is, however, only dominant in the Gulf of Mexico. OA is the primary marine phycotoxin in the North Sea and could potentially also induce negative effects upon airborne exposure to a sufficiently high dose. Prior this PhD study, the presence of both OA and YTXs in sea spray aerosols or (coastal) air had never been examined and never been detected in any natural or experimental aerosol form.

In **Chapter 3** we investigated the aerosolization processes and natural air concentrations of these phycotoxins. Using our MART, containing seawater and spiked with toxin-producing algae, we performed aerosolization experiments. As such, we provided the first (experimental) evidence and characterization of the aerosolization of OA, hYTX and dinophysistoxin-1 (DTX-1). The potential for aerosolization of these phycotoxins was demonstrated by their 78 to 1769-fold enrichment in SSAs relative to

the subsurface water. To obtain and support these results, we developed a new methodology for the extraction and analysis of phycotoxin in SSAs using ultra-high-performance liquid chromatography hyphenated to high-resolution Orbitrap mass spectrometry (UHPLC-HR-Orbitrap-MS). This analytical method showed good linearity (R^2>0.99), recovery (85.3-101.8%), and precision (RSDs≤17.2%). Natural air concentrations of these phycotoxins were subsequently investigated by combining environmental SSA sampling and concurrent MART aerosolization experiments using (unspiked) natural seawater. This approach allowed us to indirectly quantify the magnitude of OA concentrations in Belgium's coastal air ($[OA]_{coastal\ air}$ = 0.6-51 pg m^{-3}). Due to the lack of in vivo effect data we could not perform a comprehensive human risk assessment. Still considering all elements, is seems rather unlikely that these $[OA]_{coastal\ air}$ will lead to adverse health effects.

In **Chapter 4** we increased the environmental realism of our work by analyzing the potential health effects of a natural SSA sample, i.e., containing a complex and realistic mixture of marine compounds. After collection at the Belgian coast, we extracted the SSA sample and dosed it in an in vitro experiment to lung cells. By analyzing the differential gene expression, using RNA sequencing, insight into the mechanisms of the induced effects was obtained. For comparison three other treatments were also incorporated in this experiment: (1) pure homoyessotoxin (hYTX), (2) the extract of a laboratory-generated SSA containing hYTX, and (3) a known chemical mTOR inhibitor. After exposure to the natural SSA sample (extract) and the mTOR inhibitor the lung cells showed a significant decrease expression of genes related to the mTOR pathway and proprotein convertase subtilisin/kexin type 9 (PCSK9). The strong similarities in gene regulation suggest that natural SSAs indeed contain marine compounds that cause comparable effects as the known mTOR inhibitor and could therefore downregulate the mTOR pathway, as suggested by the biogenics hypothesis. In contrast, the pure hYTX and lab SSA treatments induced a significant increased expression of these genes. This does not necessarily imply that the activity of the mTOR pathway was stimulated. It does show that hYTX interacts differently with the mTOR pathway and that other marine chemicals (than hYTX) induced the effects observed in the natural SSA treatment. Overall, this study provided molecular evidence for the (biogenics) hypothesis that potential beneficial health effects can be induced at environmentally relevant doses of natural SSAs.

Chapter 5 discusses the results of a one-year SSA sampling campaign at the Belgium coast. The inorganic composition of these samples was analyzed using inductively coupled plasma - optical emission spectrometry (ICP-OES). Organic analysis of the samples was performed using UHPLC-HR-Q-Orbitrap™ hybrid mass spectrometry (MS/MS). We identified and quantified dipalmitoylphosphatidylcholine (DPPC) in nearly all SSA samples at air concentrations ranging between <1.1 and 33 pg m^{-3}. The discovery of this marine surfactant in SSAs is, due to its respiratory effects, of great importance for this research (field). Indeed, DPPC is the major component (±40%) of pulmonary surfactant in human alveoli and is used as an excipient in medical aerosol therapy to facilitate the effects of respiratory delivered drugs. The DPPC content in SSAs could play the same facilitating role for sea spray aerosolized bioactive compounds. By analyzing the inorganic content (e.g., Mg^{2+} and Ca^{2+}) of the SSA samples and the diverse environmental factors driving the enriched aerosolization of DPPC we unraveled additional processes which influence the entire SSA composition. Our findings on DPPC in SSAs are thus not only important from a human health point of view, they are also crucial for the understanding of the meteorological behavior of SSAs.

Due to the large amount of **pioneering work** that was performed, it was off course not possible to unravel all aspects of the possible linkages between SSAs and human health. Nonetheless I believe that we made **some major breakthroughs** in this young and at the same time ancient research field. The additional support we provided for the biogenics hypothesis and our discovery of DPPC in SSAs highlight the potential positive effects of the airborne exposure to sea spray aerosolized marine compounds. In addition our work suggests that the current phycotoxins concentrations at the Belgian coast do not pose a risk to human health. This **improved knowledge** of how the ocean's health status impacts human health can contribute to a better management of marine ecosystems. The **protection** of the related **ecosystem services** will also help us to live in harmony with nature and survive as a species.

Samenvatting

Kustgebieden zijn wereldwijd veruit de dichtstbevolkte regio's. Veel mensen zijn zich niet bewust of begrijpen niet hoe we het mariene milieu beïnvloeden en vice versa. De laatste decennia wordt het echter steeds duidelijker dat (veranderingen in) mariene ecosystemen een directe en indirecte invloed kunnen hebben op de menselijke gezondheid. Het hedendaagse bewustzijn van deze sterke connectie heeft geresulteerd in een nieuw interdisciplinair onderzoeksveld dat de '**oceaan en menselijke gezondheid**' met elkaar verbindt. Ondanks het feit dat kustgebieden doorheen de geschiedenis als gezondheid bevorderend werden aanschouwd, zijn epidemiologische studies pas in het laatste decennium beginnen aantonen dat kust populaties gemiddeld gezonder en gelukkiger zijn. Er zijn verschillende hypothesen voorgesteld om dit verklaren. De **biogene hypothese** van Moore stelt dat dit **positief gezondheidseffect** wordt veroorzaakt door de regelmatige blootstelling aan mariene stoffen in zeespray aerosolen (ZSA). Deze mariene stoffen zouden een (remmende) invloed hebben op cellulaire *pathways*, zoals de *mechanistic target of rapamycin* (mTOR) *pathway*. Deze hypothese, die voorheen door weinig tot geen bewijs werd ondersteund, is gebaseerd op het feit dat een verhoogde activiteit van de mTOR *pathway* gerelateerd is aan meerdere pathologische aandoeningen, terwijl het afremmen van deze *pathway* geassocieerd is met antikankertherapieën en positieve gezondheidseffecten. In tegenstelling tot deze positieve hypothese, kan het inademen van ZSA tijdens een toxine-producerende schadelijke algenbloei van *Karenia brevis* en *Ostreopsis ovata* ademhalingssyndromen veroorzaken. Blootstelling aan dergelijke mariene fycotoxines via ZSA in zeelucht baart steeds meer zorgen. Sommige giftige algensoorten verspreiden zich naar nieuwe gebieden. Tot op heden zijn **fycotoxines** de enige gekende groep van mariene stoffen die via ZSA **schadelijke gezondheidseffecten** kunnen veroorzaken.

ZSA zijn voornamelijk onderzocht in een meteorologische, klimatologische of biogeochemische context. Er zijn weinig tot geen studies die de rol van ZSA op de menselijke gezondheid hebben onderzocht. Als zodanig was het **hoofddoel van dit doctoraatsonderzoek** om een exploratieve evaluatie uit te voeren van de menselijke blootstelling aan mariene stoffen in ZSA en de daaraan gelinkte gezondheidseffecten. Potentiaal **gunstige effecten** van ZSA werden aanvankelijk onderzocht in de context

van de bovengenoemde biogene hypothese, terwijl **schadelijke effecten** van ZSA werden geëvalueerd met betrekking tot fycotoxines. Mogelijke gezondheidseffecten werden geanalyseerd met behulp van **in vitro studies** met longcellen, die als model voor het menselijk ademhalingsstelsel werden gebruikt. Om aerosolisatie processen en ZSA blootstellingscenario's te onderzoeken, hebben we een **ZSA generator** gebouwd. Deze mariene aerosol referentie tank (MART) werd gebruikt om milieu-realistische ZSA te produceren. Met behulp van zowel deze effect- als blootstelling-modelsystemen, als van enkele bestaande en nieuw ontwikkelde methodologieën, wilden we enkele belangrijke kennisleemtes in dit onderzoeksveld aanpakken.

Hoofdstuk 2 beschrijft de eerste fase van dit doctoraatsonderzoek. Via exploratieve in vitro experimenten werden zowel schadelijke als potentiële positieve gezondheid mechanismen van de respiratorische blootstelling aan fycotoxines onderzocht. Effecten op de vitaliteit van long cellen en op de mTOR-*pathway* werden respectievelijk geanalyseerd aan de hand van cytotoxiciteitstesten en western-blot methodes. Twee verschillende longcellijnen werden blootgesteld aan (1) zuivere fycotoxines en (2) het extract van een laboratorium-gegenereerde ZSA die homoyessotoxine (hYTX) bevatte. In tegenstelling tot de andere fycotoxines, initieerden de onderzochte yessotoxines (YTXs) geen mechanismen die leiden tot directe cel mortaliteit. De geobserveerde partiële effecten van YTXs op de cel vitaliteit kunnen verklaard worden door een remming van de celgroei en inductie van apoptose, beide beschermende cel mechanismen die gekoppeld zijn aan een geremde activiteit van de mTOR-*pathway.* We toonden inderdaad aan dat YTXs de activiteit van de mTOR-*pathway* afremmen. In het licht van de biogene hypothese wordt daarom verwacht dat YTXs positieve in plaats van negatieve gezondheidseffecten kunnen veroorzaken. Als zodanig toonde deze studie aan dat specifieke mariene stoffen de mTOR-*pathway* kunnen afremmen en ondersteunde ze de biogene hypothese. Okadaïnezuur (OA) en brevetoxine-2 (PbTx-2) initieerden daarentegen mechanismen die tot de directe mortaliteit van de blootgestelde longcellen leidden. PbTx-2 is het belangrijkste fycotoxine die geproduceerd wordt door schadelijke algenbloei van *Karenia brevis* en is bekend voor ademhalingsproblemen te induceren via ZSA. Deze alg is echter alleen dominant in de Golf van Mexico. OA is het meest voorkomende mariene fycotoxine in de Noordzee en zou mogelijk ook negatieve effecten kunnen hebben na respiratorische blootstelling

aan een voldoende hoge dosis. Voorafgaand aan dit doctoraatsonderzoek was de aerosolisatie of aanwezigheid in zeelucht nog nooit onderzocht voor OA en YTXs.
In **hoofdstuk 3** brachten we daar verandering in en werden de aerosolisatie processen en de natuurlijke (zeelucht) concentraties van deze fycotoxines onderzocht. Met behulp van onze MART, die zeewater bevatte waaraan toxine-producerende algen werden toegevoegd, hebben we aerosolisatie-experimenten uitgevoerd. Deze experimenten leverden het eerste (experimentele) bewijs dat OA, hYTX en dinophysistoxine-1 (DTX-1) kunnen aerosoliseren via ZSA. Hun sterke potentieel voor aerosolisatie werd aangetoond door de sterk aangerijkte concentraties waarin deze fycotoxines werden aangetroffen in de ZSA. De concentrations in de ZSA waren maar liefst een factor 78 tot 1769 hoger dan in het zeewater. Om deze kwalitatieve resultaten te verkrijgen, werd een nieuwe methodologie ontwikkeld voor de extractie en analyse van fycotoxines in ZSA. Deze analytische methode gebruikte ultra hogedrukvloeistofchromatografie gekoppeld aan hoge-resolutie Orbitrap-massaspectrometrie (UHPLC-HR-Orbitrap-MS). De methode had een goede lineariteit (R^2>0,99), *recovery* (85,3-101,8%) en precisie (RSDs≤17,2%). Natuurlijke concentraties van deze fycotoxines in zeelucht werden vervolgens onderzocht door ZSA te bemonsteren aan de Belgische kust en gelijktijdig aerosolisatie experimenten uit te voeren met natuurlijk zeewater in onze MART. Dankzij deze benadering waren we in staat de OA-concentraties in de Belgische zeelucht ($[OA]_{zeelucht}$ = 0,6-51 pg m^{-3}) in te schatten. Vanwege het gebrek aan toxicologische in-vivo data konden we geen nauwkeurige humane risicobeoordeling uitvoeren. Indien we alle elementen in beschouwing nemen, lijkt het echter eerder onwaarschijnlijk dat deze $[OA]_{zeelucht}$ nadelige gezondheidseffecten induceren.

In **hoofdstuk 4** hebben we onze in vitro experimenten, ter analyse van mogelijke gezondheidseffecten, realistischer gemaakt. Daartoe maakten we gebruik van een natuurlijk ZSA-monster, dat een complex en waarheidsgetrouw ZSA mengsel van mariene stoffen omvatte. Na de collectie van dit ZSA-monster aan de Belgische kust, werd het geëxtraheerd en gedoseerd aan longcellen in een in vitro experiment. Door de differentiële genexpressie te analyseren, met behulp van RNA-*sequencing*, werd inzicht verkregen in de moleculaire mechanismes van de geïnduceerde effecten. Ter vergelijking werden de long cellen ook aan drie andere behandelingen blootgesteld in

dit experiment: (1) zuivere hYTX, (2) het extract van een laboratorium-gegenereerde ZSA dat ook hYTX bevatte, en (3) een gekende chemische mTOR inhibitor.
Na blootstelling aan het natuurlijke ZSA-monster en de mTOR inhibitor vertoonden de longcellen een significante afname in expressie van de genen die gerelateerd zijn aan de mTOR-*pathway* en *proprotein convertase subtilisin/kexin type 9* (PCSK9). De sterke overeenkomstigheid in de regulatie van deze genen suggereert dat natuurlijke ZSA mariene stoffen bevatten die gelijkaardige effecten hebben als de mTOR inhibitor en bijgevolg de mTOR-*pathway* kunnen afremmen, zoals gesteld in de biogene hypothese. De zuivere hYTX en lab ZSA behandelingen, daarentegen, induceerden een significant verhoogde expressie van deze genen. Dit bekent niet dat de activiteit van de mTOR-*pathway* daardoor werd gestimuleerd. Wel toont het aan dat hYTX op een andere manier interageert met de mTOR-*pathway* en dat andere mariene stoffen (dan hYTX) de effecten hebben veroorzaakt waargenomen in de natuurlijke ZSA behandeling. Algemeen leverde deze studie moleculair bewijs dat potentieel gunstige gezondheidseffecten kunnen geïnduceerd worden na blootstelling aan (een realistische dosis) natuurlijke ZSA.

Hoofdstuk 5 bespreekt de resultaten van een eenjarige ZSA monstername campagne aan de Belgische kust. De anorganische samenstelling van deze ZSA monsters werd geanalyseerd met behulp van inductief gekoppelde plasma - optische emissiespectrometrie (ICP-OES). Organische analyse van de ZSA monsters werd uitgevoerd met behulp van UHPLC-HR-Q-Orbitrap ™ hybride massaspectrometrie (MS/MS). We identificeerden en kwantificeerden dipalmitoylfosfatidylcholine (DPPC) in bijna alle ZSA-monsters bij luchtconcentraties tussen <1,1 en 33 pg m^{-3}. De ontdekking van deze mariene surfactant in ZSA is vanwege zijn respiratoire effecten van groot belang voor dit onderzoek en onderzoeksveld. DPPC is de belangrijkste component (± 40%) van het pulmonale surfactantsysteem in humane longblaasjes en wordt gebruikt als voorname hulpstof bij medische aerosol therapie om de effecten van de respiratorisch-toegediende geneesmiddelen te faciliteren. Het DPPC-gehalte in ZSA zou dezelfde faciliterende rol kunnen spelen voor geaerosoliseerde bioactieve mariene stoffen in zeelucht. Door de anorganische inhoud (Mg^{2+} en Ca^{2+}) van de ZSA-monsters en de diverse omgevingsfactoren, die de zeespray aerosolisatie van DPPC bepalen, te analyseren, hebben we zeespray productie processen ontrafeld die de hele ZSA-samenstelling beïnvloeden. Onze bevindingen over DPPC in ZSA zijn dus niet

alleen belangrijk met betrekking tot de menselijke gezondheid van kustpopulaties, ze zijn ook cruciaal voor het begrijpen van het meteorologische gedrag van ZSA.

Door de grote hoeveelheid pionierswerk dat werd verricht, was het vanzelfsprekend niet mogelijk om alle aspecten van de relatie tussen ZSA en menselijke gezondheid te onderzoeken. Desalniettemin geloof ik dat we een aantal grote doorbraken hebben bereikt in dit jonge en tegelijkertijd eeuwenoude onderzoeksveld. Onze nieuwe bevindingen die de biogene hypothese ondersteunen en onze ontdekking van DPPC in ZSA, benadrukken de potentiële positieve effecten van respiratorische blootstelling aan mariene stoffen via ZSA. Bovendien suggereert ons werk dat de huidige concentraties fycotoxines (i.e., OA) aan de Belgische kust geen risico vormen voor de menselijke gezondheid. Deze nieuwe kennis, over de relatie tussen (de gezondheidstoestand van) de oceaan en menselijke gezondheid, kan bijdragen aan een beter beheer van mariene ecosystemen. De bescherming van de gerelateerde ecosysteemdiensten zal ons ook helpen om in harmonie met de natuur te leven en als soort te overleven.

Curriculum vitae

Personalia

Ir. Emmanuel Van Acker
Kasteelstraat 29, 8580 Avelgem, Belgium
Born 18th of January 1991, Menen, Belgium
Married to Laura Anrijs
✆ +32 471 44 69 61
✉ emmanuel_van_acker@hotmail.com

Professional experience

2015-2021 Ghent University, Faculty of Bioscience Engineering
Academic assistant Department of Animal Sciences and Aquatic Ecology
PhD student Laboratory of Environmental Toxicology & Aquatic Ecology

Education

2015-2021 Ghent University
Doctor (PhD) of Bioscience Engineering

2014-2015 Ghent University & University of Antwerp
M.Sc. in Technology for Integrated Water Management *(Magna cum laude)*

2012-2014 University of Leuven (KU Leuven)
M.Sc. in Bioscience Engineering, Environmental Technology *(Cum laude)*

2009-2012 University of Leuven (KU Leuven)
B.Sc. in Bioscience Engineering

2003-2009 Sint-Jan Berchmanscollege Avelgem
Science-Mathematics

Scientific awards

2019 HYDRO vzw and the Flanders Marine Institute (VLIZ)
Dr Edouard Delcroix Incentive Award

2018 at the 53rd European Marine Biology Symposium
Best poster award - 2nd runner up

2017 Flanders Marine Institute (VLIZ) philanthropy
VLIZ Brilliant Marine Research Idea grant

A1 Publications

Van Acker E.; De Rijcke M.; Liu Z.; Asselman J.; De Schamphelaere K.A.C.; Vanhaecke L.; Janssen C.R. Algal phospholipids in sea spray aerosols: a surprising parallel with medical aerosol therapy. *Submitted to Environmental Science and Technology.*

Van Acker E.; Huysman S.; De Rijcke M.; Asselman J.; De Schamphelaere K.A.C.; Vanhaecke L.***§***; Janssen C.R.***§*** **2021**. Phycotoxin-Enriched Sea Spray Aerosols: Methods, Mechanisms, and Human Exposure. Environmental Science and Technology, 55, 6184-6196. *(***§** *shared last)*

Van Acker E.; De Rijcke M.; Asselman J.; Beck I.M.; Huysman S.; Vanhaecke L.; De Schamphelaere K.A.C.; Janssen C.R. **2020**. Aerosolizable Marine Phycotoxins and Human Health Effects: In Vitro Support for the Biogenics Hypothesis. Marine Drugs, 18, 1-13.

Asselman J.***§***; **Van Acker E.*****§***; De Rijcke M.; Tilleman L.; Van Nieuwerburgh F.; Mees J.; De Schamphelaere K.A.C.; Janssen C.R. **2019**. Marine biogenics in sea spray aerosols interact with the mTOR signaling pathway. Scientific Reports, 9, 1-10. *(***§** *shared first)*

De Rijcke M.; **Van Acker E.**; Nevejan N.; De Schamphelaere K.A.C.; Janssen C.R. **2016**. Toxic dinoflagellates and *Vibrio* spp. act independently in bivalve larvae. Fish & Shellfish Immunology 57, 236-242.

Platform presentations *(first author)*

Van Acker E.; De Rijcke M.; Huysman S.; Vandegehuchte M.; Vanhaecke L.; De Schamphelaere K.; Janssen C. Assessing human exposure to background levels of algal toxins via sea spray. 18th International Conference on Harmful Algae (ICHA), 21-27 October **2018** Nantes, France.

Van Acker E.; Asselman J.; De Rijcke M.; De Schamphelaere K.A.C.; Janssen C.R. Do marine aerosols improve human health? An exploratory "holistic" approach. VLIZ Marine Science Day March 21st **2018**, Bredene, Belgium.

Van Acker E.; De Rijcke M.; De Schamphelaere K.A.C.; Janssen C. Occurrence and effects of bio-active substances in marine bioaerosols. SETAC Europe 27th Annual Meeting, May 8th **2017**, Brussels, Belgium. *(invited speaker)*

Van Acker E.; De Rijcke M.; De Schamphelaere K.; Janssen C. Phycotoxins in sea spray aerosols: Friend or Foe? VLIZ Marine Scientist Day, March 3rd **2017** Bruges, Belgium.

Poster presentations *(first author)*

Van Acker E.; Asselman J.; De Rijcke M.; De Schamphelaere K.; Janssen C.; 2020. Sea spray exposure to man: initial risk benefit assessment. SOPHIE People, Health and the Ocean Conference. March 30th **2020**. Brussels, Belgium.

Webinar due to covid-19 crisis.

Van Acker E.; Asselman J.; De Rijcke M.; Huysman S.; Vanhaecke L.; De Schamphelaere K.; Janssen C. Marine sea spray exposure to man: initial risk benefit assessment. VLIZ Marine Science Day, March 13th **2019**, Bredene, Belgium.

Van Acker E.; De Rijcke M.; Huysman S.; Vanhaecke L.; De Schamphelaere K.; Janssen C. Human exposure to algal toxins via sea spray aerosols. 53rd European Marine Biology Symposium, 17-21 September **2018**, Ostend, Belgium.

Van Acker E.; De Rijcke M.; De Schamphelaere K..; Janssen C.; 2016. Right place, wrong time: mixture toxicity effects of pathogens and HABs on bivalve recruitment. VLIZ Marine Scientist Day, February 2nd **2018**, Bruges, Belgium.

Educational activities

Tutor of 7 M.Sc. dissertation students (of which 2 awarded)

Eeckhout J. **2020**. Characterisation of marine bioactive compounds in sea spray aerosols. UGent. M.Sc. in Bioscience Engineering.

Goossens E. **2019**. Characterisation of antioxidant capacity in sea spray aerosols. UGent. M.Sc. in Bioscience Engineering.

D'Hondt W. **2018**. Identification of biogenic chemicals in sea spray aerosols. UGent. M.Sc. in Bioscience Engineering.

Lodewijks E. **2017**. Potential human health effects of phycotoxins in marine bioaerosols. UGent. M.Sc. in Environmental Sanitation.

VLIZ Thesis Award

Baelus S. **2017**. Characterization of phycotoxins in sea spray aerosols. UGent. M.Sc. in Bioscience Engineering.

ArcelorMittal Indaver Thesis Award

Vergote T. **2016**. Production and detection of aerosolized marine phycotoxins. UGent. M.Sc. in Bioscience Engineering.

Van Hal M. **2016**. Marine bioaerosols: human health effects of aerosolized Phycotoxins. UGent. M.Sc. in Bioscience Engineering.

Tutor of 4 B.Sc. dissertation students

De Keersmaeker G.; Vermeesh G.; Moeyersoons M.; Van der Hauwaert L. **2018**. Transformeren we onze zeeën in actieve luchtvervuilers? B.Sc. in Bioscience Engineering.

Coordinating assistant of the courses of Prof. Janssen and Prof. De Schamphelaere

This included schedule planning, course site management, exam planning, exam supervision, being the first contact person for students, teaching exercise and practicum sessions, and giving excursions for the following courses:

Applied Marine Ecology (6y)

(previously the Marine Ecology partim of the courses: Aquatic and Terrestrial Ecology, Environmental ecology and Aquatic ecology)

Environmental Risk Assessment (3y)

(previously named Ecological Risk Assessment)

Ecosystem modelling (4y)

(previously named Ecotechnology)

UGain – *Milieucoördinator* – Ecotoxicology module (4y)

(previously named IVPV)

Other involement

GhEnToxLab

Coordinated a 2y research project of VMM on the microplastic emission and pollution in freshwater environments in Flanders.

Coordinated a half year research project of Aquafin of the microplastic removal in STP effluent using a discfilter set-up.

Coordinated scientific lab seminars (2y) and monthly social activities (4y)

Coordinated the PlaneetZee@Work for high school students (2y)

Maintained the GhEnToxLab website (2y)

Presented my PhD research to the general public on:

"*Dag van de wetenschap"*, November 26th 2017, Ostend, Belgium.

"Pint of Science", May 22nd 2019, Ostend, Belgium.

Private

Head leader (4y) and leader (7y) at Scouts & Gidsen Moen

Board member of De Mouwebokkers vzw (*since 2015*)

Board member of Mbc De Steenbakkers vzw (*since 2020*)